

AD-A133 350

REPORT OF TESTS OF A COMPRESSOR CONFIGURATION OF DCA  
BLADING(U) NAVAL POSTGRADUATE SCHOOL MONTEREY CA

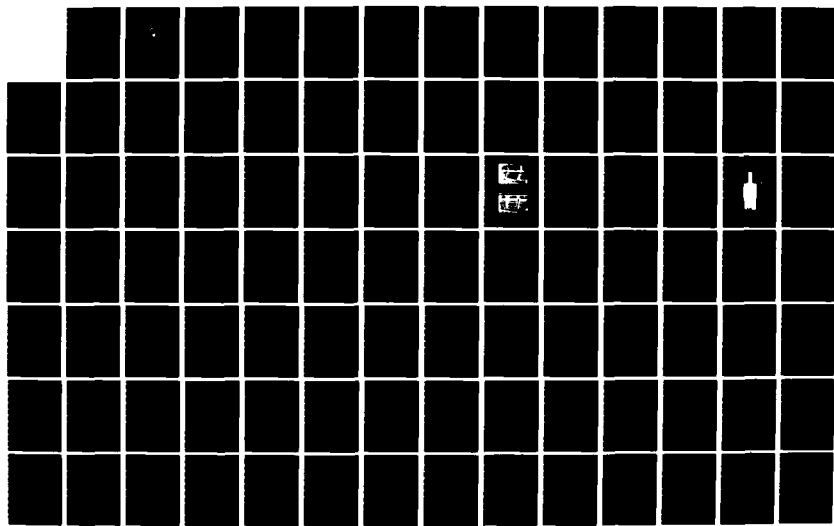
1/2

S J HIMES JUN 83

UNCLASSIFIED

F/G 20/4

NL



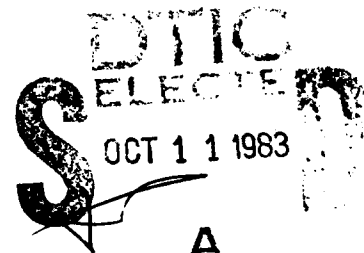


MICROCOPY RESOLUTION TEST CHART  
NATIONAL BUREAU OF STANDARDS-1963-A

AD-A233350

# NAVAL POSTGRADUATE SCHOOL

## Monterey, California



# THESIS

A

REPORT OF TESTS OF A COMPRESSOR  
CONFIGURATION OF DCA BLADING

by

Stephen J. Himes

June 1983

Thesis Advisor:

R. P. Shreeve

Approved for public release: distribution unlimited.

DMC FILE COPY

83 10 07 034

## UNCLASSIFIED

SECURITY CLASSIFICATION OF THIS PAGE (When Data Entered)

REPORT DOCUMENTATION PAGE		READ INSTRUCTIONS BEFORE COMPLETING FORM
1. REPORT NUMBER	2. GOVT ACCESSION NO.	3. RECIPIENT'S CATALOG NUMBER
4. TITLE (and Subtitle) Report of Tests of a Compressor Configuration of DCA Blading		5. TYPE OF REPORT & PERIOD COVERED Master's Thesis June 1983
7. AUTHOR(s) Stephen J. Himes		6. PERFORMING ORG. REPORT NUMBER
9. PERFORMING ORGANIZATION NAME AND ADDRESS Naval Postgraduate School Monterey, California 93940		10. PROGRAM ELEMENT, PROJECT, TASK AREA & WORK UNIT NUMBERS
11. CONTROLLING OFFICE NAME AND ADDRESS Naval Postgraduate School Monterey, California 93940		12. REPORT DATE June 1983
		13. NUMBER OF PAGES 180
14. MONITORING AGENCY NAME & ADDRESS (if different from Controlling Office)		15. SECURITY CLASS. (of this report) Unclassified
		15a. DECLASSIFICATION/DOWNGRADING SCHEDULE
16. DISTRIBUTION STATEMENT (of this Report)  Approved for public release: distribution unlimited.		
17. DISTRIBUTION STATEMENT (of the abstract entered in Block 20, if different from Report)		
18. SUPPLEMENTARY NOTES		
19. KEY WORDS (Continue on reverse side if necessary and identify by block number)  Cascade DCA Blading		
20. ABSTRACT (Continue on reverse side if necessary and identify by block number)  Results of an experimental program to measure the performance of a compressor stator cascade consisting of 20 DCA blades of chord 5.01 inches, aspect ratio 2.0 and solidity 1.67 under conditions of varying incidence angle and Reynolds number are reported. Flow quality and blade performance data were obtained using pneumatic probe surveys and surface pressure measurements. Changes in Reynolds		

Unclassified

SECURITY CLASSIFICATION OF THIS PAGE (When Data Entered)

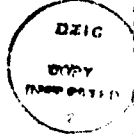
(20. ABSTRACT Continued)

number in the range of 500,000 to 770,000 did not measurably affect either flow quality or blade performance. Changes in incidence angle over the range -15 to 10 degrees produced generally well behaved blade performance parameters.

Accession For

SEARCHED	INDEXED
SERIALIZED	FILED
APR 19 1968	
FBI - LOS ANGELES	

A



S-N 0102-LF-014-6601

Approved for public release: distribution unlimited.

REPORT OF TESTS OF A COMPRESSOR CONFIGURATION OF DCA BLADING

by

Stephen J. Himes  
Lieutenant Commander, United States Navy  
B. S. A. E. United States Naval Academy, 1974

Submitted in partial fulfillment of the  
requirements for the degree of

MASTER OF SCIENCE IN AERONAUTICAL ENGINEERING

from the

NAVAL POSTGRADUATE SCHOOL

June 1983

Author: Stephen J. Himes

Approved by: Raymond P. Sherrill  
Thesis Advisor

Donald M. Layton  
Chairman, Department of Aeronautics

J. M. Dwyer  
Dean of Science and Engineering

ABSTRACT

Results of an experimental program to measure the performance of a compressor stator cascade consisting of 20 (DCA) blades of chord 5.01 inches, aspect ratio 2.0 and solidity 1.67 under conditions of varying incidence angle and Reynolds number are reported. Flow quality and blade performance data were obtained using pneumatic probe surveys and surface pressure measurements. Changes in Reynolds number in the range of 500,000 to 770,000 did not measurably affect either flow quality or blade performance. Changes in incidence angle over the range -15 to 10 degrees produced generally well behaved blade performance parameters.

## TABLE OF CONTENTS

I.	INTRODUCTION .....	13
II.	TEST FACILITY .....	15
	A. HIGH REYNOLDS NUMBER CASCADE .....	15
	1. Wind Tunnel .....	15
	2. Plenum Modifications .....	15
	3. Cascade North Wall Composition .....	15
	4. Inlet Guide Vane Assembly .....	15
	5. Test Section .....	16
	B. INSTRUMENTATION .....	16
	1. Survey Probes .....	16
	2. Reference Probes .....	16
	3. Wall Pressure Taps .....	16
	4. Acquisition and Reduction System .....	17
	5. Measurement Uncertainty .....	17
III.	EXPERIMENTAL PROCEDURES .....	18
	A. GENERAL .....	18
	1. Flow Quality .....	18
	2. Flow Geometry .....	18
	3. Reference Quantities .....	19
	4. Performance Parameters .....	19
	B. SPECIFIC TEST PROCEDURES .....	19
	1. Probe Calibration .....	19
	2. Test Section Setup and Adjustment .....	19

3. Test Measurements .....	20
a. Blade-to-Blade Survey .....	20
b. Spanwise Survey .....	21
c. Instrumented Blade Pressure Distribution .....	21
<b>IV. TEST CASCADE AND PROGRAM OF TESTS.....</b>	<b>22</b>
A. CASCADE CONFIGURATION .....	22
1. Blading .....	22
B. TEST PARAMETERS .....	22
1. Incidence Angle .....	22
2. Reynolds Number .....	23
<b>V. RESULTS .....</b>	<b>24</b>
A. FLOW QUALITY .....	24
B. CASCADE PERFORMANCE .....	24
C. TEST REPEATABILITY .....	24
<b>VI. DISCUSSION .....</b>	<b>25</b>
A. FLOW QUALITY .....	25
1. Uniformity .....	25
2. Periodicity .....	25
3. Pseudo Two-Dimensionality .....	26
4. Effect of North Wall Composition .....	26
B. CASCADE PERFORMANCE .....	27
1. Effect of Reynolds Number .....	27
C. TEST REPEATABILITY .....	27
D. COMPARISON WITH CINA .....	28
<b>VII. CONCLUSIONS .....</b>	<b>29</b>

VIII. RECOMMENDATIONS.....	31
APPENDIX A .....	56
A. FLOW QUALITY DOCUMENTATION .....	56
1. Uniformity .....	56
2. Periodicity .....	56
3. Pseudo Two-Dimensionality .....	56
4. Notation .....	56
APPENDIX B .....	170
A. STORAGE OF EXPERIMENTAL DATA .....	170
1. Storage Devices .....	170
a. Cassette Tape .....	170
b. File Naming Scheme .....	170
2. Thesis Logbook .....	172
B. PROBE CALIBRATION DATA .....	172
APPENDIX C .....	174
LIST OF REFERENCES .....	178
INITIAL DISTRIBUTION LIST .....	180

## LIST OF FIGURES

### Figure

1.	Test Facility Schematic .....	32
2.	McGuire's Plenum Modification .....	33
3a.	Cascade Test Section, Plexiglass Wall Installed ..	34
3b.	Cascade Test Section, Steel Wall Installed .....	34
4.	Test Section Instrumentation and Physical Dimensions .....	35
5.	Cascade Geometry, and Definition of Angles .....	36
6.	DCA Blade Pressure Tap Locations .....	37
7.	Photograph of Center Instrumented Blade .....	38
8.	AVDR versus Incidence Angle .....	39
9.	Loss Coefficient versus Incidence Angle .....	40
10.	Deviation Angle versus Incidence Angle .....	41
11.	Static Pressure Coefficient versus Incidence Angle .....	42
12.	AVDR versus Diffusion Factor .....	43
13.	Loss Coefficient Parameter versus Diffusion Factor .....	44
C.1.	Blade Space Control Volume .....	174
C.2.	Assumed Pressure Function .....	176

LIST OF TABLES

Table

I.	Measurement Uncertainty .....	45
II.	Cascade Performance Formulas .....	46
III.	Cascade Configuration Parameters .....	48
IV.	Test Blade Coordinates .....	49
V.	Variable Test Parameters .....	50
VI.	Flow Uniformity Summary .....	51
VII.	Flow Periodicity and Pseudo Two-Dimensionality Summary .....	54
VIII.	Cascade Performance Summary .....	55
B.1.	Raw Data Storage .....	173

### LIST OF SYMBOLS

ADVR	Axial Velocity--Density Ratio
$C_{fB}$	Coefficient of force based on surface pressure integration
$C_{fM}$	Coefficient of force based on momentum conservation
$C_{P_{static}}$	Coefficient of static pressure rise
$C_{xB}$	Coefficient of force in the x direction based on blade surface pressure integration
$C_{yB}$	Coefficient of force in the y direction based on blade surface pressure integration
$C_{xM}$	Coefficient of force in the x direction based on momentum conservation
$C_{yM}$	Coefficient of force in the y direction based on momentum conservation
c	Blade chord (inches)
D	Diffusion factor
$h_i$	Spanwise depth of control volume at inlet ( $i = 1$ ) or outlet ( $i = 2$ )
i	Incidence angle (degrees)
$k_1$	$[\int_0^S \rho_1 V_1 \cos \beta_1 dx] / [\int_0^S \rho_{ref} V_{ref} \cos \beta_1 dx]$
$k_2$	$[\int_0^S \rho_2 V_2 \cos \beta_2 dx] / [\int_0^S \rho_{ref} V_{ref} \cos \beta_2 dx]$
P	Pressure (in $H_2O$ )
Q	Dynamic Pressure (in $H_2O$ )
s	Blade-to-blade spacing (inches)
T	Temperature ( $^{\circ}R$ )
v	Velocity (ft/sec)
w	Relative velocity (ft/sec)

x	Velocity, non-dimensionalized by the "limiting" velocity, $V_T = \sqrt{2} C_p T_t$
x	Coordinate in the blade-to-blade direction (inches)
y	Coordinate in the axial direction (inches)
z	Coordinate in the spanwise direction (inches)
$\beta$	Air angle, measured in the blade-to-blade plane (degrees)
$\gamma$	Stagger angle (degrees)
$\delta$	Deviation angle (degrees)
$\sigma$	Solidity (c/s)
$\phi$	Pitch angle (of air flow), measured in the spanwise, blade-to-blade plane
$\psi$	Blade camber angle (degrees)
$\Omega$	$[\bar{\omega} \cos^3 \beta_2 / 2\sigma \cos^2 \beta_1]$ Loss coefficient parameter
$\bar{\omega}$	Loss coefficient

#### Subscripts

i	Refers to traversing plane; i = 1 for inlet, i = 2 for outlet
p	Pressure
plen	Plenum (supply)
s	Static
t	Total
u	In the blade-to-blade (x) direction
wl	North wall, lower plane
1	Inlet plane
2	Outlet plane

ACKNOWLEDGMENTS

I would like to express my thanks and appreciation to Dr. R. P. Shreeve, Director, Turbopropulsion Laboratory, for his efforts in making this study a worthwhile and enjoyable learning experience. Special notes of thanks go to Jim Hammer, Kelly Harris, John Morris, Al McGuire and Friedrich Neuhoff for their prompt and efficient assistance. Finally, to my wife, Melissa and son, Michael, thank you for your patience and support during the course of this study.

## I. INTRODUCTION

The on and off-design blade element performance of, and flow through a double-circular-arc (DCA) compressor cascade is being examined in a large subsonic cascade wind tunnel. Tests are to be made subsequently of a controlled-diffusion (CD) cascade configuration designed to replace it as the midspan section of the stator of an axial transonic compressor.

Previous phases of the work involving tests with the present DCA blading were reported by Cina [Ref. 1] and Molloy [Ref. 2]. Cina's test results were considered to be preliminary because the cascade flow was found not to be periodic from one blade passage to the next, but was periodic from blade pair to blade pair. As a result of Cina's work, a modification to the inlet guide vane (IGV) assembly was made, decreasing the space between vanes from 2 inches to 1 inch. Molloy set out to repeat Cina's experiments, but encountered IGV blade flutter (which resulted in some blade damage) when adjusting the vanes with the cascade running. Facility modifications were made which included first the installation of plenum chamber turning vanes. This reduced the large scale flow fluctuations which had prevented the use of tufts to determine the cause of the flutter problem. Also, the vane actuating mechanism was stiffened and new cascade operating procedures were adopted. Following these improvements,

the immediate test objective was to document flow quality and the performance of the reference DCA cascade. Added features of the test program were to investigate the possible effects of Reynolds number and to determine the degree of repeatability of test data from run to run and also from cascade build to build. Additionally, an improvement of the analysis required to derive blade force coefficients from probe survey data was attempted. In the absence of wall suction, side wall boundary layer thickening from inlet to outlet measurement planes causes the control volume to take on a three-dimensional character. An attempt was made to account for the additional pressure-area terms on the control volume surfaces which accompany the streamtube contraction by using the Axial Velocity Density Ratio (AVDR) and an assumed linear distribution of static pressure acting on the streamtube walls. Details of this analysis are presented in Appendix C.

The following report documents a program of 20 tests carried out using the DCA cascade following the facility improvements. Results are given and are discussed, particularly from the viewpoint of flow quality and test repeatability. Details of the results are summarized in figures, tables and appendices. Appendix A contains flow quality documentation, Appendix B, a description of experimental data storage and Appendix C, a discussion of blade force coefficient analysis.

## II. TEST FACILITY

### A. HIGH REYNOLDS NUMBER CASCADE

#### 1. Wind Tunnel

A schematic of the test facility as originally configured is shown in Fig. 1. A complete description is given in [Ref. 3].

#### 2. Plenum Modifications

The plenum chamber (located in the basement of the cascade building) has undergone successive modifications to provide acceptably uniform inlet conditions measured at the inlet guide vane station. Modifications conducted by Bartocci [Ref. 4] and Moebius [Ref. 5] were superceded by those of McGuire [Ref. 6]. McGuire's modification to the plenum is illustrated in Fig. 2. McGuire's plenum modification was in place for all tests reported herein.

#### 3. Cascade North Wall Composition

A plexiglass north wall used during cascade tests enabled McGuire to conduct a concurrent flow visualization experiment. The regular steel wall was used for two of the twenty test runs.

#### 4. Inlet Guide Vane Assembly

The inlet guide vane assembly was the same as that used by Molloy, with vanes at one inch spacing.

## 5. Test Section

Views of the cascade test section are shown in Fig. 3a, Fig. 3b, and Fig. 4. Fig. 3a shows the cascade test section with the plexiglass wall installed and the DCA blade row in place. Fig. 3b shows the test section with the steel wall in place. Fig. 4 illustrates instrumentation placement and physical dimensions.

## B. INSTRUMENTATION

### 1. Survey Probes

Two United Sensor Corporation five-hole probes were used for surveys at the upper and lower planes. A DC-125-24-F-22-CD probe, serial number A981-2 was used at the upper plane and a DA-125 probe, serial A847-1 was used at the lower plane.

### 2. Reference Probes

Plenum chamber reference total pressure was sensed using a pressure tube suspended in the plenum. Reference static pressure was sensed using a static port located on the lower portion of the cascade south wall. Redundancy of reference pressures was provided by a standard pitot-static probe located approximately 2 inches from the entrance to the blade row at midspan and aligned with the inlet flow.

### 3. Wall Pressure Taps

Two rows of static pressure taps were located on the cascade south wall 16.25 inches ahead and 6.5 inches

behind mid-chord. Twenty taps per row spaced two inches apart in the blade-to-blade direction, each connected to a water manometer board, allowed visual inspection of the inlet and outlet static pressure distributions.

#### 4. Acquisition and Reduction System

Data was acquired, reduced and plotted using a modified Hewlett Packard HP-3052A Data Acquisition System [Ref. 7]. Two 48-port Scanivalves connected to a HP-9845A desktop computer via a NPS/TPL HG-78K Scanivalve Controller and a HP-98034A HP-IB Interface Bus allowed all probe and reference pressures to use a single transducer. Blade surface pressures were sensed by the second Scanivalve transducer. The desktop computer acted as the system controller and used acquisition, reduction and plotting software programs documented in [Ref. 8].

#### 5. Measurement Uncertainty

Table I summarizes measurement uncertainties.

### **III. EXPERIMENTAL PROCEDURES**

#### **A. GENERAL**

##### **1. Flow Quality**

Flow uniformity, periodicity, and pseudo two-dimensionality criteria (which implies that area change is permitted) must be satisfied before any calculated cascade performance parameters can be considered meaningful. These flow quality criteria are discussed extensively in [Ref. 9], [Ref. 10] and [Ref. 11].

Uniformity generally describes the degree of constancy of measured values in the blade-to-blade and spanwise directions at the inlet plane and in the spanwise direction at the outlet plane. Periodicity is indicated by a correspondence of measured values from one blade space to the next at the outlet plane. The pseudo two-dimensionality condition is met when the integrated blade surface pressure distribution gives a blade force vector coincident with the blade force vector calculated using the principle of conservation of momentum.

##### **2. Flow Geometry**

Definition of geometrical parameters describing flow through a cascade are given in Fig. 5. Angle measurements were taken from a vertical reference line, clockwise being positive.

### 3. Reference Quantities

To remove time dependency of inlet dynamic pressure caused by atmospheric fluctuations and variations in blower speed, each pressure measurement was referenced to plenum conditions, a procedure validated earlier by Duval [Ref. 11].

### 4. Performance Parameters

Cascade performance parameters were calculated using the formulas listed in Table II. Note that the effect of AVDR on loss coefficient, static pressure rise coefficient, diffusion factor and blade force coefficient derived from momentum conservation was accounted for in each expression.

## B. SPECIFIC TEST PROCEDURES

### 1. Probe Calibration

Prior to testing, both United Sensor five-hole probes were calibrated in a free jet flow. The calibration was represented using Zebner's analytical procedure [Ref. 12] and computer software developed by Neuhoff [Ref. 13].

### 2. Test Section Setup and Adjustment

Tests were conducted at constant stagger angle while varying only air inlet angle and velocity magnitude. To set an inlet condition, before starting the cascade the lower end walls were set to the desired inlet air angle with end wall spacings set to 1.5 inches (one-half blade space). The IGVs were set to deliver the desired inlet air angle following a schedule established in preliminary tests conducted

without test blades. Finally, upper end walls were positioned approximately. The cascade was started and the upper end wall angles were fine-tuned to give a uniform static pressure distribution at the outlet plane. A check of the inlet air angle was made with the lower probe placed at mid-span in the center of the blade-to-blade traverse. If adjustment of the IGVs was required, the cascade was first shut down, the IGVs were readjusted, the cascade was restarted and the inlet air angle was checked again after the cascade had stabilized at the inlet dynamic pressure required for the test.<sup>1</sup>

### 3. Test Measurements

#### a. Blade-to-Blade Survey

Blade-to-blade surveys were conducted using the upper and lower probes simultaneously. Both probes were located at midspan with the lower probe trailing the upper by two inches. Measurements were recorded over four adjacent blade spaces located in the center portion of the cascade test section. The two innermost blade spaces bracketed the center blade which was instrumented with 39 pressure taps. Survey points were spaced 0.25 inches apart over the outermost spaces and at 0.125 inches over the two innermost spaces.

---

<sup>1</sup>Inlet guide vane flutter similar to that reported by Molloy [Ref. 2] reoccurred while adjusting the IGV assembly at relatively high inlet dynamic pressure (about 17 inches of water). Thus it is essential not to adjust the inlet guide vanes while the cascade is operating.

Closely spaced survey points over two blade passages insured that one full blade wake would be surveyed with good spatial resolution.

b. Spanwise Survey

Two spanwise surveys were carried out to establish the spanwise extent of uniform conditions. First, measurements were taken with the upper probe 1 inch from the suction side of the centermost blade and the lower probe 1 inch from the pressure side of the centermost blade. Once the first spanwise traverse was complete, the upper probe was placed 1 inch from the pressure side, the lower placed 1 inch from the suction side and the spanwise traverse was repeated.

c. Instrumented Blade Pressure Distribution

After completing the blade-to-blade and spanwise traverse, one or more sets of blade pressure distribution data were recorded.

#### **IV. TEST CASCADE AND PROGRAM OF TESTS**

##### **A. CASCADE CONFIGURATION**

Constant parameters for the cascade configuration are summarized in Table III.

###### **1. Blading**

Test blading consisted of twenty constant cross-section double circular arc (DCA) blades of aspect ratio 2.0 and chord 5.01 inches. Coordinates for the test blades are given in Table IV. Three of the twenty blades were instrumented with static pressure taps at midspan in order to provide measurements of blade static pressure distribution. The center blade contained 39 pressure taps while each adjacent blade had 6 taps. Adjacent blade instrumentation provided a measure of the uniformity of pressure distribution from one blade to the next. Pressure tap locations for the center instrumented blade are illustrated in Fig. 6. Fig. 7 shows a photo of the center instrumented blade.

##### **B. TEST PARAMETERS**

The results of 20 tests are reported for which the test parameters are summarized in Table V.

###### **1. Incidence Angle**

Seven test values of incidence angle were chosen. Five of the seven angles were approximately those reported

by Cina to allow a comparison to be made of corresponding data sets.

2. Reynolds Number

In order to investigate the possible dependence of cascade flow quality and performance on Reynolds number, each incidence angle was tested at at least two Reynolds numbers. The Reynolds number based on chord was varied between 491,000 and 773,000.

## V. RESULTS

### A. FLOW QUALITY

Uniformity, periodicity and pseudo two-dimensionality were evaluated from data presented in Appendix A and are summarized in Tables VI and VII.

### B. CASCADE PERFORMANCE

Cascade performance is summarized in Figs. 8 through 13 and in Table VIII.

### C. TEST REPEATABILITY

Run-to-run repeatability of cascade performance parameters is indicated in Figs. 8 to 13 by double-headed solid arrows. The arrow indicates the observed range of the applicable cascade performance parameter. Tunnel build-to-build repeatability was investigated at the design incidence angle of 2.2 degrees. Double-headed broken arrows indicate build-to-build repeatability.

## VI. DISCUSSION

### A. FLOW QUALITY

#### 1. Uniformity

As seen in Table VI, the dynamic pressure, static pressure, total pressure and non-dimensional velocity were acceptably uniform over at least twenty percent of blade span at the inlet and outlet planes, and over the entire twelve inch blade-to-blade traverse at the inlet plane.

Inlet and outlet air angle were acceptably uniform in the spanwise direction. Beta 1 was indicated to vary slightly in the blade-to-blade direction. The average total change in Beta 1 from beginning to end of a 12 inch blade-to-blade traverse was approximately one degree. Since adjustment of the inlet guide vane assembly with the cascade running was prohibited, this variation was accepted. If the IGV mechanism was stiffened further to allow adjustment during cascade operation, strict uniformity of inlet air angle would probably be assured.

#### 2. Periodicity

With the exception of the most negative incidence angle of -12.5 degrees, good periodicity was obtained over the three centermost blades. Surface pressures from the left, center and right blades were in excellent agreement except at  $i = -12.5$  degrees. Also, all flow parameters

measured at the outlet plane at midspan were closely periodic from one blade space to the next with the exception of the most negative incidence angle.

### 3. Pseudo Two-Dimensionality

Despite the revision which was made to the calculation of  $C_{fM}$ , (the blade force coefficient derived from probe survey data; Appendix C), agreement between  $C_{fM}$  and  $C_{fB}$ , (the blade force coefficient derived from surface pressure measurements), was achieved in only about 50 percent of the tests (Table VII). The problem is thought to lie in the calculation of the axial component of  $C_{fM}$ . An order of magnitude comparison of the terms that make up the axial component  $C_{fM}$  (Eqn. C. 14) revealed that the first two terms were of order 1.0, the third and fourth terms of order 10.0, and the fifth term of order 0.01. The difference between the first two pairs of terms, however, were both less than order 1.0, with the pressure-area integrals contributing the most. Thus, the value of  $C_{fM}$  was highly sensitive to small inaccuracies in the survey data and too coarse spacing of data points. The more satisfactory results obtained for the tangential components of  $C_{fM}$  can be explained because its evaluation does not involve pressure-area integration terms.

### 4. Effect of North Wall Composition

At one incidence angle the more rigid and slightly better-fitting steel wall was used. The resultant spanwise distribution of flow parameters was generally indistinguishable

from the distributions obtained when using the plexiglass wall. (See Figs. A.51 to A.76 and Figs. A.139 to A.144).

## B. CASCADE PERFORMANCE

### 1. Effect of Reynolds Number

Figs. 8 to 13, and Appendix A show that varying Reynolds number from approximately 500,000 to 770,000 had no measurable effect on the blading performance or on the cascade flow quality. This can probably be explained as being due to the controlling influence of a leading edge separation bubble on the suction side boundary layer transition [Ref. 6]. Conducting tests significantly above a prescribed threshold Reynolds number is therefore unnecessary for this blade set. It is noted that when operating at Reynolds numbers of 500,000, adjustment of the IGV assembly with the cascade running may be possible in the future after further stiffening of the actuating mechanism.

## C. TEST REPEATABILITY

Run-to-run repeatability of cascade performance parameters was satisfactory as was build-to-build repeatability. The total uncertainties in the measurements of AVDR, loss coefficient, deviation angle and static pressure rise coefficient were about 0.01, 0.005, 0.4 degree, and 0.02 respectively.

#### D. COMPARISON WITH CINA

Figs. 8 through 13 each contain a broken line showing the results of Cina's DCA cascade tests. Differences between the two data sets are apparent. Given a specific incidence angle, Cina reported a lower loss coefficient, deviation angle and AVDR, and higher static pressure rise coefficient. Three contributing factors can be cited. First, and most importantly, Cina operated with a different IGV assembly that did not deliver periodic conditions blade-passage to blade-passage. Secondly, he used a plenum which gave less stable, more turbulent supply conditions. Finally, the upper and lower traverse probes were carefully recalibrated after Cina completed his tests.

## VII. CONCLUSIONS

Based on an examination of experimental data the following conclusions are drawn.

1. The cascade flow was satisfactorily uniform. Uniformity existed at the upper and lower planes over at least 20% of blade span near midspan and at the lower plane (midspan) in the blade-to-blade direction for all measured flow parameters at all tested inlet conditions.
2. The cascade flow was satisfactorily periodic. Periodicity existed at the upper plane (midspan) in the blade-to-blade direction for all inlet conditions tested.
3. The cascade flow was not shown consistently to be strictly pseudo two-dimensional. Accounting for streamtube contraction due to side wall boundary layer thickening from lower to upper measuring planes introduced additional small terms into the equation for the axial force component. However, the calculation of the axial force is dominated by the difference between two pressure-area integrals of much greater magnitude.
4. Cascade performance parameters were not measurably affected by varying Reynolds number in the range 500,000 to 770,000.
5. Test conditions can be repeated within an acceptable uncertainty from run-to-run. Build-to-build conditions can

also be successfully repeated.

6. Use of the plexiglass north wall instead of a steel wall had no measurable effect on the results.

7. Inlet guide vanes cannot be safely adjusted with the cascade operating.

## VIII. RECOMMENDATIONS

It is recommended that the following actions be considered.

1. The inlet guide vane assembly should be modified to allow adjustment of the IGVs while the cascade is running.
2. Yaw balancing manometers should be inclined in order to provide the experimenter with better inlet and outlet air angle measurement sensitivity.
3. The motor driven yaw and spanwise positioning systems mounted on the upper traverse caused a significant bending moment to be placed on the probe blade-to-blade slide. Noticeable wear of the upper traverse mechanism took place during the course of twenty test runs. Removal of the power yaw and span drives in favor of a lighter-weight mount similar to that at the lower plane is recommended.
4. Provide ready data file transfer from the HP-9845A cassette tapes to the IBM 3033 computer so that advantage can be taken of the DISSPLA graphics capability available at the NPS Computer Center.

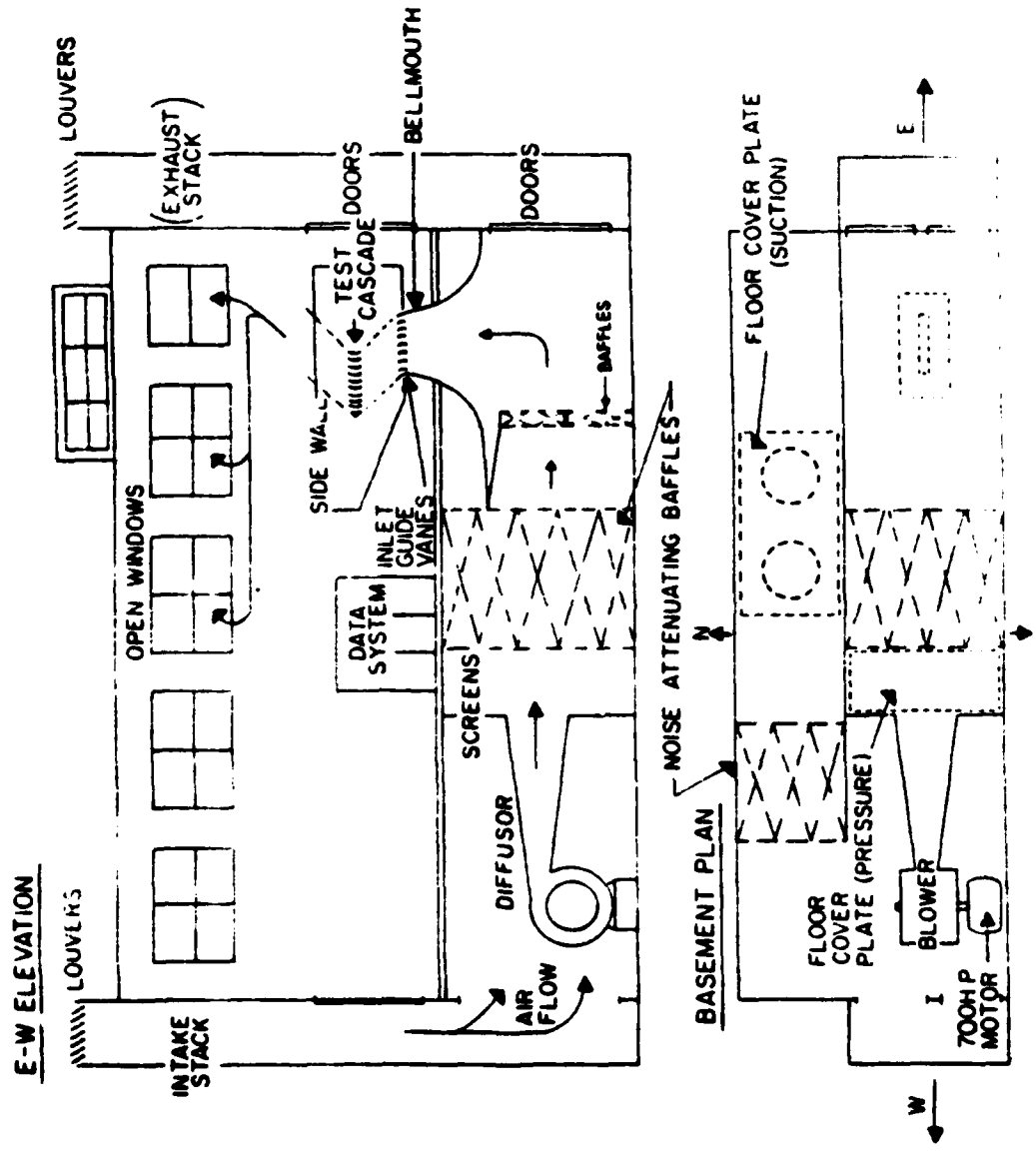


Fig. 1. Test Facility Schematic

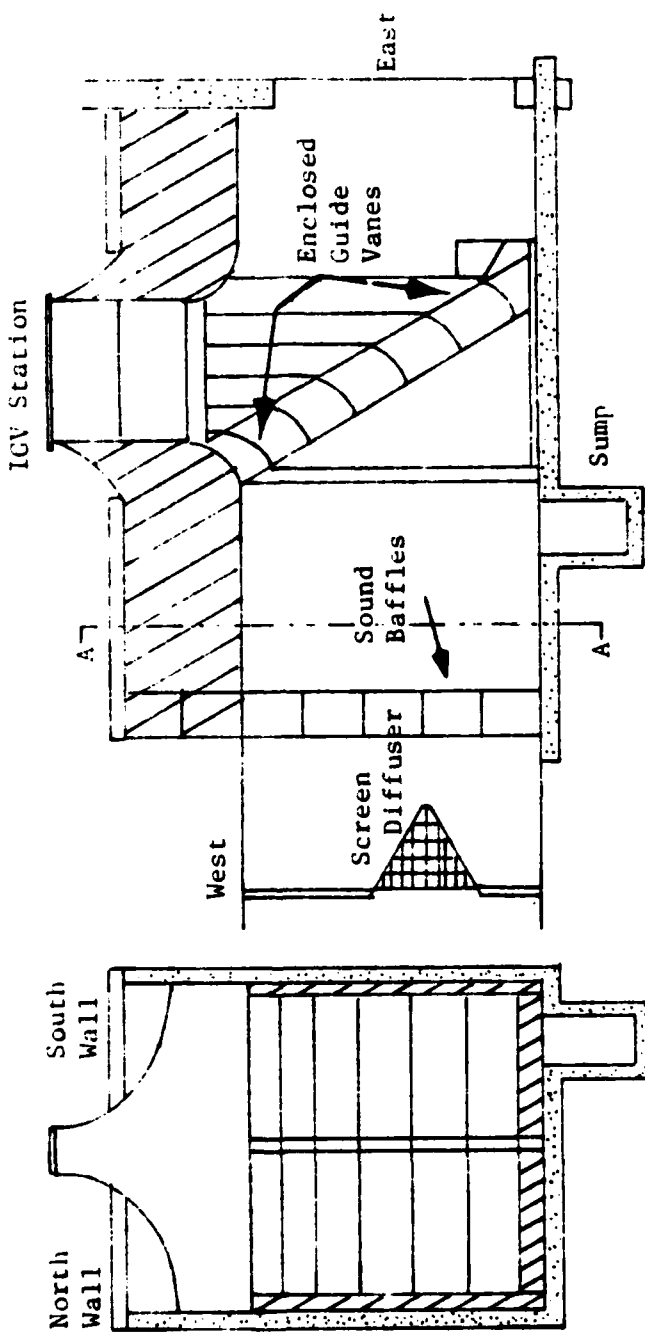
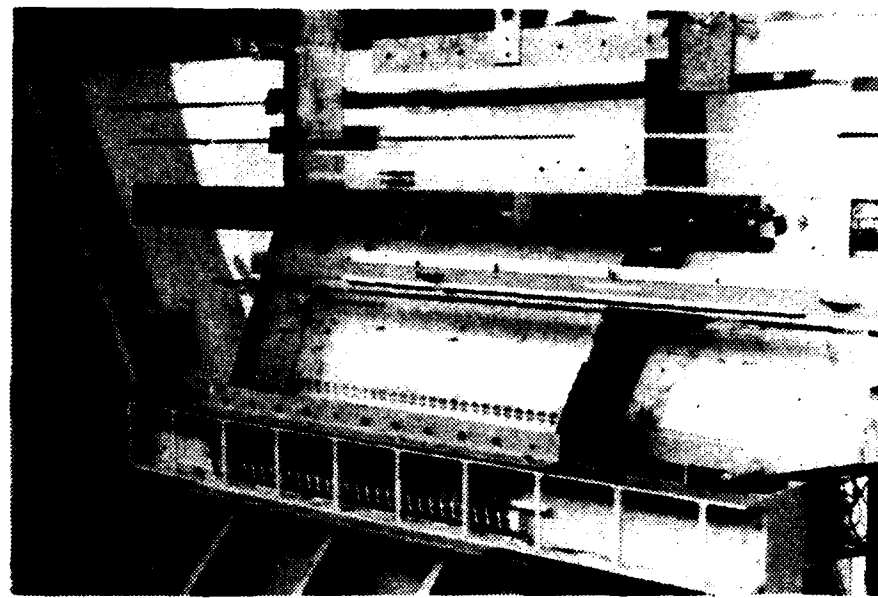
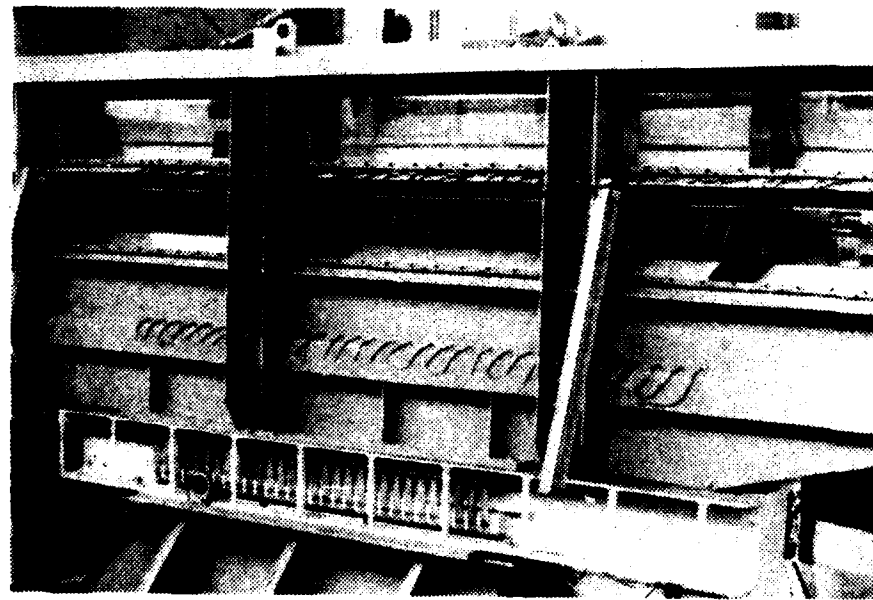


Fig. 2. McGuire's Plenum Modification



**Fig. 3a. Cascade Test Section, Plexiglass Wall  
Installed**



**Fig. 3b. Cascade Test Section, Steel Wall  
Installed**

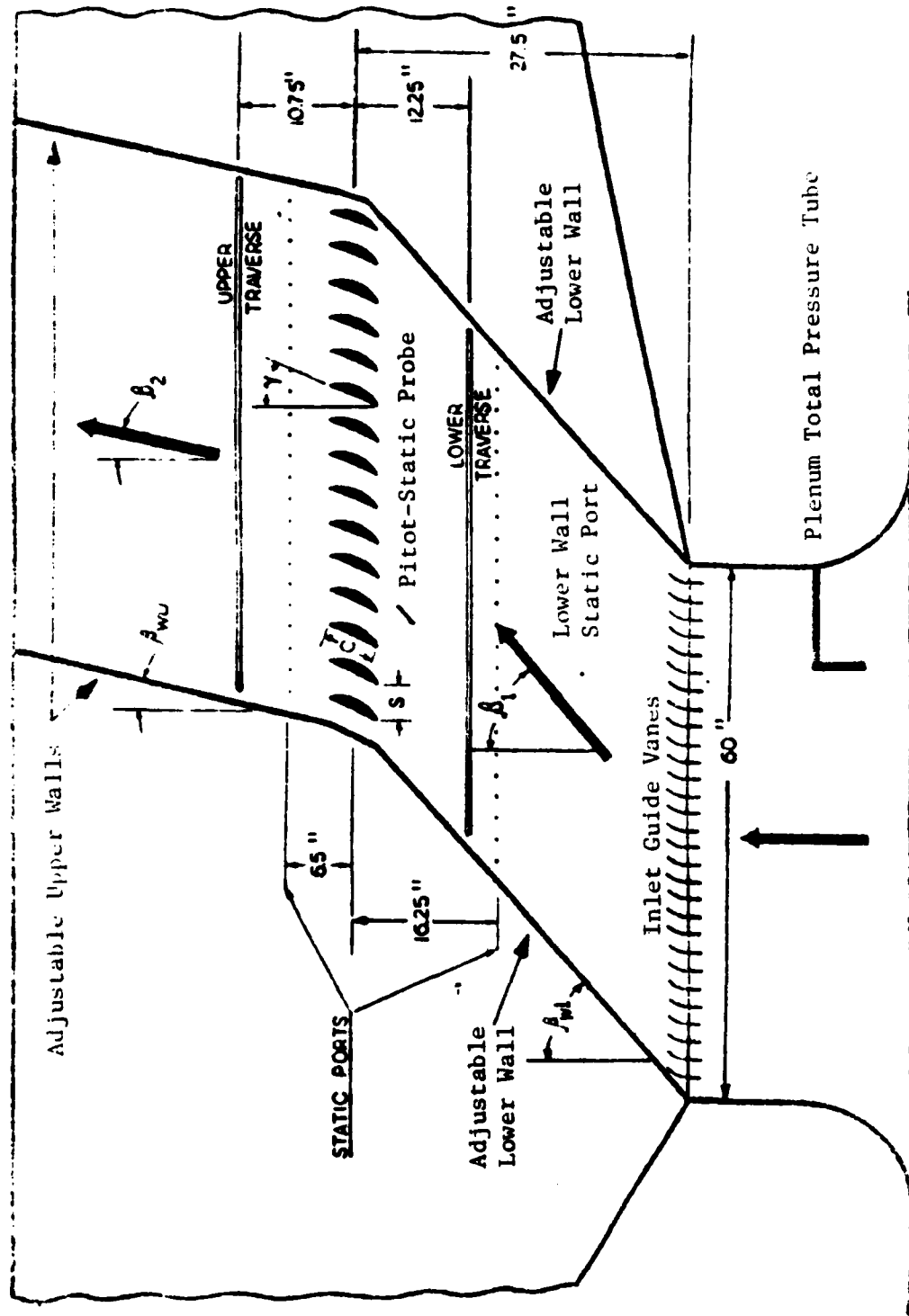


Fig. 4. Test Section Instrumentation and Physical Dimensions

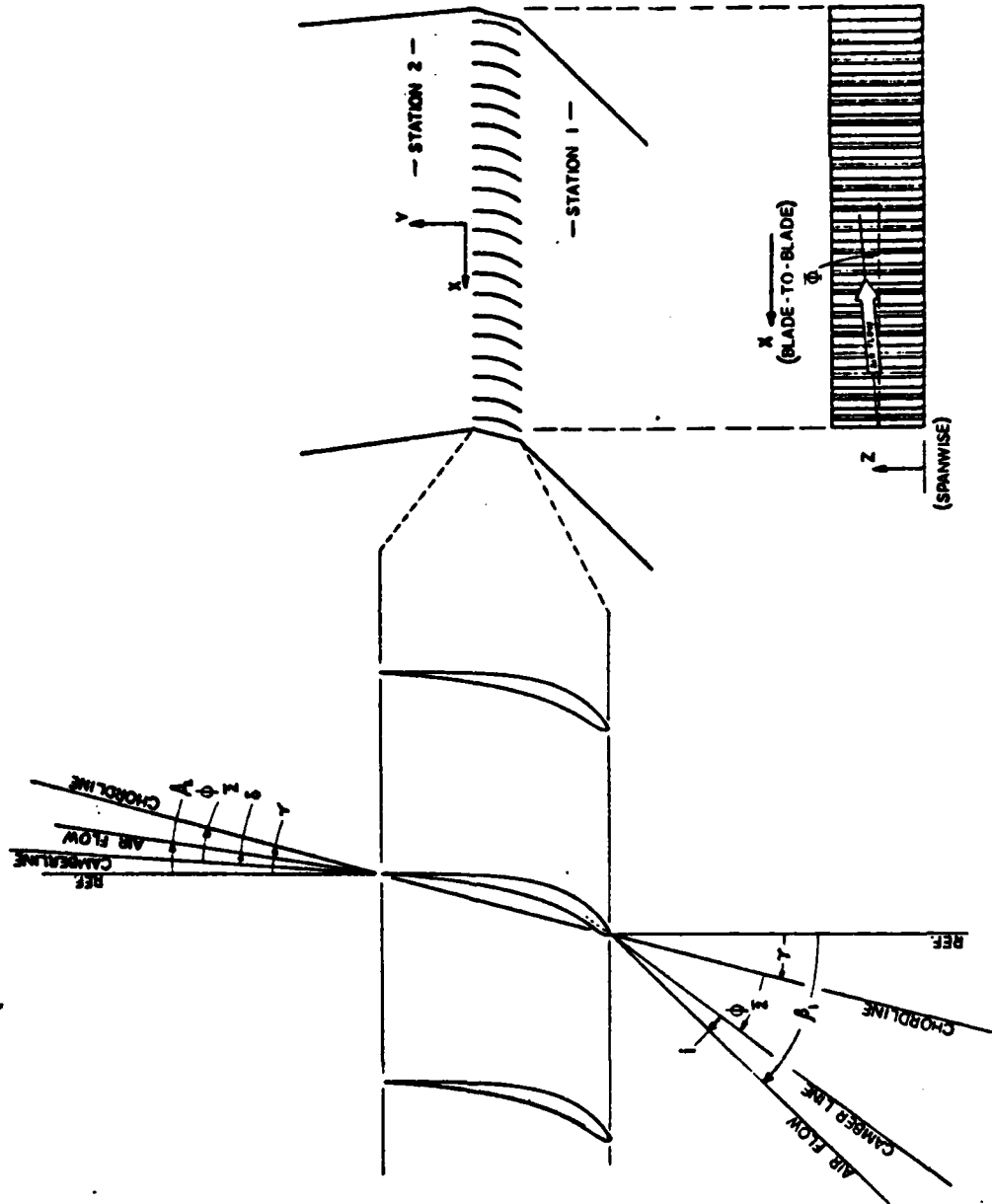


Fig. 5. Cascade Geometry, and Definition of Angles

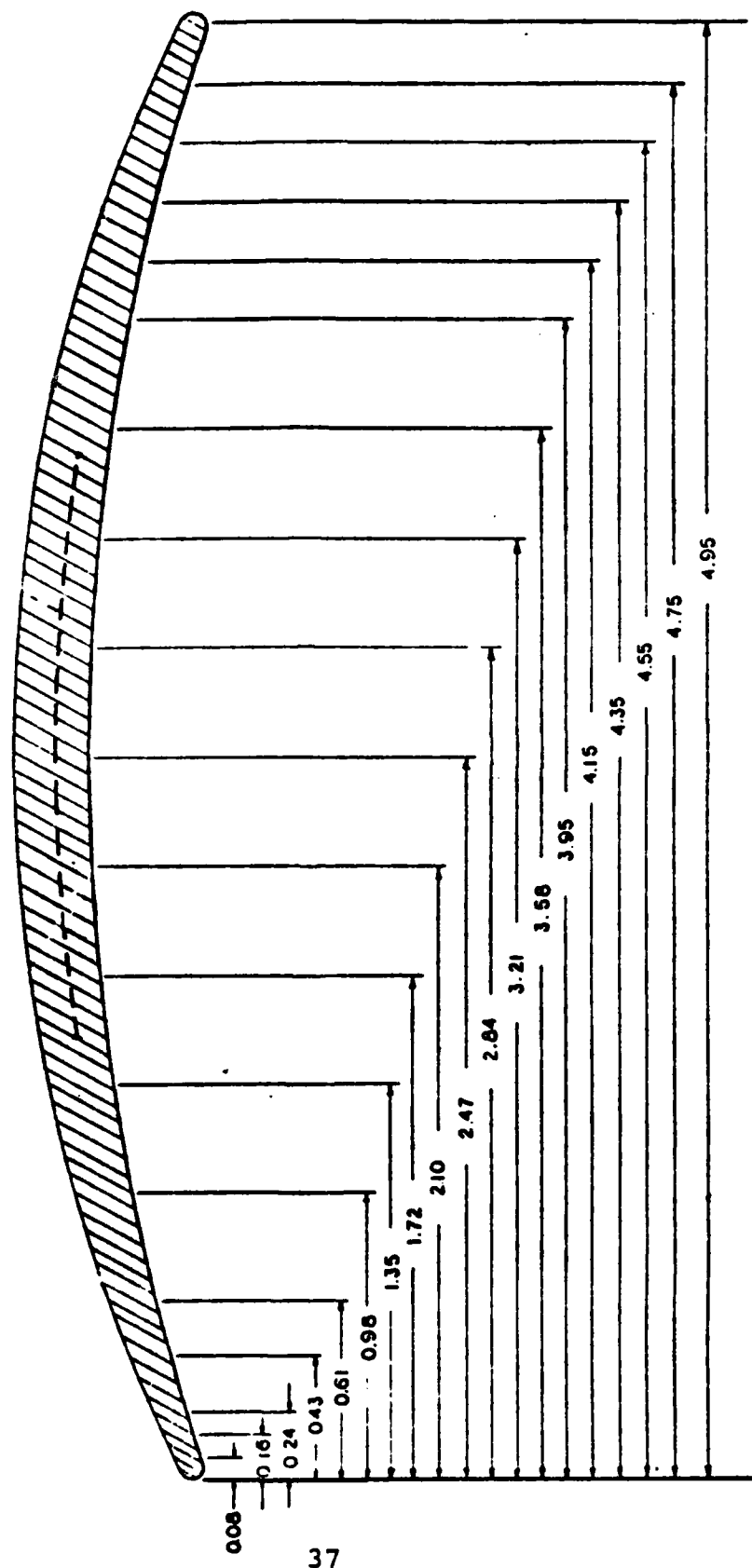


Fig. 6. DCA Blade Pressure Tap Locations

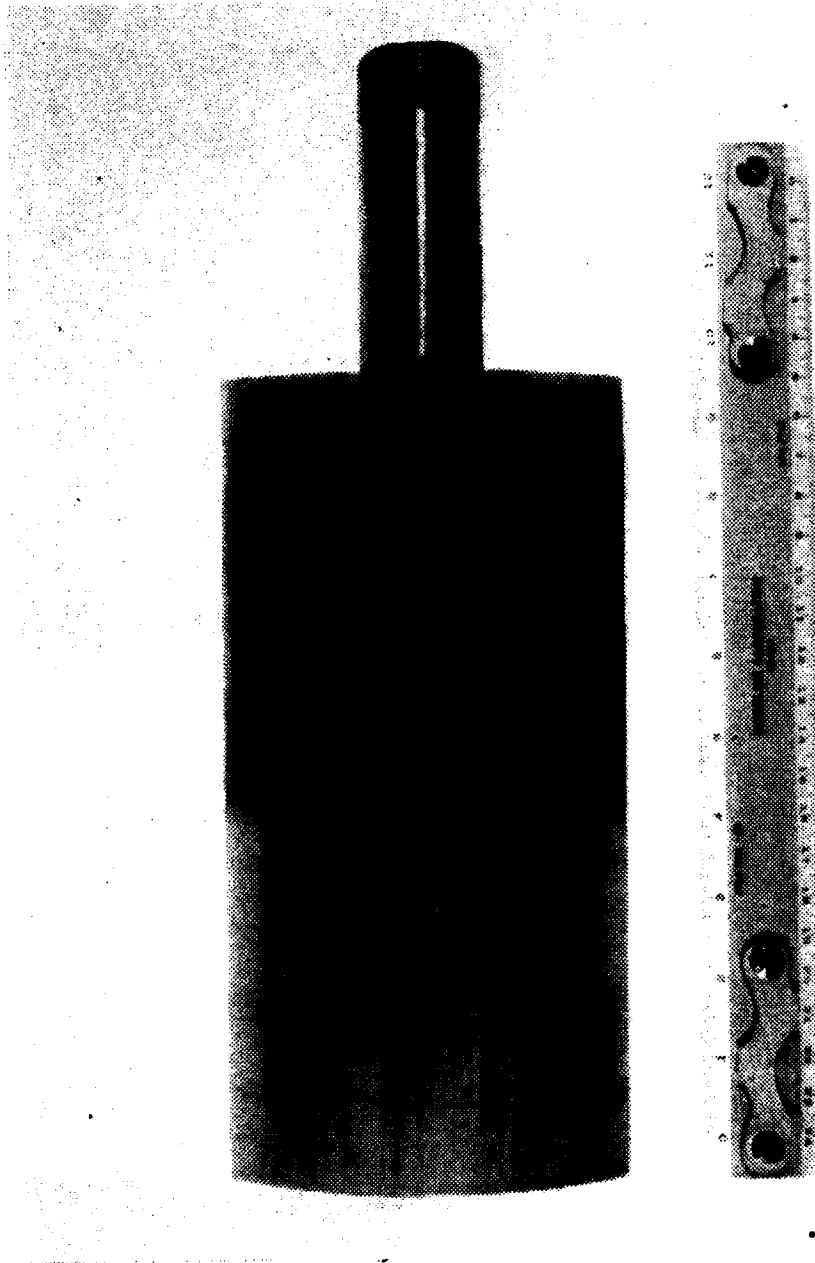


Fig. 7. Photograph of Center Instrumented Blade

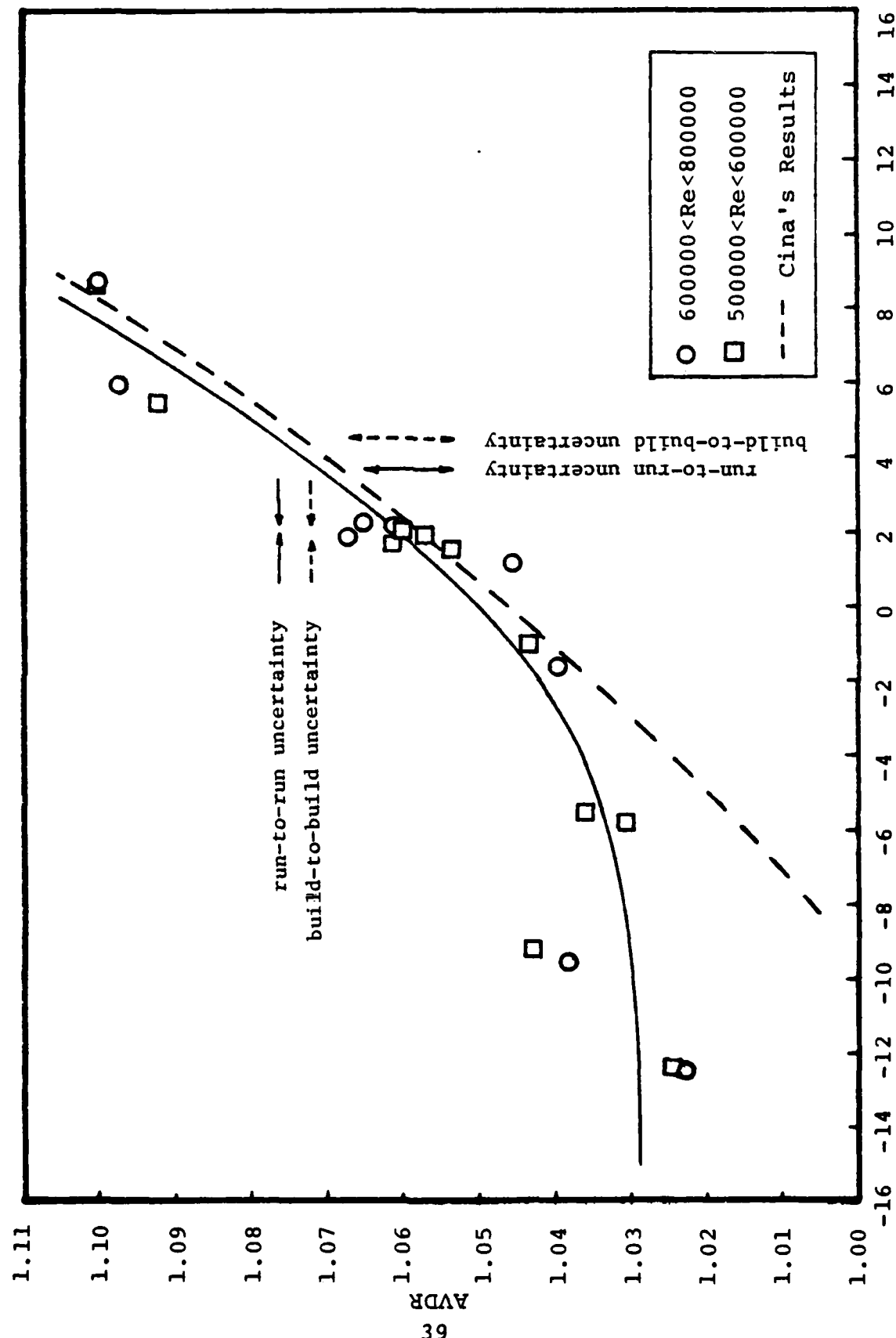


Fig. 8. AVDR versus Incidence Angle

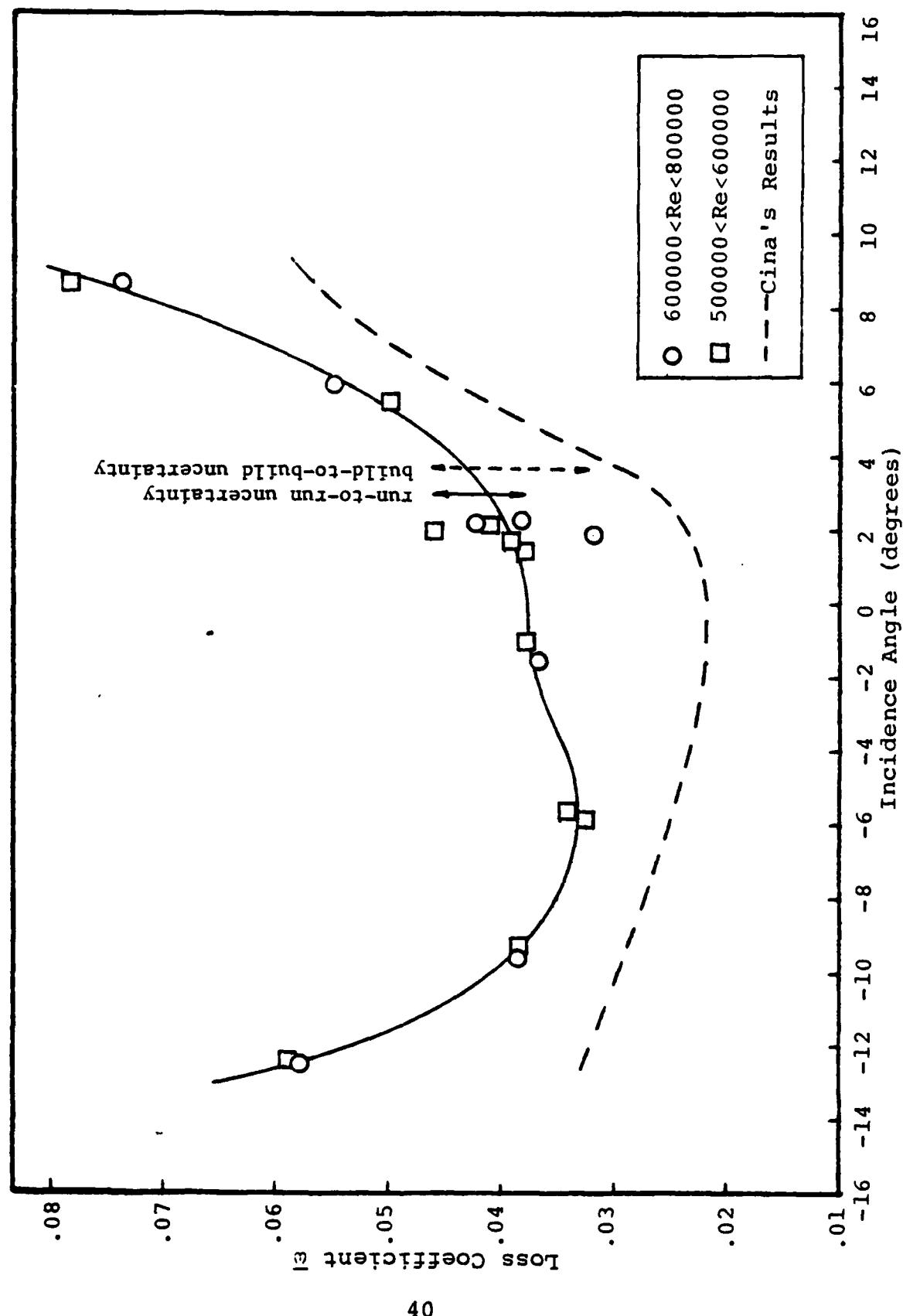


Fig. 9. Loss Coefficient versus Incidence Angle

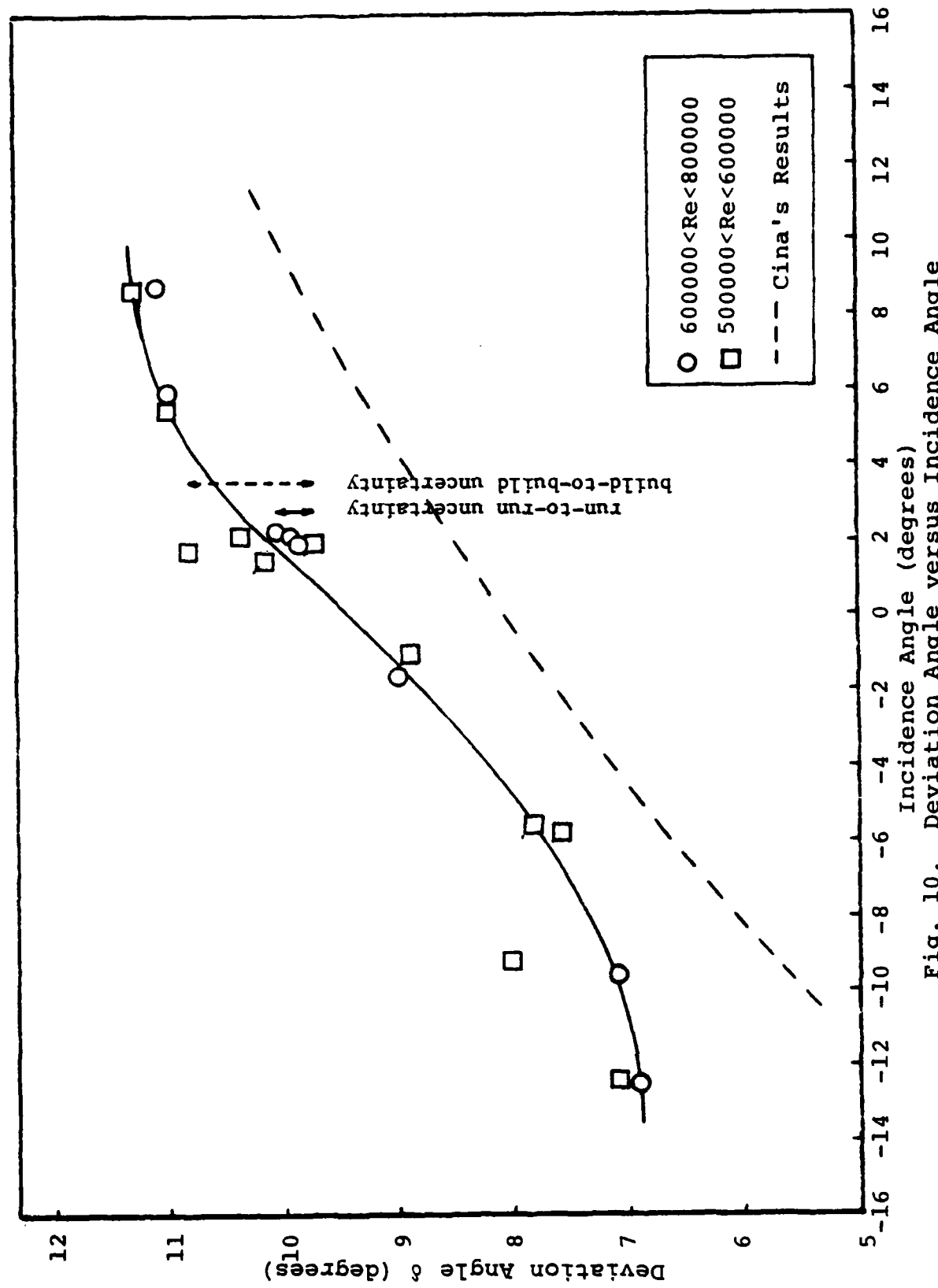


Fig. 10. Deviation Angle versus Incidence Angle

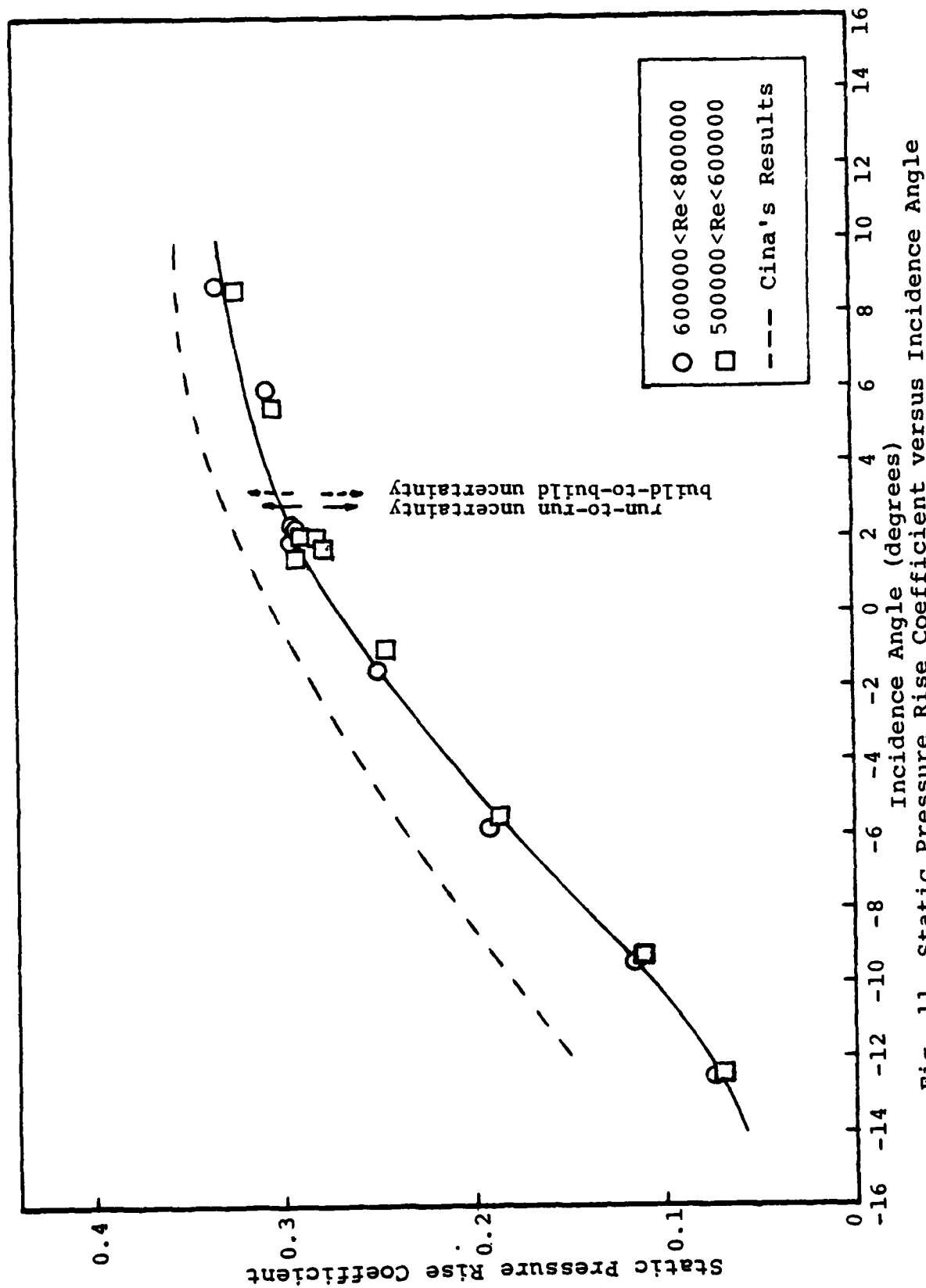


Fig. 11. Static Pressure Rise Coefficient versus Incidence Angle

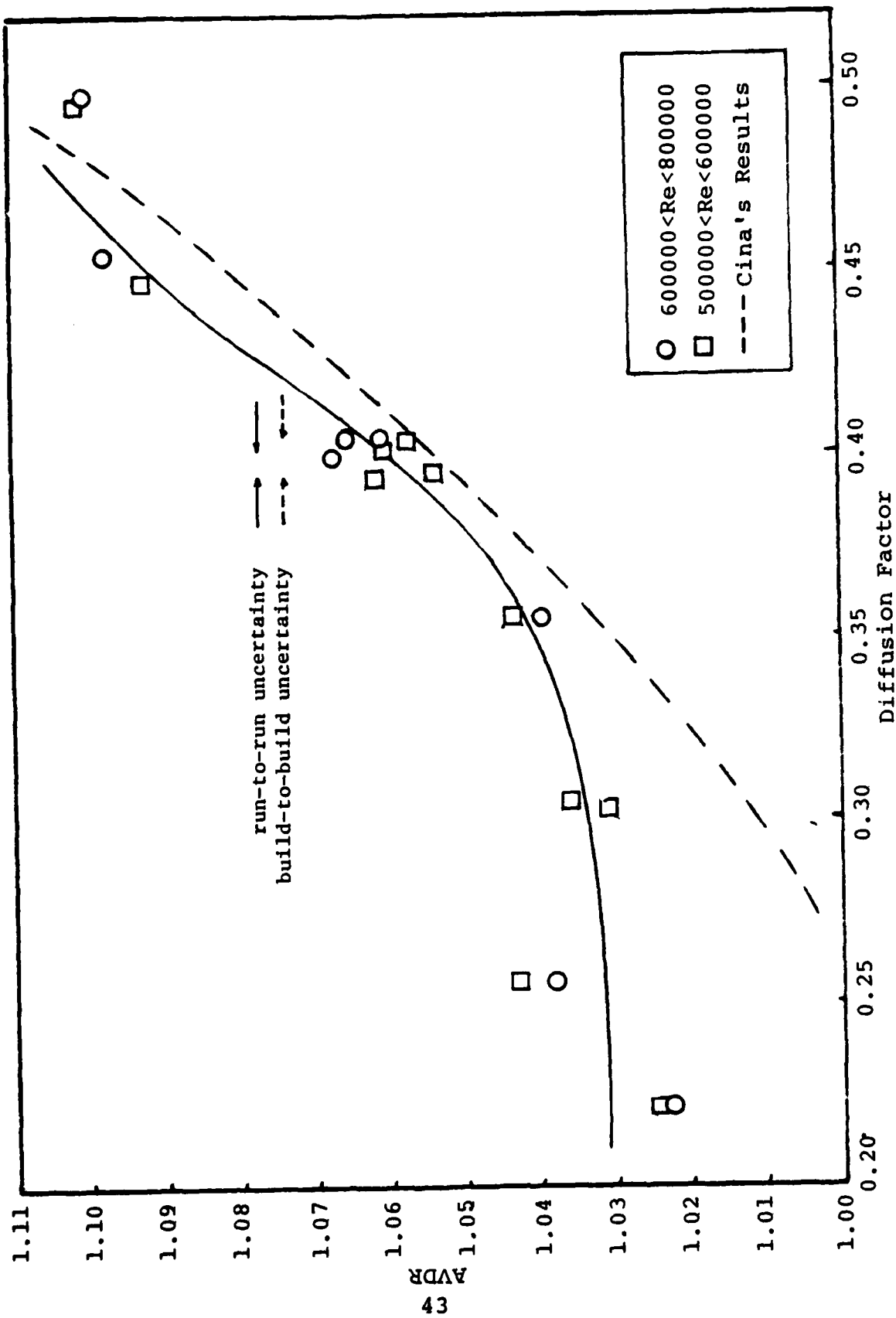


Fig. 12. AVDR versus Diffusion Factor

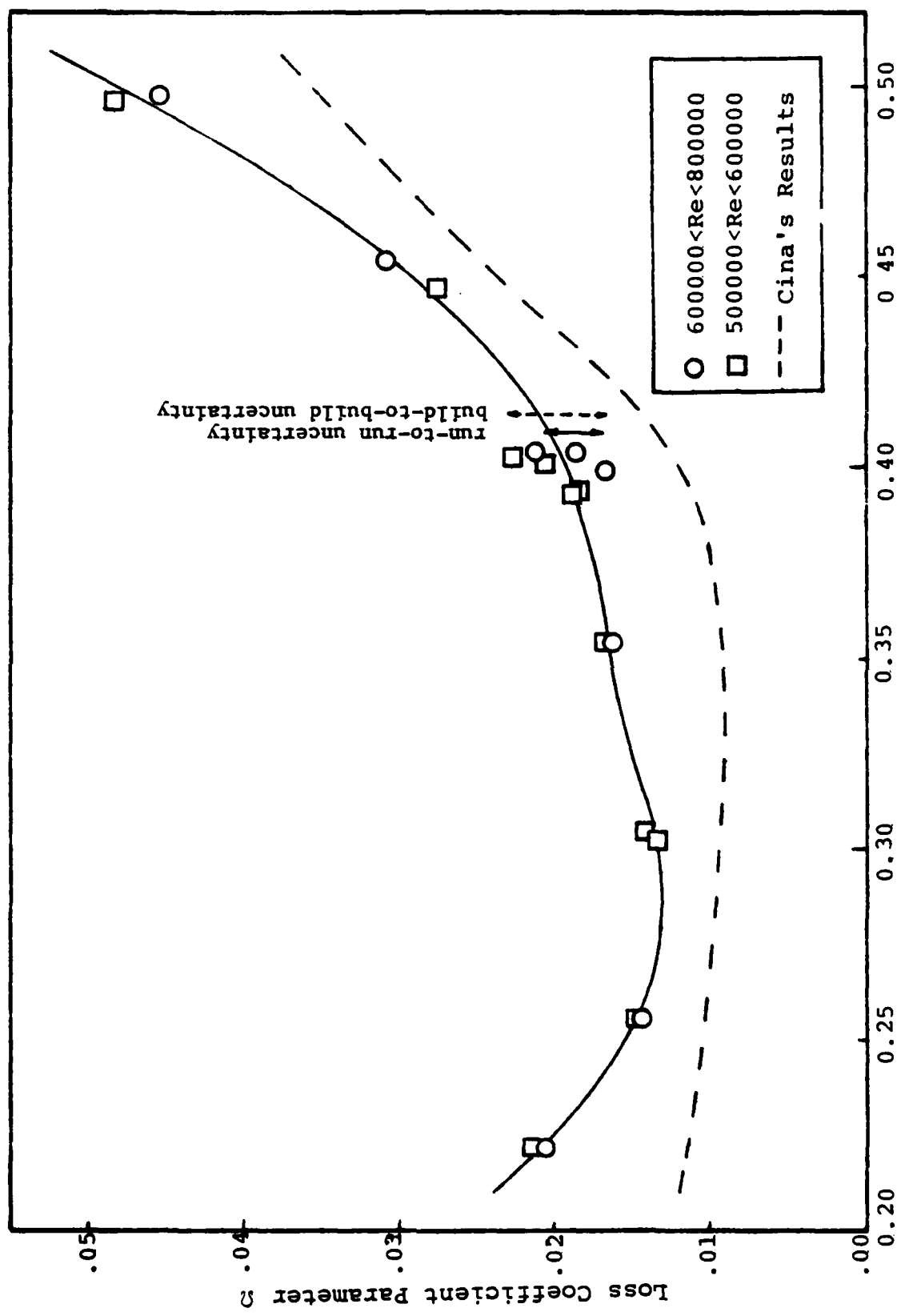


Fig. 13. Loss Coefficient Parameter versus Diffusion Factor

TABLE I. MEASUREMENT UNCERTAINTY

Item	Description	Method	Uncertainty
x	Blade-to-blade displacement x = 0 in. West end x = 60 in. East end	Position potentiometer	± .01 in.
z	Spanwise displacement z = 0 in. North wall z = 10 in. South wall	Position potentiometer on probe mount	± .01 in.
$\beta_1$	Inlet flow yaw angle	Angle potentiometer on probe mount (hand adjustment)	± .2 deg.
$\beta_2$	Outlet flow yaw angle	Angle potentiometer on probe mount (motor driven adjustment)	± .5 deg.
$P_{plen}$	Plenum total pressure	Tube in plenum chamber $V = 0$	± .01 in. $H_2O$ gauge
$P_s$	Static pressure at the test plane	Calibrated pneumatic probe	± .1 in. $H_2O$ gauge
$P_{w1}$	Static pressure at x = 0 in., y = -16.25 in., z = 0 in.	Static tap on North wall	± .01 in. $H_2O$ gauge
$P_{ATM}$	Atmospheric pressure	Mercury barometer	
P	Pressure	Scanivalve transducer	± .01 in. $H_2O$ gauge

TABLE II. CASCADE PERFORMANCE FORMULAS

Parameter	General Expression	Programmed Expression
Loss Coefficient $\frac{1}{\omega}$	(Note 1) $(\bar{C}_{Pt_1} - \bar{C}_{Pt_2}) / (\bar{C}_{Pt_1} - \bar{C}_{Pt_2})$	$\frac{\int_0^S C_{Pt_1} k_1 dx - \frac{1}{AVDR} \int_0^S C_{Pt_1} k_2 dx}{\int_0^S C_{Pt_1} k_1 dx - \int_0^S C_{Pt_1} k_1 dx}$ (Note 2)
Diffusion Factor D	$1 - \frac{W_2 + \Delta W_u}{W_1}$	$1 - \frac{\cos \bar{\beta}_1 + \cos \bar{\beta}_1 (\tan \bar{\beta}_1 - AVDR (\tan \bar{\beta}_2))}{\cos \bar{\beta}_2}$
Axial Velocity Density Ratio AVDR	$h_1/h_2$	$\frac{\int_0^S \left(\frac{Pt_2}{Pt_{ref}}\right) \left(\frac{X_2}{X_{ref}}\right)^{\frac{Y-2}{2}} \cos \beta_2 dx}{\int_0^S \left(\frac{Pt_1}{Pt_{ref}}\right) \left(\frac{X_1}{X_{ref}}\right)^{\frac{Y-2}{2}} \cos \beta_1 dx}$ (Note 2)
Static Pressure Rise Coefficient $C_{P static}$	$\frac{\bar{P}_2 - \bar{P}_1}{\bar{P}_{t1} - \bar{P}_1}$	$\frac{\frac{1}{AVDR} \int_0^S C_{P2} k_2 dx - \int_0^S C_{P1} k_1 dx}{\int_0^S C_{P_{t1}} k_1 dx - \int_0^S C_{P1} k_1 dx}$

TABLE II. (continued)

<b>Loss Coefficient Parameter</b>	$\bar{\Omega} \cos^3 \beta_2$ $\frac{1}{2\bar{\Omega}\cos^2 \beta_1}$
<b>Incidence Angle</b>	$\beta_1 - \gamma - \phi/2$ $\bar{\beta}_1 - \gamma - \phi/2$
<b>Deviation Angle</b>	$\phi/2 - \gamma + \beta_2$ $\phi/2 - \gamma + \bar{\beta}_2$

Note 1: "Barred" quantities are average values computed over a selected integration interval--usually one blade space.

Note 2: Derivation of programmed expression is given in Reference 1.

TABLE III. CASCADE CONFIGURATION PARAMETERS

Constants

Blade type	DCA
Number of blades	20
Spacing (inches)	3.0
Solidity	1.67
Thickness (% chord)	7.0
Camber angle (degrees)	45.72
Stagger angle (degrees)	14.27

TABLE IV. TEST BLADE COORDINATES

X-COORD.	Y-PRESS.	Y-SUCT.
-0.044	0.000	0.000
-0.021	-----	0.039
0.013	-0.042	-----
0.178	0.007	0.142
0.400	0.067	0.244
0.622	0.120	0.333
0.844	0.164	0.413
1.067	0.207	0.480
1.289	0.242	0.538
1.511	0.271	0.584
1.733	0.293	0.620
1.956	0.309	0.649
2.178	0.320	0.664
2.399	0.324	0.673
2.622	0.324	0.671
2.844	0.318	0.660
3.066	0.304	0.640
3.288	0.284	0.607
3.511	0.260	0.567
3.732	0.229	0.515
3.955	0.191	0.453
4.177	0.147	0.380
4.400	0.098	0.298
4.621	0.040	0.200
4.844	-0.022	0.091
4.908	-0.042	-----
4.943	-----	0.040
4.966	0.000	0.000

TABLE V. VARIABLE TEST PARAMETERS

Test Number	$\beta_1^{\circ}$	i <sup>o</sup>	Reynolds Number
1	39.02	1.89	773,000
2	38.68	1.55	511,000
3*	38.34	1.21	701,000
4	38.89	1.76	491,000
5	42.66	5.54	518,000
6	43.13	5.99	771,000
7	45.92	8.79	768,000
8	45.89	8.76	493,000
9	31.32	-5.81	560,000
10	31.56	-5.57	503,000
11	27.90	-9.23	502,000
12	27.55	-9.58	626,000
13	39.28	2.15	545,000
14	39.40	2.27	676,000
15	39.16	2.03	527,000
16	39.36	2.23	604,000
17	35.50	-1.59	643,000
18	35.60	-1.50	525,000
19	24.74	-12.39	535,000
20	24.63	-12.50	611,000

\*Note: Data from run number 3 not plotted because data set was judged to be too coarse.

TABLE VI. FLOW UNIFORMITY SUMMARY

( $\frac{\Delta Q}{Q}$ ) shows the maximum positive and negative deviation of the tabulated uniformity parameter with respect to its average value computed over the distance indicated.

Inlet plane: mid 20% of span

$i(^{\circ})$	$\frac{\Delta Q}{Q}(z)$	$\frac{\Delta(P_{s-Pt})}{\bar{Q}}(z)$	$\frac{\Delta(P_{plen-Pt})}{\bar{Q}}(z)$	$\frac{\Delta X}{X}(z)$	$\frac{\Delta \beta}{\beta}(^{\circ})$
-12.50	(1.6/-1.5)	(0.2/-0.1)	(1.4/-1.6)	(0.8/-0.6)	(.05/-0.05)
-12.39	(1.3/-1.1)	(0.8/-0.1)	(0.8/-0.1)	(0.6/-0.4)	(0/0)
- 9.58	( 0/ 0)	( 0/-0.1)	(0.4/-0.5)	(0.2/-0.1)	( 0/ 0)
- 9.23	(0.3/-0.2)	(0.2/-0.1)	(0.1/-0.1)	( 0/ 0)	( 0/ 0)
- 5.81	(0.1/-0.1)	(0.3/-0.2)	(0.5/-0.4)	(0.3/-0.1)	( 0/ 0)
- 5.57	(0.2/-0.2)	(0.3/-0.3)	(0.5/-0.4)	(0.2/-0.1)	(.33/-0.17)
- 1.59	(0.5/-0.4)	(1.2/-0.6)	(0.2/-0.1)	(0.4/-0.7)	( 0/ 0)
- 1.50	(0.1/-0.2)	(0.1/-0.1)	(0.3/-0.3)	(0.1/-0.2)	(.17/-0.09)
2.27	(0.3/-0.3)	(1.6/-0.9)	(0.4/-0.4)	(0.5/-0.9)	(.08/-0.6)
2.23	(0.3/-0.4)	(0.5/-0.3)	(0.3/-0.3)	(0.3/-0.4)	( 0/ 0)
5.99	(0.2/-0.1)	(0.1/-0.1)	(0.1/-0.1)	(0.1/ 0)	(.05/-0.09)
5.54	(0.2/-0.3)	(2.8/-1.4)	(0.4/-0.2)	(0.7/-1.2)	( 0/ 0)
8.79	(0.1/-0.1)	(0.1/-0.1)	(0.1/-0.1)	(0.11/ 0)	( 0/ 0)
8.76	(0.5/-0.4)	(0.2/-0.1)	(0.2/-0.2)	(0.1/-0.1)	( 0/ 0)

TABLE VI. (Continued)

( $\frac{1}{Q}$ ) shows the maximum positive and negative deviation of the tabulated uniformity parameter with respect to its average value computed over the distance indicated.

Outlet plane: mid 20% of span					
$i(^{\circ})$	$\frac{\Delta Q}{Q}(z)$	$\frac{\Delta(P_{s-Pw})}{Q}(\%)$	$\frac{\Delta(P_{plen-Pt})}{Q}(\%)$	$\frac{\Delta X}{X}(z)$	$\frac{\Delta \beta}{\beta}(^{\circ})$
-12.50	(1.1/-0.7)	(0/ 0)	(0.9/-0.8)	(0.4/-0.4)	(.09/-0.06)
-12.39	(0.5/-0.4)	(0.2/-0.1)	(0.2/-0.1)	(0.5/-0.4)	(.02/-0.06)
- 9.58	(0.1/-0.1)	(0.3/-0.2)	(0.2/-0.2)	( 0/ 0)	( 0/ 0)
- 9.23	(0.4/-0.2)	(0.1/-0.1)	(0.3/-0.3)	(0.1/-0.2)	( 0/ 0)
- 5.81	(0.2/-0.2)	( 0/ 0)	(0.3/-0.3)	(0.1/-0.1)	(.05/-0.09)
- 5.57	(0.6/-0.5)	(0.3/-0.3)	(2.0/-1.3)	(0.4/-0.7)	(.10/-0.20)
- 1.59	(0.7/-0.9)	(1.3/-0.8)	(0.1/-0.1)	(0.4/-0.5)	( 0/ 0)
- 1.50	(0.1/-0.2)	(0.2/-0.3)	(0.1/-0.1)	(0.1/ 0)	( 0/ 0)
2.27	(0.2/-0.3)	(0.1/-0.1)	(0.2/-0.2)	( 0/ 0)	(.03/-0.07)
2.25	( 0/ 0)	(0.4/-0.3)	(0.1/-0.2)	(0.1/-0.2)	( 0/ 0)
5.99	(0.5/-0.5)	(4.1/-2.1)	(0.5/-0.4)	(0.7/-1.0)	( 0/ 0)
5.54	(0.7/-1.2)	(0.4/-0.6)	(1.4/-0.9)	(0.3/-0.5)	( 0/ 0)
8.79	(0.4/-0.4)	(0.2/-0.1)	(0.1/-0.2)	( 0/ 0)	(.04/-0.02)
8.76	(4.2/-6.2)	(5.3/-3.0)	(7.0/-4.8)	(2.7/-4.5)	(.08/-0.17)

TABLE VI. (Continued)

( $\frac{\Delta Q}{\bar{Q}}$ ) shows the maximum positive and negative deviation of the tabulated uniformity parameter with respect to its average value computed over the distance indicated.

Inlet plane: -3 to 0 blade-to-blade direction

$\theta(^{\circ})$	$\frac{\Delta Q}{\bar{Q}}(z)$	$\frac{\Delta(P_{sl}-P_{wl})}{\bar{Q}}(\%)$	$\frac{\Delta(P_{plen}-P_t)}{\bar{Q}}(\%)$	$\frac{\Delta X}{X}(z)$	$\frac{\Delta B}{B}(^{\circ})$
-12.50	(1.3/-1.7) (2.6/-2.2)	(4.4/-0.5) (0.4/-0.3)	(2.2/-1.4) (2.3/-2.1)	(0.8/-1.1) (1.1/-0.8)	(.32/-0.30) (.23/-0.28)
-12.39					
- 9.58	(1.9/-1.9) (1.5/-2.2)	(0.5/-0.6) (0.6/-0.4)	(2.3/-2.8) (2.8/-1.6)	(1.4/-1.0) (0.8/-1.3)	(0/ 0) (.15/-0.34)
- 9.23					
- 5.81	(1.6/-2.1) (2.4/-3.0)	(0.7/-0.5) (0.4/-0.5)	(1.3/-1.2) (3.1/-2.5)	(0.5/-0.6) (1.2/-1.5)	(.43/-0.31) (.27/-0.25)
- 5.57					
- 1.59	(2.7/-5.2) (2.1/-1.3)	(1.4/-0.8) (0.4/-0.4)	(2.1/-1.7) (0.8/-1.0)	(0.9/-1.3) (0.6/-0.6)	(.27/-0.32) (.27/-0.19)
- 1.50					
2.27	(1.1/-1.2) (1.2/-1.0)	(2.2/-0.8) (0.6/-0.6)	(1.0/-0.8) (0.7/-0.6)	(0.7/-1.2) (0.5/-0.7)	(.26/-0.30) (.30/-0.20)
2.23					
5.99	(2.1/-1.4)	(0.2/-0.1)	(1.2/-1.9)	(0.9/-0.5)	(.28/-0.22)
5.54	(2.2/-2.3)	(0.5/-0.2)	(1.3/-1.5)	(0.6/-0.6)	(.31/-0.20)
8.79	(0.4/-0.6)	(0.4/-0.5)	(0.5/-0.4)	(0.3/-0.2)	(.20/-0.17)
8.76	(0.8/-1.0)	(4.3/-1.6)	(0.9/-1.1)	(0.5/-2.3)	(0/ 0)

TABLE VII. FLOW PERIODICITY AND PSEUDO TWO-DIMENSIONALITY SUMMARY\*

Incidence angle (degrees)	Periodicity based on blade static pressures	Pseudo Two-Dimensionality based on blade force coefficient diagrams Δmagnitude(%) Δdirection( $^{\circ}$ )
-12.50	imperfect	- 2.1      10.0 $^{\circ}$
-12.39	imperfect	13.0      25.0 $^{\circ}$
- 9.58	acceptable	- 1.5      3.0 $^{\circ}$
- 9.23	good	41.3      27.0 $^{\circ}$
- 5.81	good	-19.1      7.5 $^{\circ}$
- 5.57	good	-20.0      3.5 $^{\circ}$
- 1.59	good	-25.2      24.5 $^{\circ}$
- 1.50	good	16.5      22.5 $^{\circ}$
2.27	good	- 4.6      2.5 $^{\circ}$
2.23	good	- 2.4      2.0 $^{\circ}$
5.99	good	- 0.7      7.0 $^{\circ}$
5.54	good	- 6.1      4.0 $^{\circ}$
8.79	good	- 3.4      1.5 $^{\circ}$
8.76	good	-16.2      -5.0 $^{\circ}$

\*Note: Data from six additional runs at design incidence angle are not presented.

TABLE VIII. CASCADE PERFORMANCE SUMMARY

$\beta_1$	1	$\beta_2$	$\delta$	D	$\omega$	$\frac{\omega \cos^3 \beta_2}{20 \cos^2 \beta_1}$	$\frac{\omega \cos \beta_2}{20}$	AVDR	$C_p$ static	$Cx_M$	$Cy_M$	$Cx_B$	$Cy_B$	Re
24.63	-12.50	-1.68	6.9	0.222	.0574	0.02077	0.0172	.0752	-0.7734	-.3176	-.8347	-.1825	611,000	
24.74	-12.39	-1.50	7.1	0.222	.0592	0.02147	0.0177	.0716	-0.7699	-.6142	-.8486	-.1988	535,000	
27.55	-9.58	-1.51	7.1	0.256	.0378	0.01438	0.0113	.1.0383	.1155	-0.8851	-.2214	-.8963	-2334	626,000
27.90	-9.23	-0.59	8.0	0.256	.0374	0.01433	0.0112	.1.0432	.1129	-0.8420	-.7120	-.7609	-1730	502,000
31.32	-5.81	-0.94	7.6	0.303	.0328	0.01345	0.0098	.1.0309	.1931	-1.0101	-.4745	-.1.2751	-.5261	560,000
31.56	-5.57	-0.83	7.8	0.305	.0346	0.01426	0.0103	.1.0360	.1874	-1.0003	-.4076	-.1.0997	-.3762	503,000
35.50	-1.59	0.37	9.0	0.355	.0363	0.01640	0.0109	.1.0396	.2517	-1.1210	-.1.0897	-.1.1788	-.4119	643,000
35.60	-1.50	0.36	8.9	0.356	.0370	0.01675	0.0111	.1.0432	.2454	-1.1060	-.9981	-.1.2037	-.4329	525,000
39.02	1.89	1.16	9.8	0.400	.0320	0.01586	0.0096	.1.0672	.2875	-1.1967	-.3833	-.1.2794	-.4741	773,000
38.34	1.21	2.48	11.1	0.386	.0478	0.02320	0.0143	.1.0455	.2823	-1.1510	-.2054	-.6540	-.2746	701,000
39.40	2.27	1.53	10.1	0.405	.0378	0.01893	0.0113	.1.0653	.2871	-1.1821	-.5270	-.1.2642	-.4930	676,000
39.36	2.23	1.32	9.9	0.405	.0425	0.02127	0.0127	.1.0612	.2863	-1.1873	-.5551	-.1.2478	-.4967	604,000
39.28	2.15	1.77	10.4	0.402	.0412	0.02056	0.0123	.1.0605	.2851	-1.1611	-.8821	-.1.2732	-.5267	545,000
39.16	2.03	1.12	9.7	0.404	.0461	0.02294	0.0138	.1.0573	.2814	-1.1743	-.4652	-.1.2732	-.5336	527,000
38.68	1.55	1.61	10.2	0.395	.0378	0.01855	0.0113	.1.0538	.2863	-1.1737	-.7848	-.1.3500	-.5603	511,000
38.89	1.76	2.24	10.8	0.394	.0385	0.01898	0.0115	.1.0618	.2786	-1.1352	-.2153	-.1.2751	-.5261	491,000
43.13	5.99	2.47	11.1	0.455	.0552	0.03094	0.0165	.1.0974	.3046	-1.2015	-.6695	-.1.2816	-.5266	771,000
42.66	5.54	2.45	11.0	0.448	.0498	0.02750	0.0149	.1.0923	.3025	-1.1786	-.6086	-.1.2946	-.5669	518,000
45.92	8.79	2.46	11.1	0.499	.0737	0.04547	0.0220	.1.0999	.3341	-1.2605	-.5957	-.1.3924	-.6218	768,000
45.89	8.76	2.75	11.3	0.497	.0785	0.04835	0.0235	.1.1024	.3231	-1.2459	-.4875	-.1.2977	-.6342	493,000

## APPENDIX A

### A. FLOW QUALITY DOCUMENTATION

#### 1. Uniformity

Uniformity of dynamic pressure ( $Q/\bar{Q}$ ), static pressure ( $\Delta Ps/\bar{Q}$ ), total pressure ( $\Delta Pt/\bar{Q}$ ), non dimensional velocity ( $X/\bar{X}$ ), and Beta for spanwise surveys at the inlet and outlet planes and blade-to-blade surveys at the inlet plane at each test condition are shown in Figs. A.1 through A.105. Photographs of upper and lower static pressure distributions for each incidence angle and Reynolds number comprise Figs. A.106 to A.119.

#### 2. Periodicity

Periodicity of ( $Q/\bar{Q}$ ), ( $\Delta Ps/\bar{Q}$ ), ( $\Delta Pt/\bar{Q}$ ), ( $X/\bar{X}$ ) and Beta for blade-to-blade surveys at the outlet plane and adjacent blade pressure distribution for each test condition are shown in Figs. A.120 through A.168.

#### 3. Pseudo Two-Dimensionality

Blade force coefficients for each test condition are plotted in Figs. A.169 to A.182.

#### 4. Notation

The parameters plotted in Figs. A.1 to A.105 and Figs. A.122 to A.154 are defined as follows:

Parameter	Meaning
$Q/\bar{Q}$	local value of $Q/\bar{Q}$ <sup>2</sup>
$\Delta P_s/\bar{Q}$	$(P_s - P_{wl})/\bar{Q}$
$\Delta P_t/\bar{Q}$	$(P_{plen} - P_t)/\bar{Q}$
$X/\bar{X}$	local value of $X/\bar{X}$

---

<sup>2</sup>"Barred" quantities apply to the specific measurement plane and are calculated over a prescribed integration interval--usually one blade space.

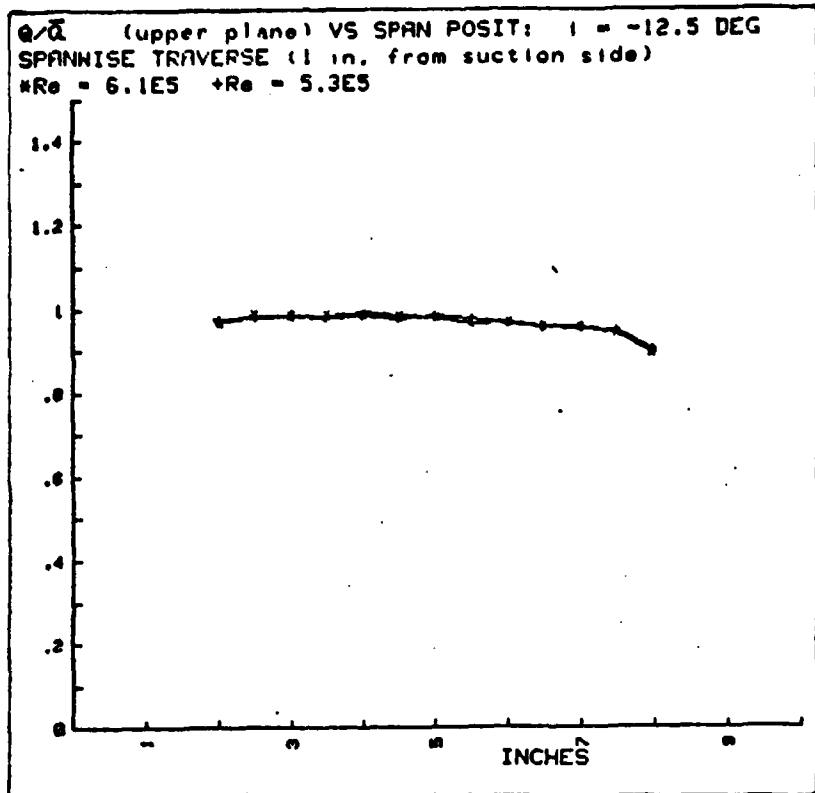


Fig. A.1

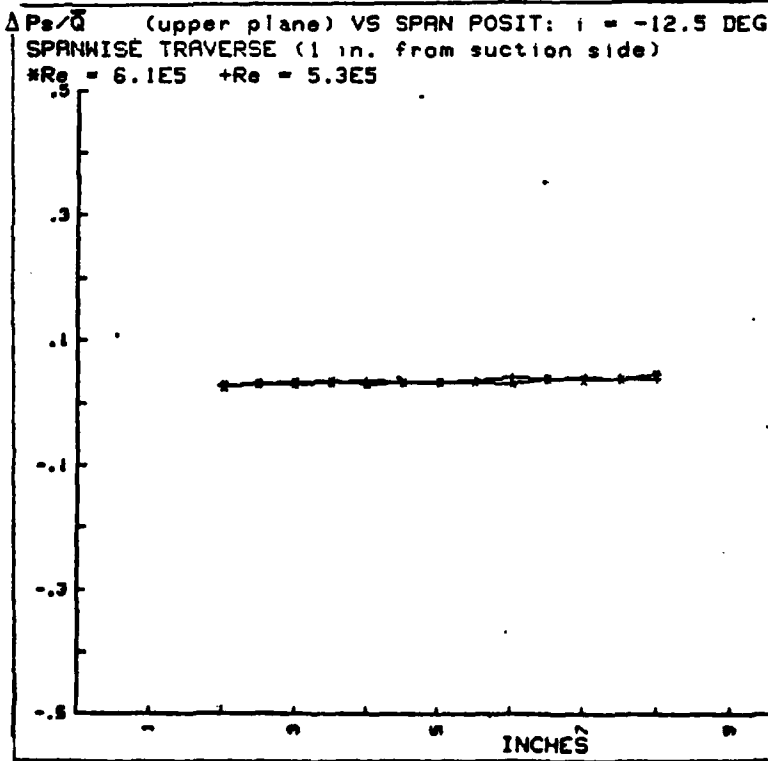


Fig. A.2

$\Delta Pt/\bar{Q}$  (upper plane) VS SPAN POSIT:  $i = -12.5$  DEG  
SPANWISE TRAVERSE (1 in. from suction side)  
 $*Re = 6.1E5 +Re = 5.3E5$

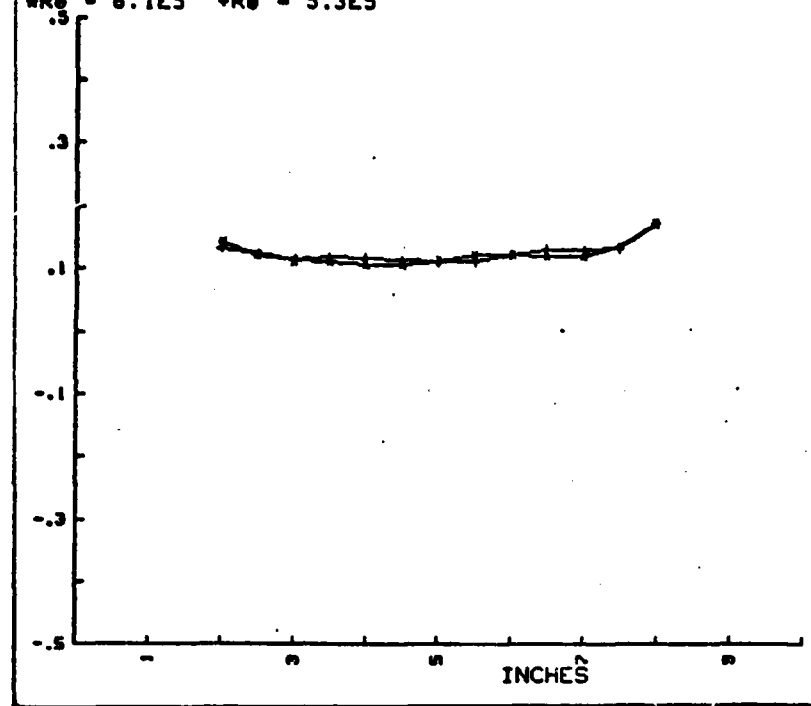


Fig. A.3

$X/\bar{X}$  (upper plane) VS SPAN POSIT:  $i = -12.5$  DEG  
SPANWISE TRAVERSE (1 in. from suction side)  
 $*Re = 6.1E5 +Re = 5.3E5$

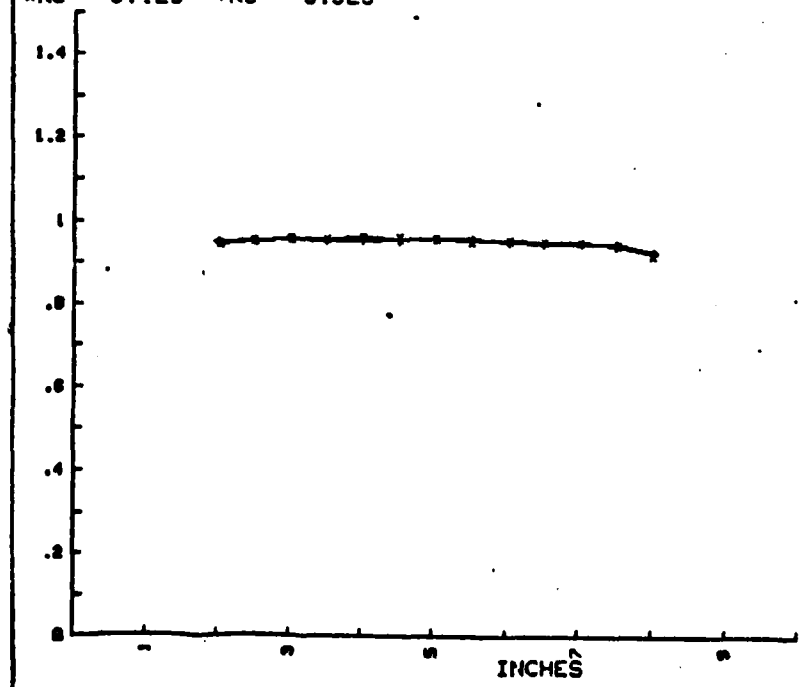


Fig. A.4

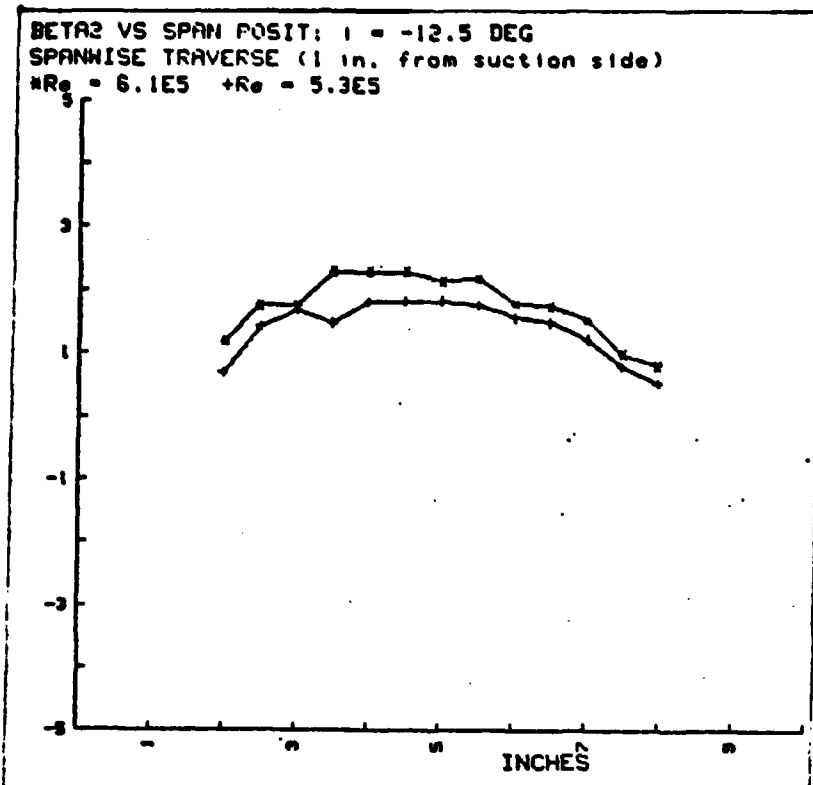


Fig. A.5

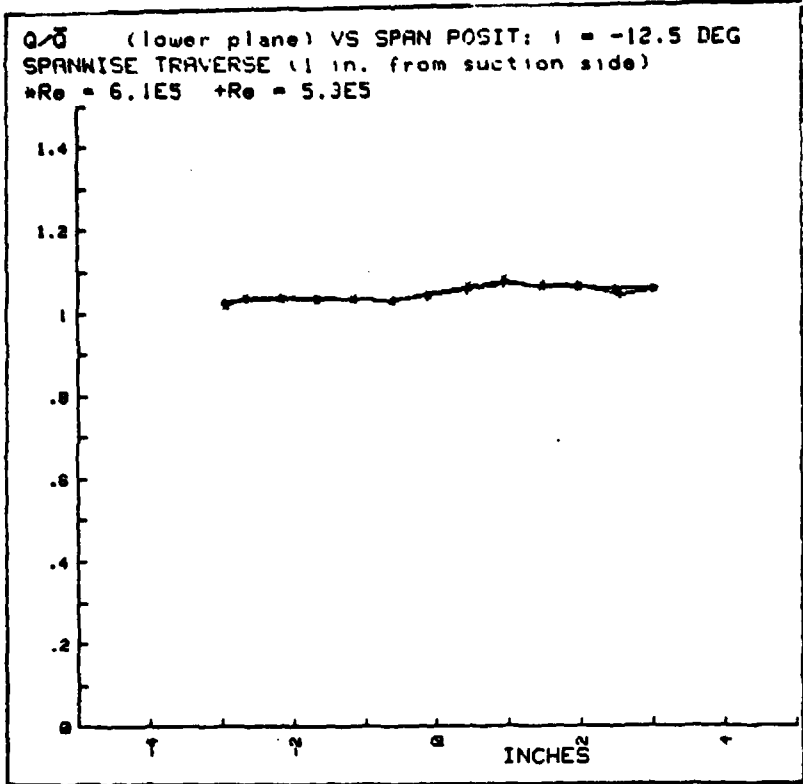


Fig. A.6

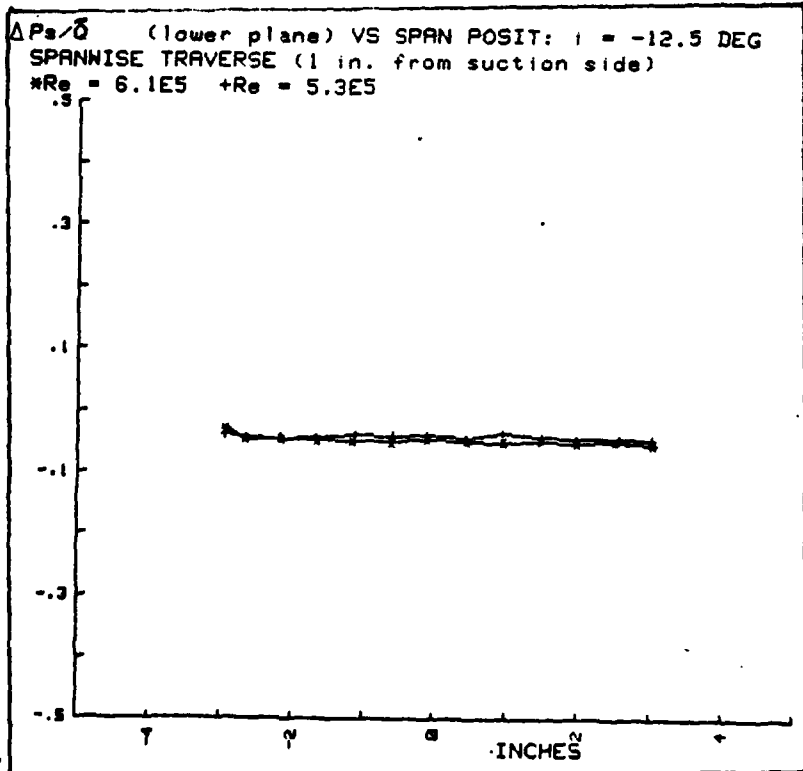


Fig. A.7

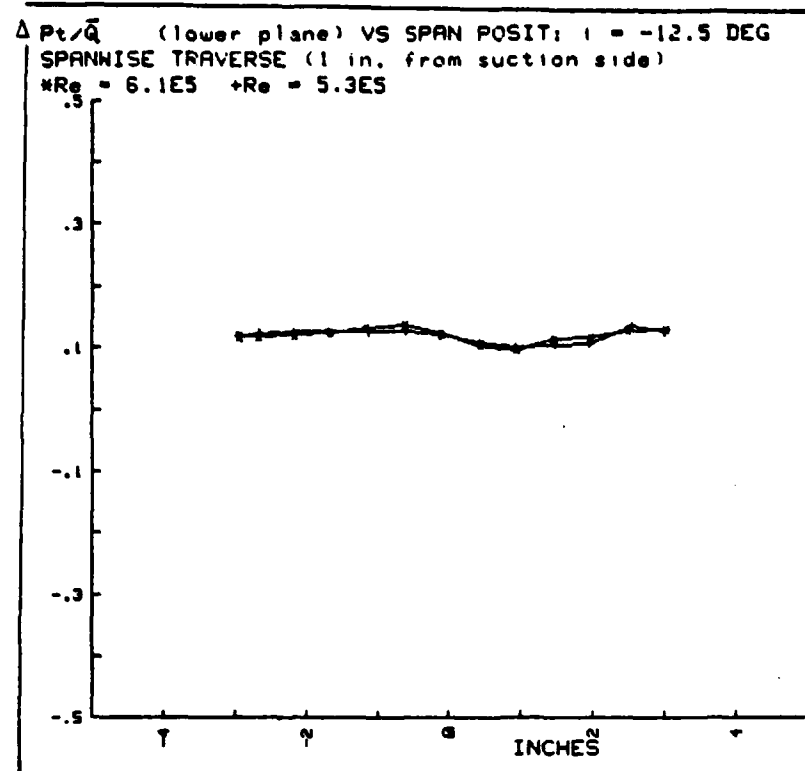


Fig. A.8

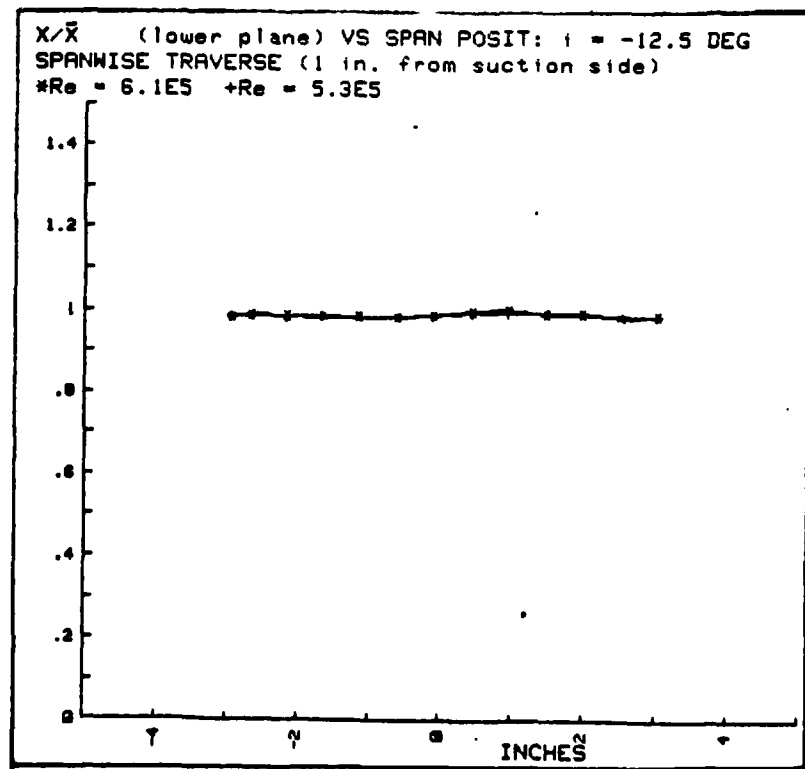


Fig. A.9

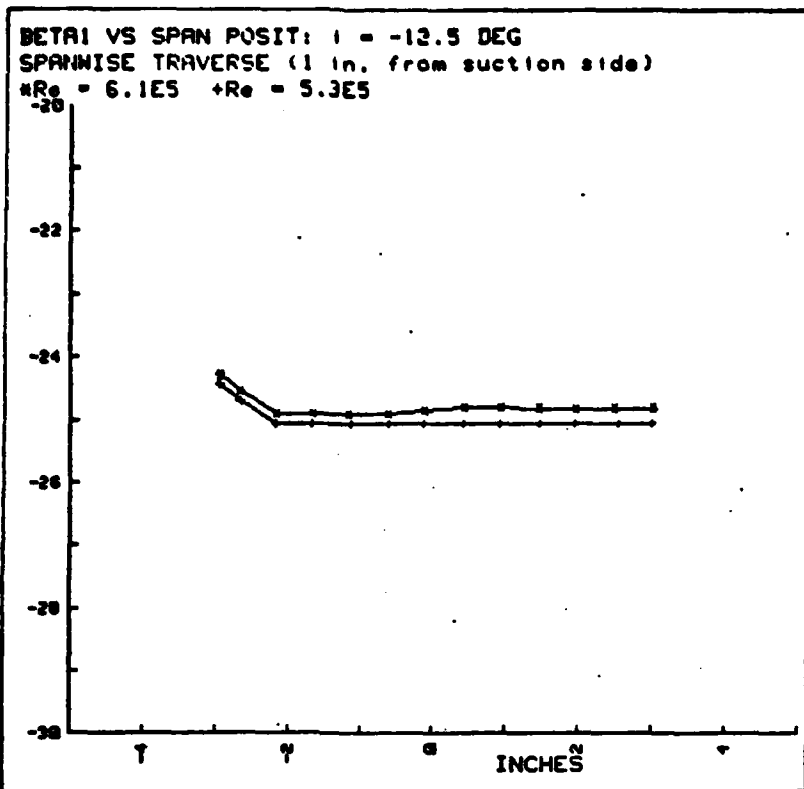


Fig. A.10

$Q/\bar{Q}$  (lower plane) VS BTOB POSIT:  $i = -12.5$  DEG  
BLADE TO BLADE TRAVERSE (midspan)  
 $*Re = 6.1E5 \quad +Re = 5.3E5$

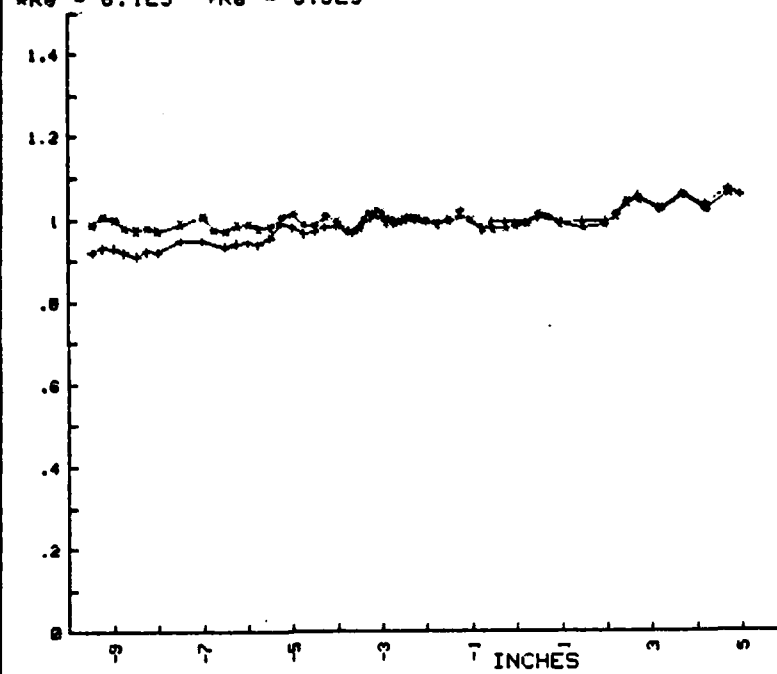


Fig. A.11

$\Delta P_s/\bar{Q}$  (lower plane) VS ETOB POSIT:  $i = -12.5$  DEG  
BLADE TO BLADE TRAVERSE (midspan)  
 $*Re = 6.1E5 \quad +Re = 5.3E5$

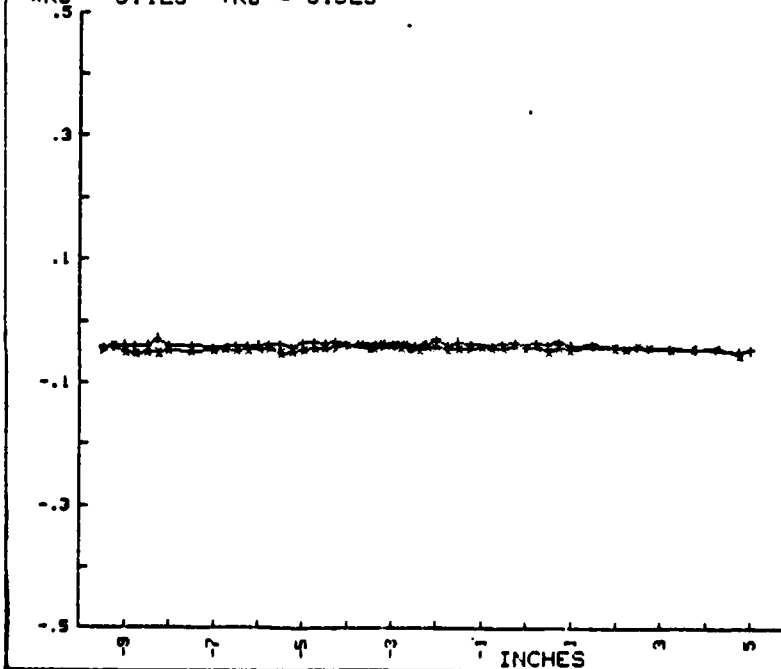


Fig. A.12

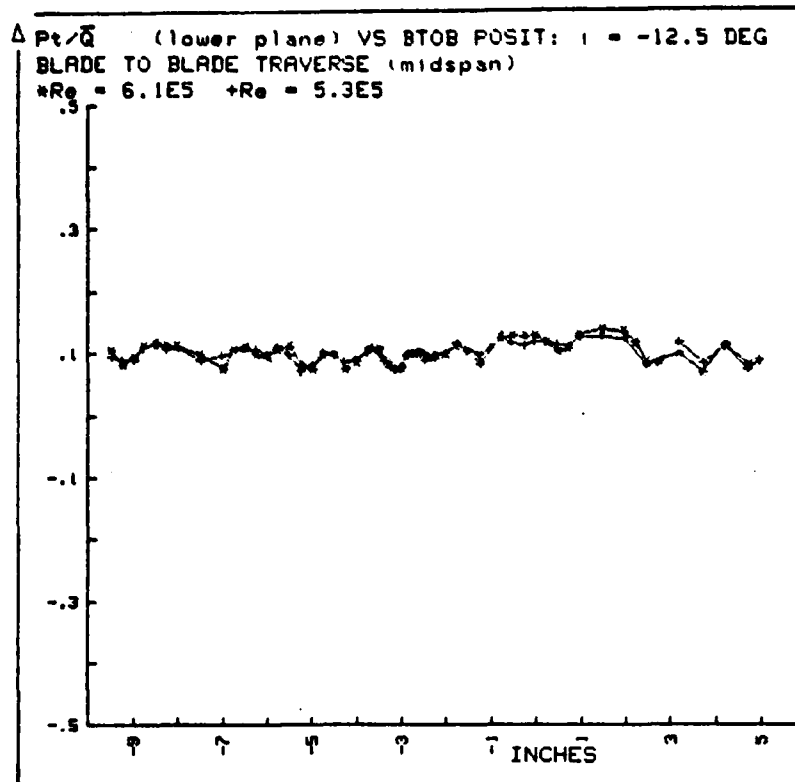


Fig. A.13

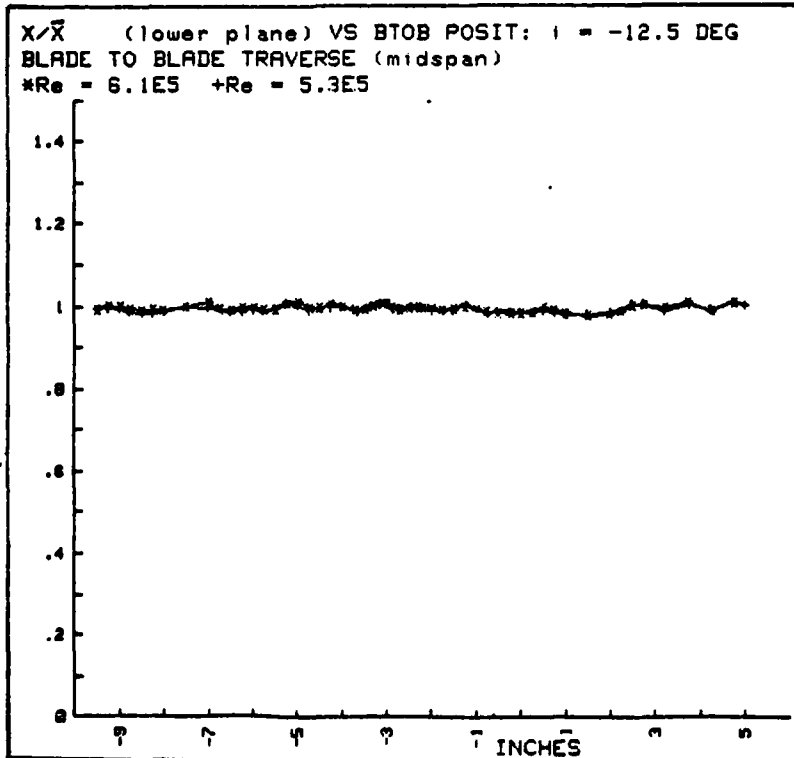


Fig. A.14

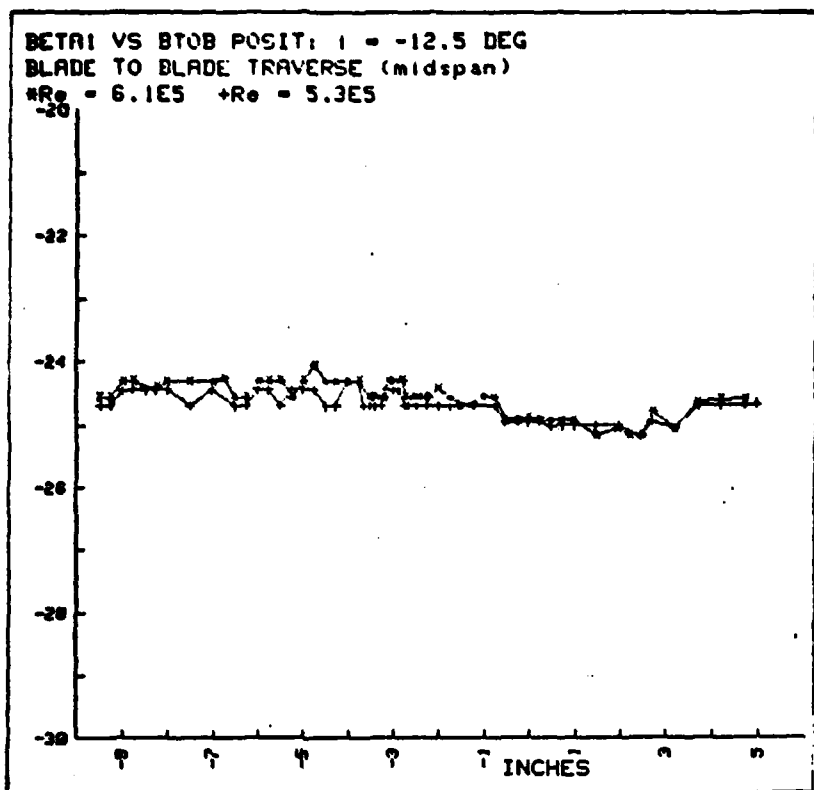


Fig. A.15

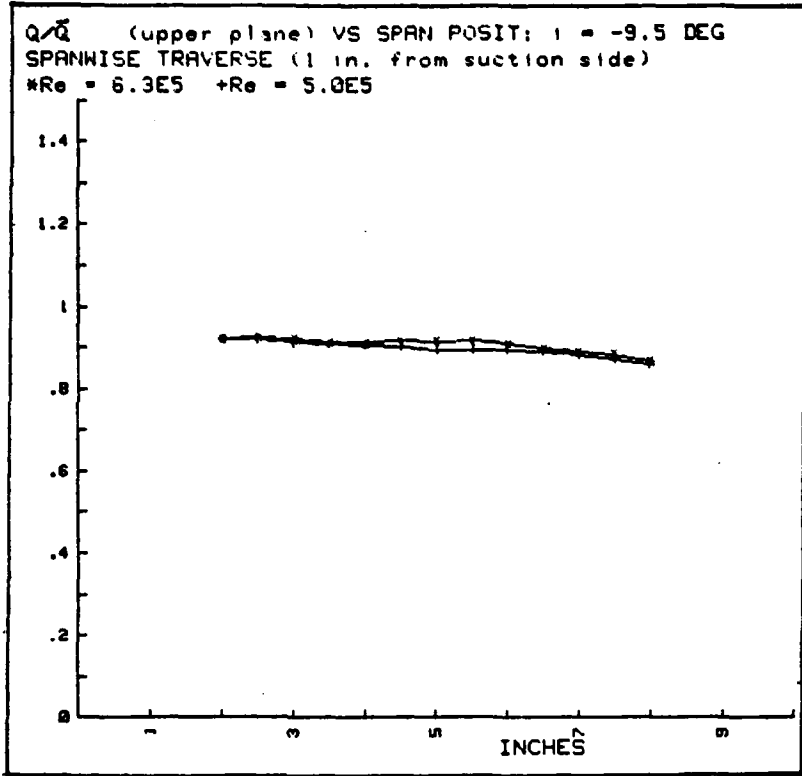


Fig. A.16

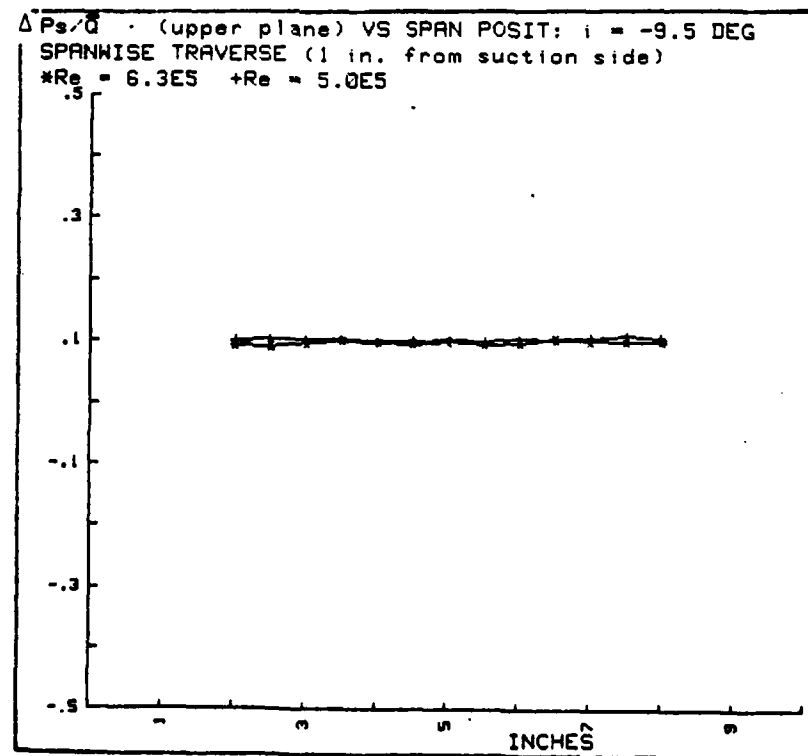


Fig. A.17

$\Delta P_t/\bar{Q}$  (upper plane) VS SPAN POSIT:  $i = -9.5$  DEG  
SPANWISE TRAVERSE (1 in. from suction side)  
 $*Re = 6.3E5 +Re = 5.0E5$

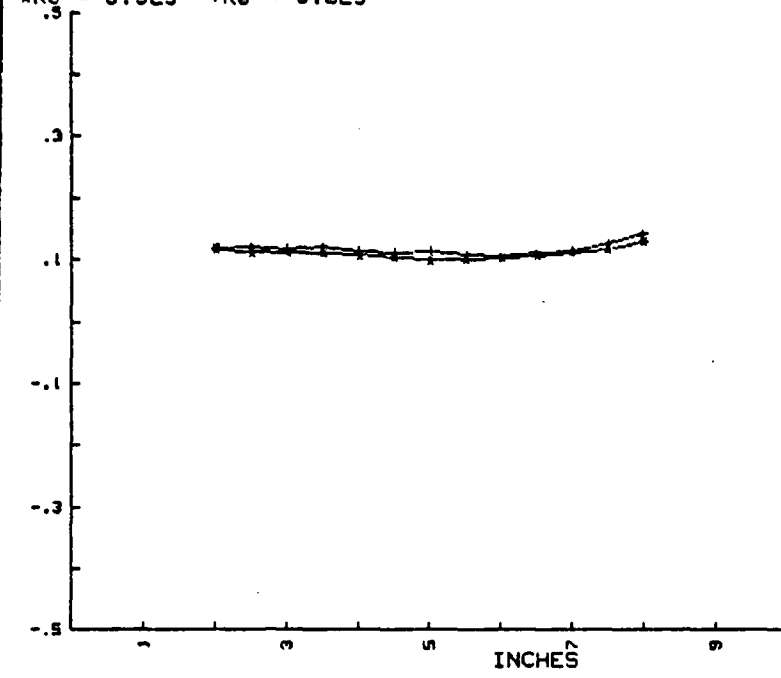


Fig. A.18

$X/\bar{X}$  (upper plane) VS SPAN POSIT:  $i = -9.5$  DEG  
SPANWISE TRAVERSE (1 in. from suction side)  
 $*Re = 6.3E5 +Re = 5.0E5$

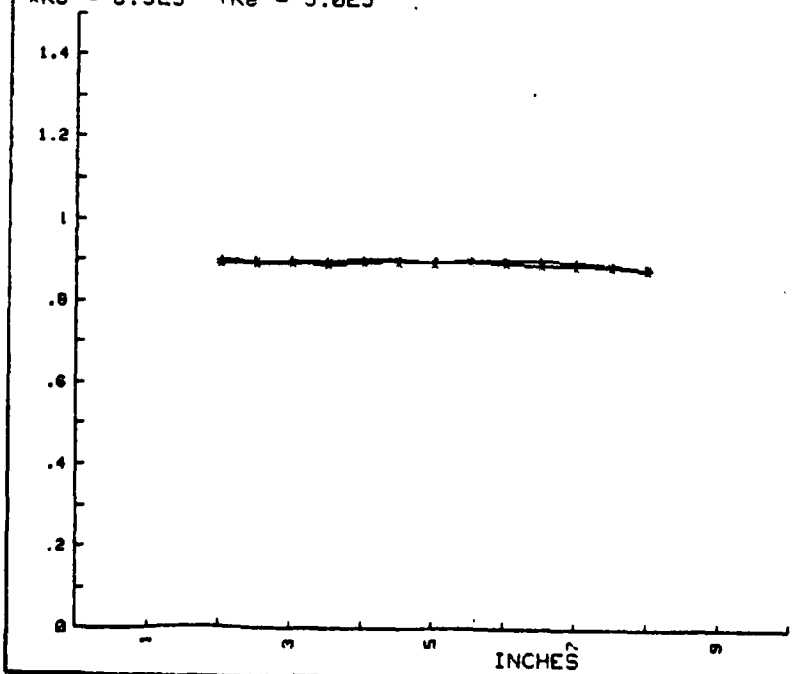


Fig. A.19

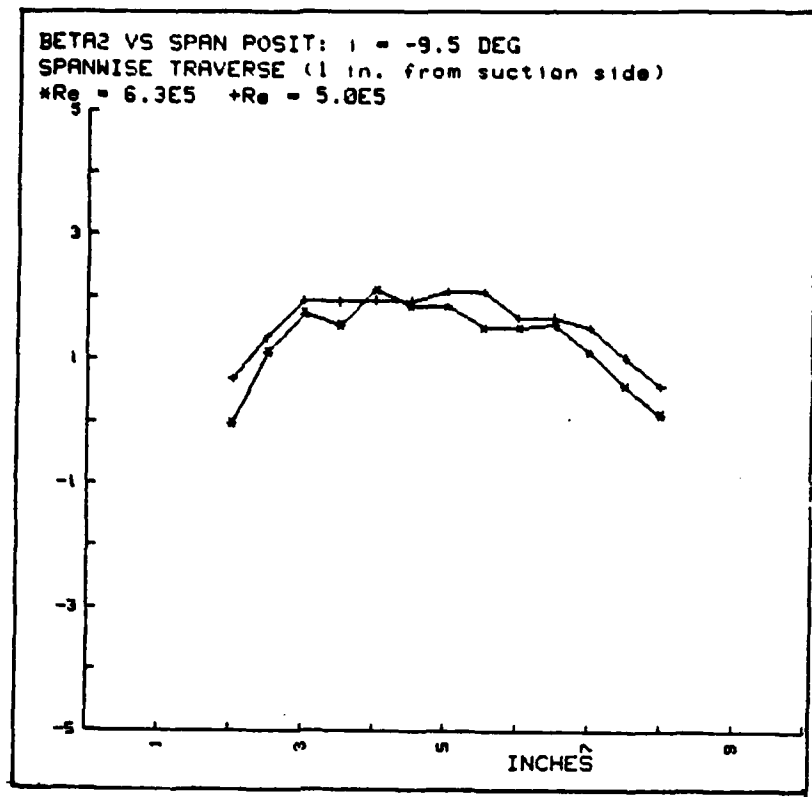


Fig. A.20

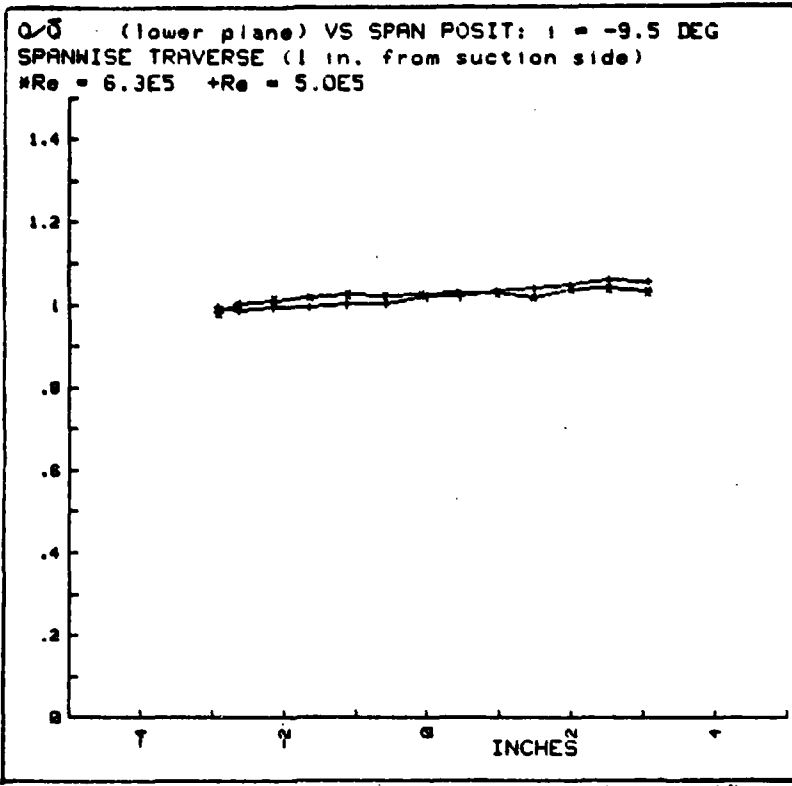


Fig. A.21

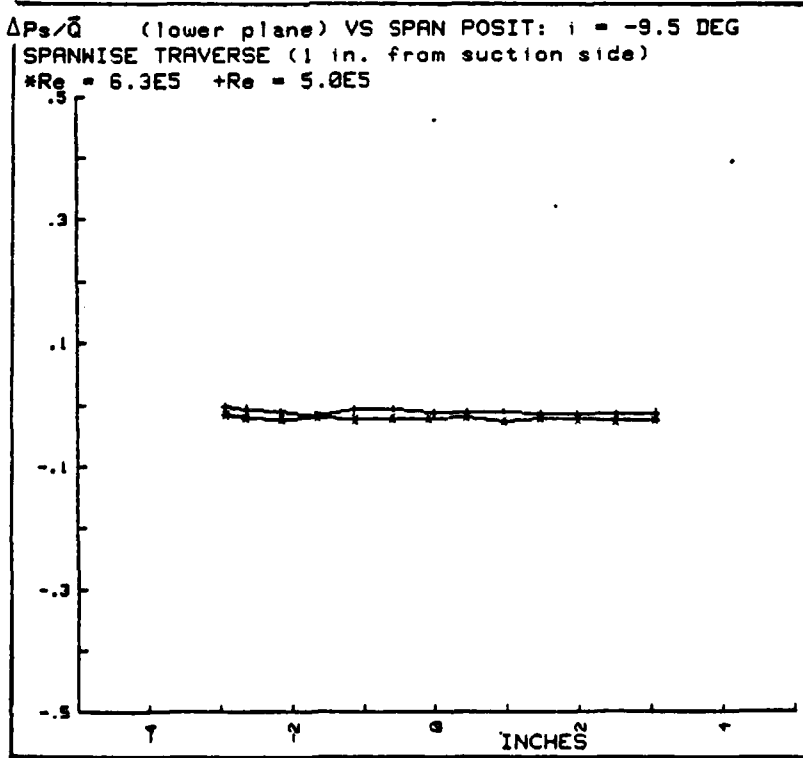


Fig. A.22

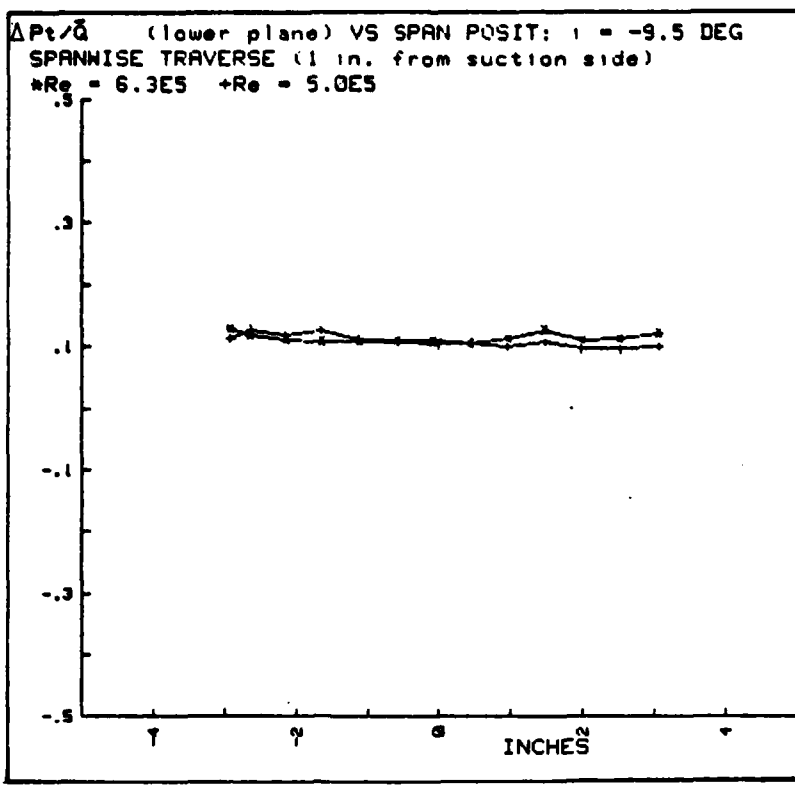


Fig. A.23

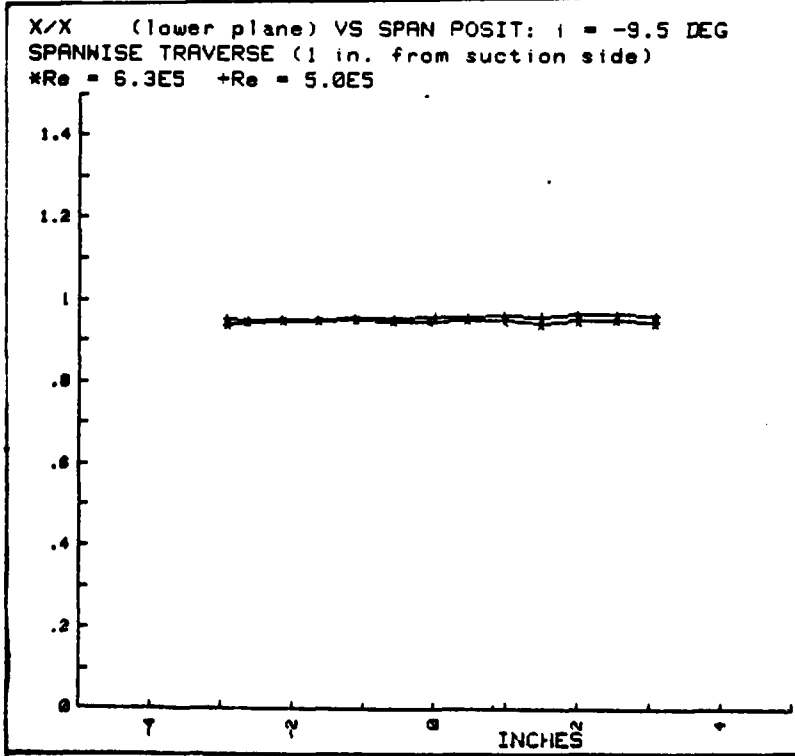


Fig. A.24

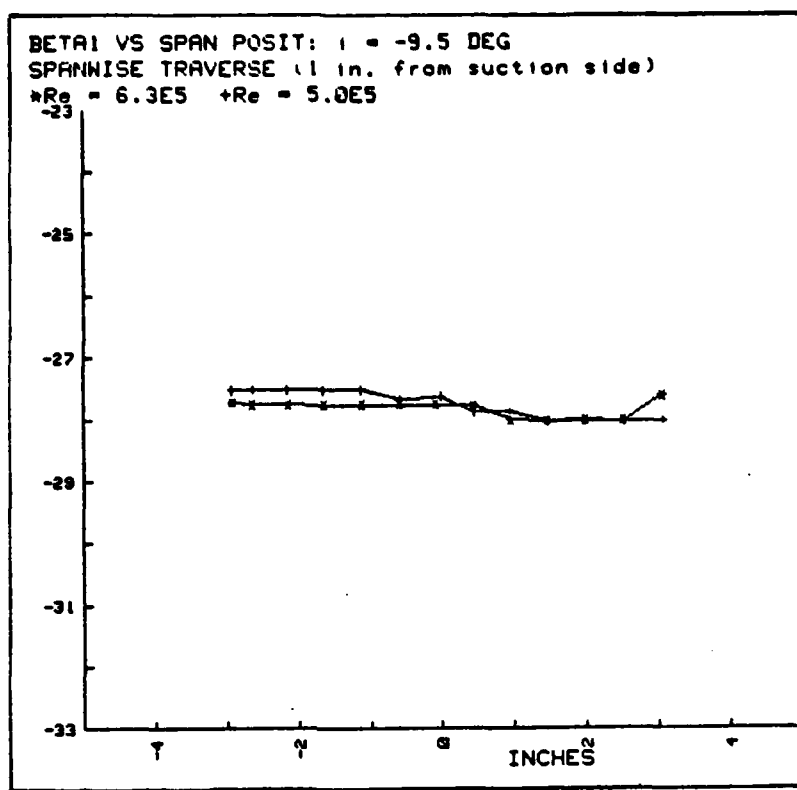


Fig. A.25

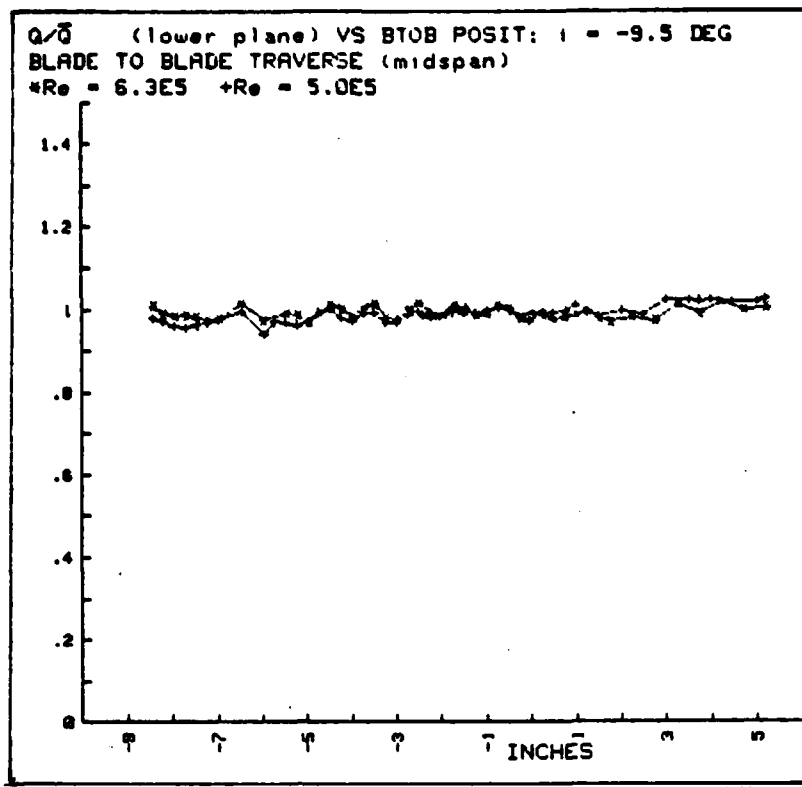


Fig. A.26

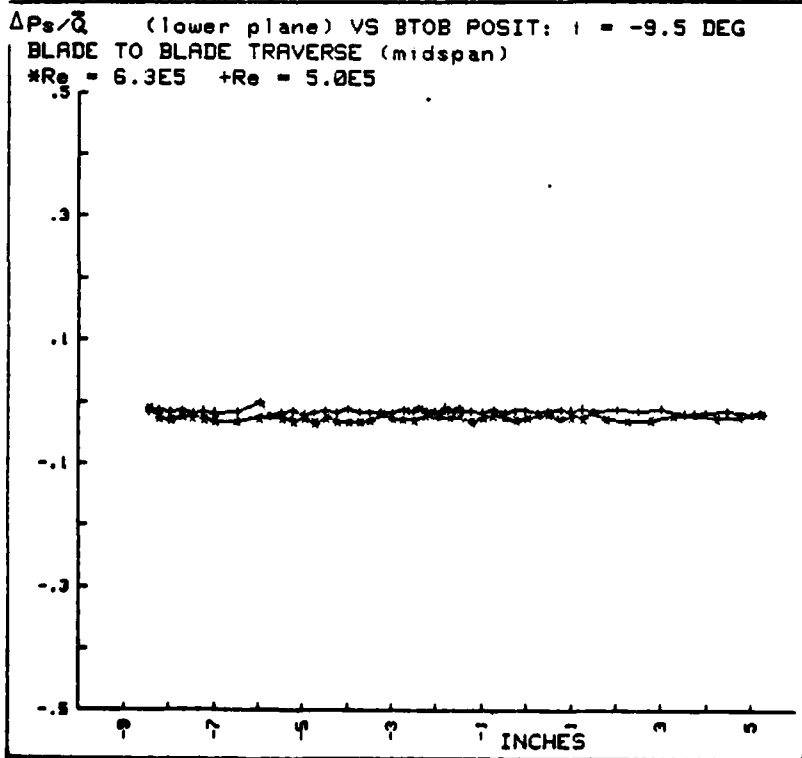


Fig. A.27

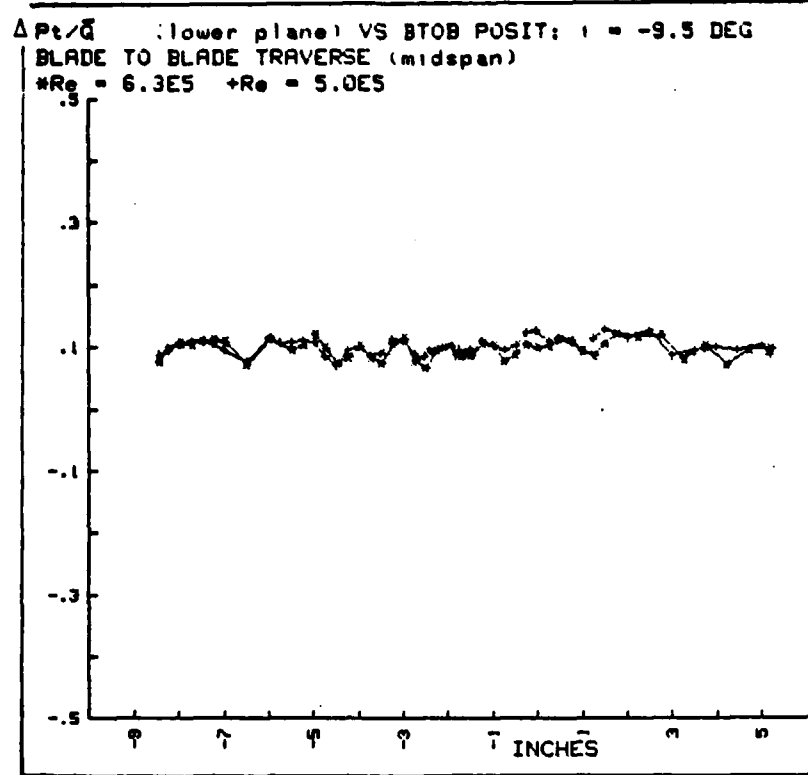


Fig. A.28

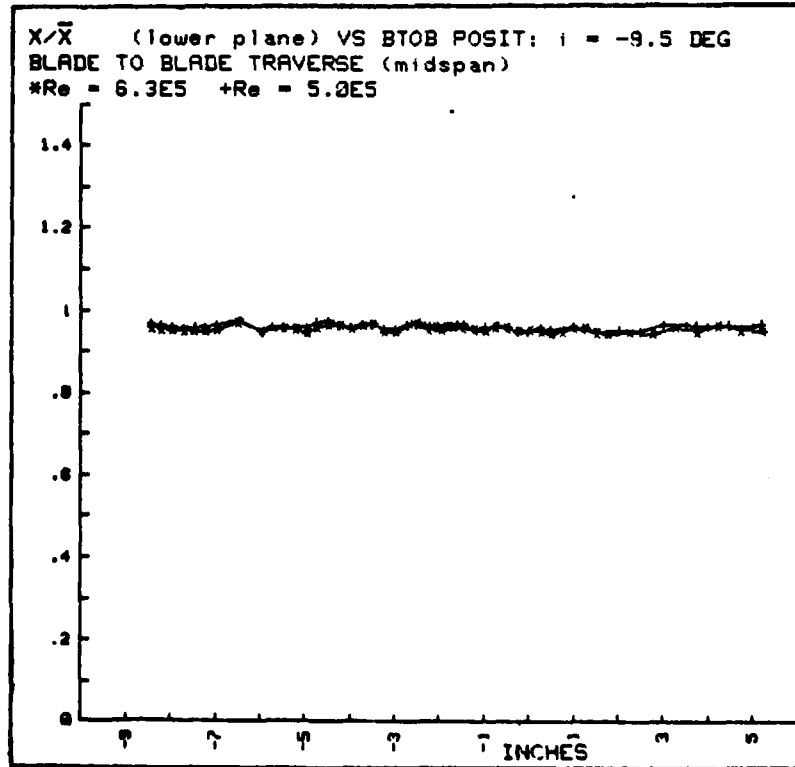


Fig. A.29

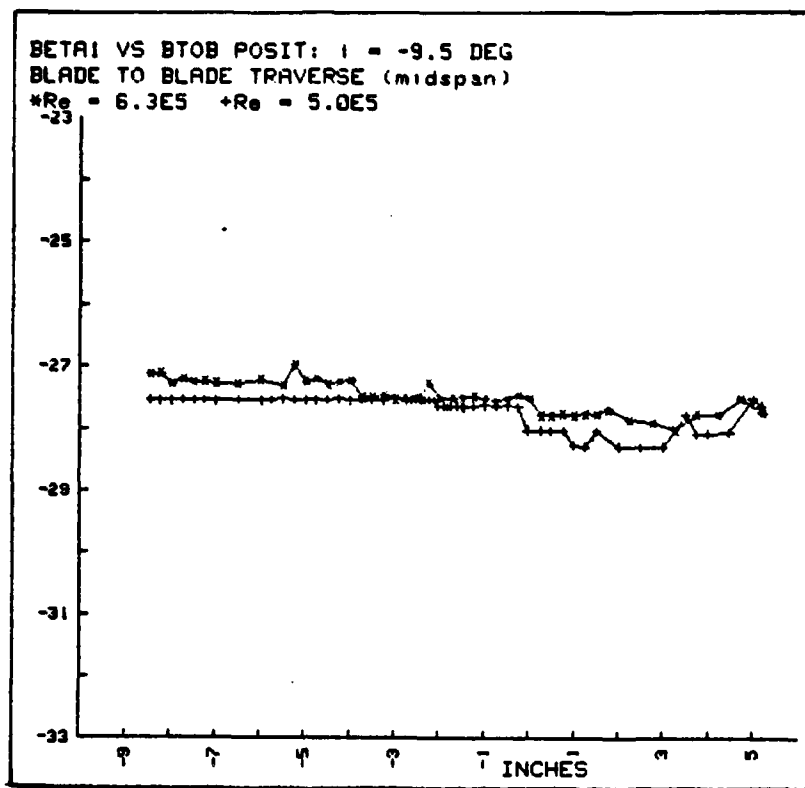


Fig. A.30

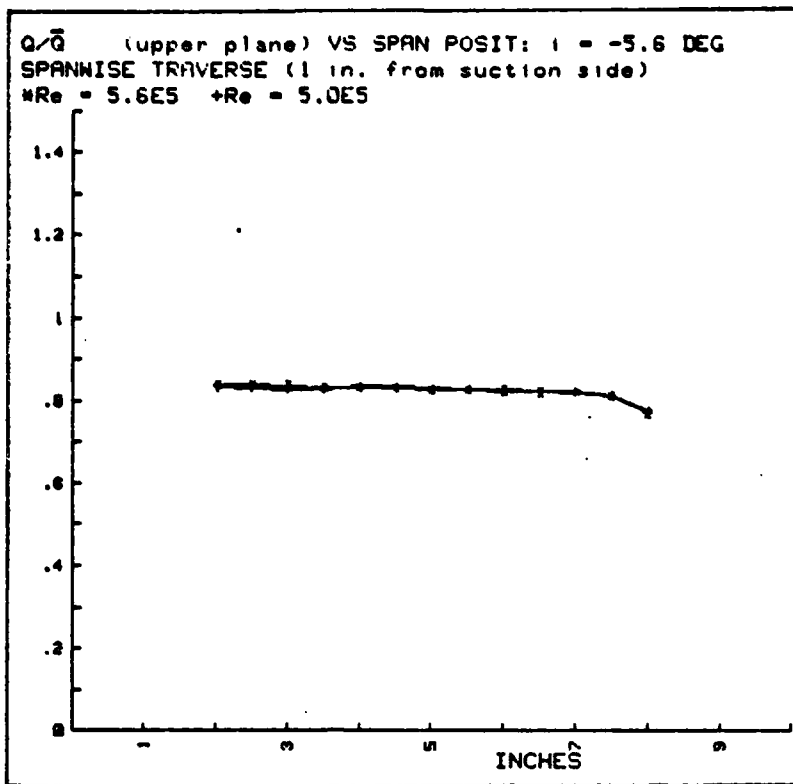


Fig. A.31

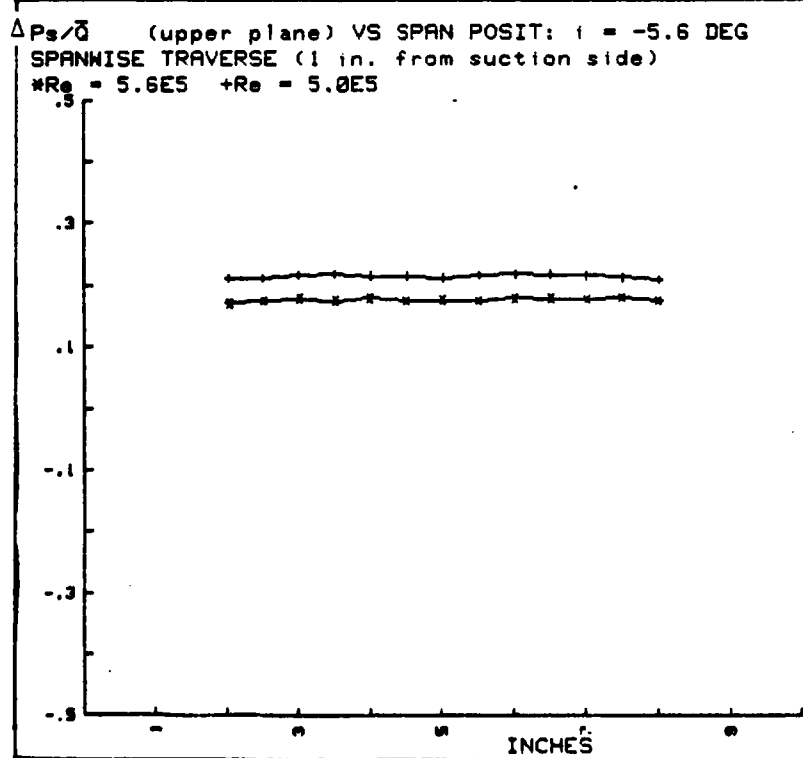


Fig. A.32

$\Delta P_t/Q$  (upper plane) VS SPAN POSIT:  $i = -5.6$  DEG  
SPANWISE TRAVERSE (1 in. from suction side)  
 $*Re = 5.6E5 +Re = 5.0E5$

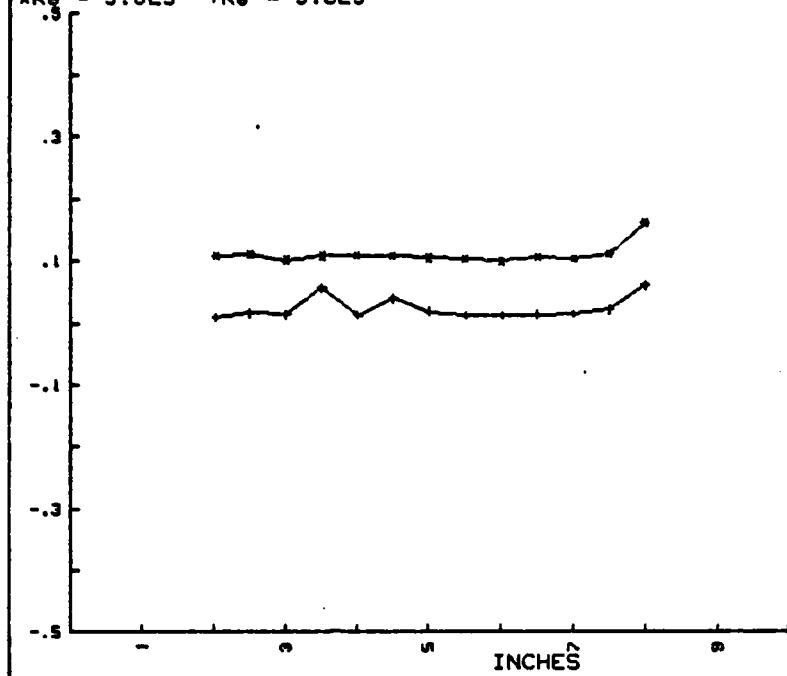


Fig. A.33

$X/\bar{X}$  (upper plane) VS SPAN POSIT:  $i = -5.6$  DEG  
SPANWISE TRAVERSE (1 in. from suction side)  
 $*Re = 5.6E5 +Re = 5.0E5$

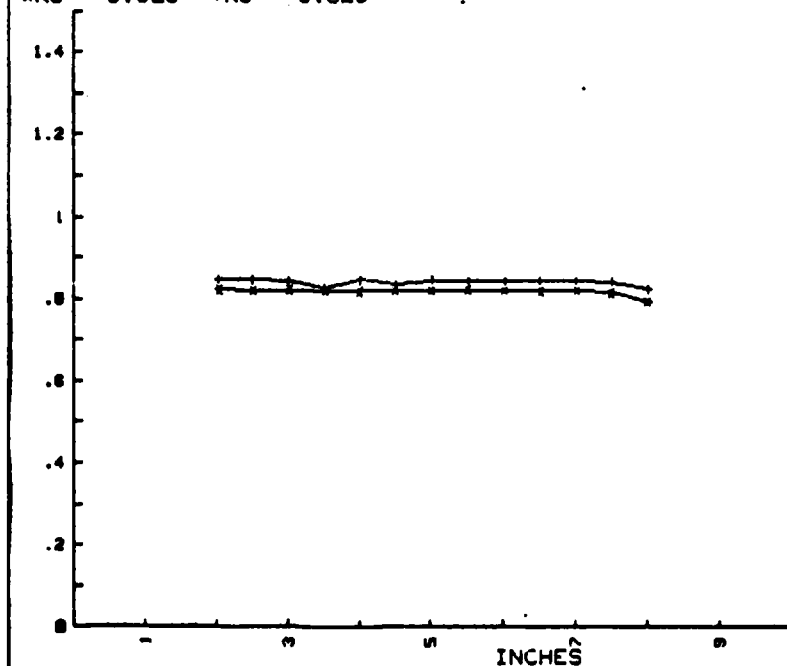


Fig. A.34

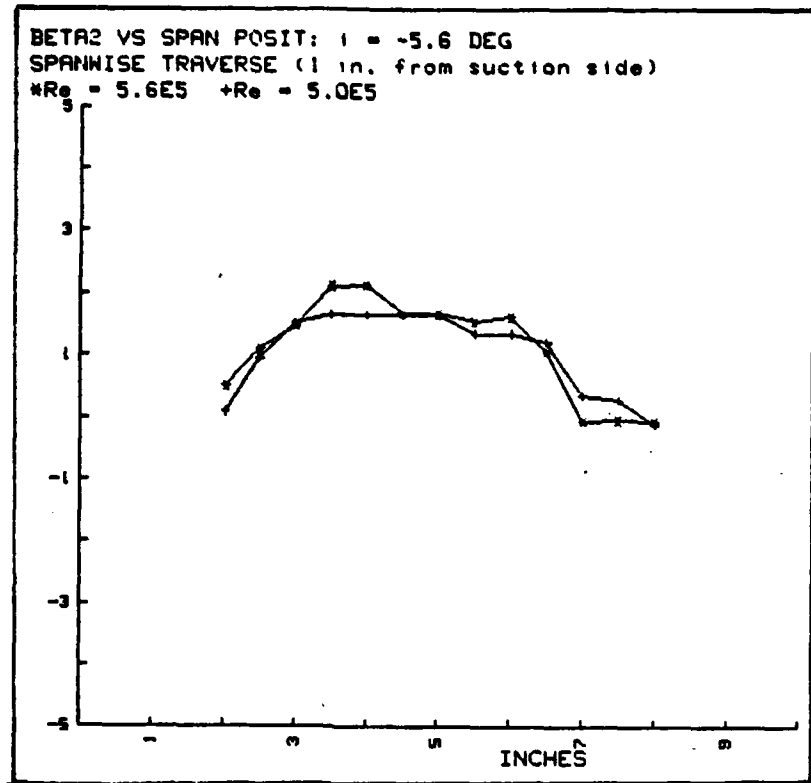


Fig. A.35

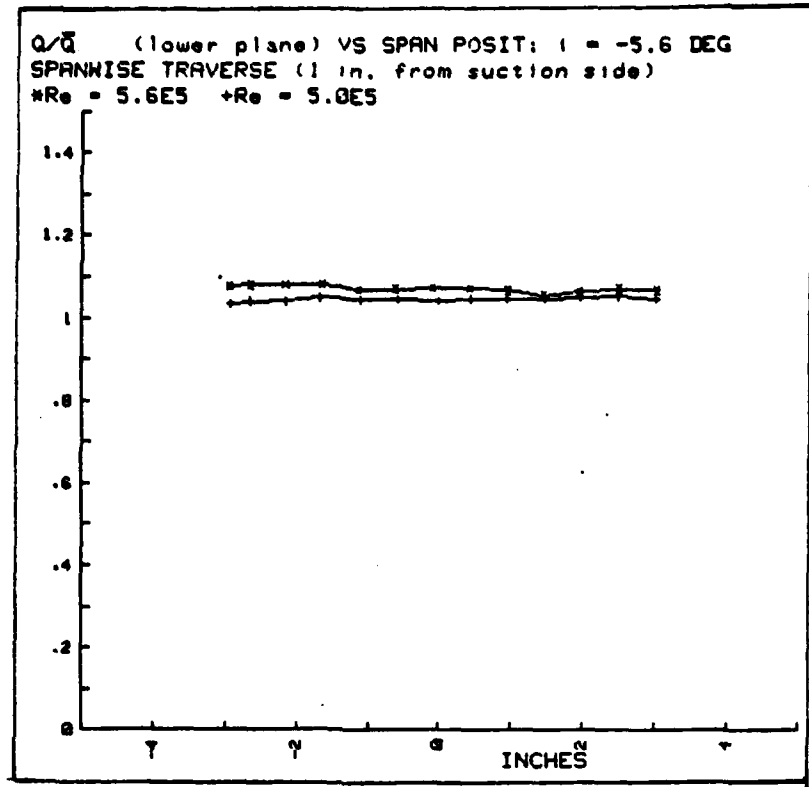


Fig. A.36

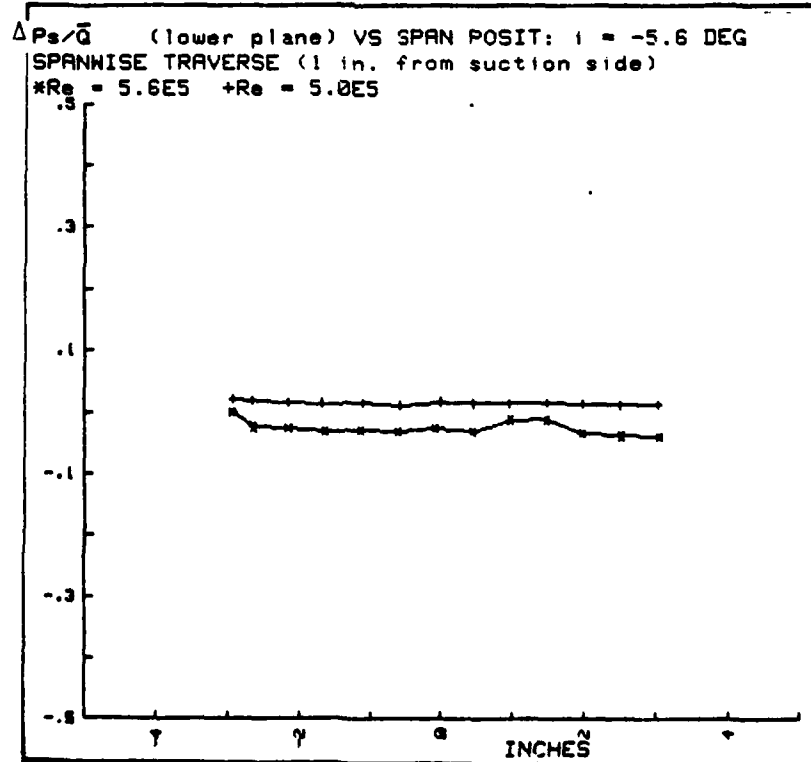


Fig. A.37

$\Delta P_t/Q$  (lower plane) VS SPAN POSIT:  $i = -5.6$  DEG  
SPANWISE TRAVERSE (1 in. from suction side)  
 $*Re = 5.6E5 + Re = 5.0E5$

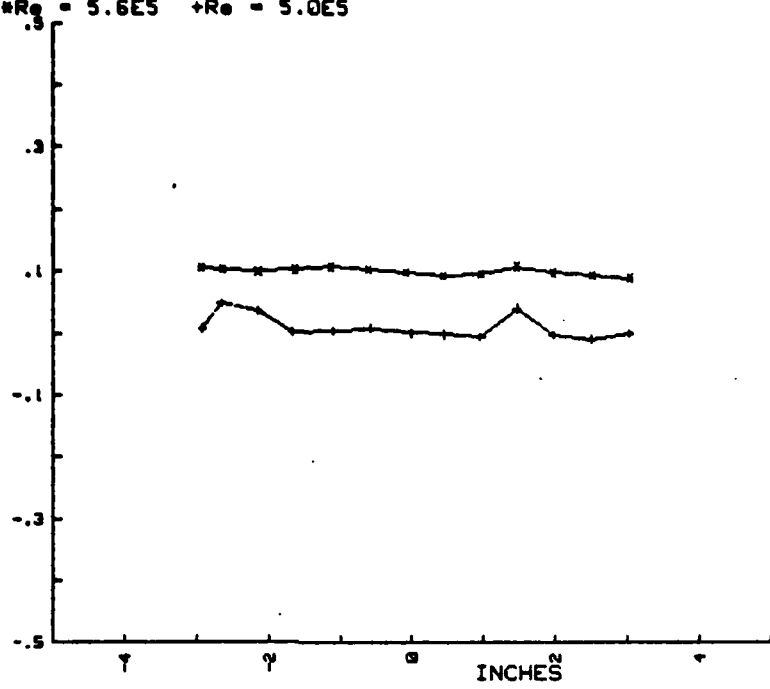


Fig. A.38

$X/\bar{X}$  (lower plane) VS SPAN POSIT:  $i = -5.6$  DEG  
SPANWISE TRAVERSE (1 in. from suction side)  
 $*Re = 5.6E5 + Re = 5.0E5$

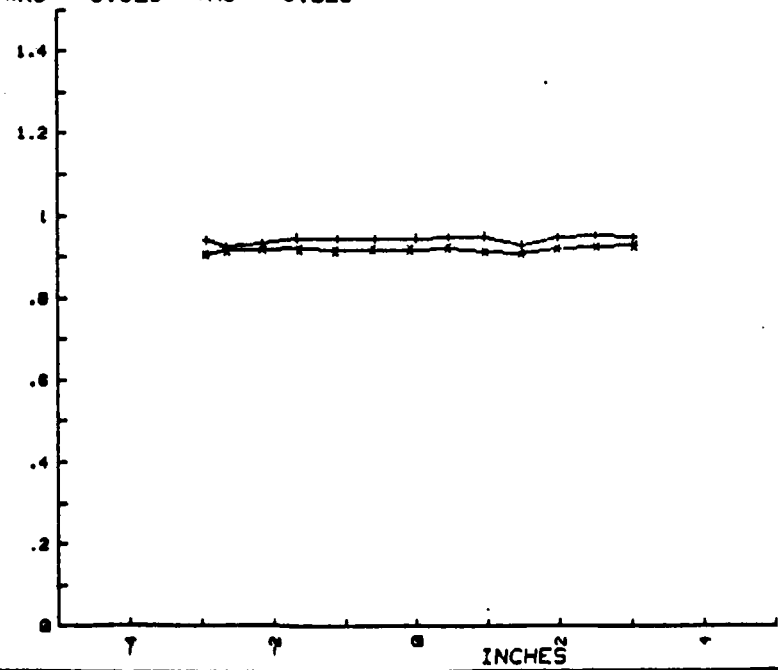


Fig. A.39

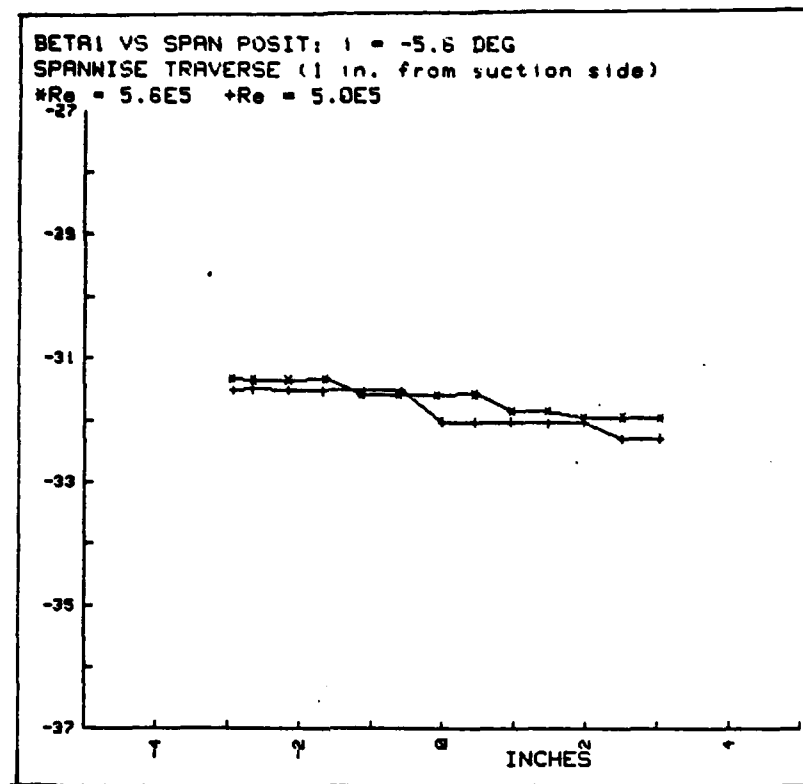


Fig. A.40

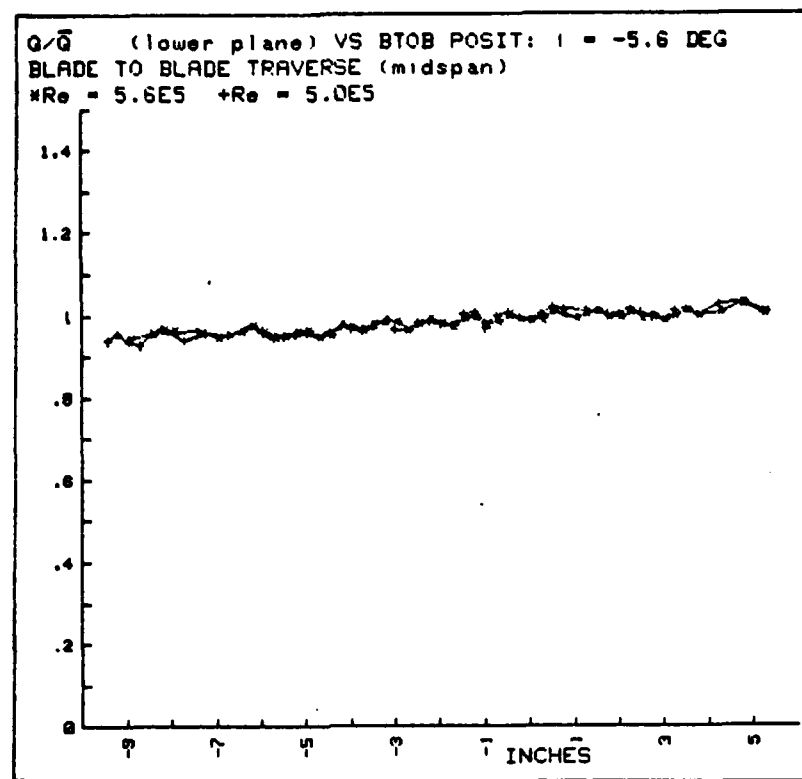


Fig. A.41

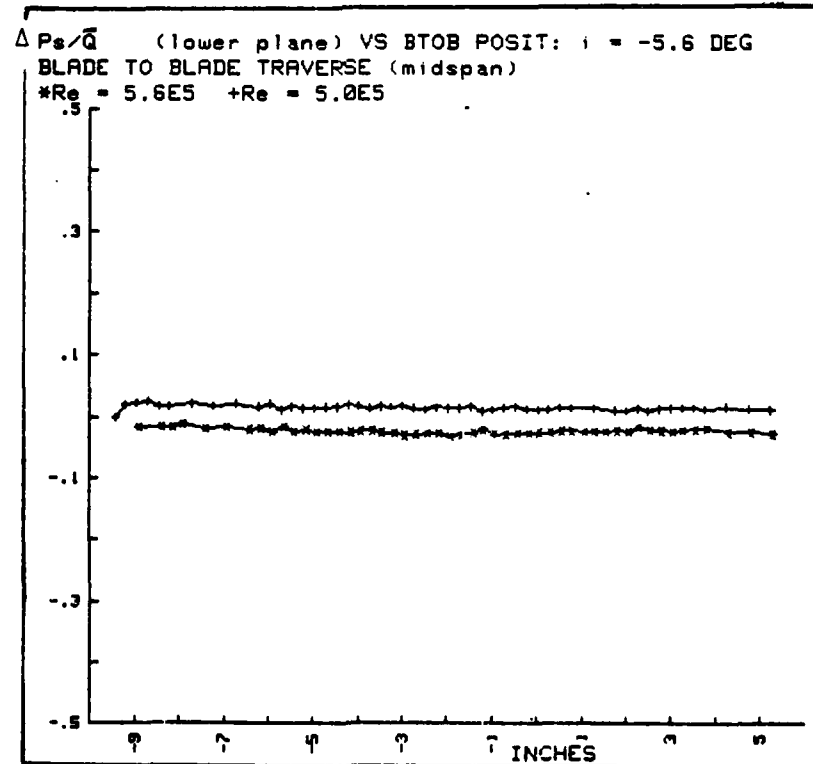


Fig. A.42

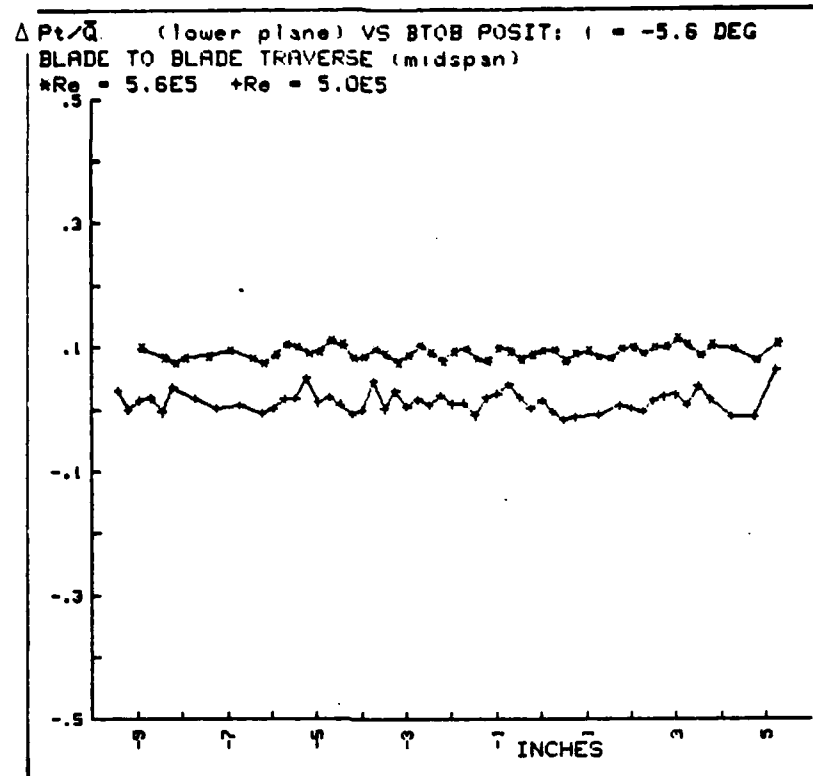


Fig. A.43

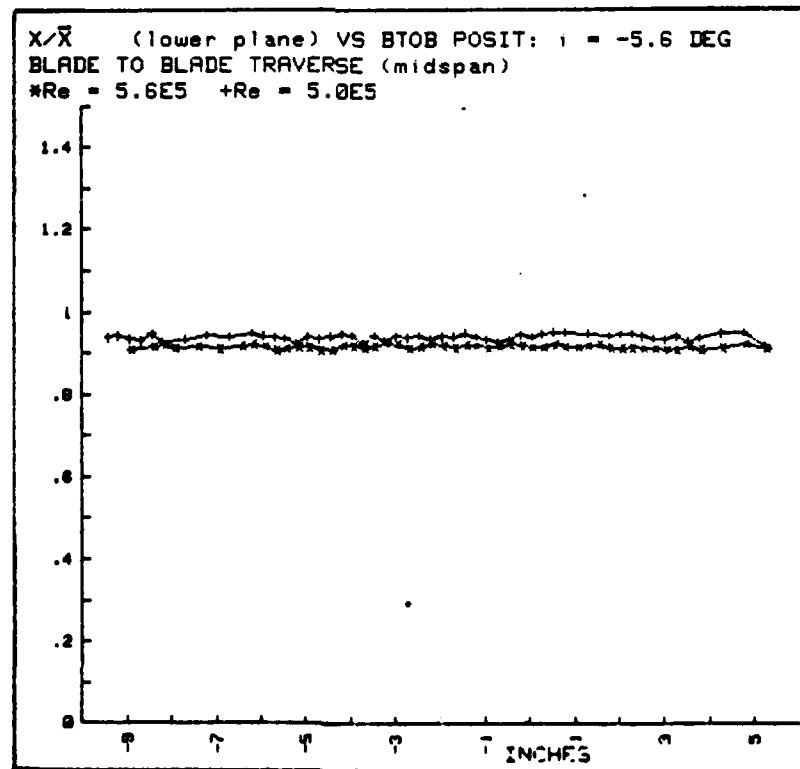


Fig. A.44

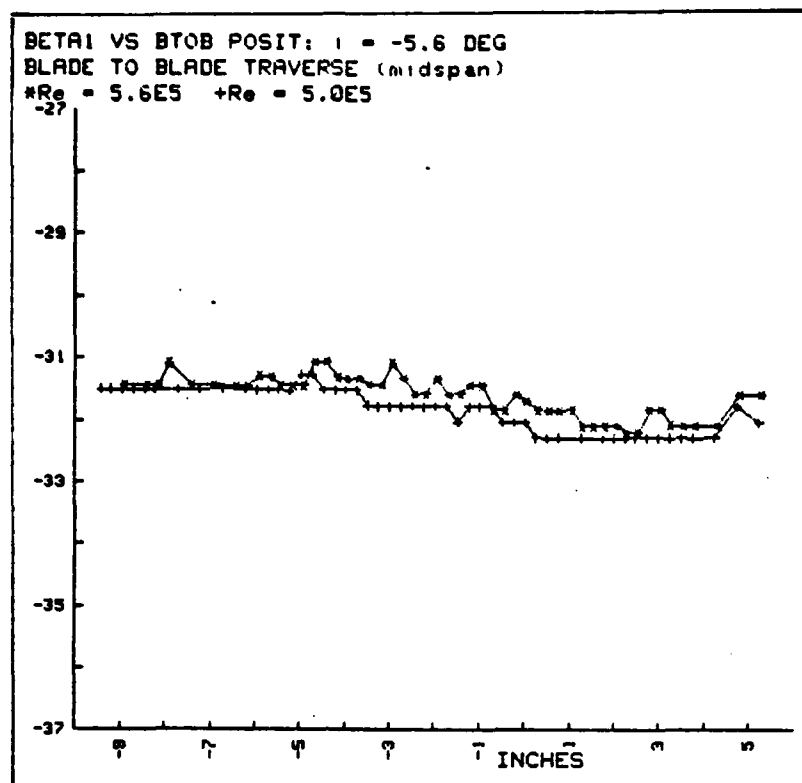


Fig. A.45

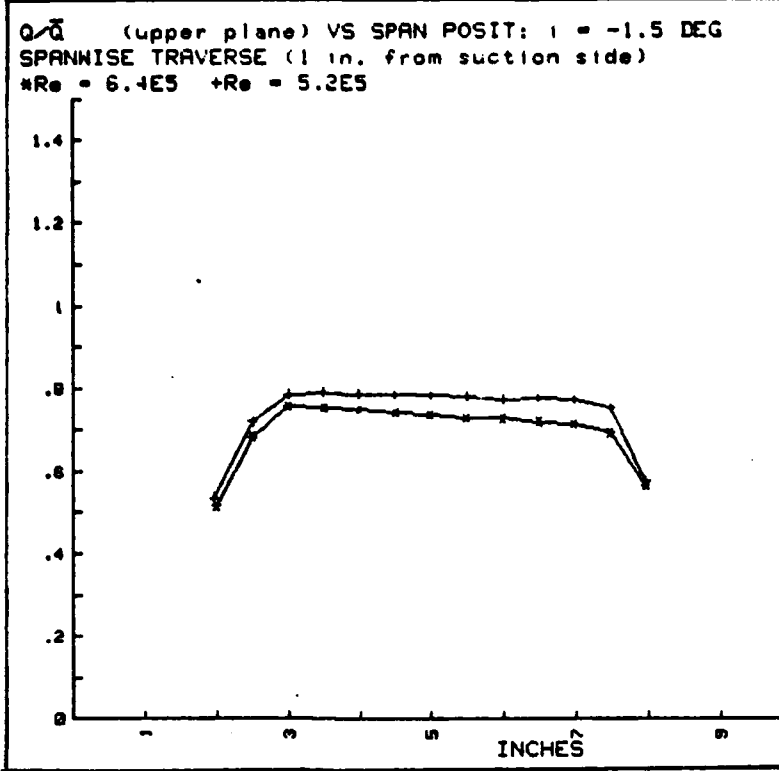


Fig. A.46

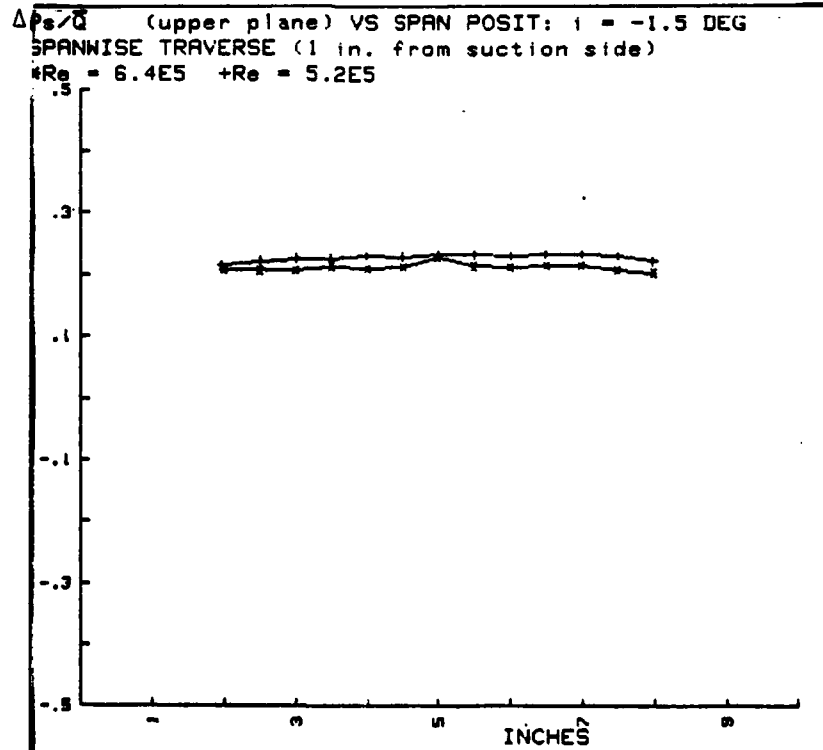


Fig. A.47

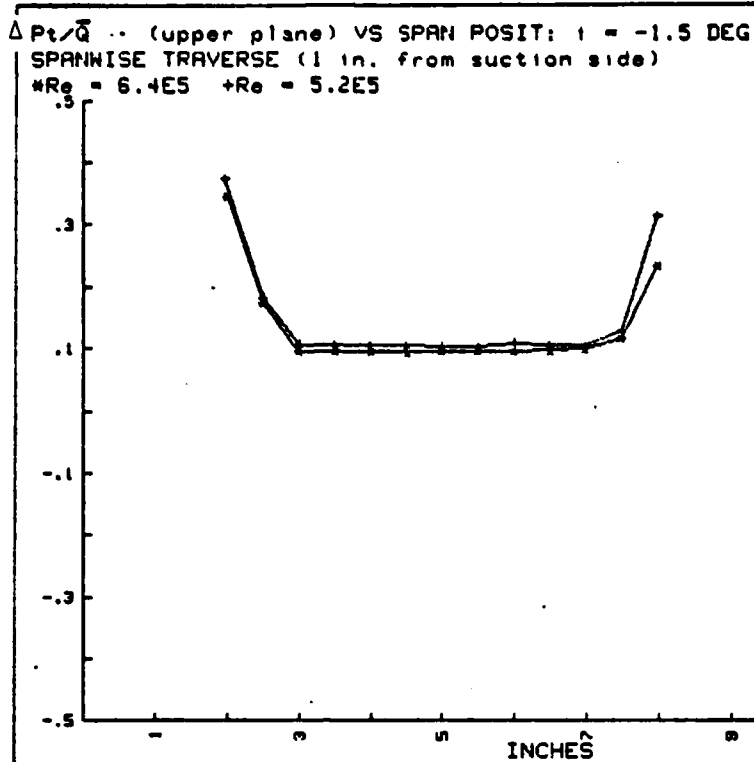


Fig. A.48

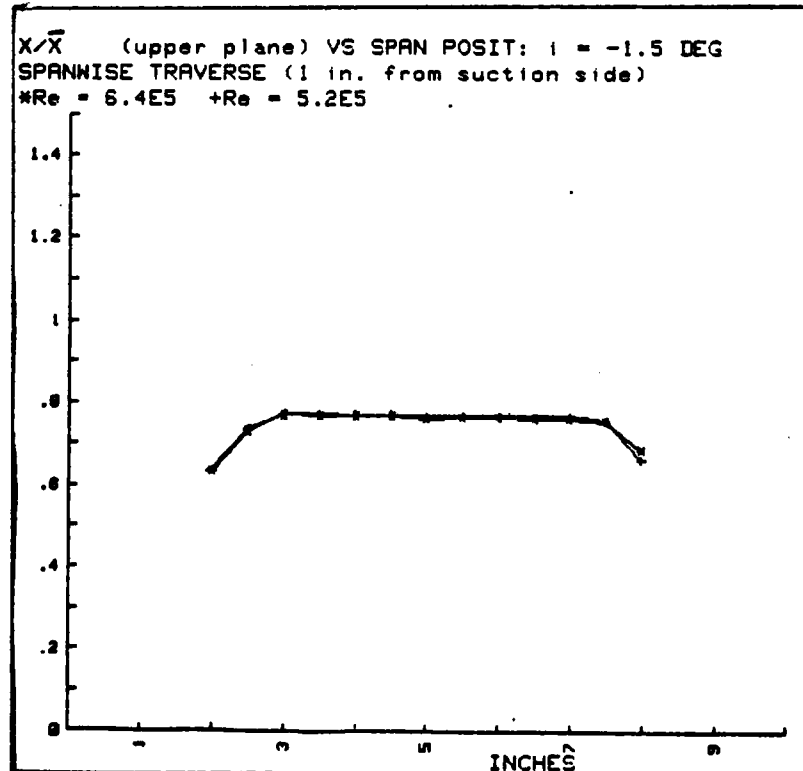


Fig. A.49

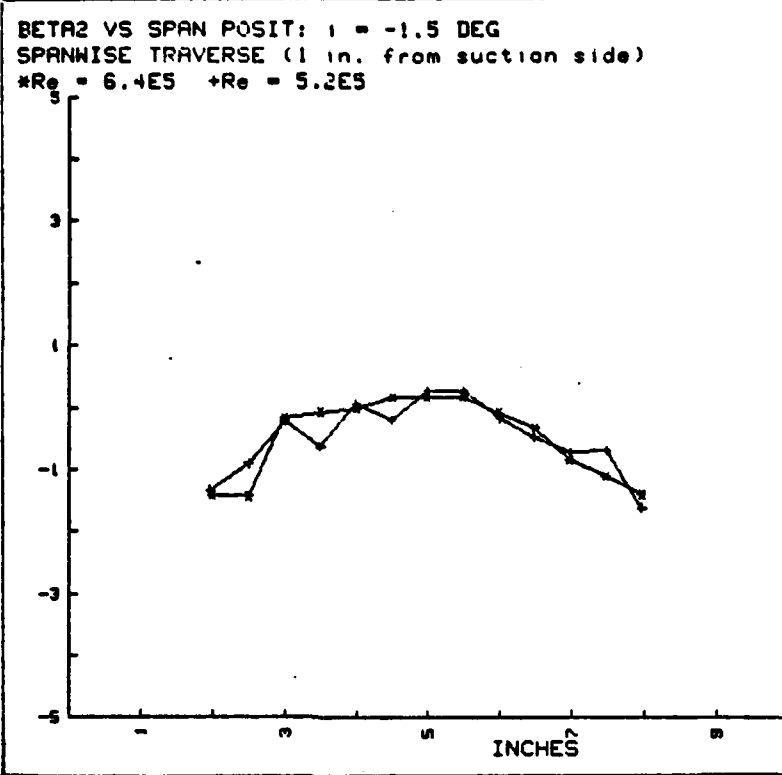


Fig. A.50

$Q/Q$  (lower plane) VS SPAN POSIT:  $i = -1.5$  DEG  
SPANWISE TRAVERSE (1 in. from suction side)  
 $*Re = 6.4E5 +Re = 5.2E5$

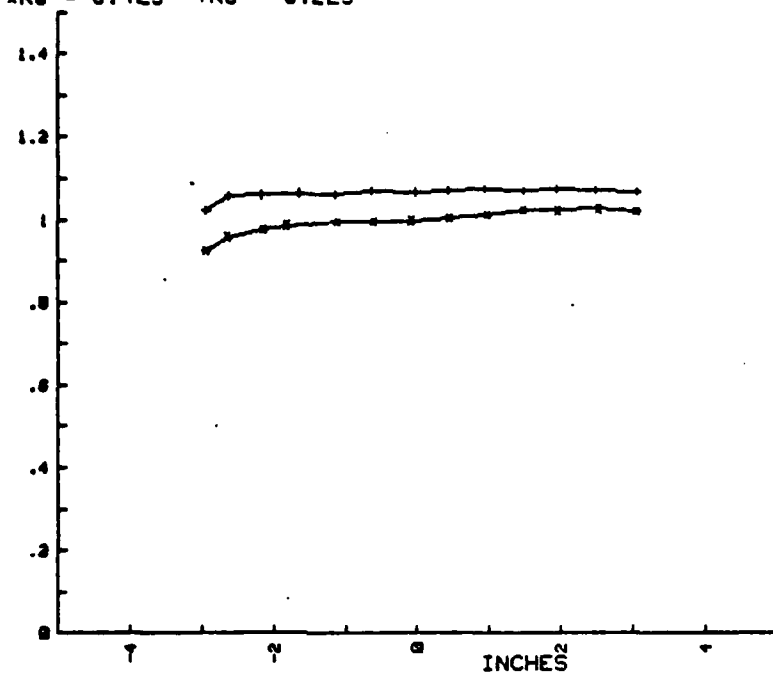


Fig. A.51

$\Delta P_s/\bar{Q}$  (lower plane) VS SPAN POSIT:  $i = -1.5$  DEG  
SPANWISE TRAVERSE (1 in. from suction side)  
 $*Re = 6.4E5 +Re = 5.2E5$

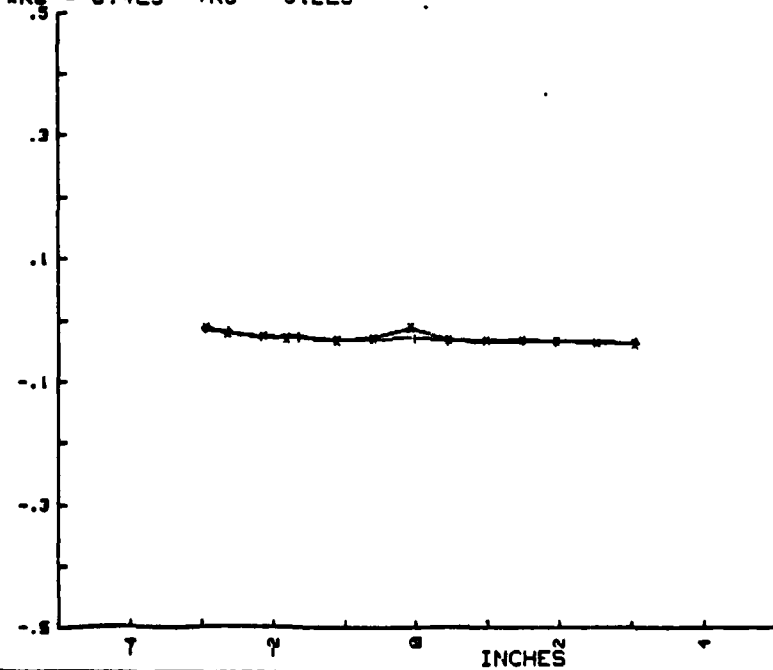


Fig. A.52

$\Delta P_t / \bar{Q}$  (lower plane) VS SPAN POSIT:  $i = -1.5$  DEG  
SPANWISE TRAVERSE (1 in. from suction side)  
 $*Re = 6.4E5 +Re = 5.2E5$

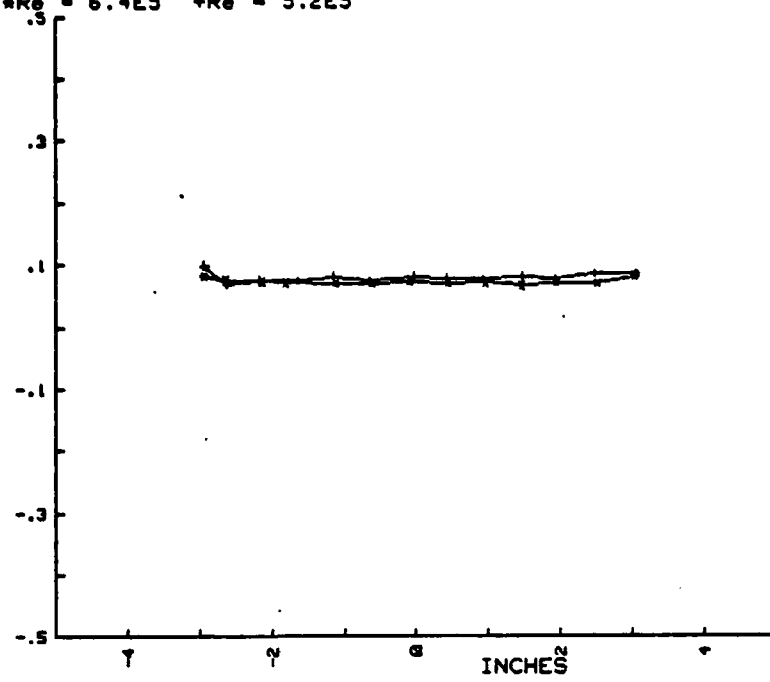


Fig. A.53

$X/\bar{X}$  (lower plane) VS SPAN POSIT:  $i = -1.5$  DEG  
SPANWISE TRAVERSE (1 in. from suction side)  
 $*Re = 6.4E5 +Re = 5.2E5$

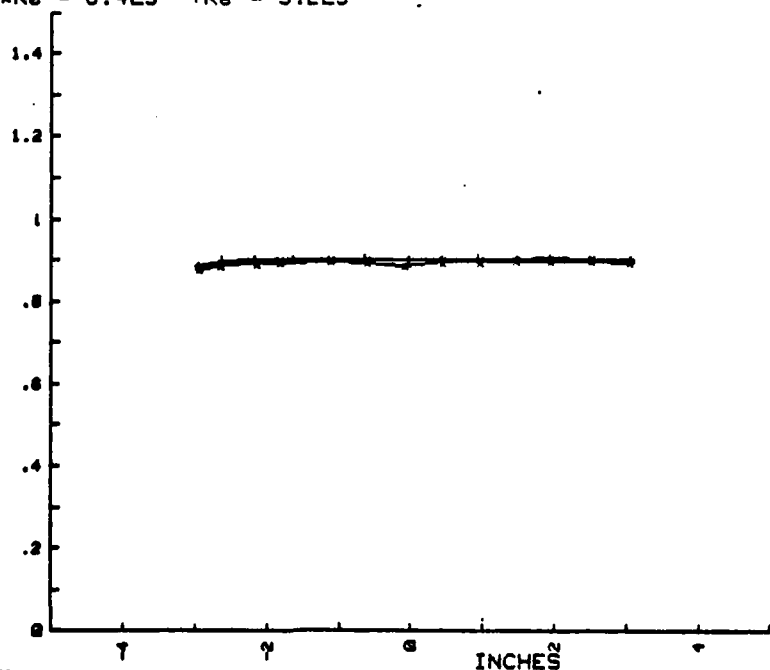


Fig. A.54

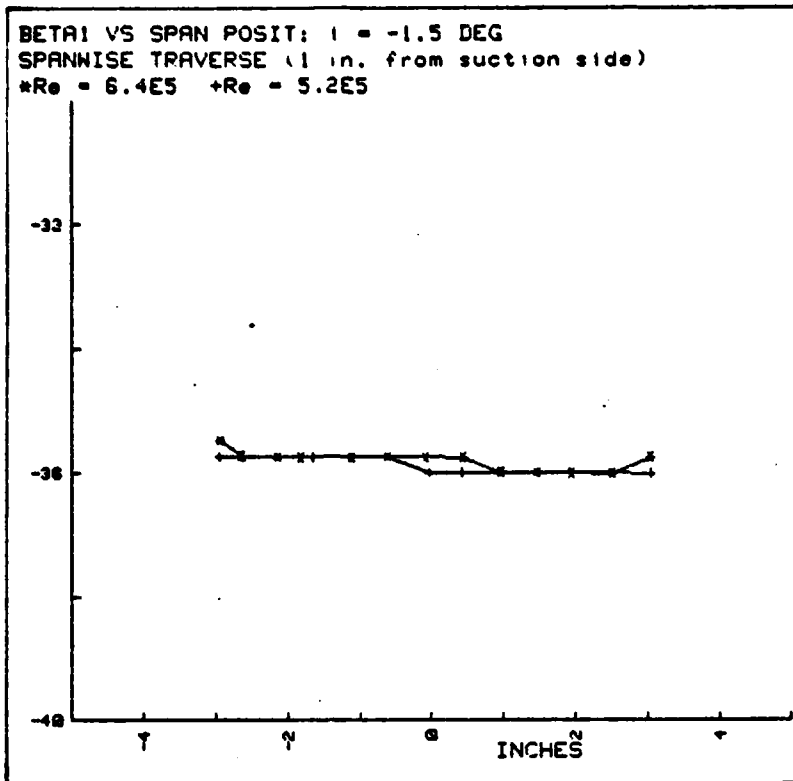


Fig. A.55

$Q/\bar{Q}$  (lower plane) VS BTOB POSIT:  $i = -1.5$  DEG  
BLADE TO BLADE TRAVERSE (midspan)  
 $*Re = 6.4E5 +Re = 5.2E5$

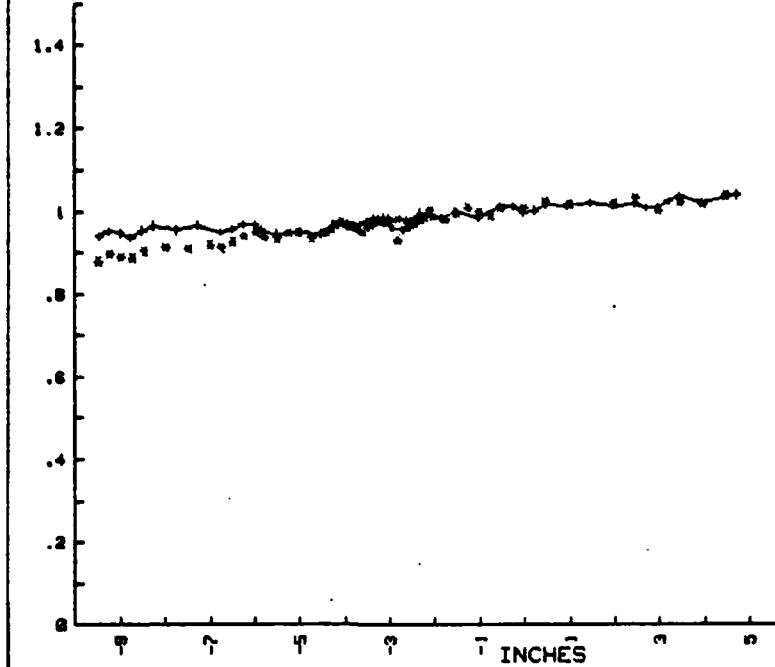


Fig. A.56

$\Delta P_s/\bar{Q}$  (lower plane) VS BTOB POSIT:  $i = -1.5$  DEG  
BLADE TO BLADE TRAVERSE (midspan)  
 $*Re = 6.4E5 +Re = 5.2E5$

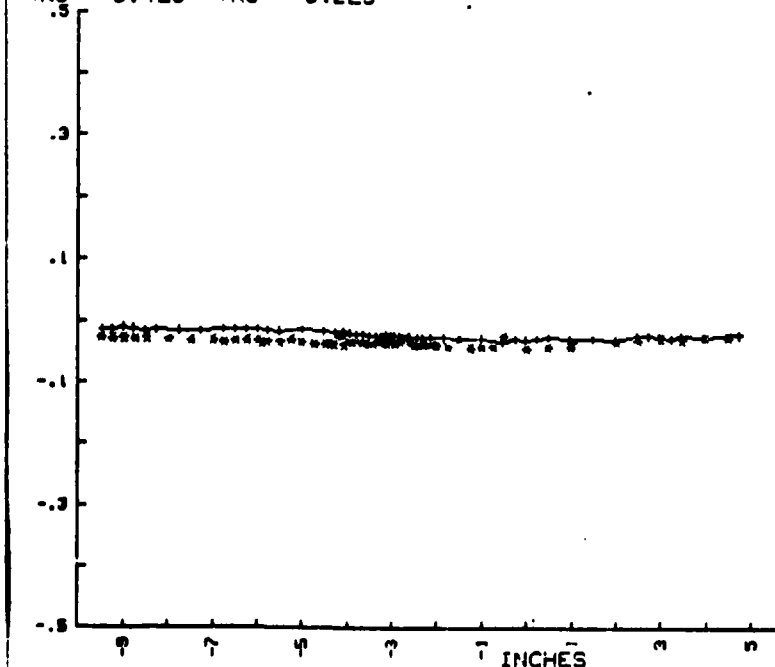


Fig. A.57

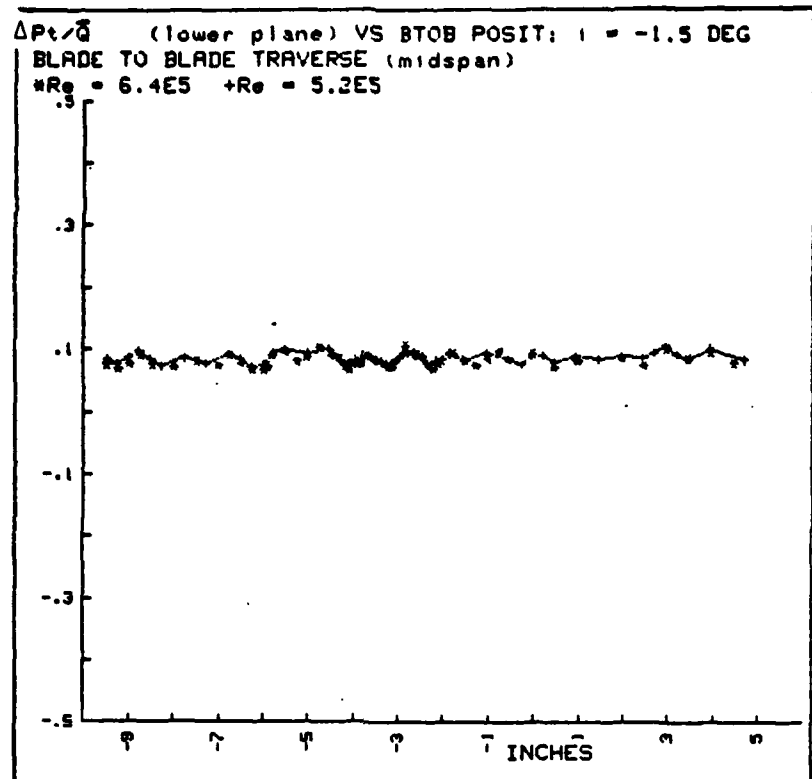


Fig. A.58

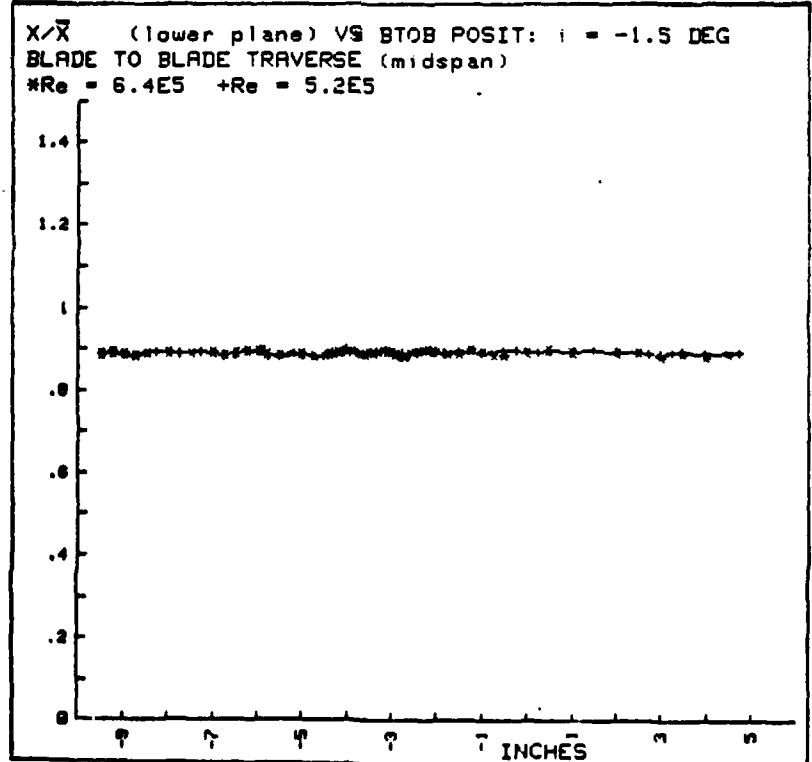


Fig. A.59

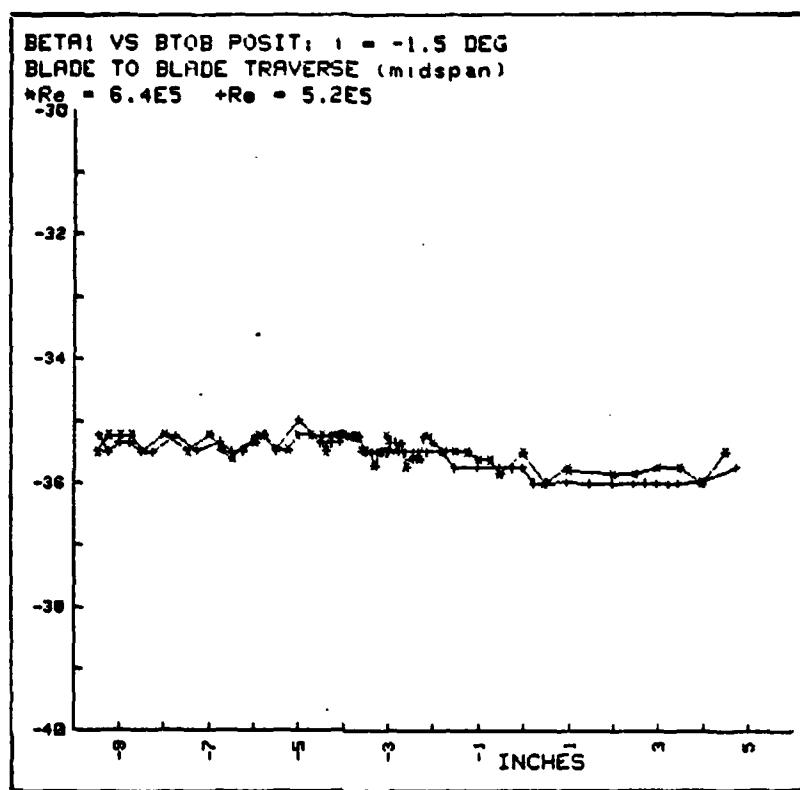


Fig. A.60

$Q/\bar{Q}$  (upper plane) VS SPAN POSIT:  $i = 2.2$  DEG  
 SPANWISE TRAVERSE (1 in. from suction side)  
 $*Re=6.7E5$ (plexiglass wall)  $+Re=6.0E5$ (steel wall),

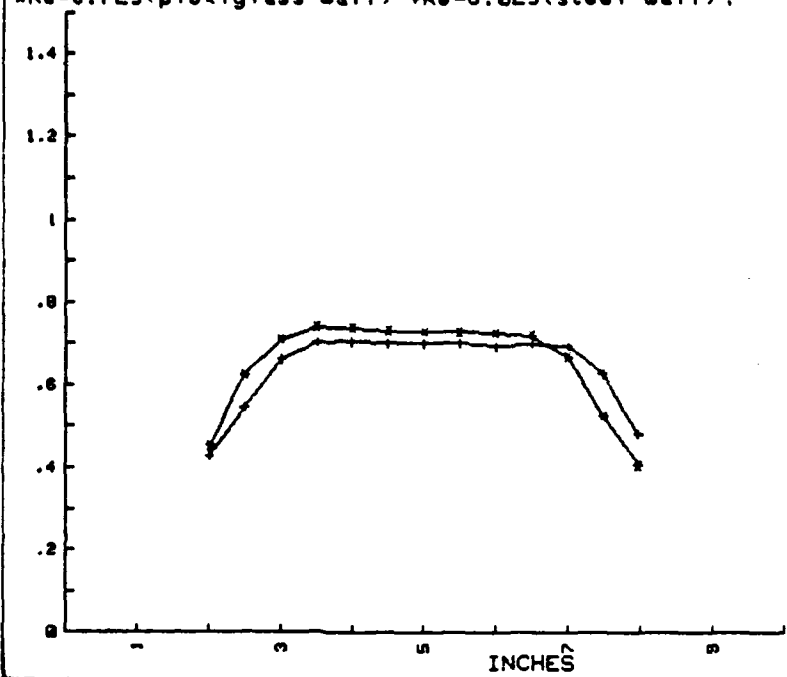


Fig. A.61

$\Delta P_s/\bar{Q}$  (upper plane) VS SPAN POSIT:  $i = 2.2$  DEG  
 SPANWISE TRAVERSE (1 in. from suction side)  
 $*Re=6.7E5$ (plexiglass wall)  $+Re=6.0E5$ (steel wall)

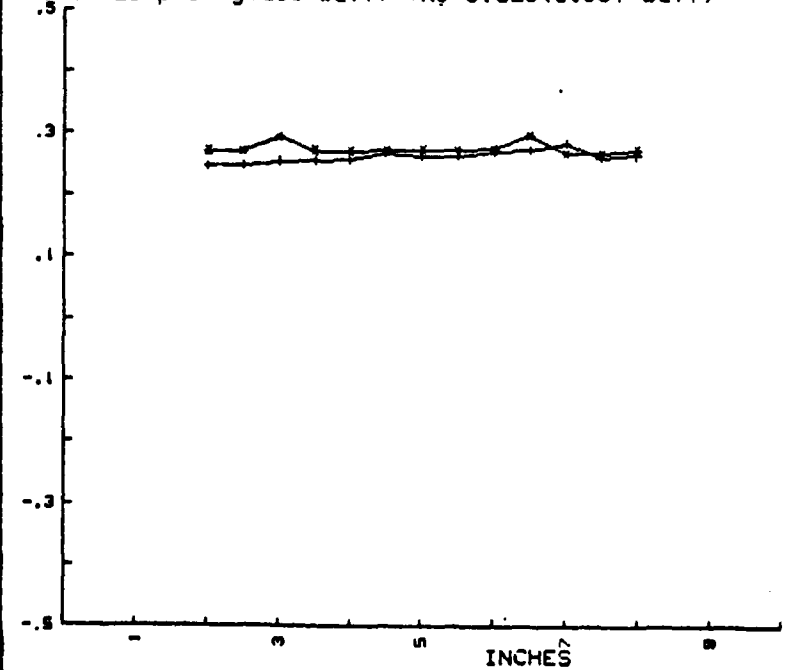


Fig. A.62

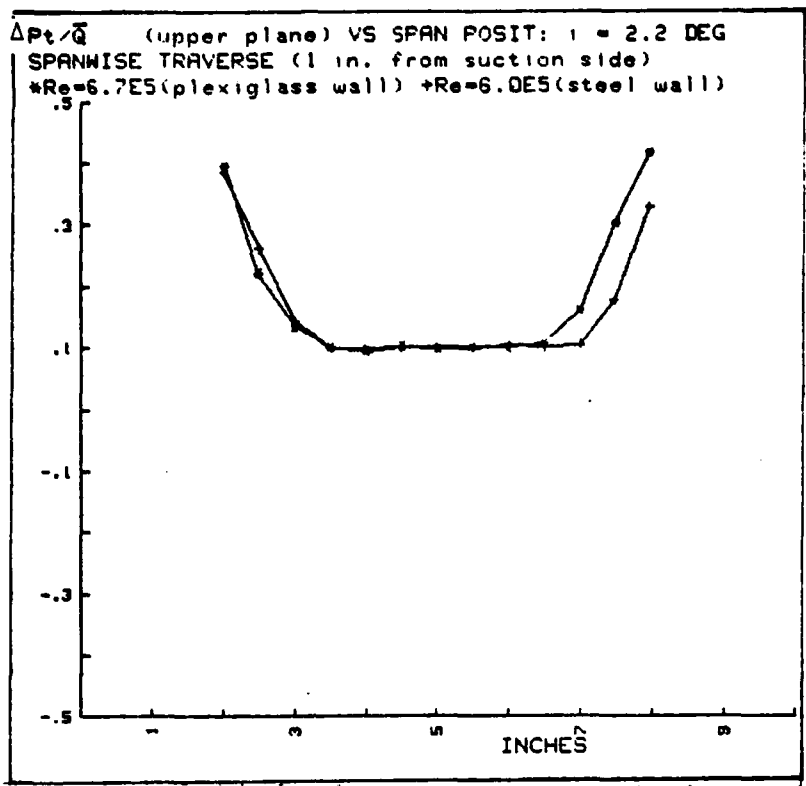


Fig. A.63

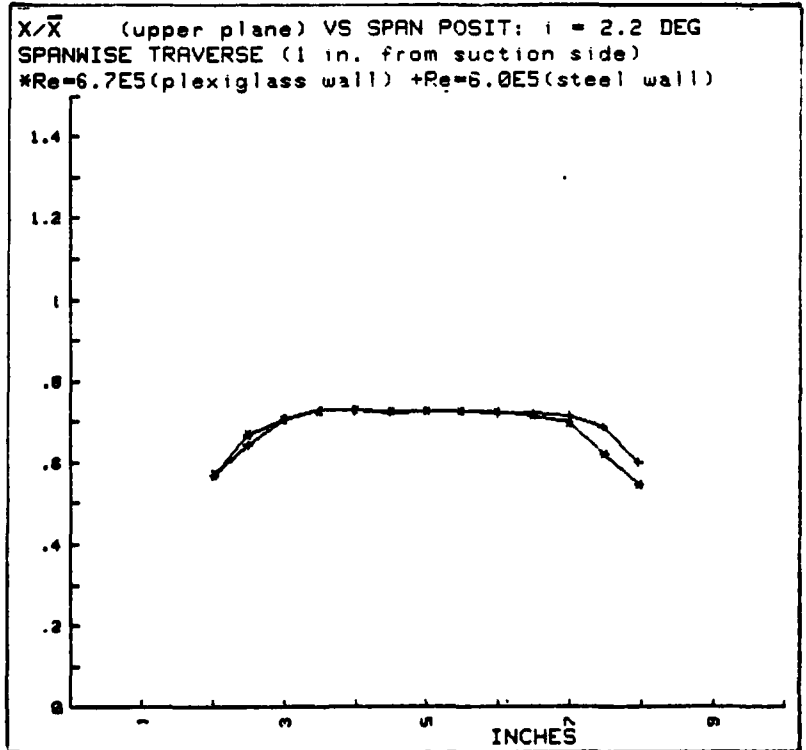
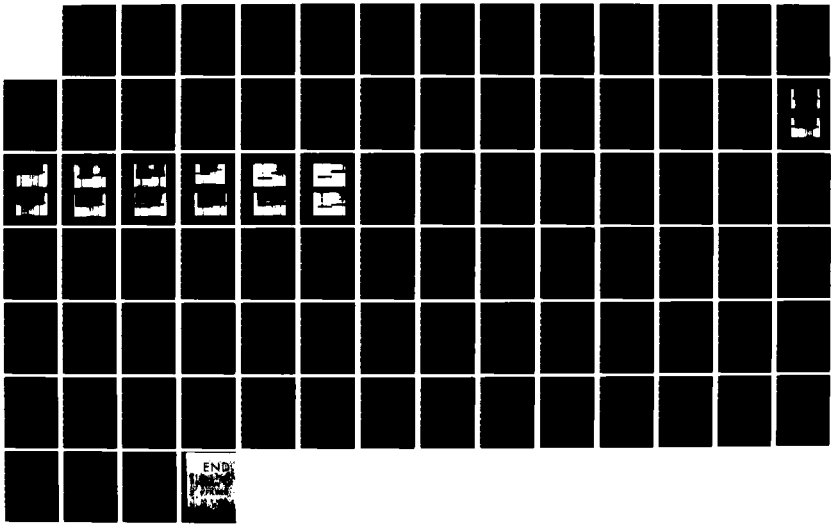


Fig. A.64

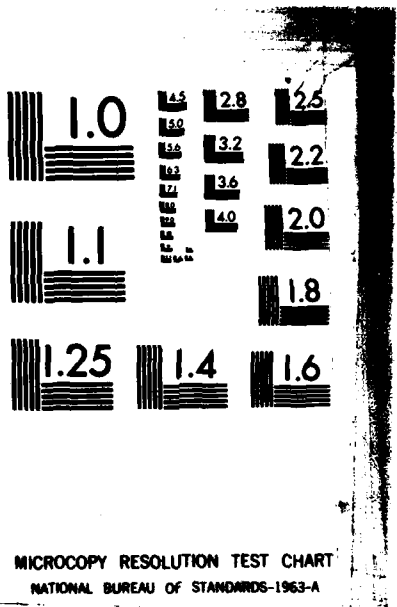
AD-A133 350 REPORT OF TESTS OF A COMPRESSOR CONFIGURATION OF DCR 2/2  
BLADING(U) NAVAL POSTGRADUATE SCHOOL MONTEREY CA  
S J HIMES JUN 83

UNCLASSIFIED

F/G 20/4 NL



END



MICROCOPY RESOLUTION TEST CHART  
NATIONAL BUREAU OF STANDARDS-1963-A

BETA2 VS SPAN POSIT:  $\delta = 2.2$  DEG  
SPANWISE TRAVERSE (1 in. from suction side)  
 $*Re=6.7E5$ (plexiglass wall) + $Re=6.0E5$ (steel wall)

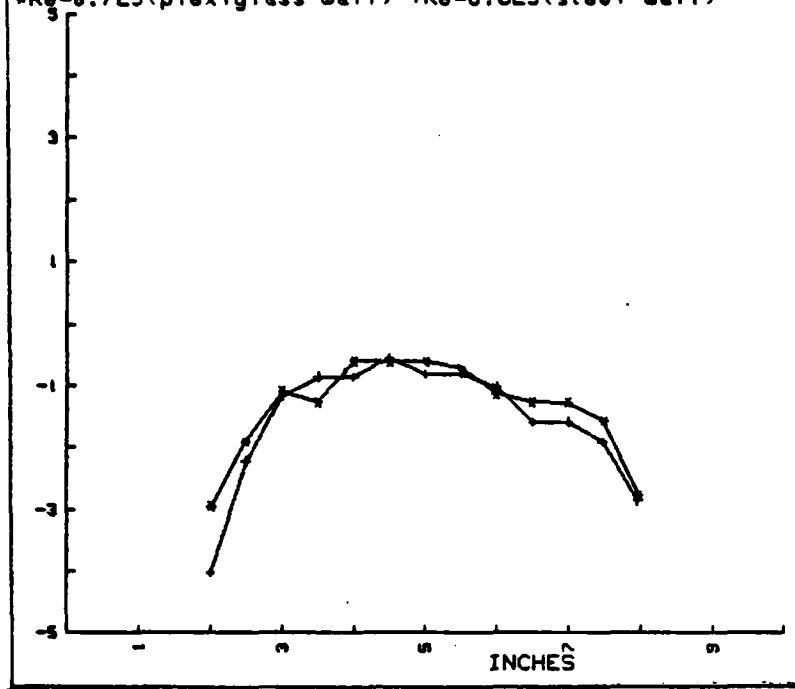


Fig. A.65

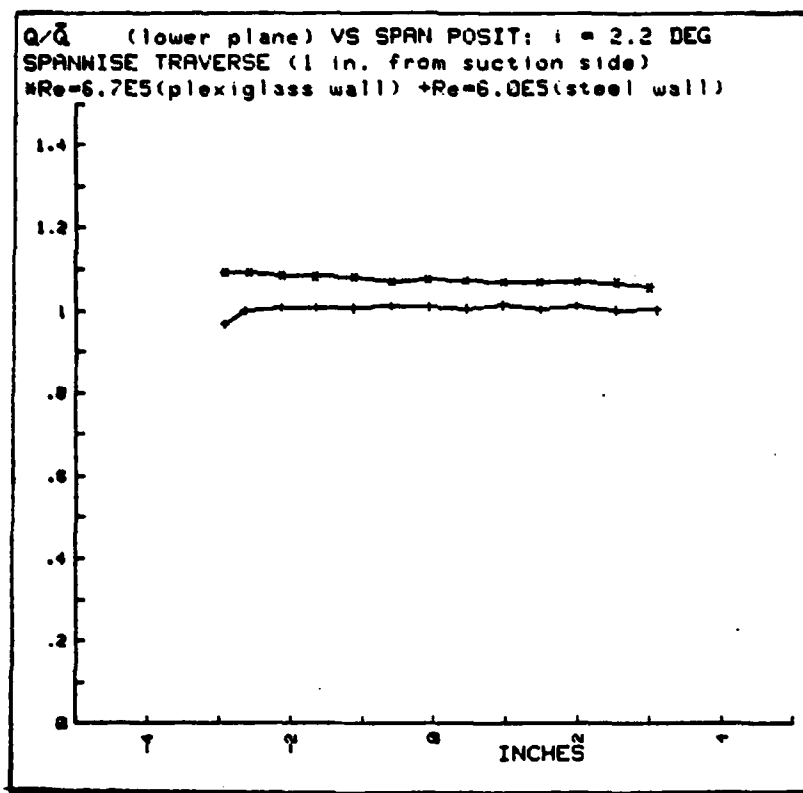


Fig. A.66

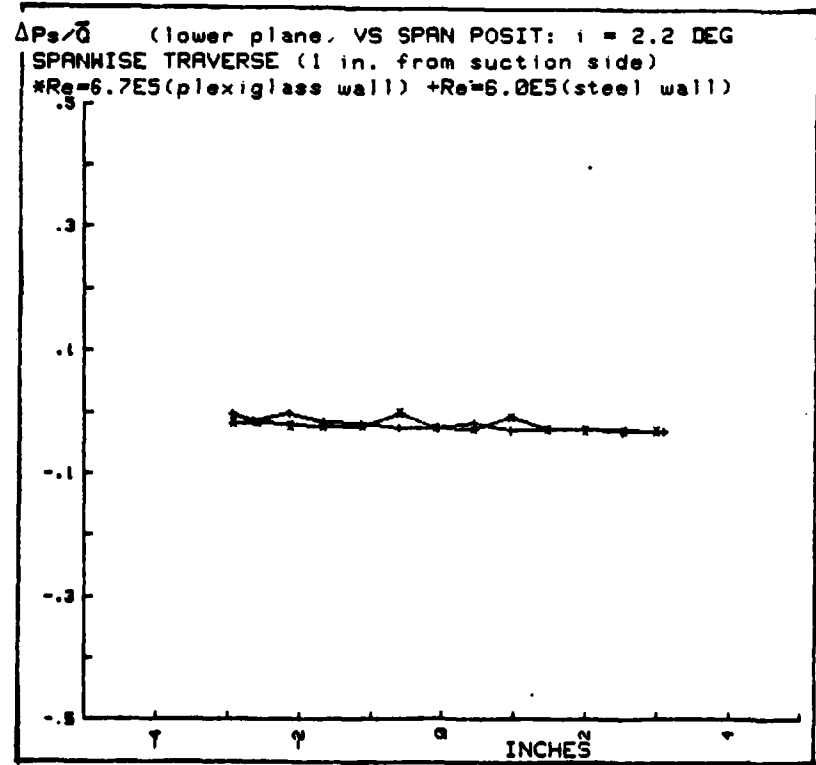


Fig. A.67

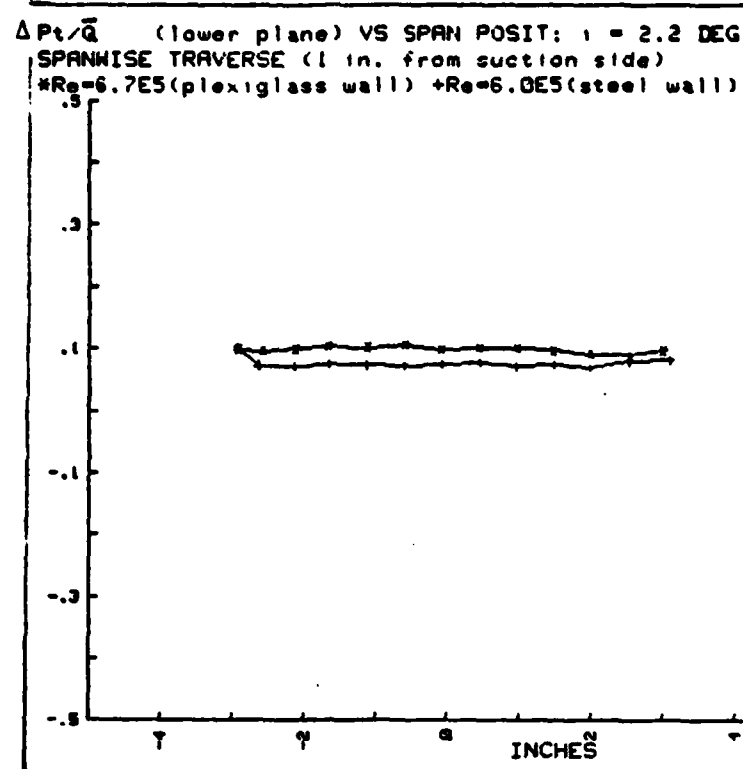


Fig. A.68

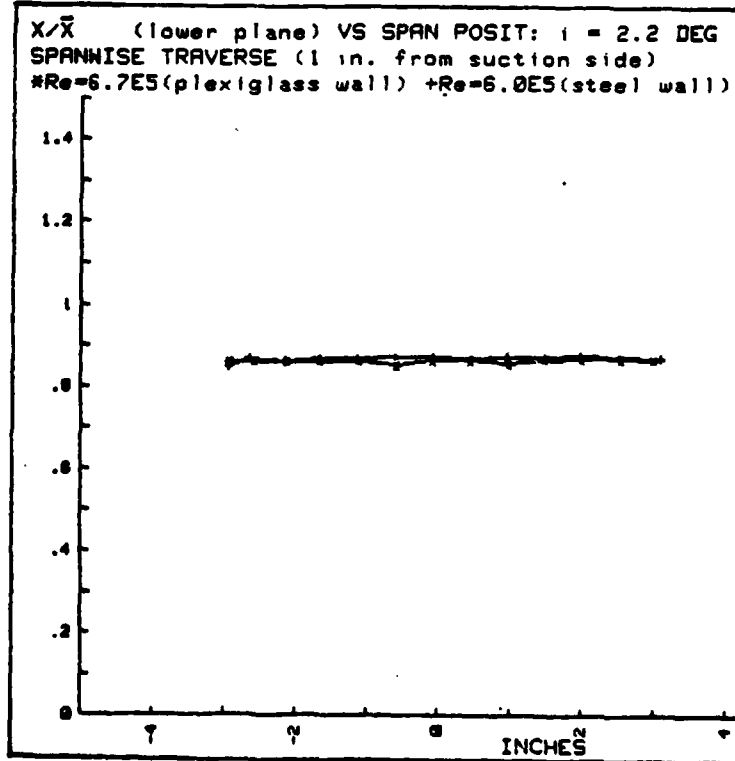


Fig. A.69

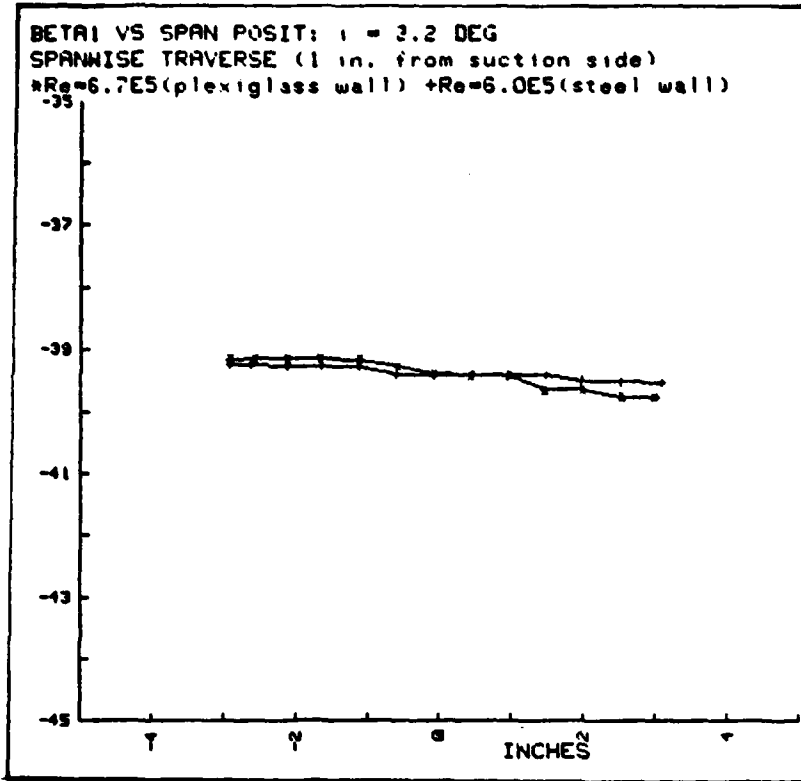


Fig. A.70

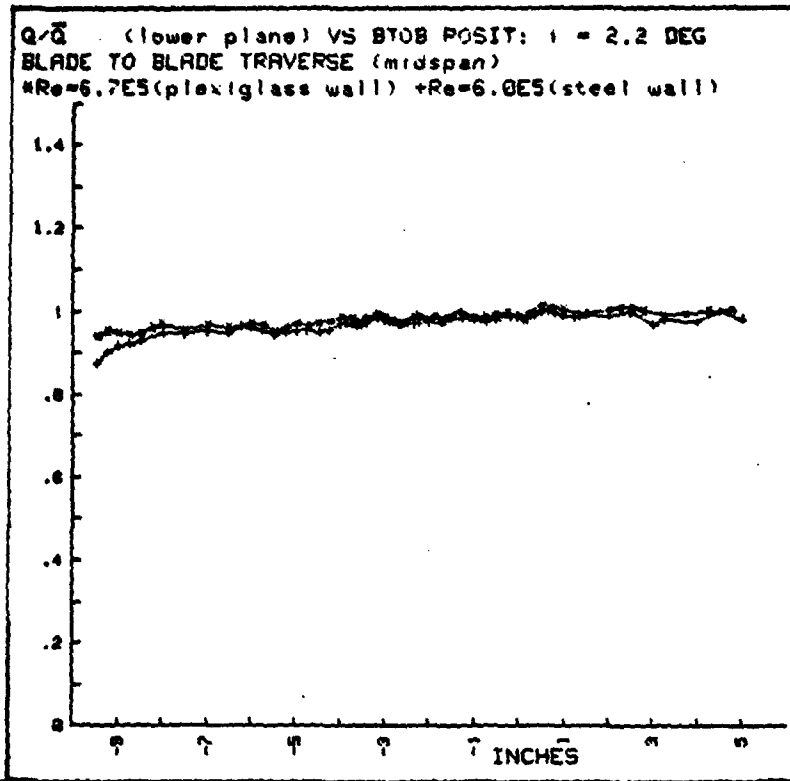


Fig. A.71

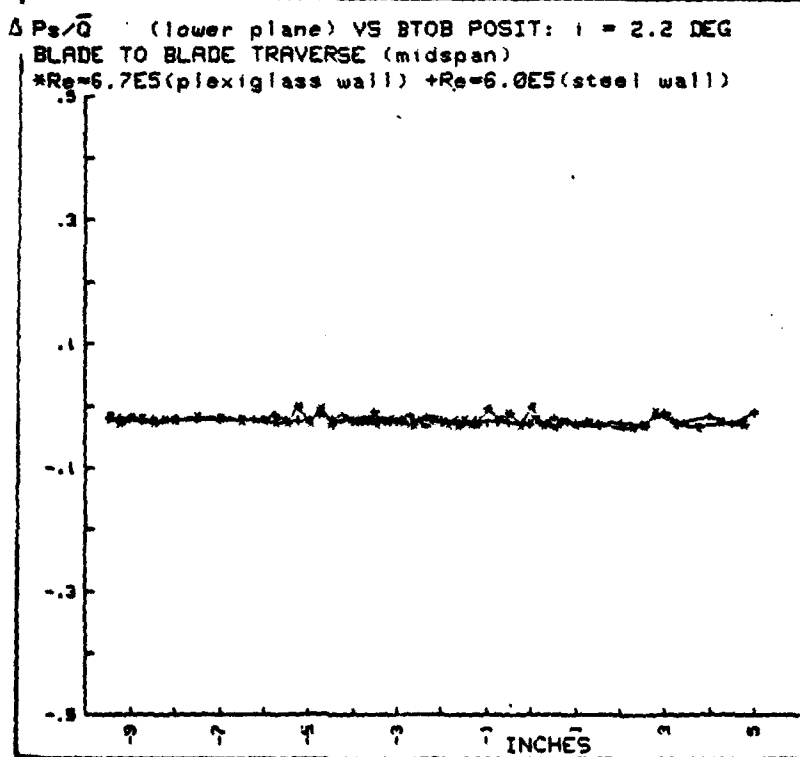


Fig. A.72

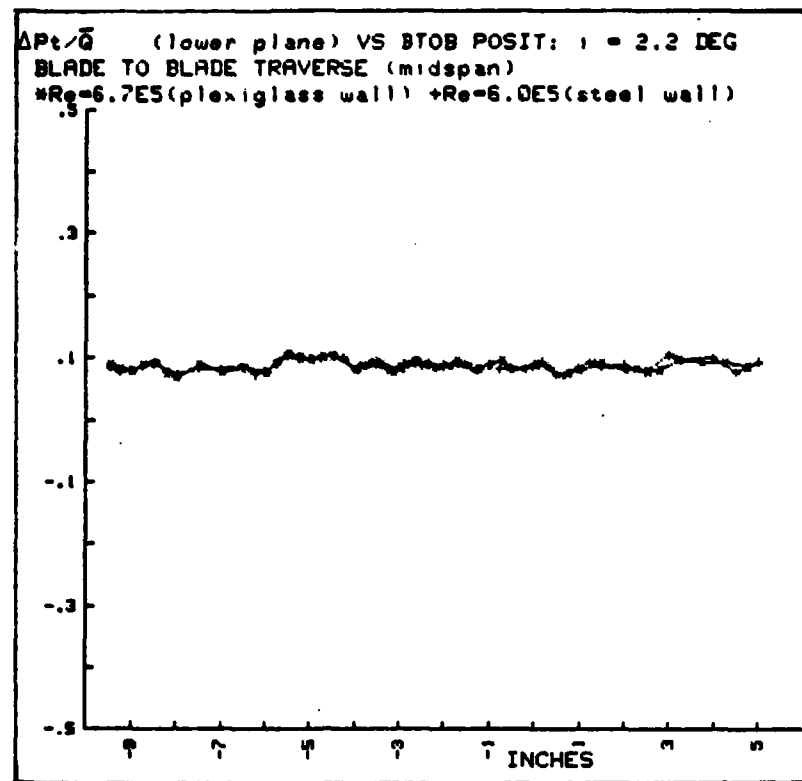


Fig. A.73

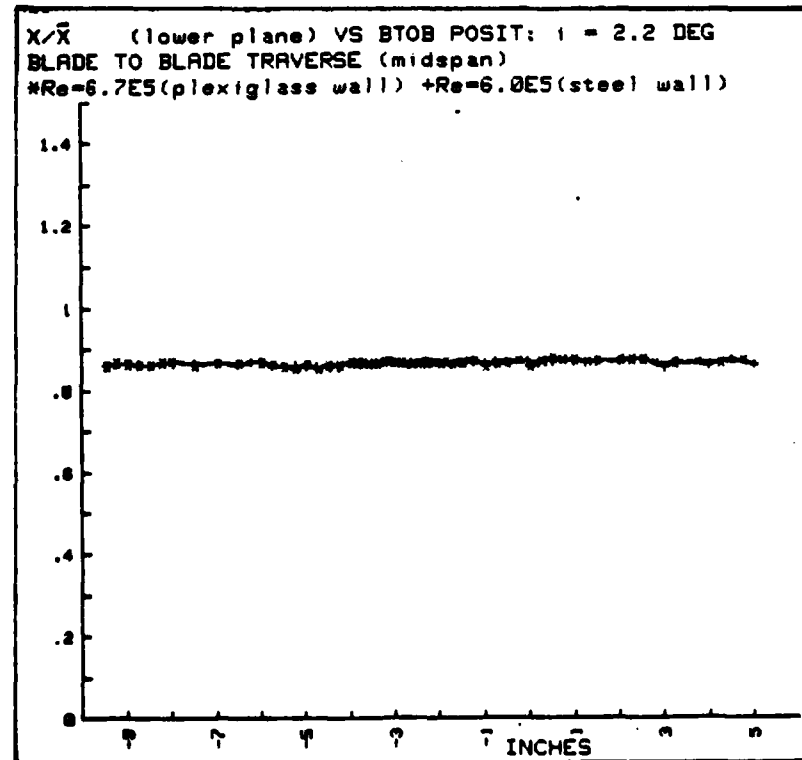


Fig. A.74

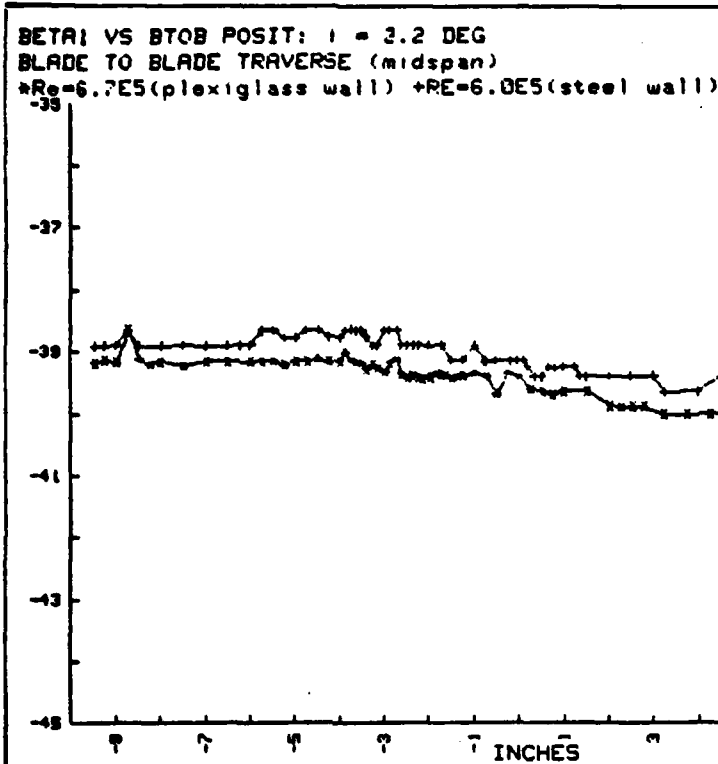


Fig. A.75

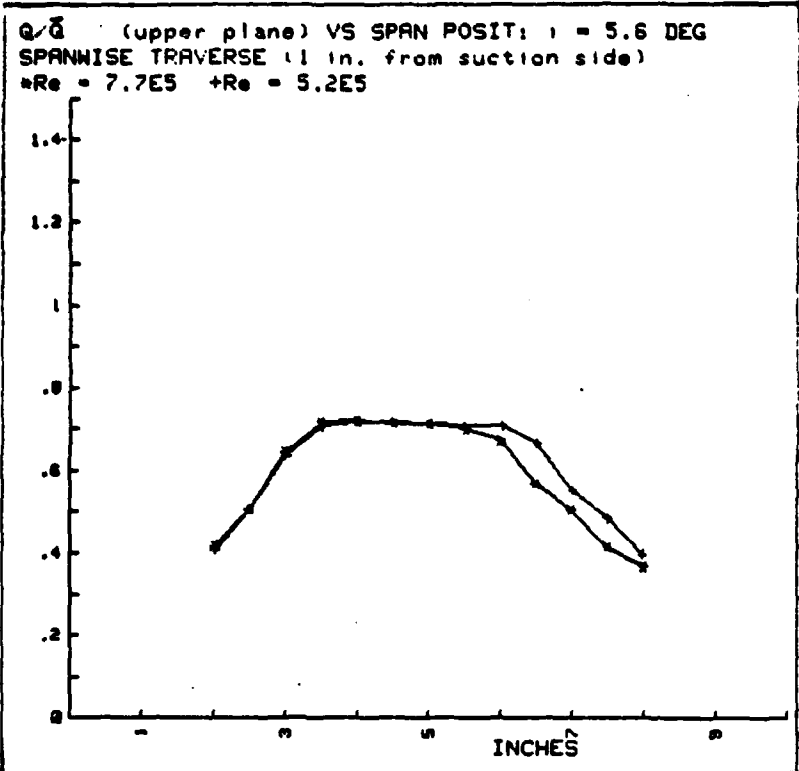


Fig. A.76

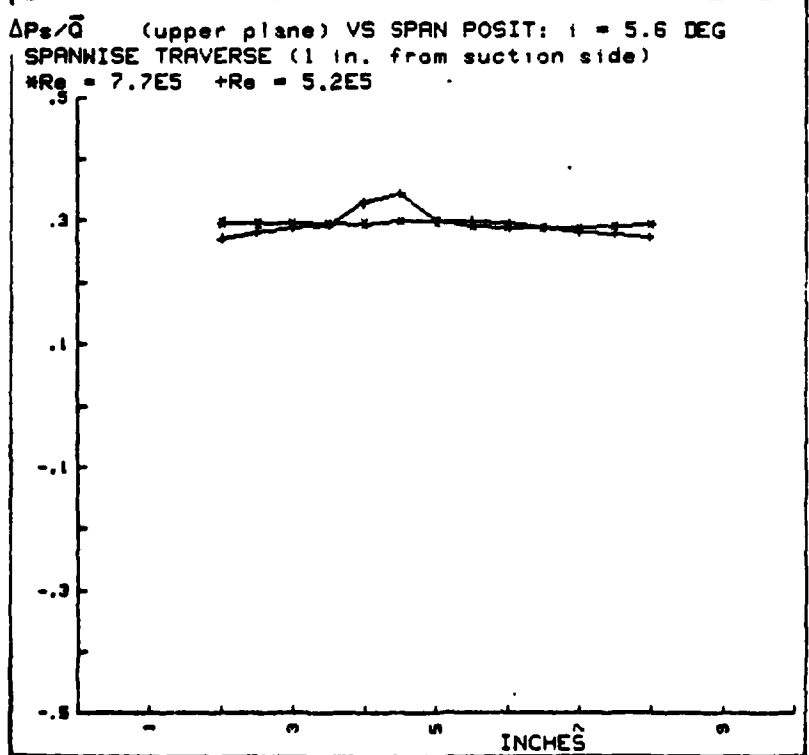


Fig. A.77

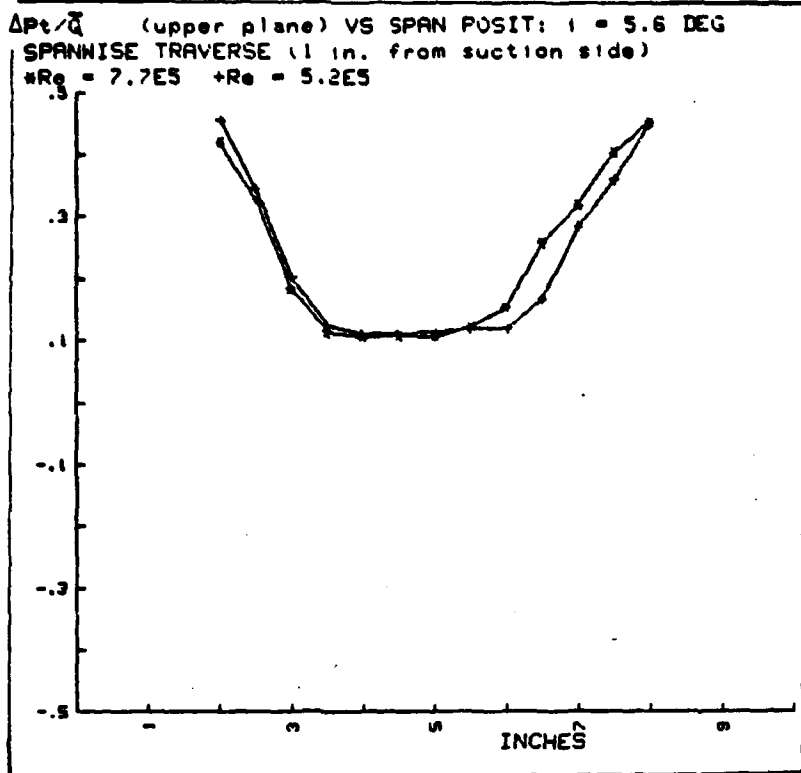


Fig. A.78

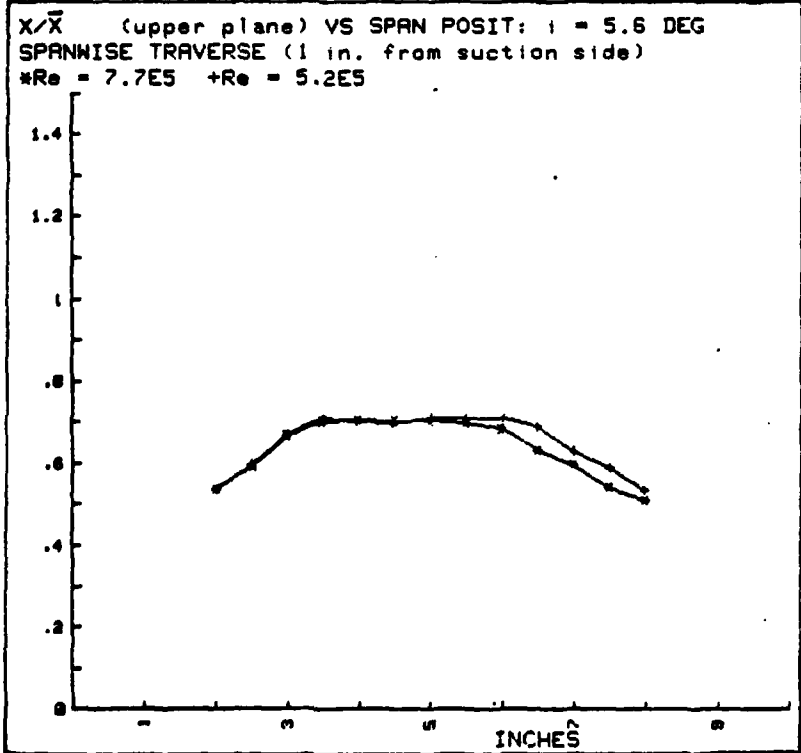


Fig. A.79

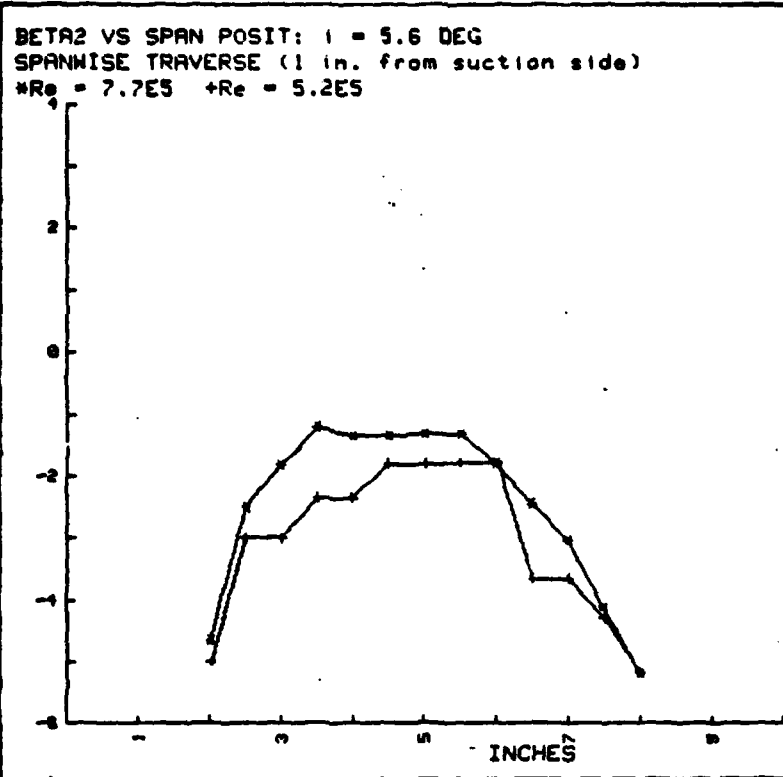


Fig. A.80

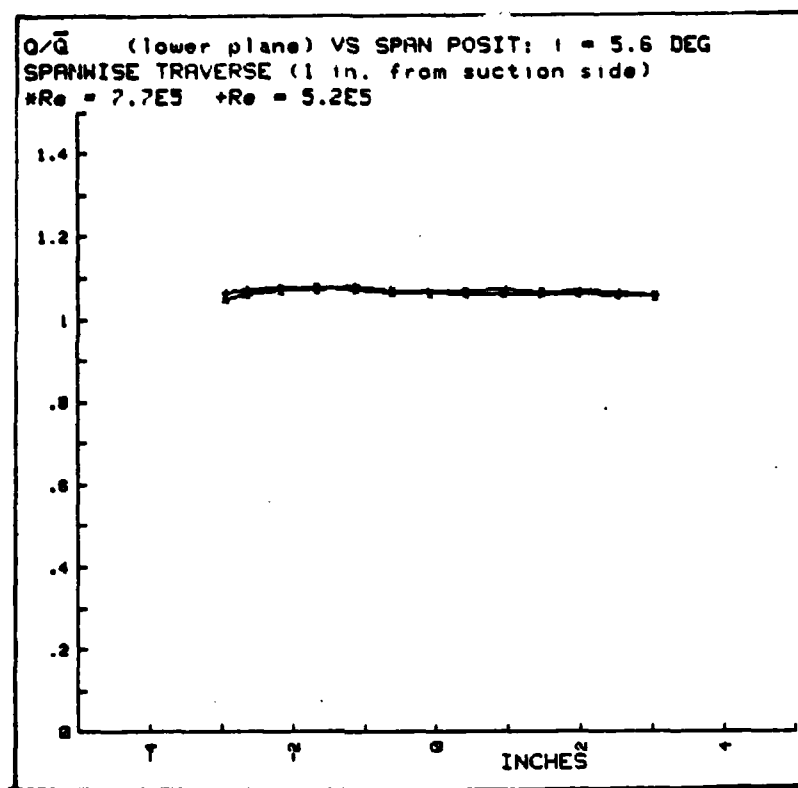


Fig. A.81

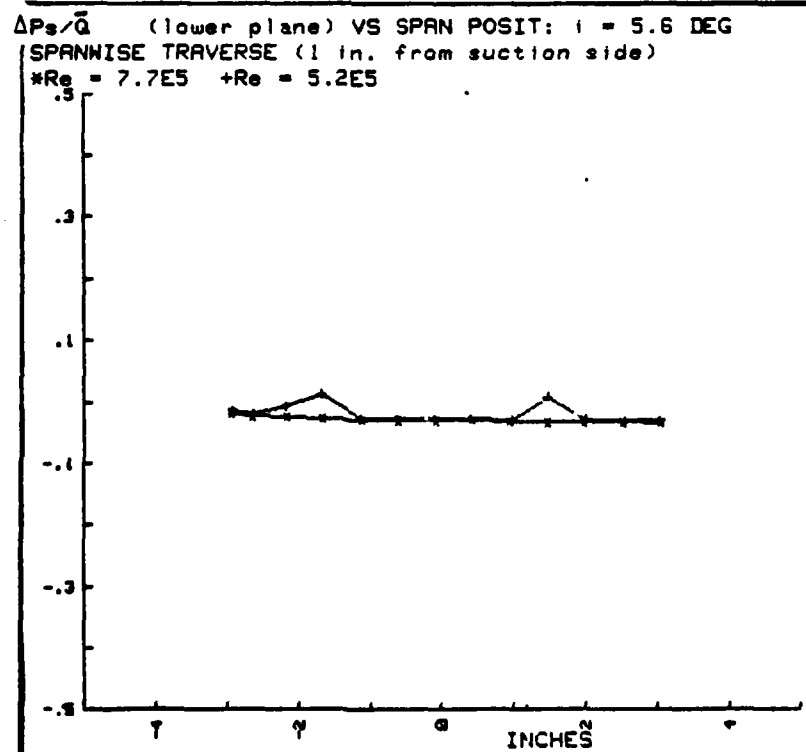


Fig. A.82

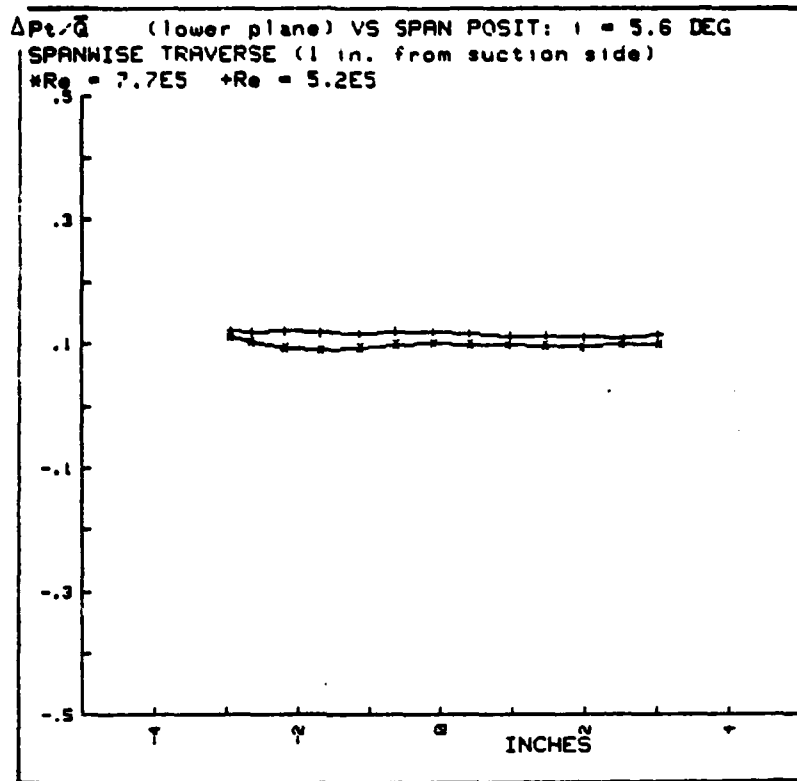


Fig. A.83

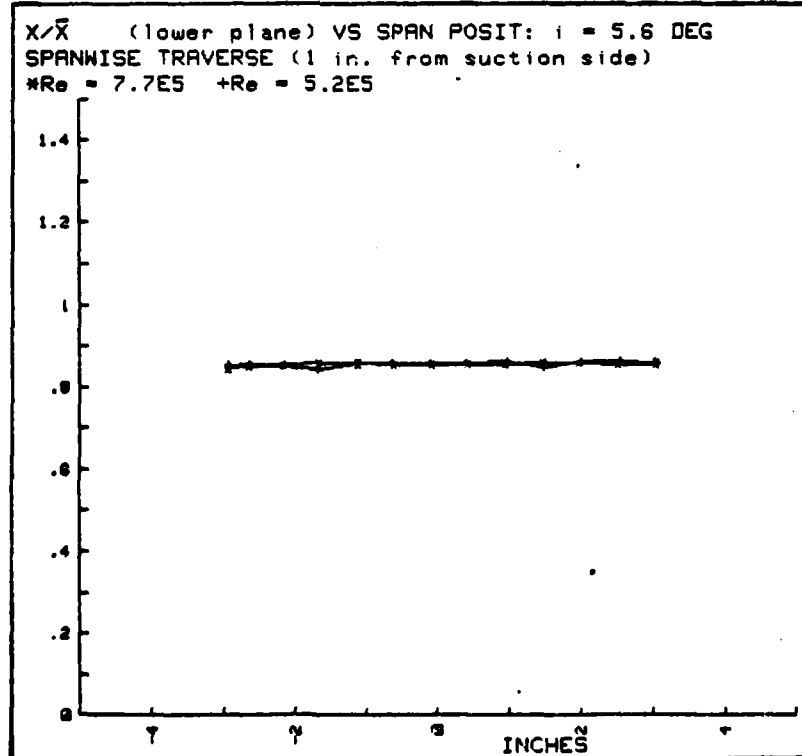


Fig. A.84

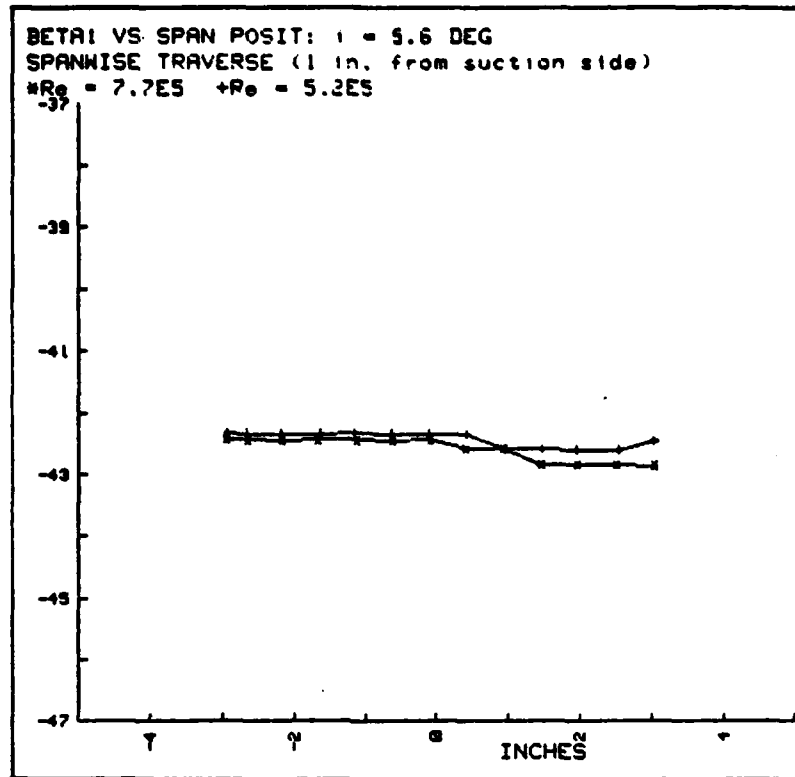


Fig. A.85

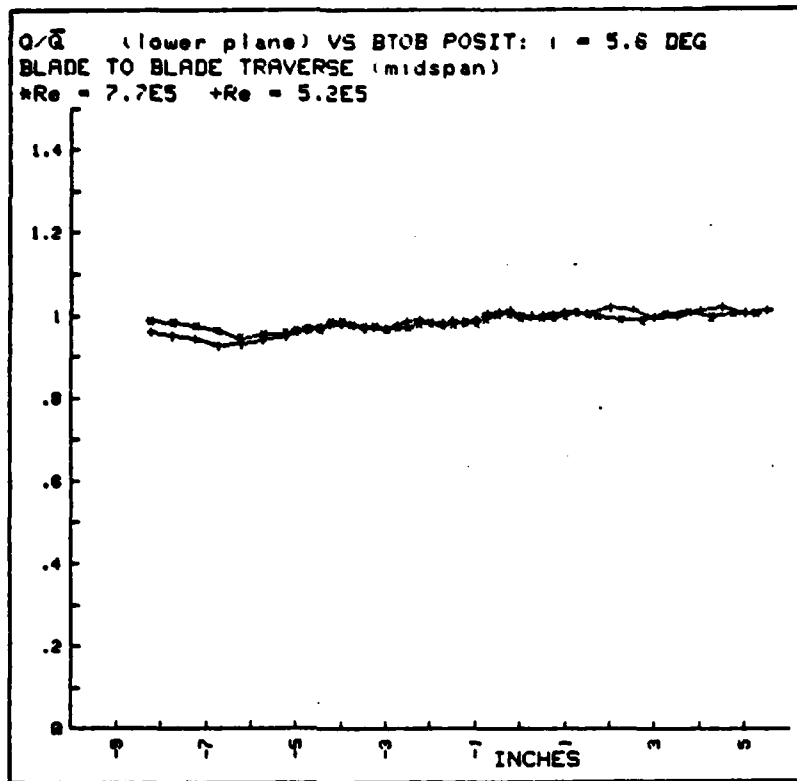


Fig. A.86

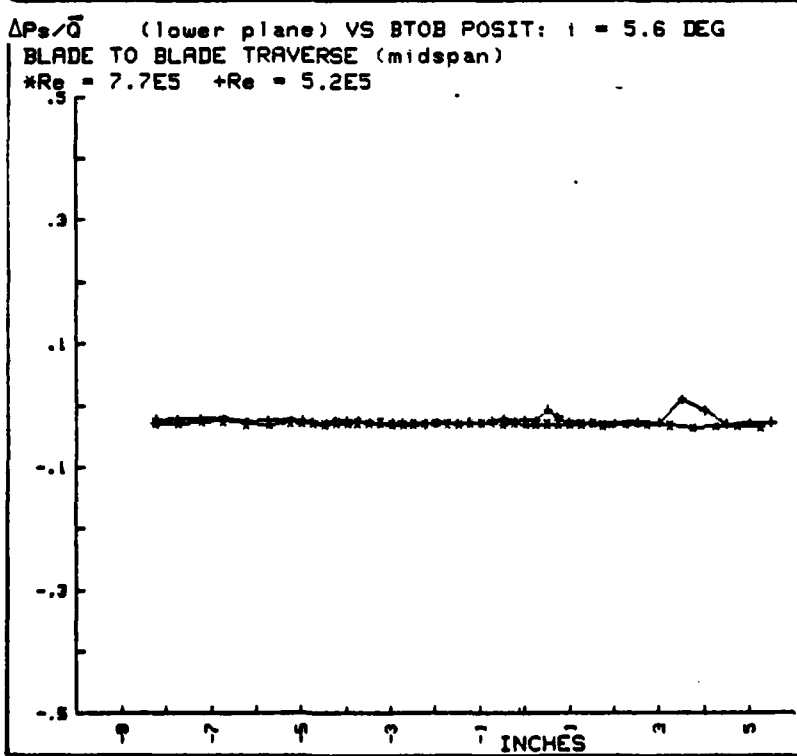


Fig. A.87

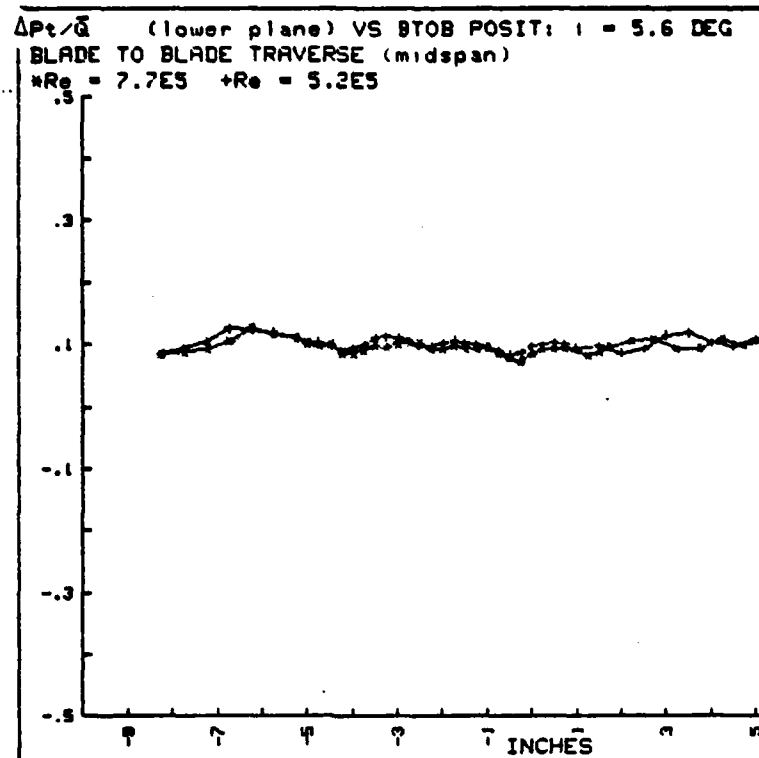


Fig. A.88

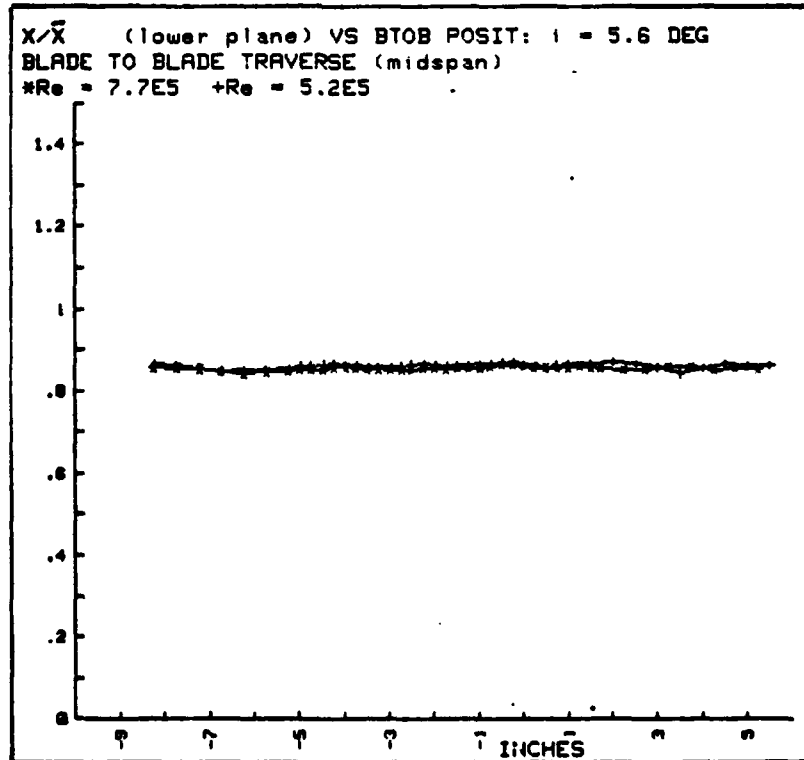


Fig. A.89

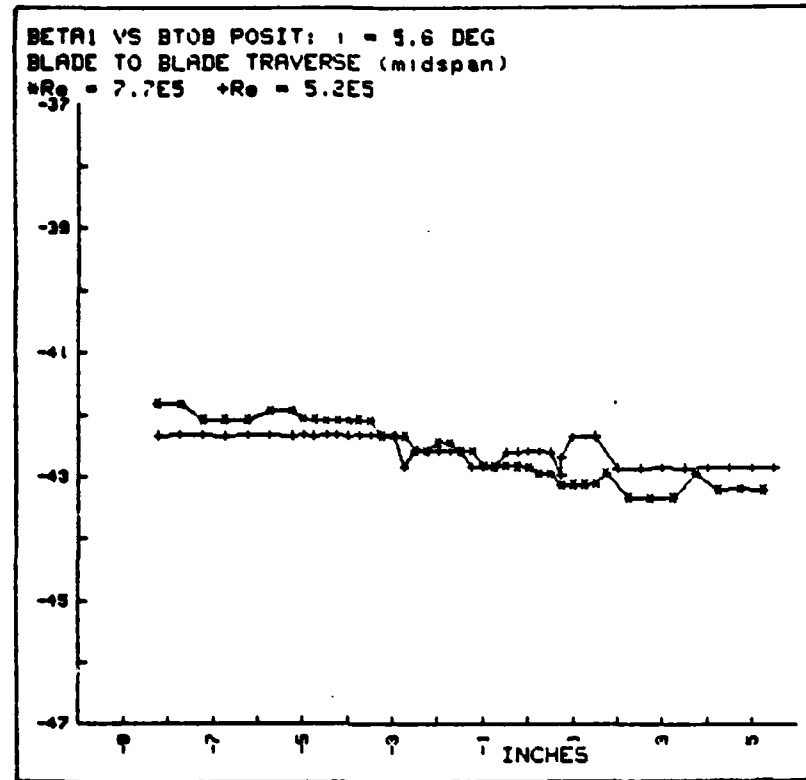


Fig. A.90

$Q/\bar{Q}$  (upper plane) VS SPAN POSIT:  $i = 8.8$  DEG  
SPANNWISE TRAVERSE (1 in. from suction side)  
 $*Re = 7.7E5 + Re = 4.9E5$

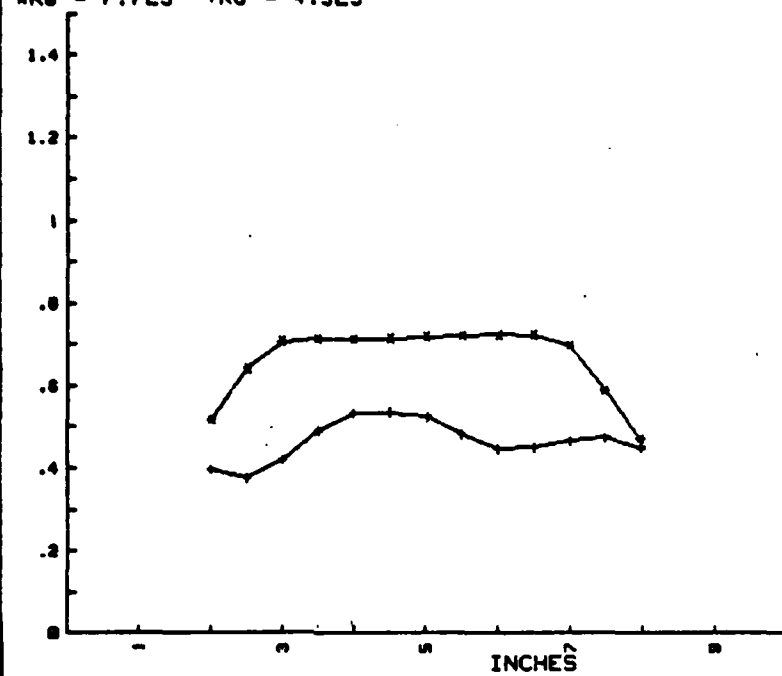


Fig. A.91

$\Delta P_s/\bar{Q}$  (upper plane) VS SPAN POSIT:  $i = 8.8$  DEG  
SPANNWISE TRAVERSE (1 in. from suction side)  
 $*Re = 7.7E5 + Re = 4.9E5$

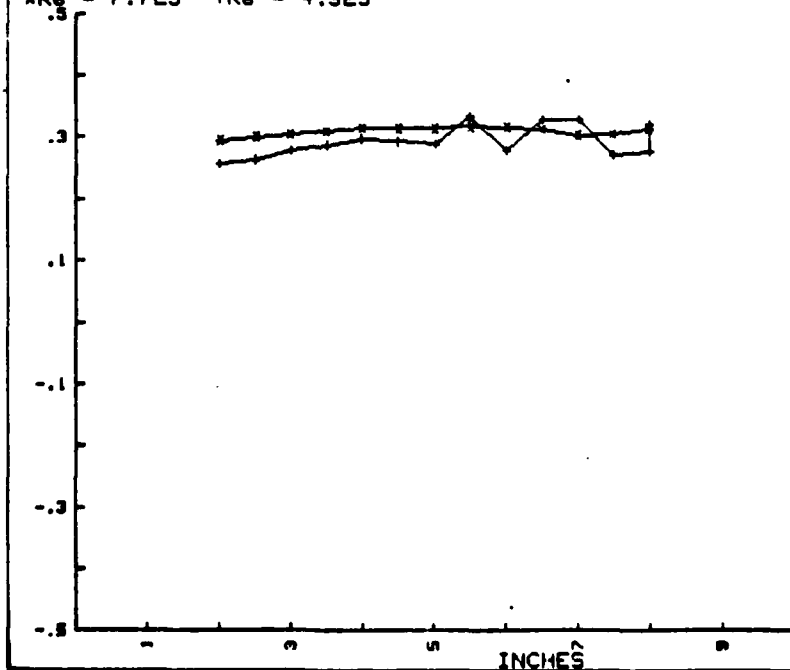


Fig. A.92

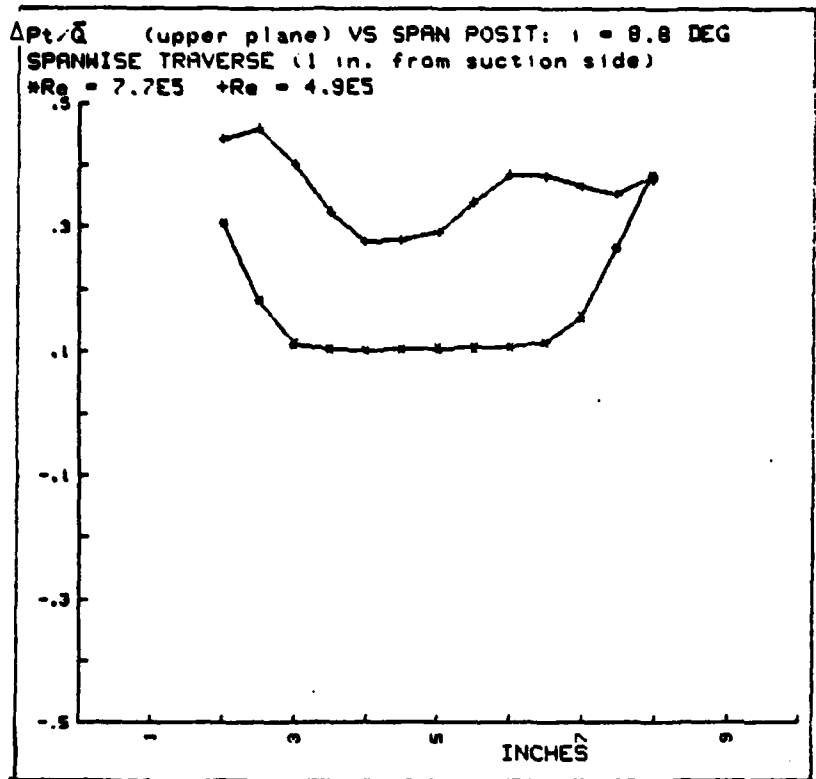


Fig. A.93

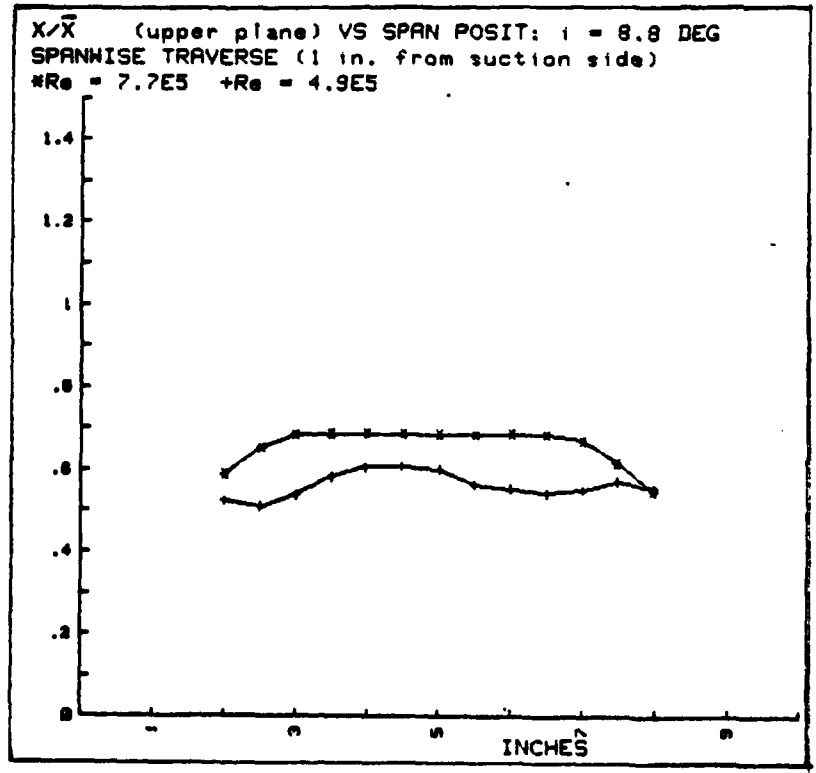


Fig. A.94

BETA2 VS SPAN POSIT:  $\delta = 0.8$  DEG  
SPANWISE TRAVERSE (1 in. from suction side)  
 $*R_g = 7.7E5$   $+Re = 4.9E5$

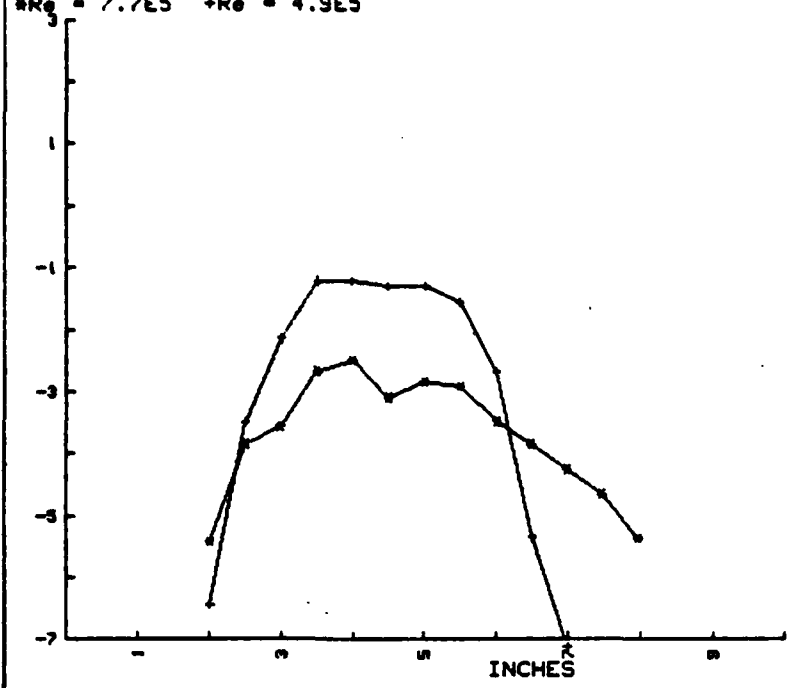


Fig. A.95

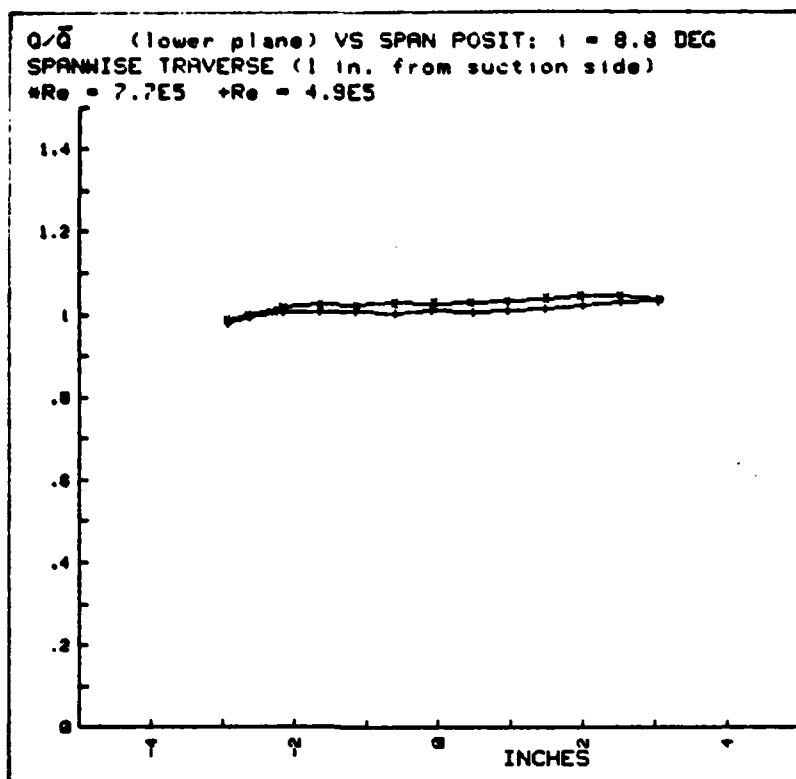


Fig. A.96

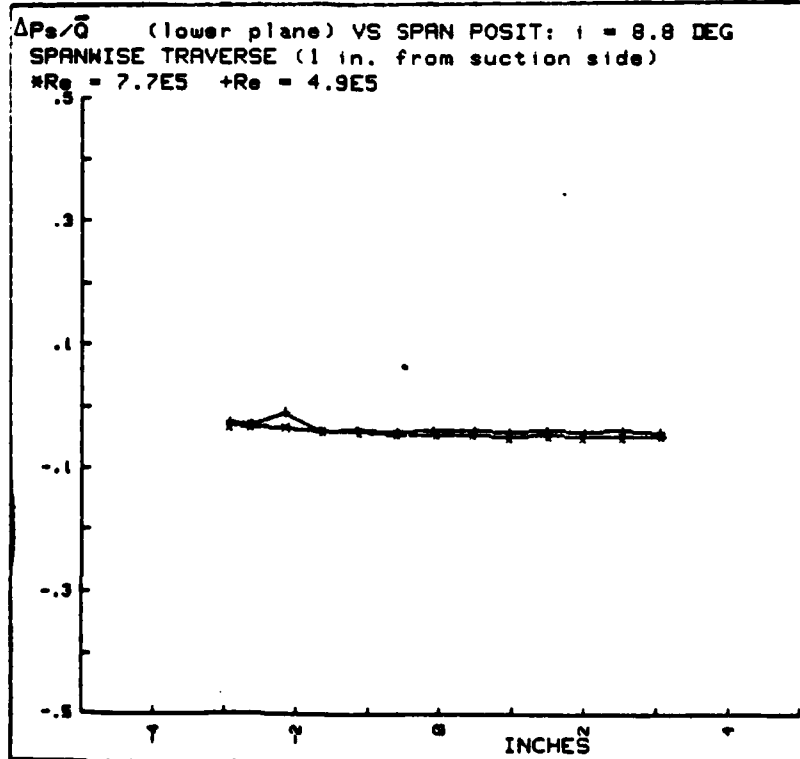


Fig. A.97

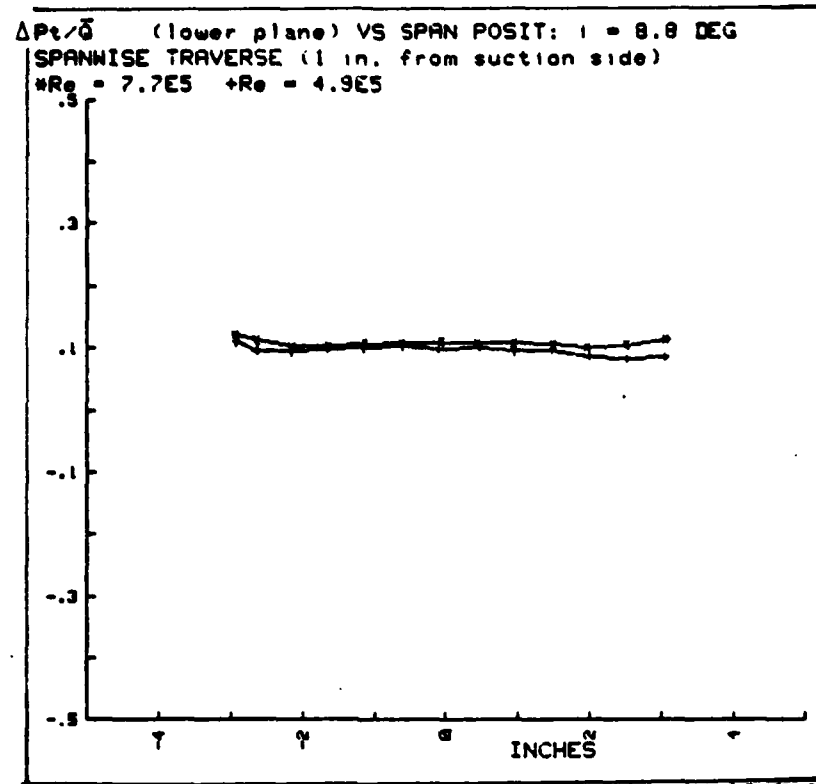


Fig. A.98

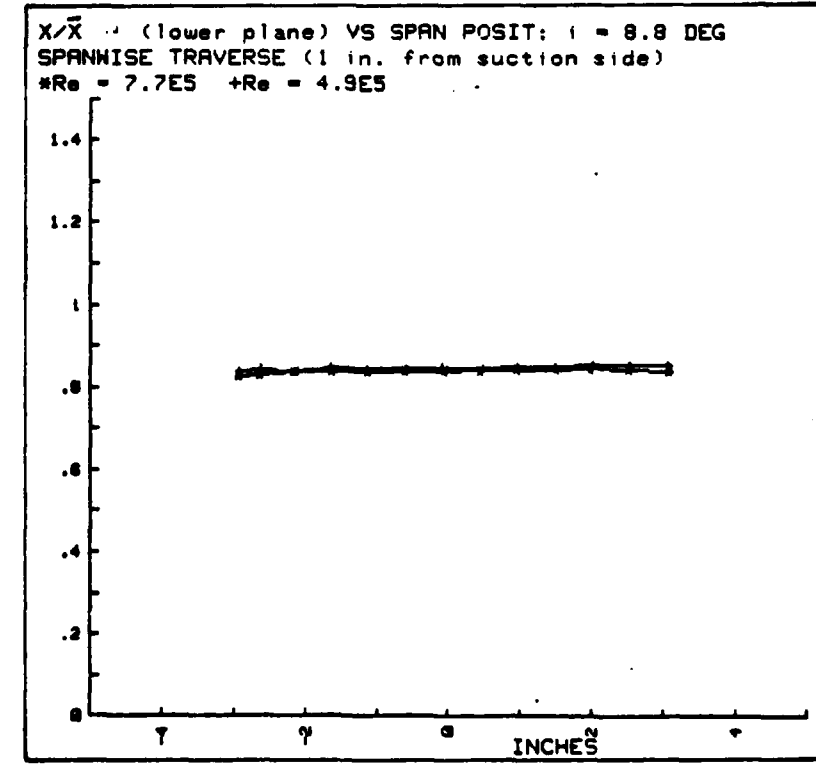


Fig. A.99

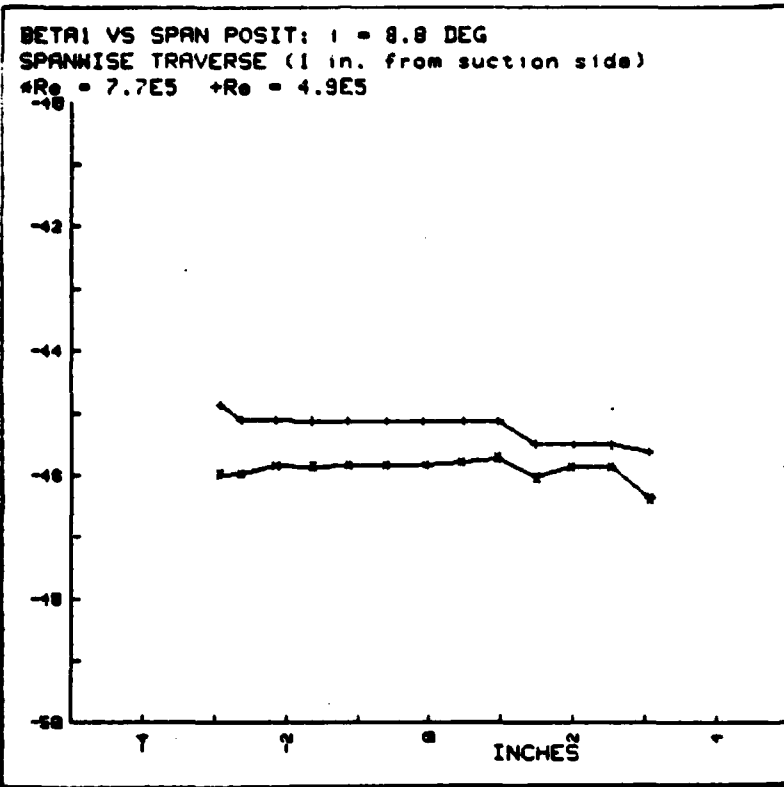


Fig. A.100

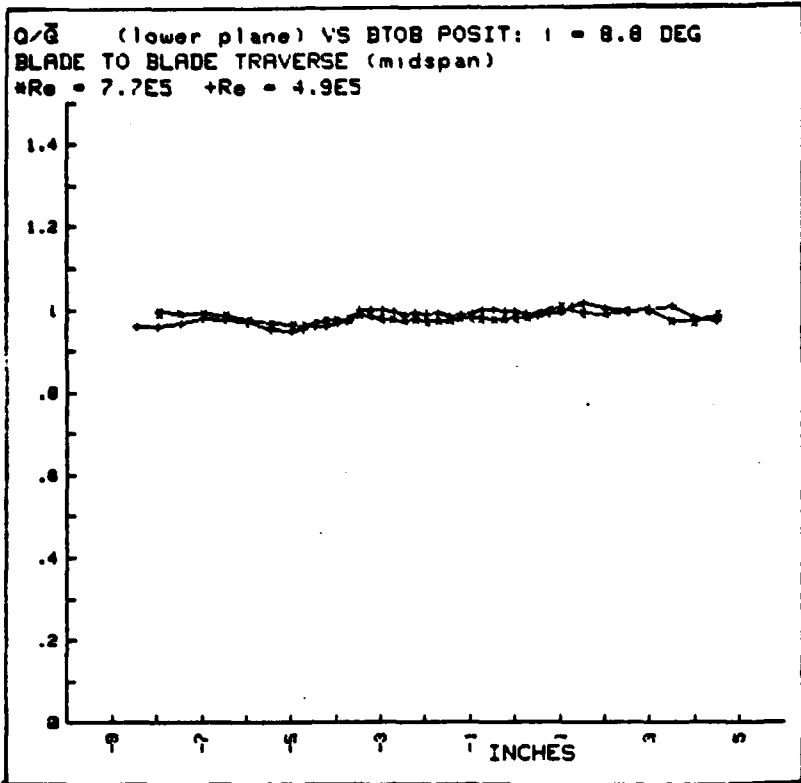


Fig. A.101

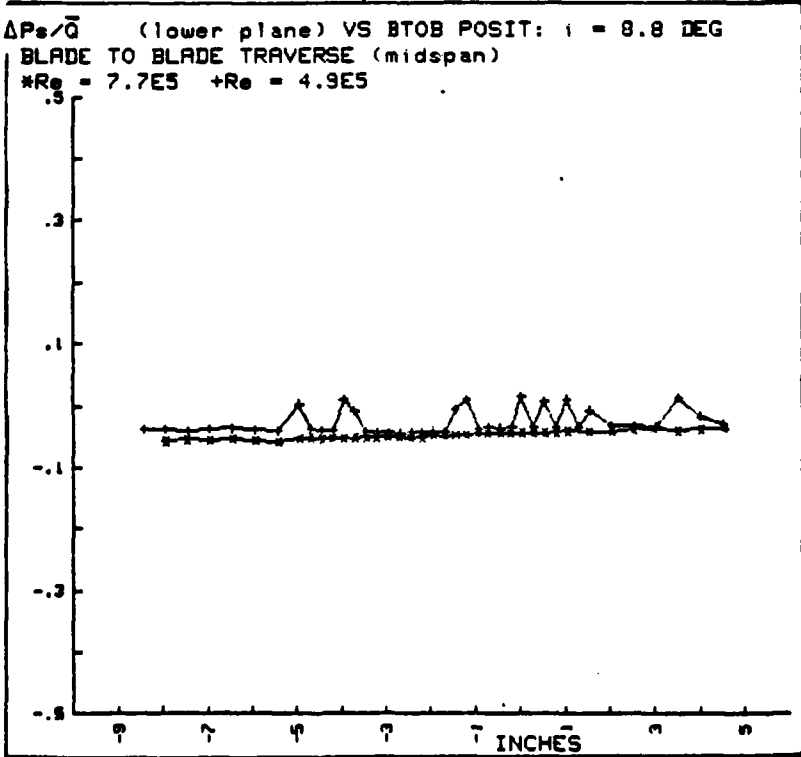


Fig. A.102

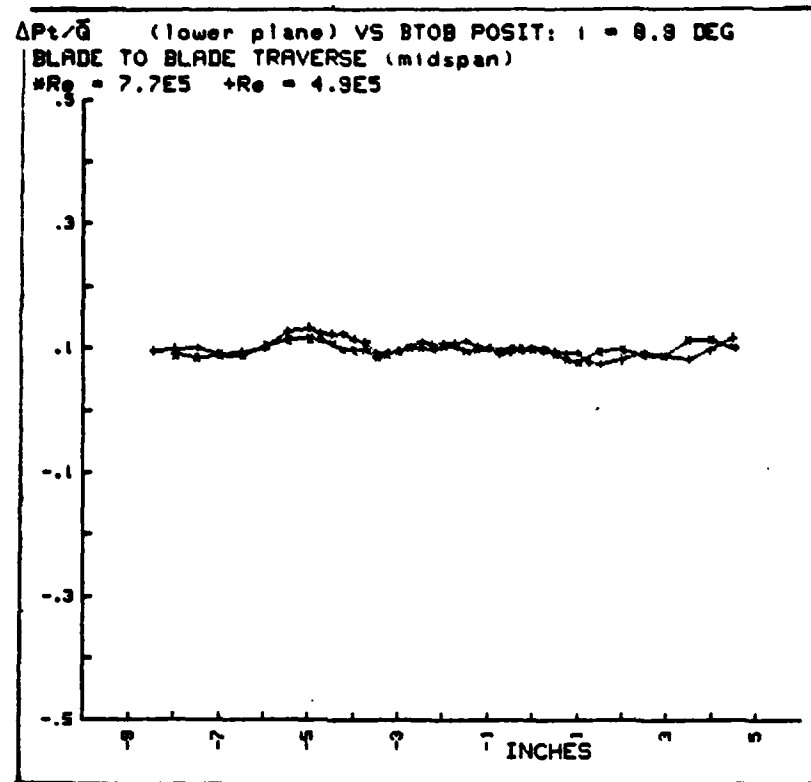


Fig. A.103

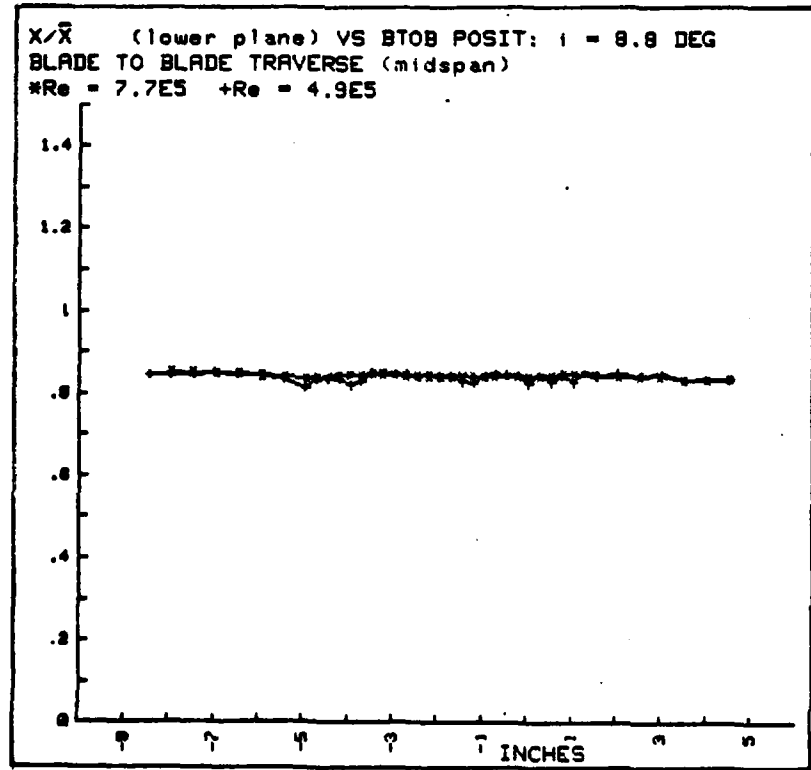


Fig. A.104

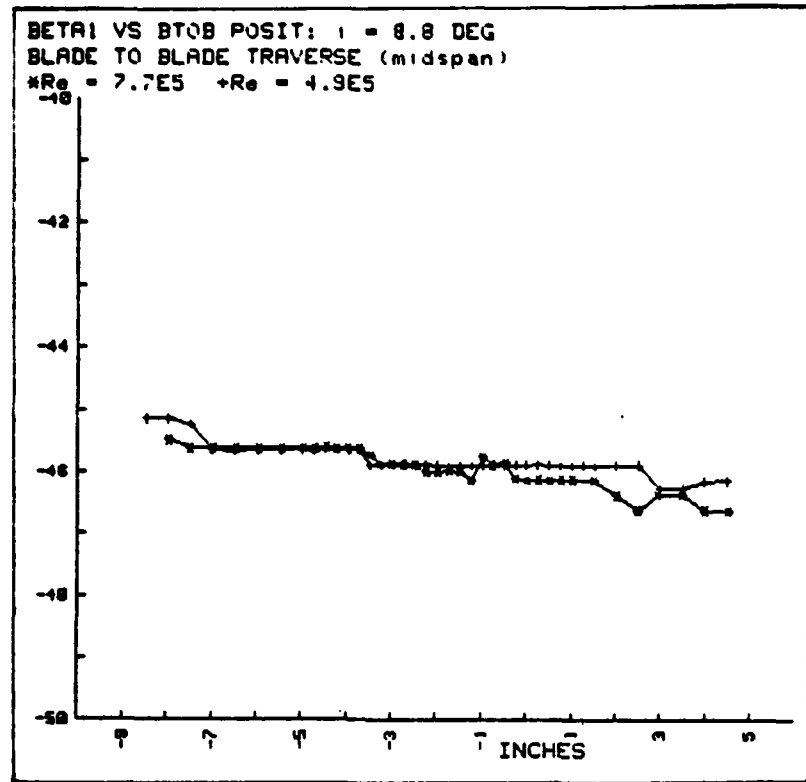


Fig. A.105

$i = -12.50^\circ$ ,  $Re = 611,000$

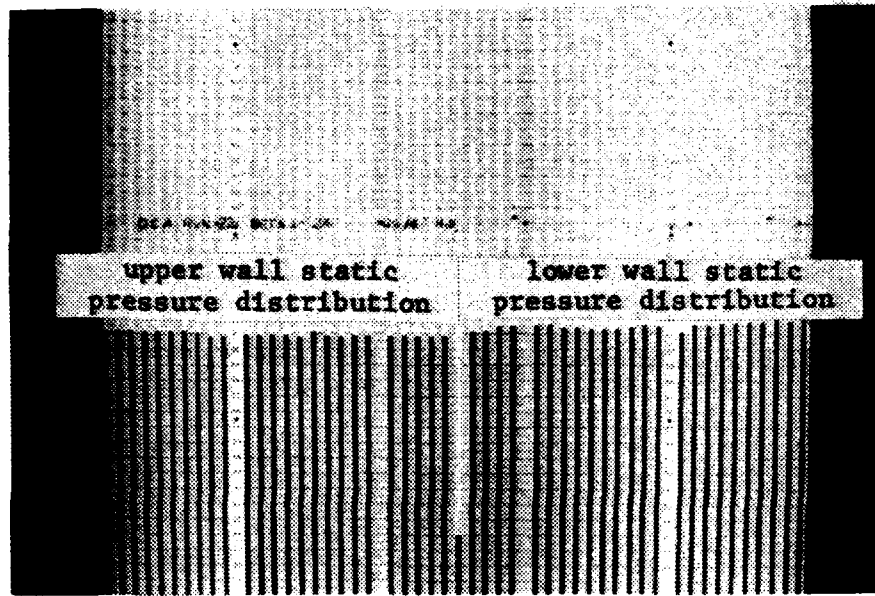


Fig. A.106

$i = -12.39^\circ$ ,  $Re = 535,000$

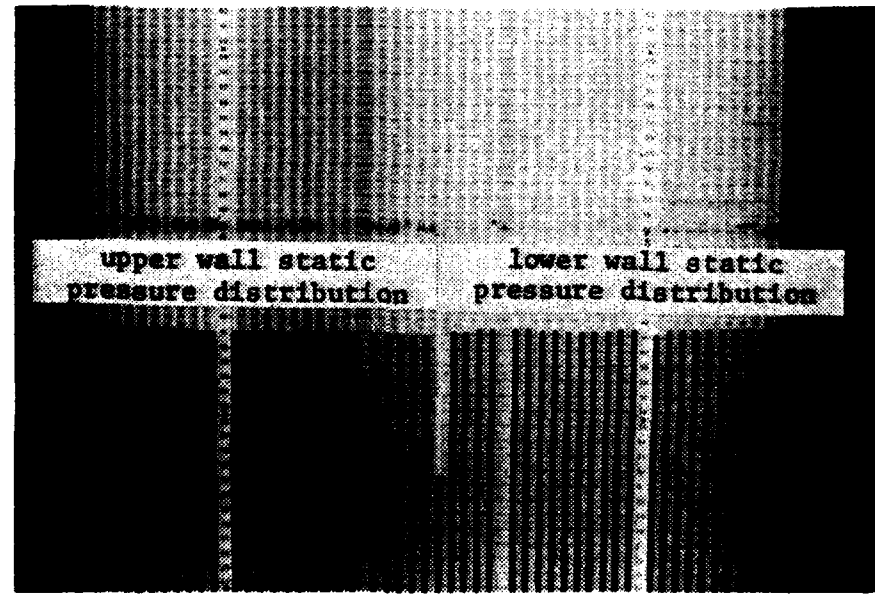


Fig. A.107

$i = -9.58^\circ$ ,  $Re = 626,000$

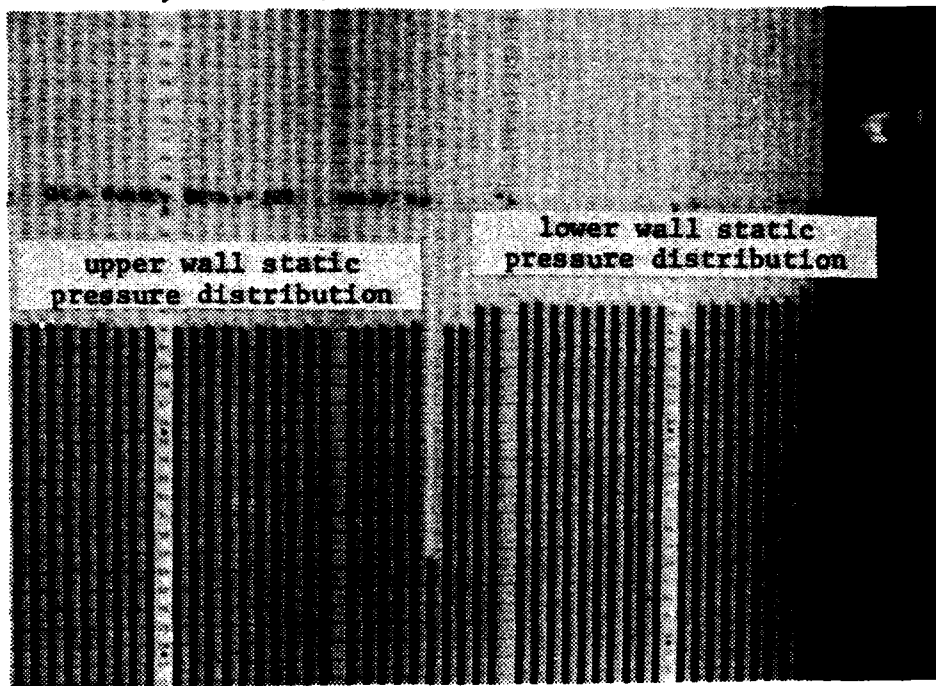


Fig. A.108

$i = -9.23$ ,  $Re = 502,000$

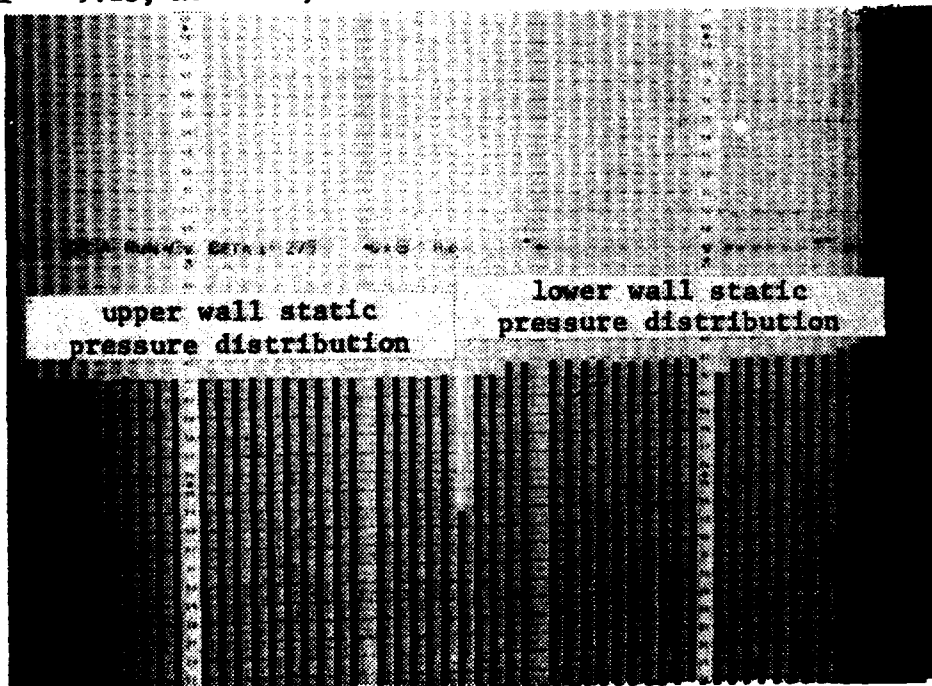


Fig. A.109

$$i = -5.81^\circ, Re = 560,000$$

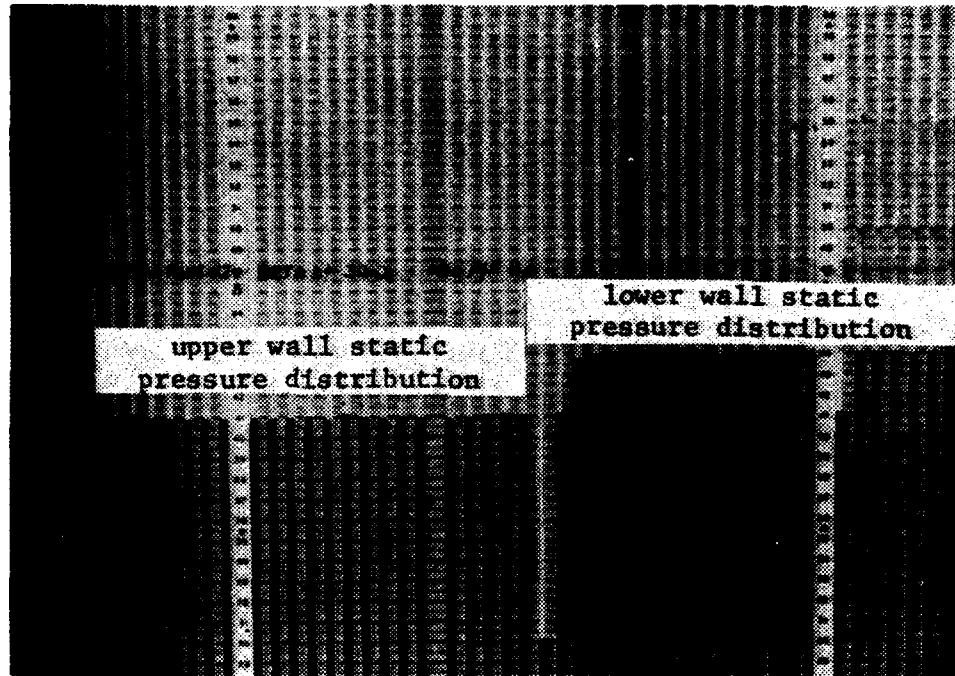


Fig. A.110

$$i = -5.57^\circ, Re = 503,000$$

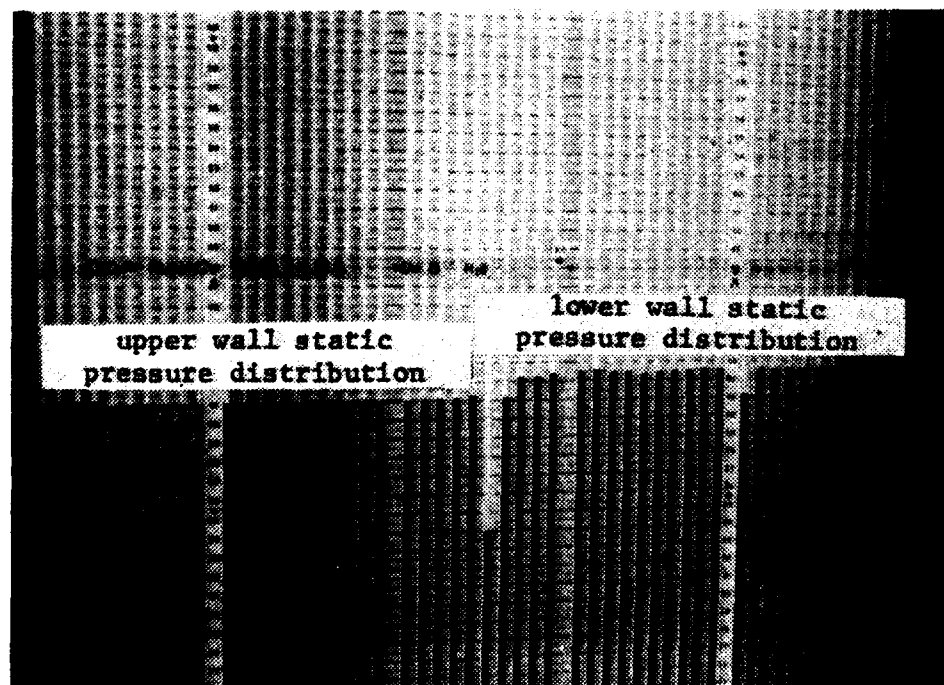


Fig. A.111

$i = -1.59^\circ$ ,  $Re = 643,000$

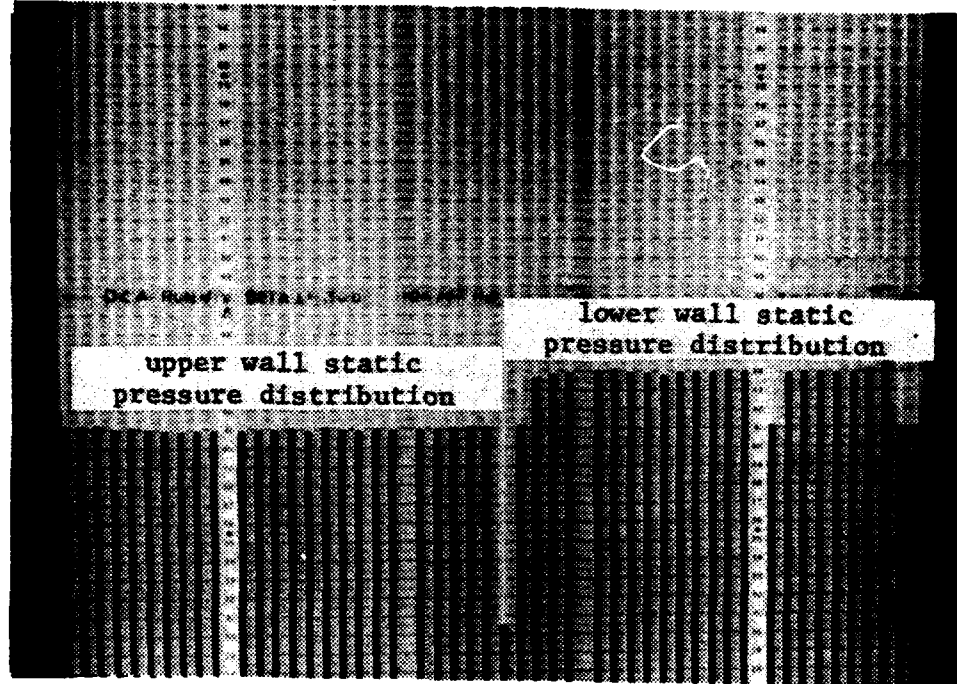


Fig. A.112

$i = -1.50^\circ$ ,  $Re = 525,000$

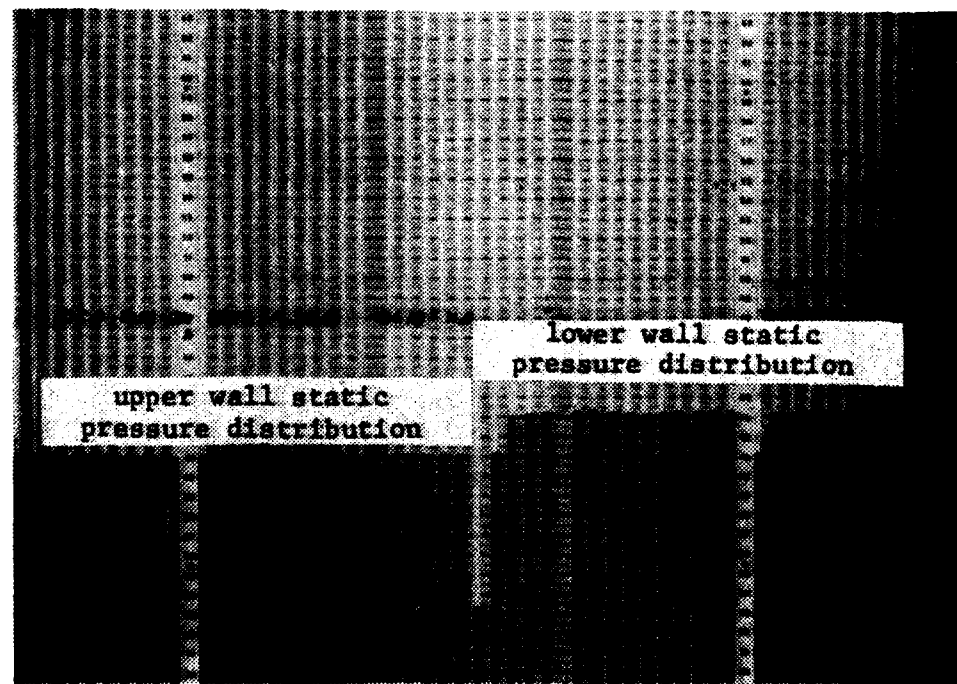


Fig. A.113

$i = 2.27^\circ$ ,  $Re = 676,000$

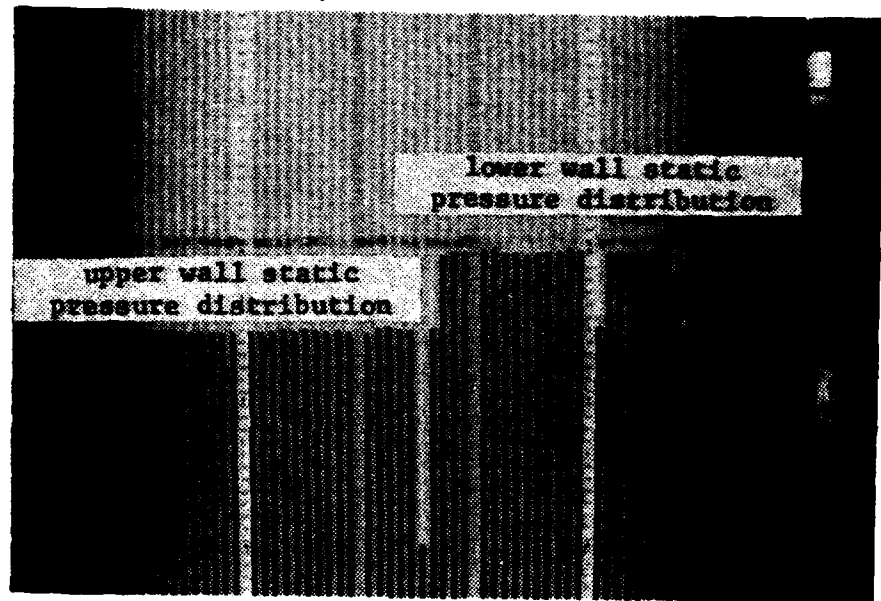


Fig. A.114

$i = 2.23^\circ$ ,  $Re = 604,000$

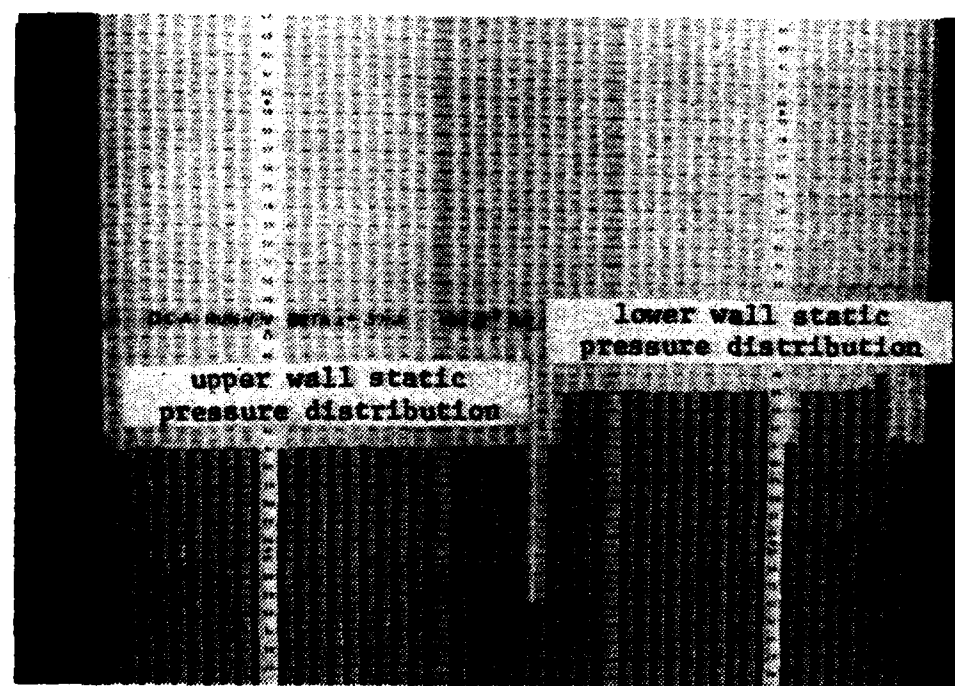


Fig. A.115  
125

$i = 5.99^\circ$ ,  $Re = 771,000$

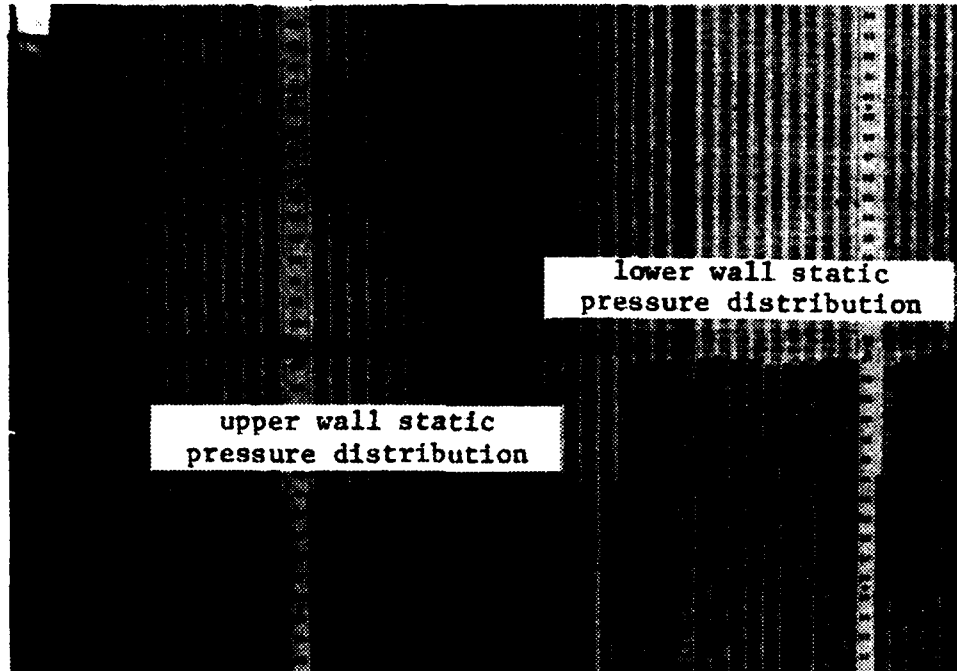


Fig. A.116

$i = 5.54^\circ$ ,  $Re = 518,000$

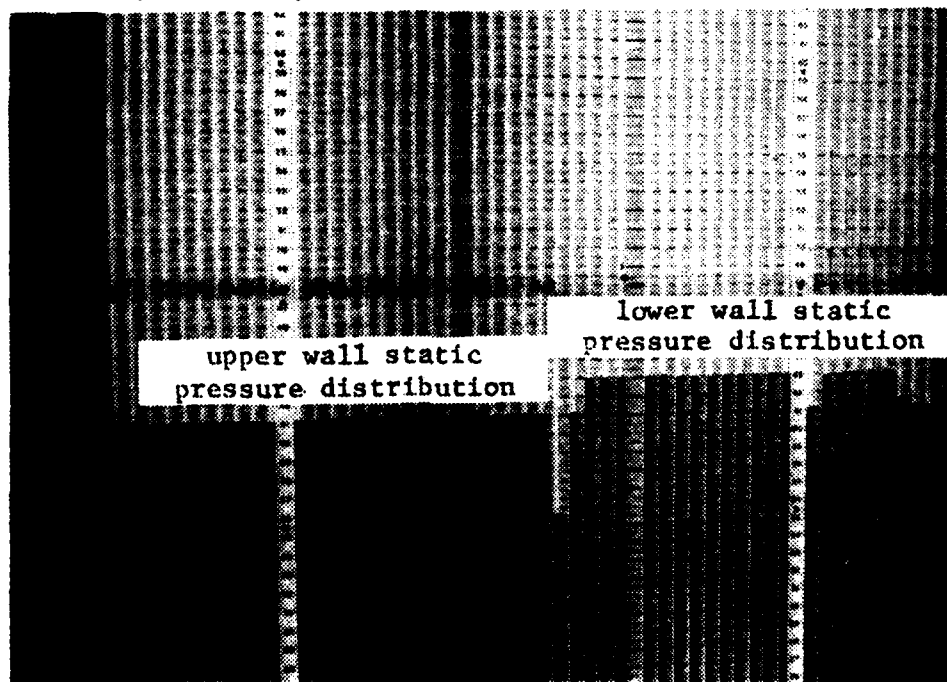


Fig. A.117  
126

$i = 8.79^\circ$ ,  $Re = 768,000$

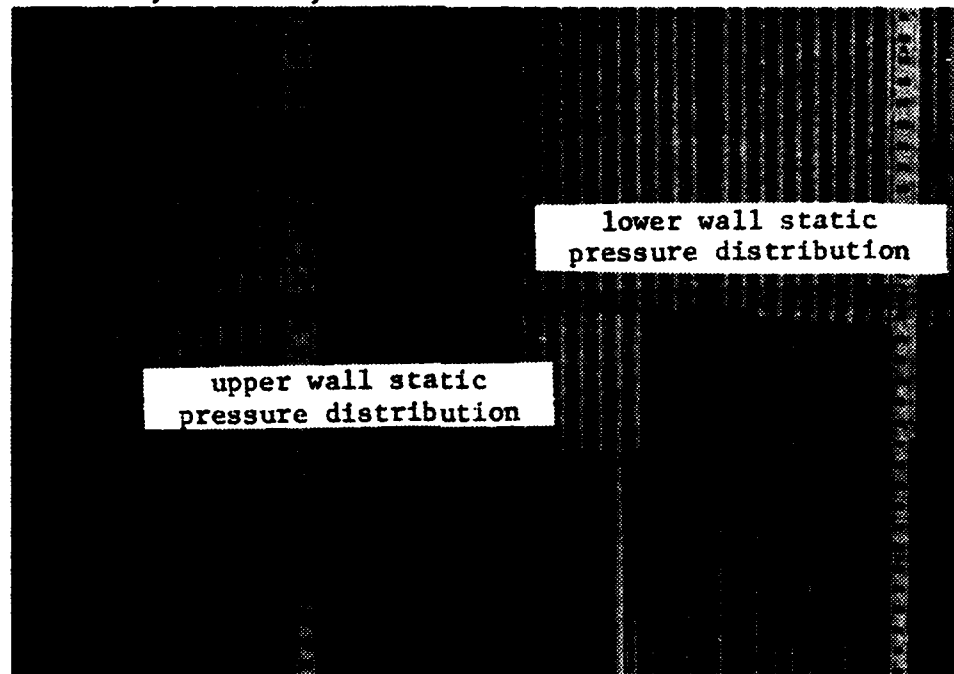


Fig. A.118

$i = 8.76^\circ$ ,  $Re = 493,000$

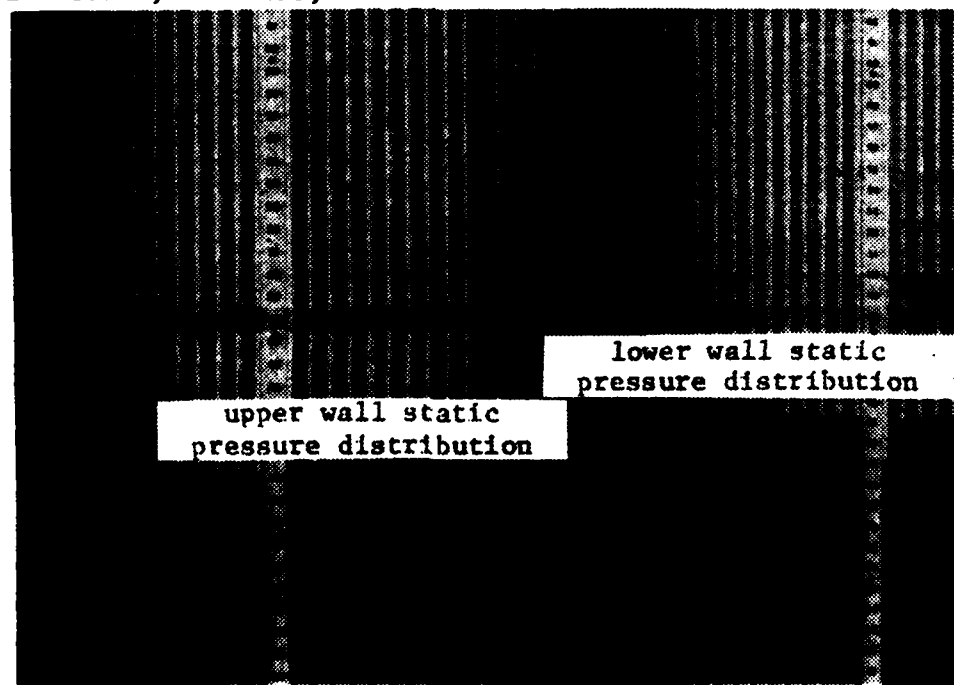


Fig. A.119  
127

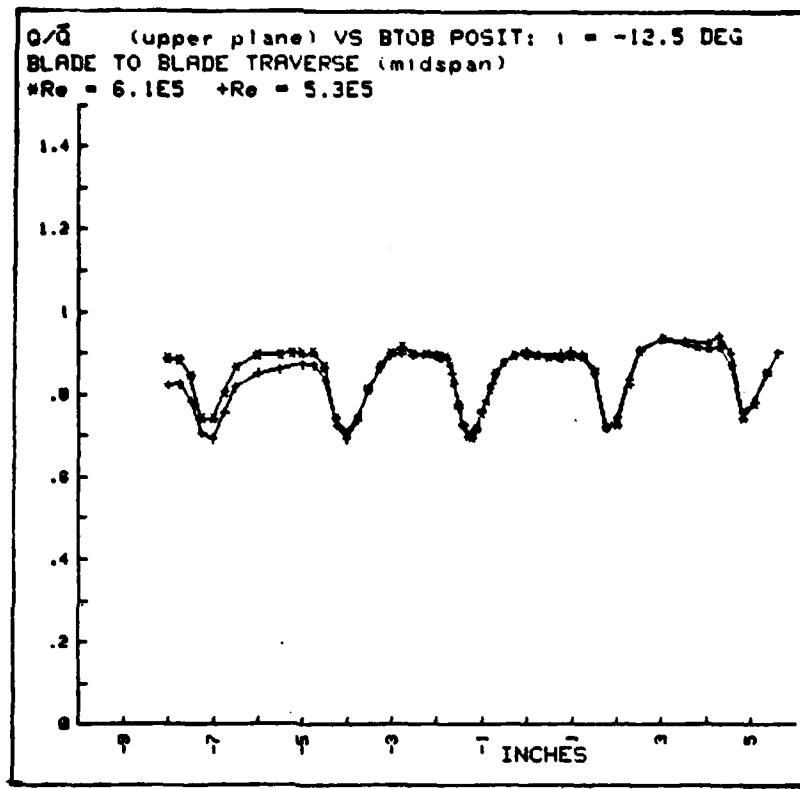


Fig. A.120

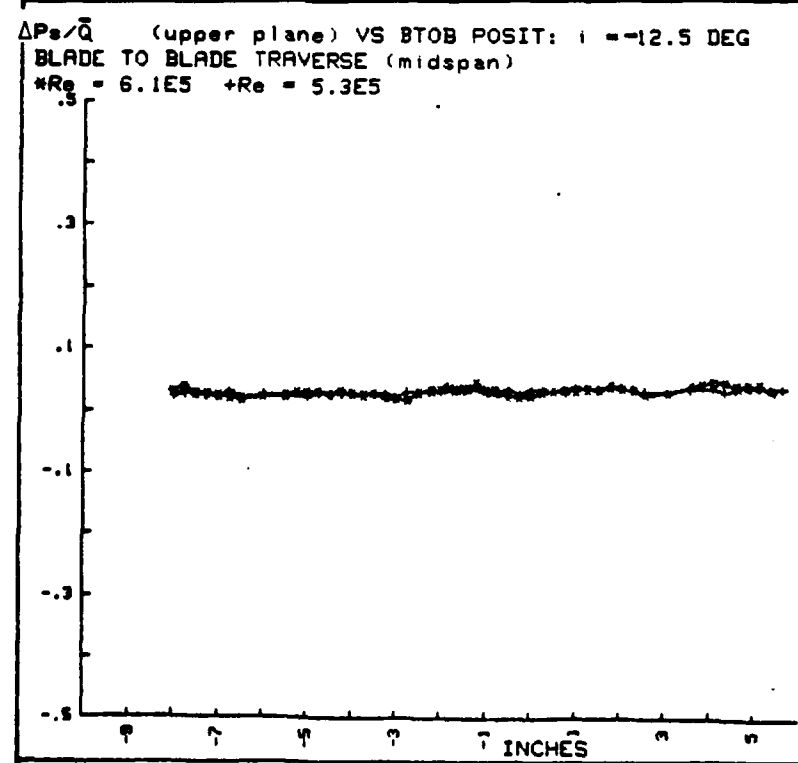


Fig. A.121

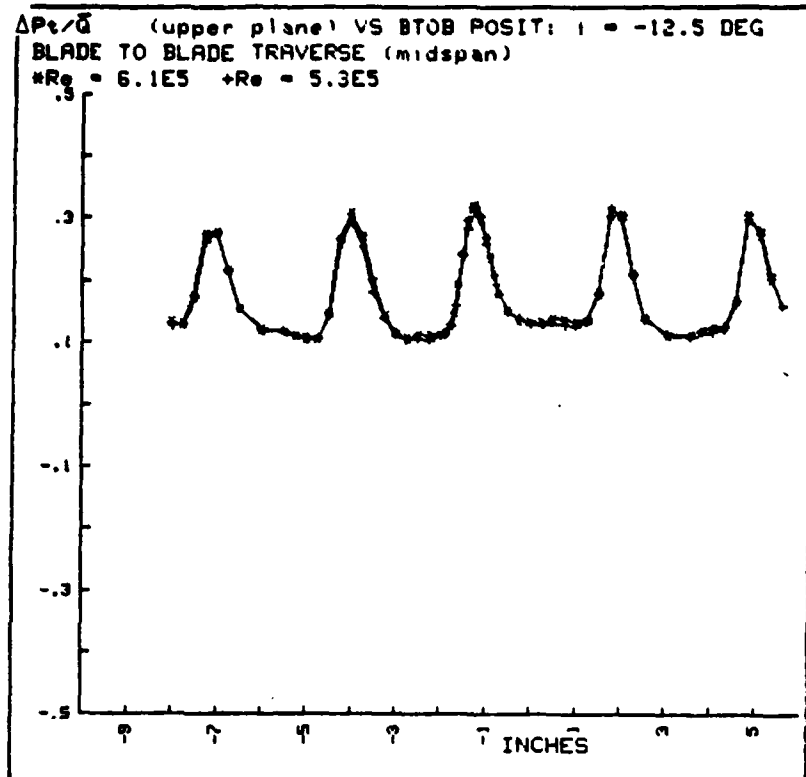


Fig. A.122

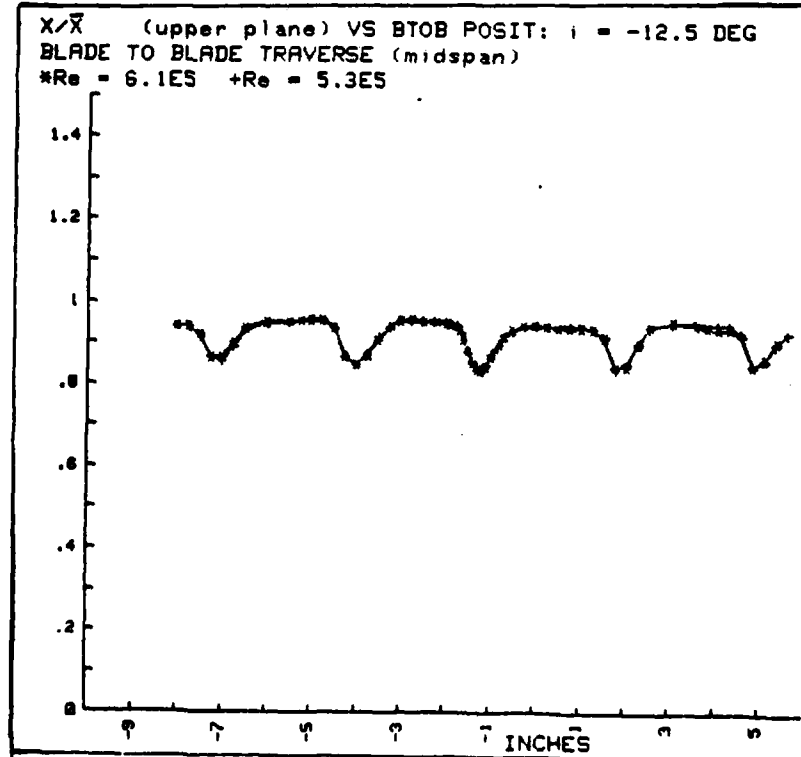


Fig. A.123

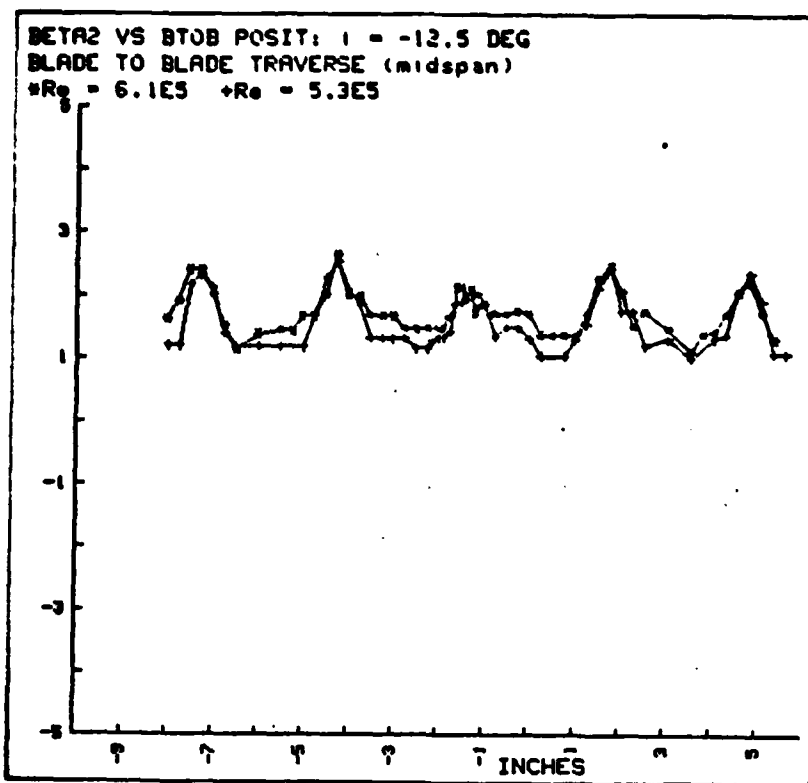


Fig. A.124

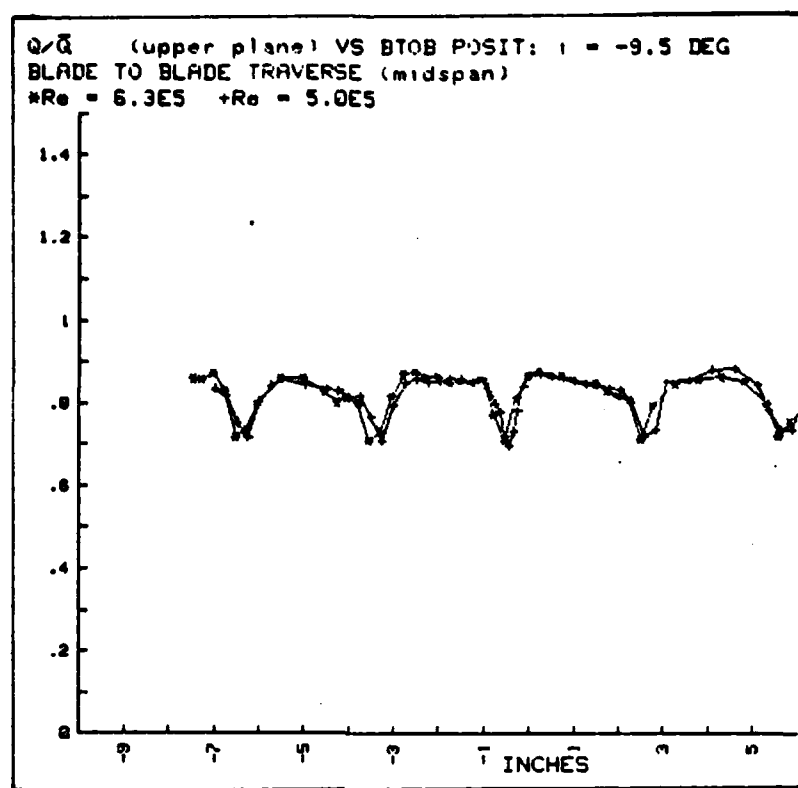


Fig. A.125

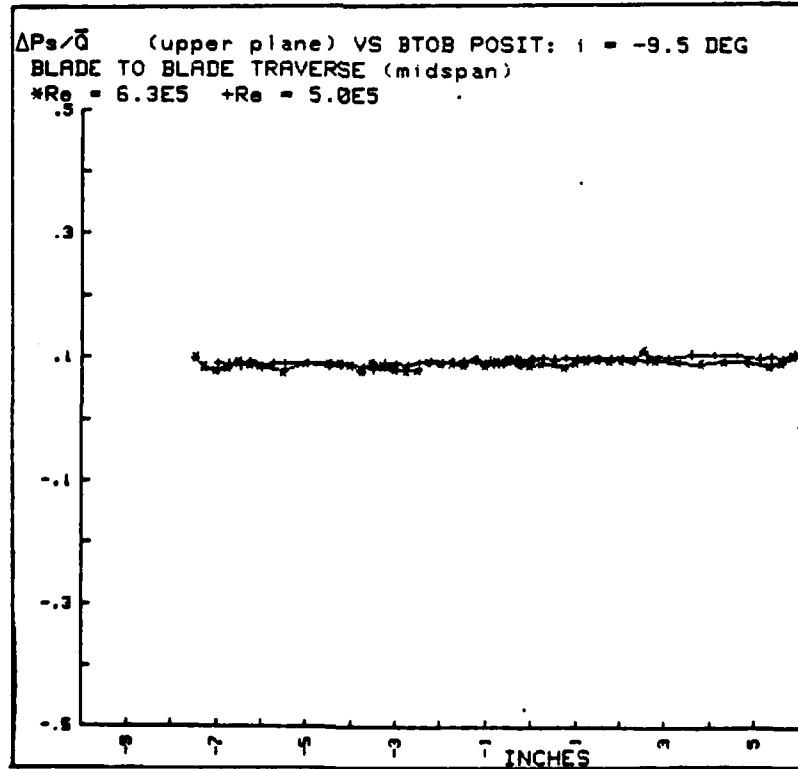


Fig. A.126

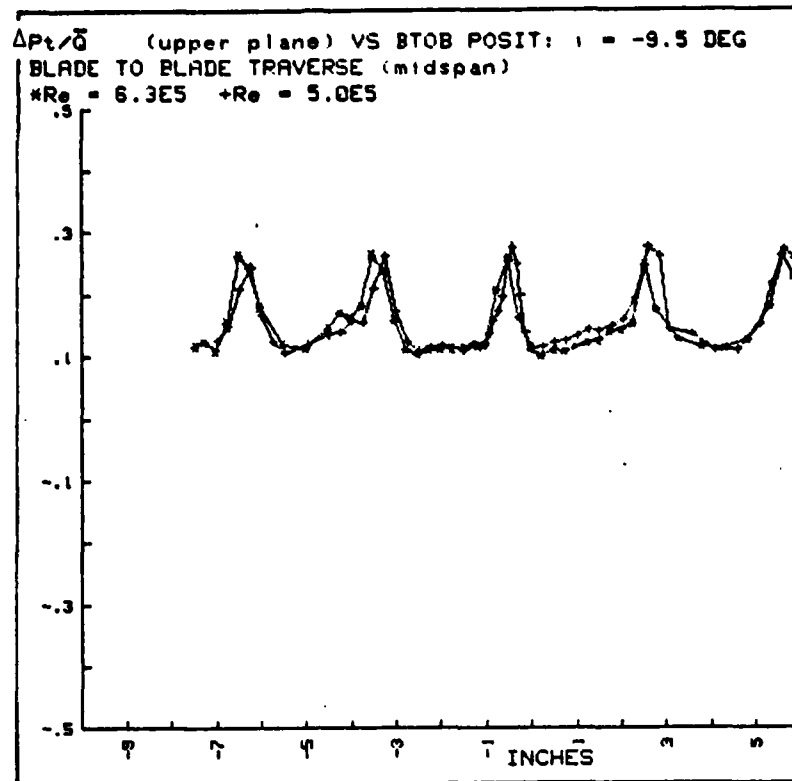


Fig. A.127

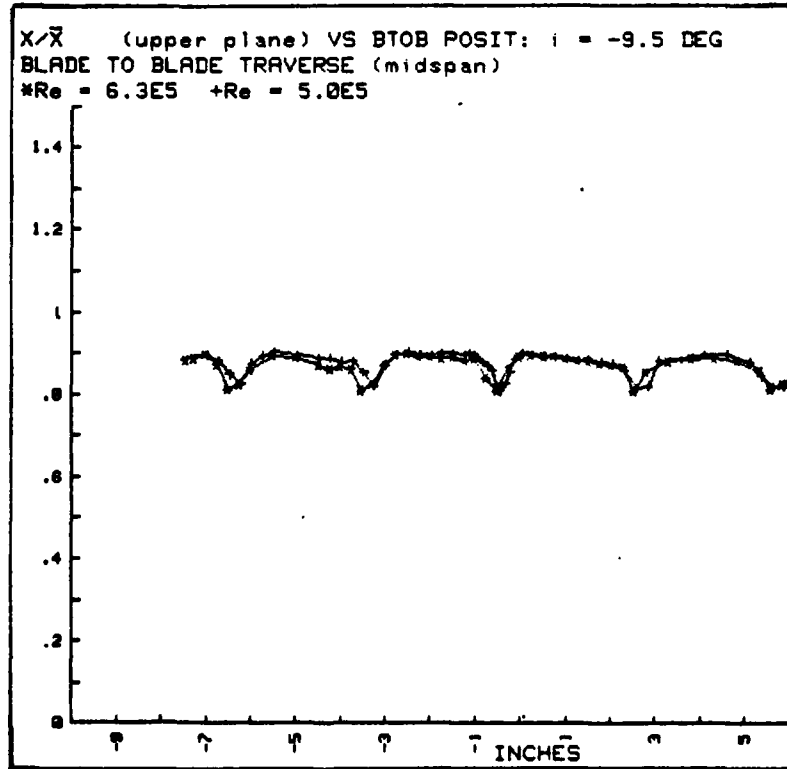


Fig. A.128

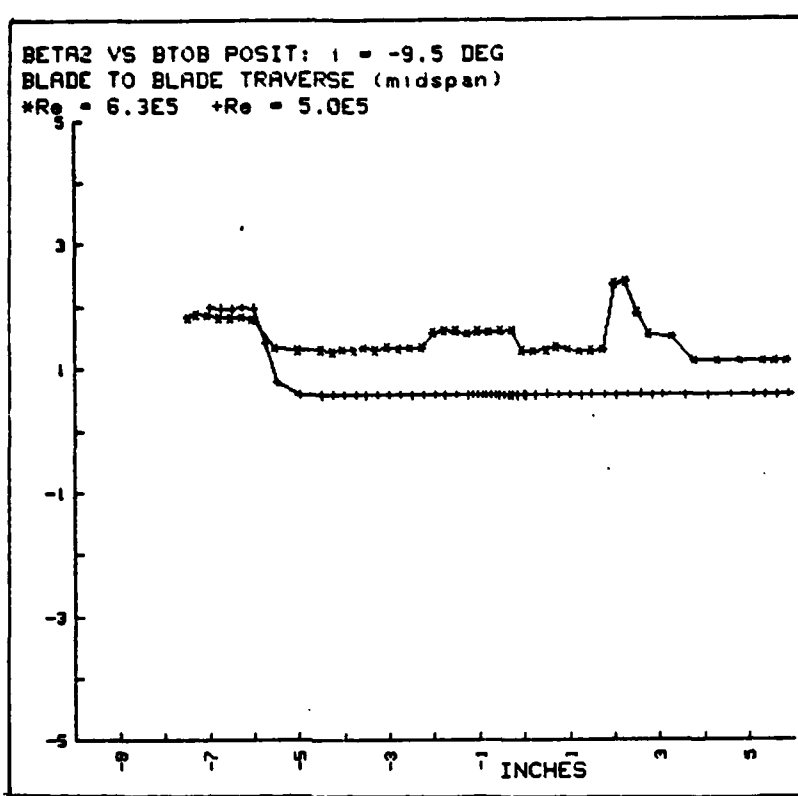


Fig. A.129

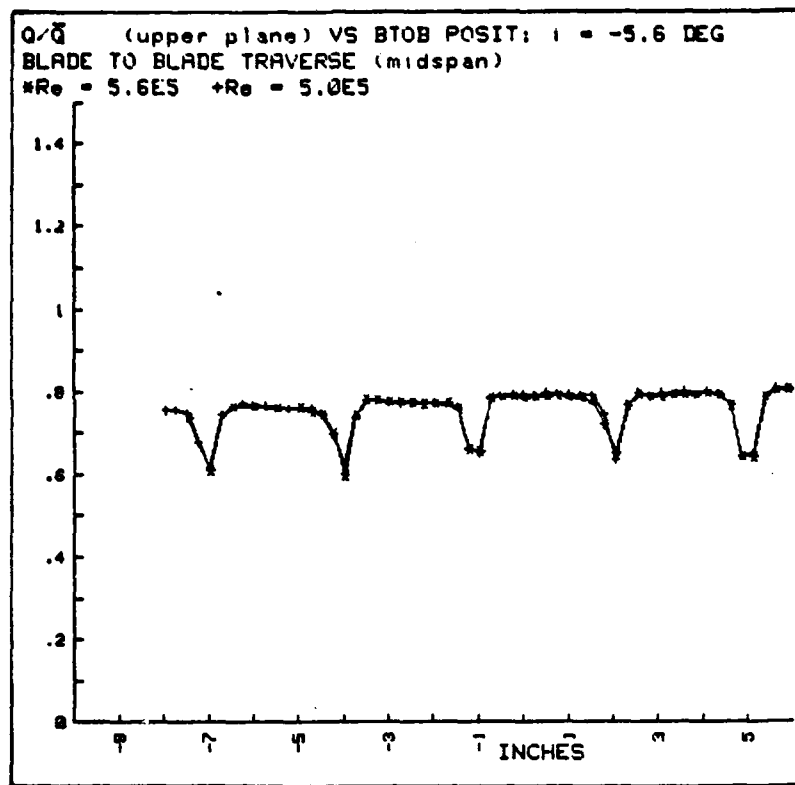


Fig. A.130

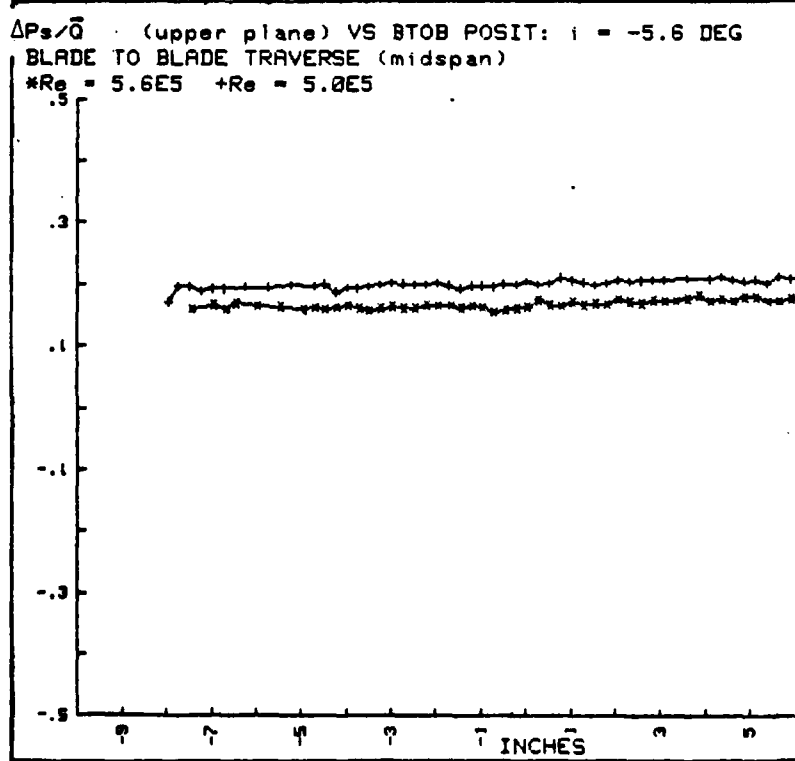


Fig. A.131

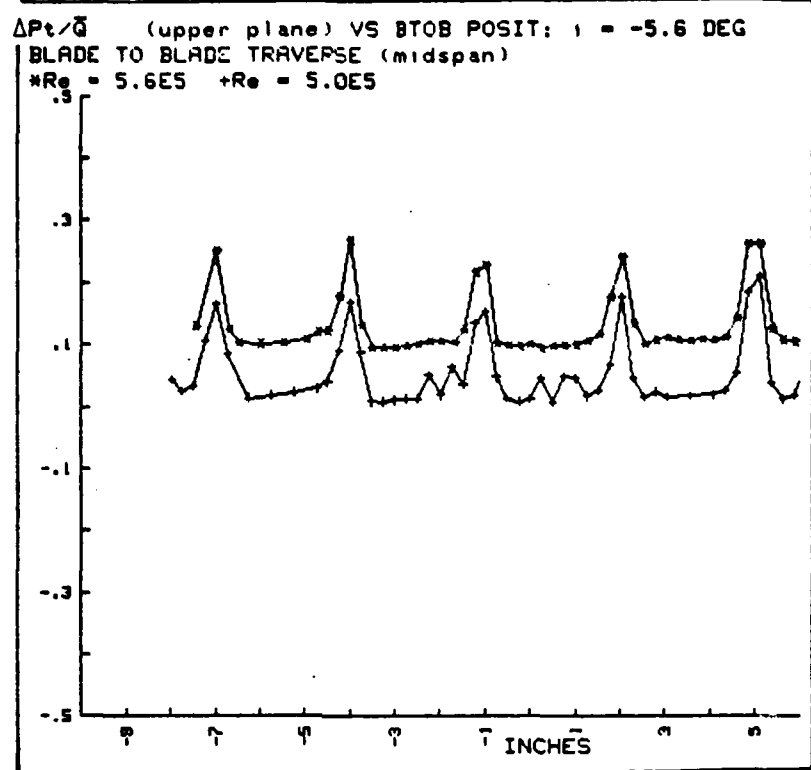


Fig. A.132

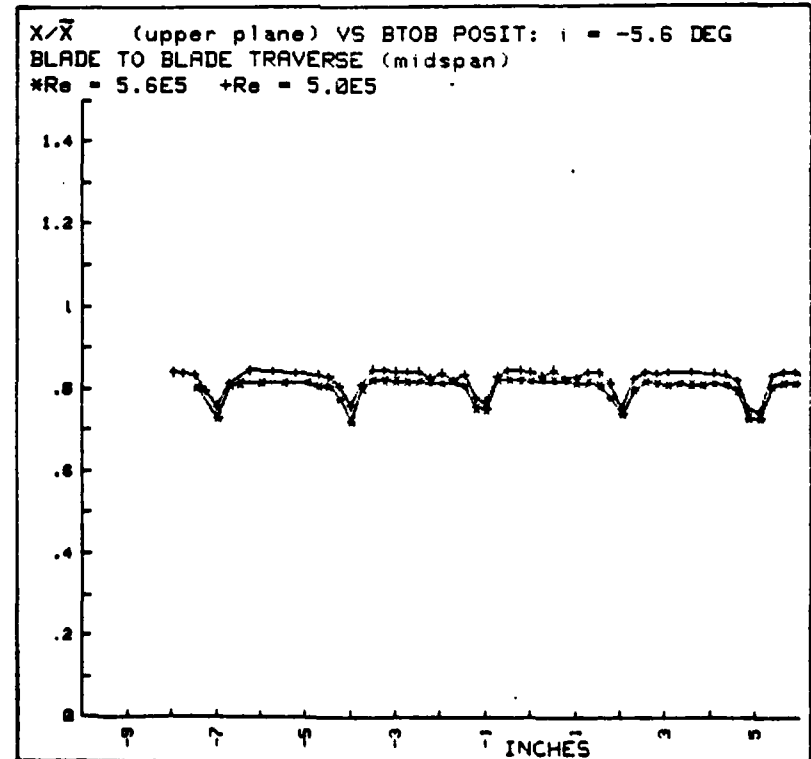


Fig A.133

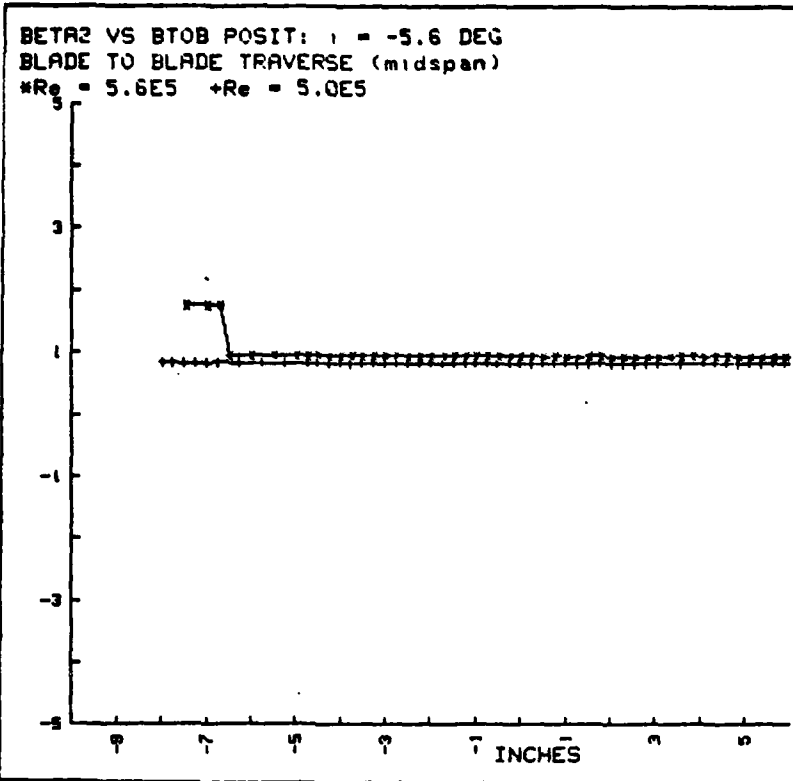


Fig. A.134

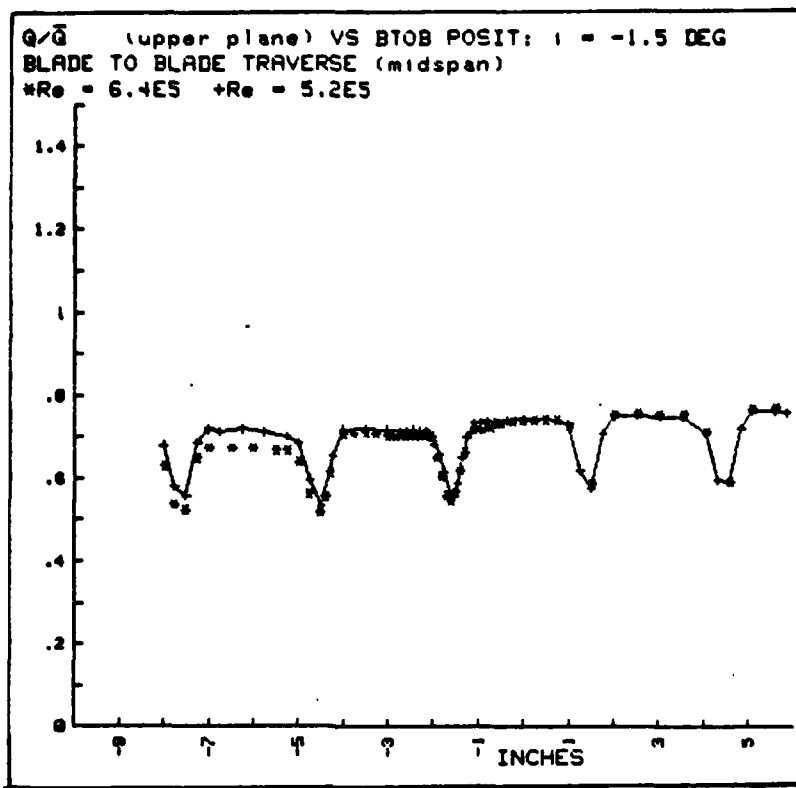


Fig. A.135

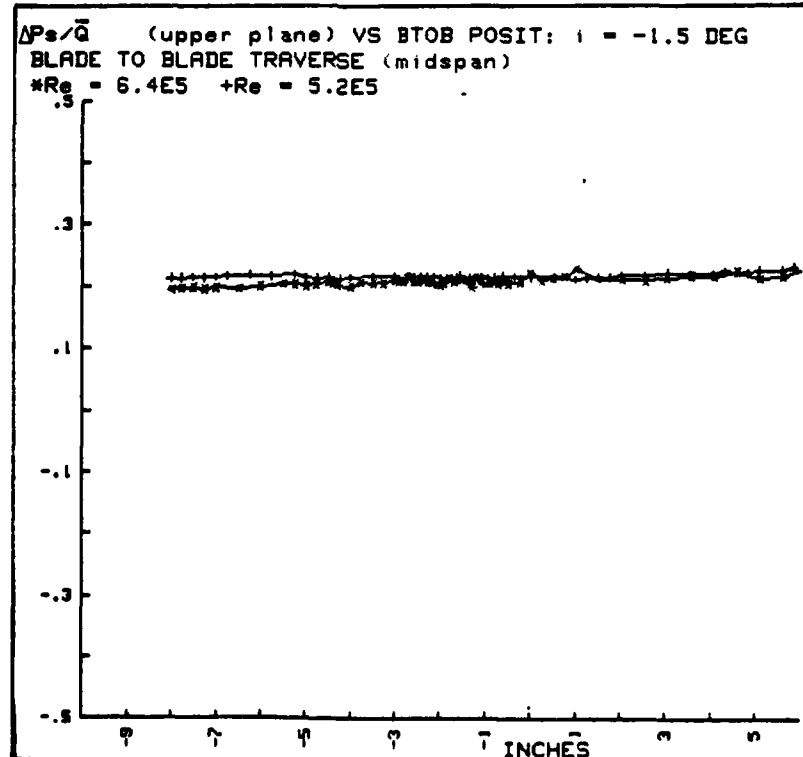


Fig. A.136

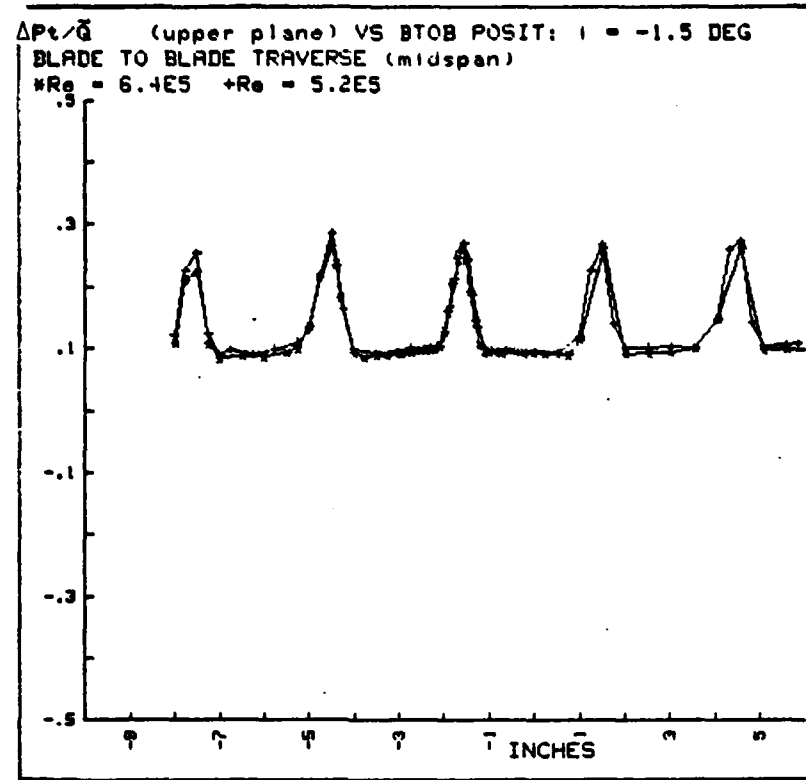


Fig. A.137

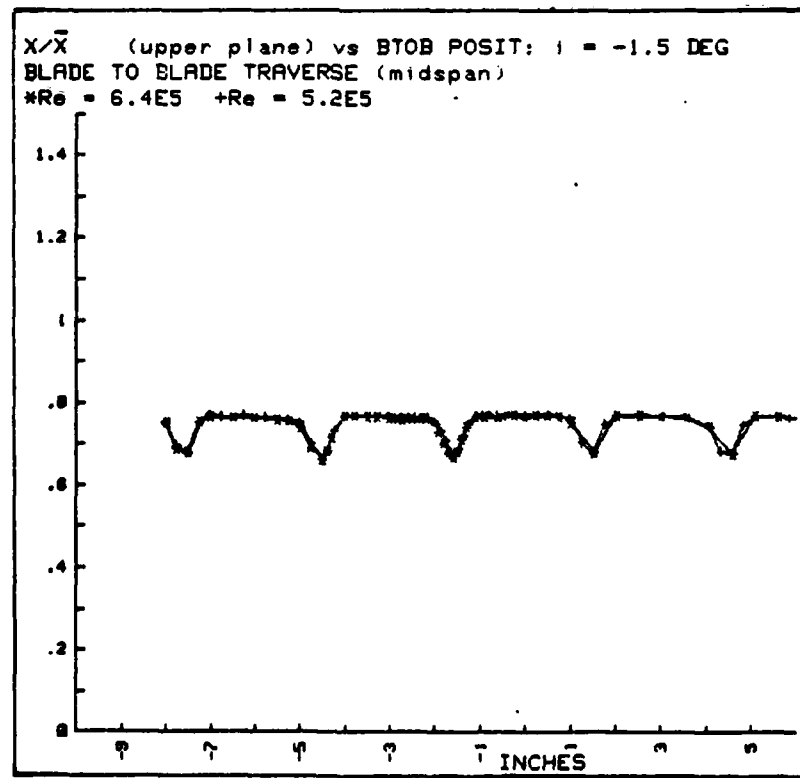


Fig. A.138

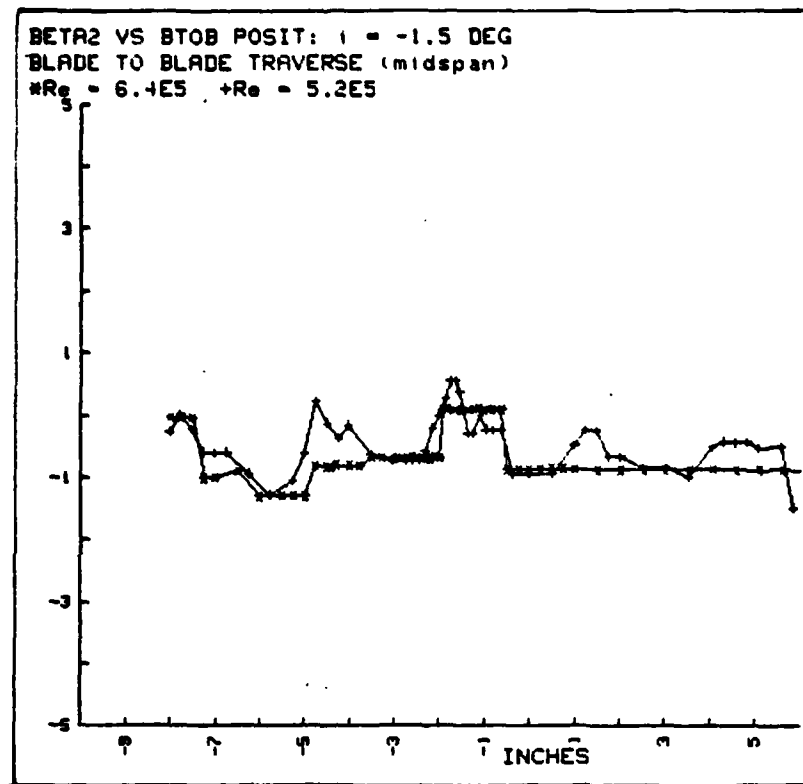


Fig. A.139

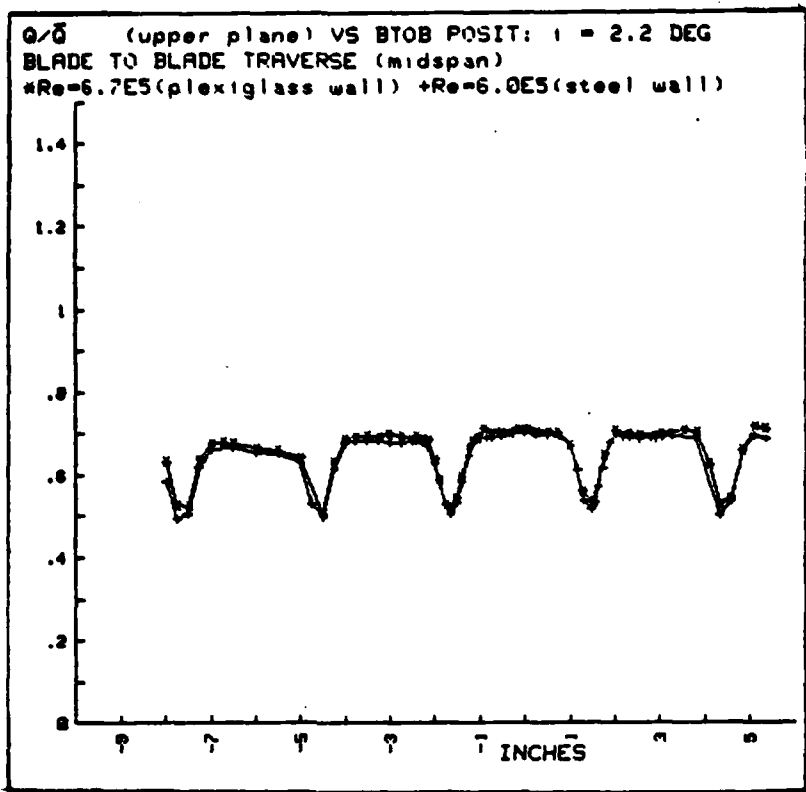


Fig. A.140

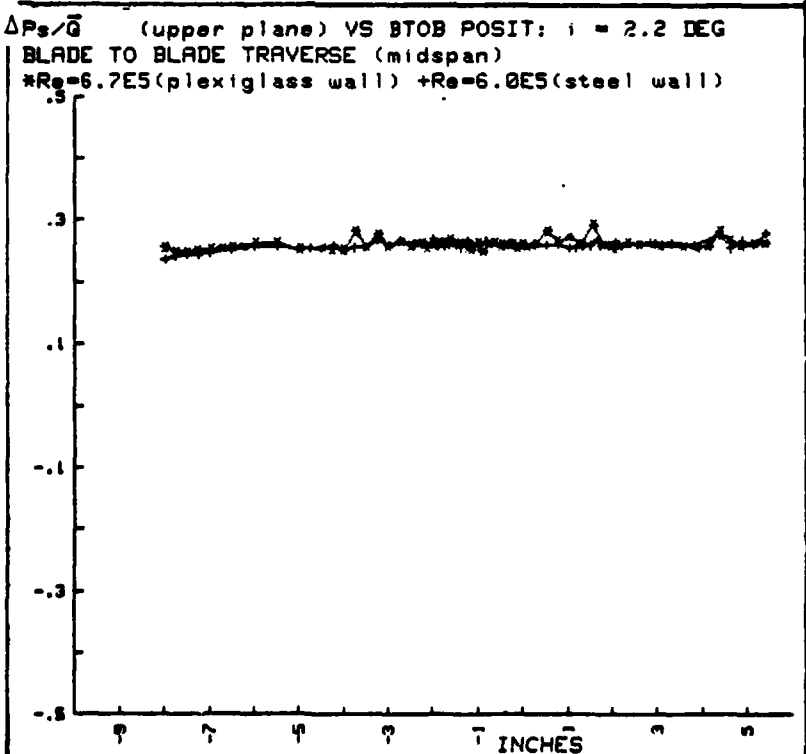


Fig. A.141

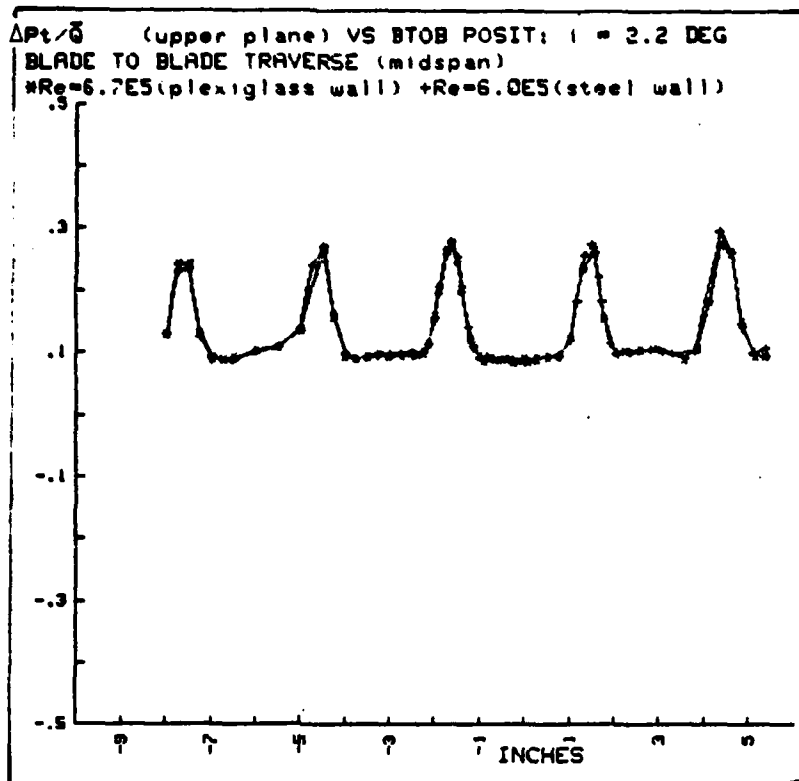


Fig. A.142

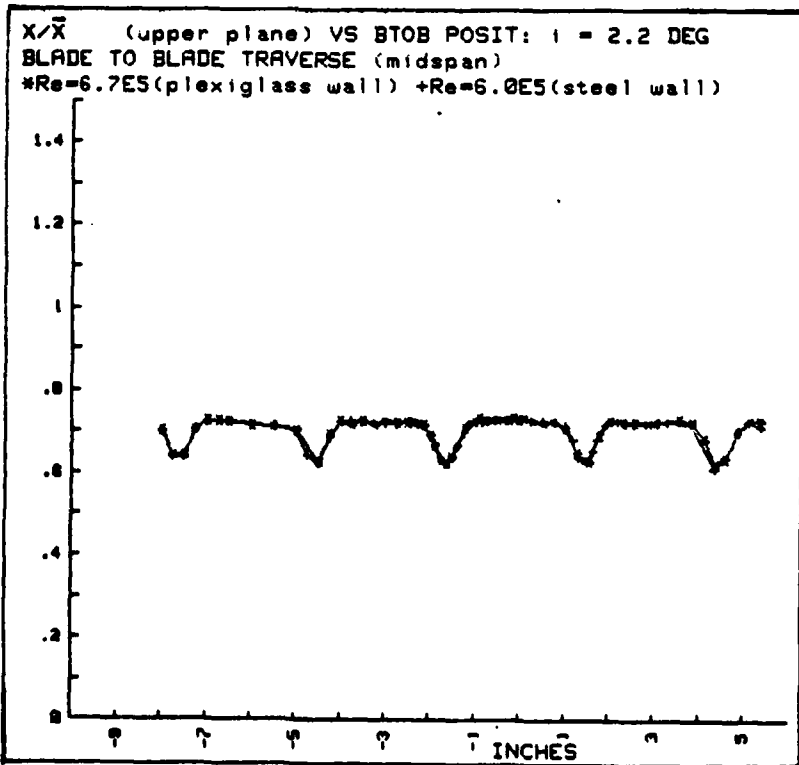
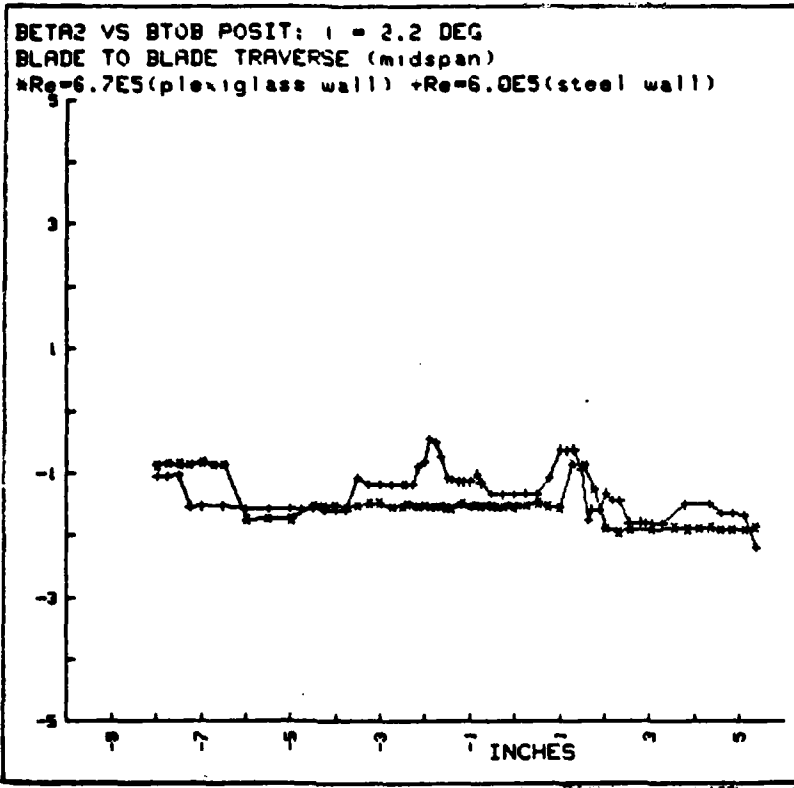


Fig. A.143



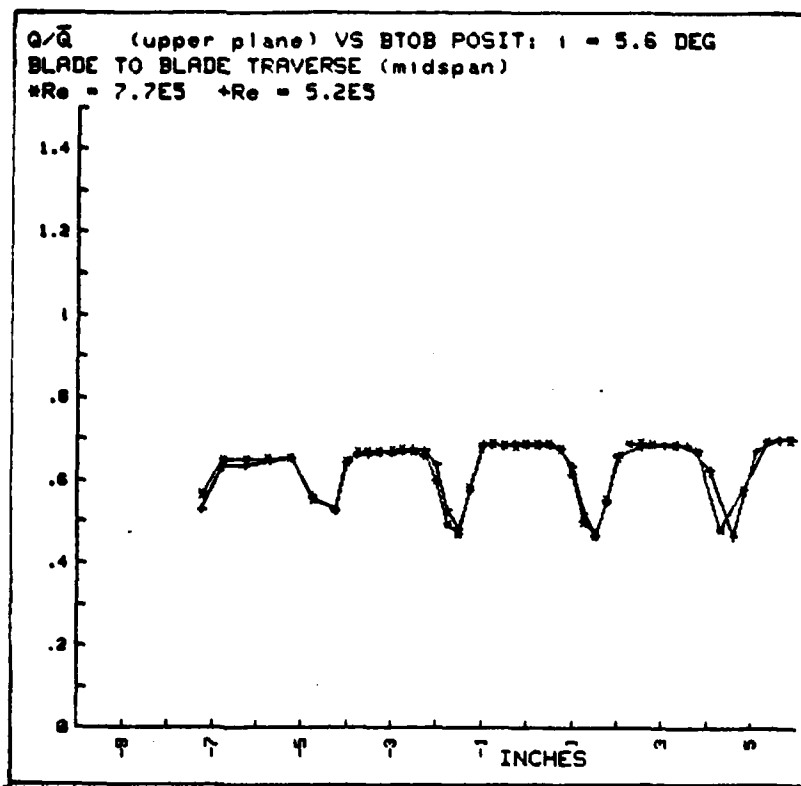


Fig. A.145

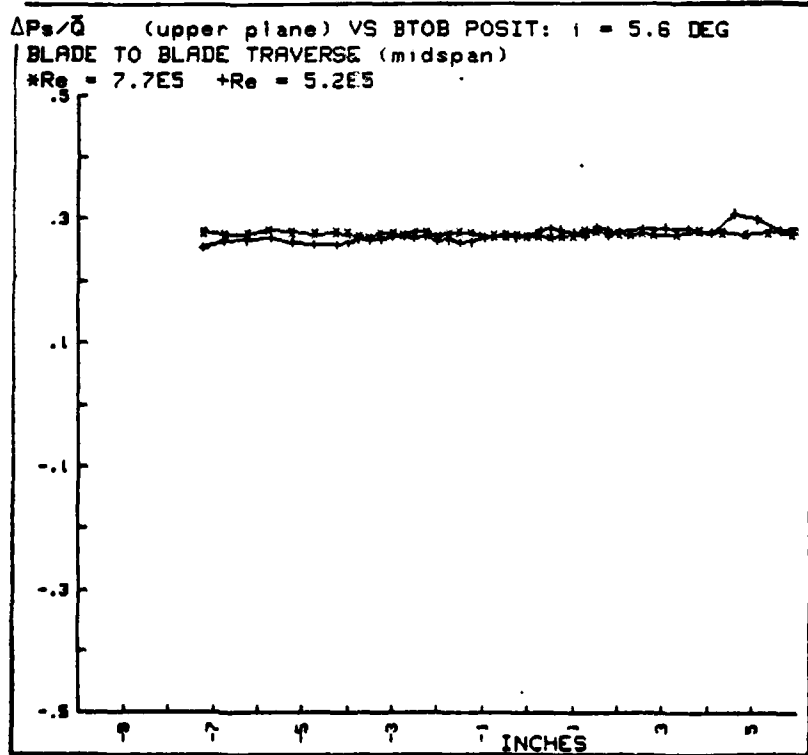


Fig. A. 146

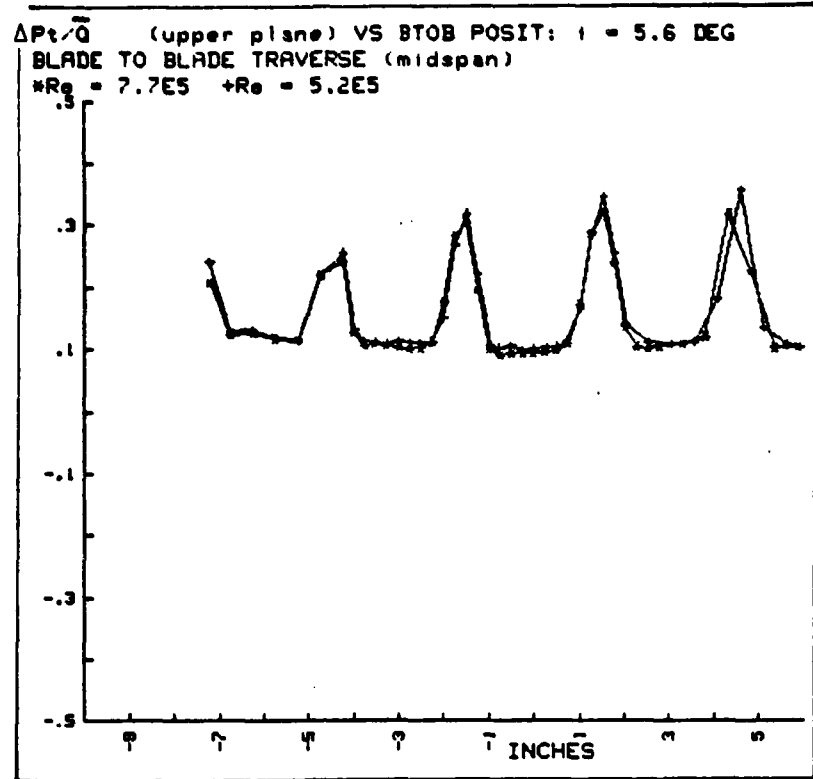


Fig. A.147

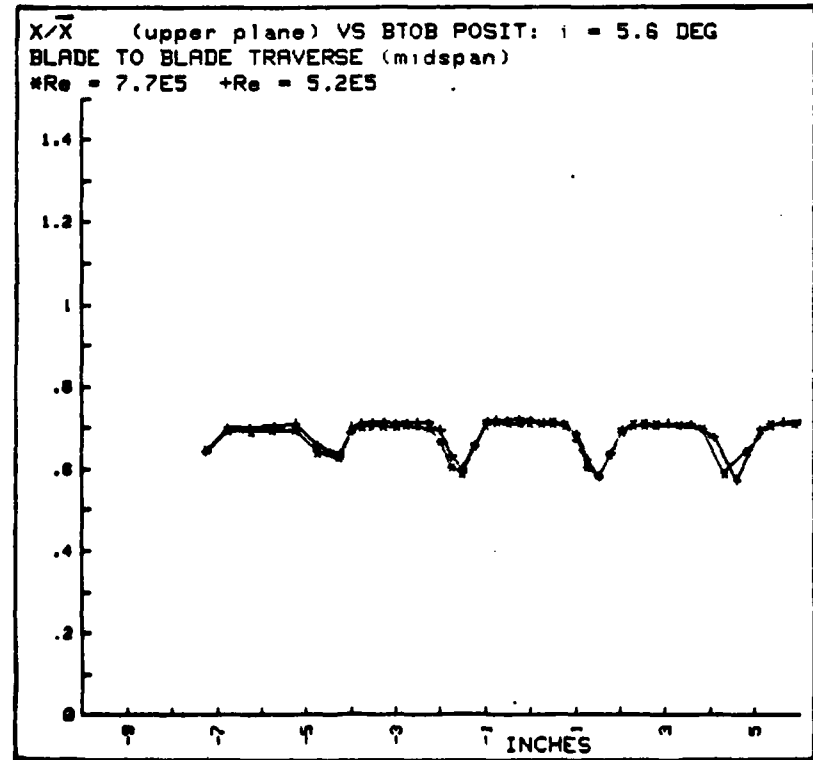


Fig. A.148

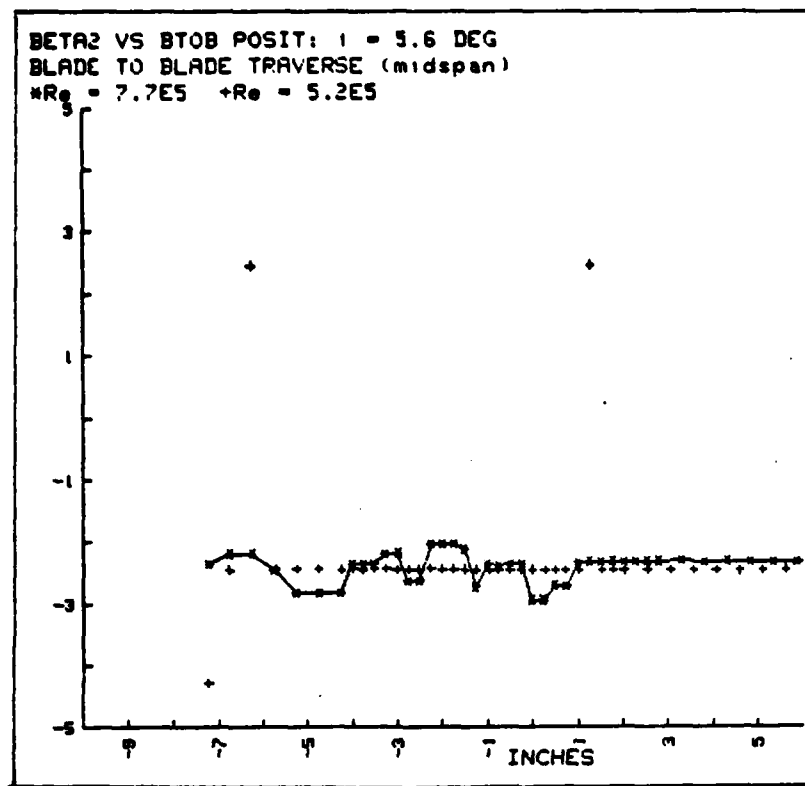


Fig. A.149

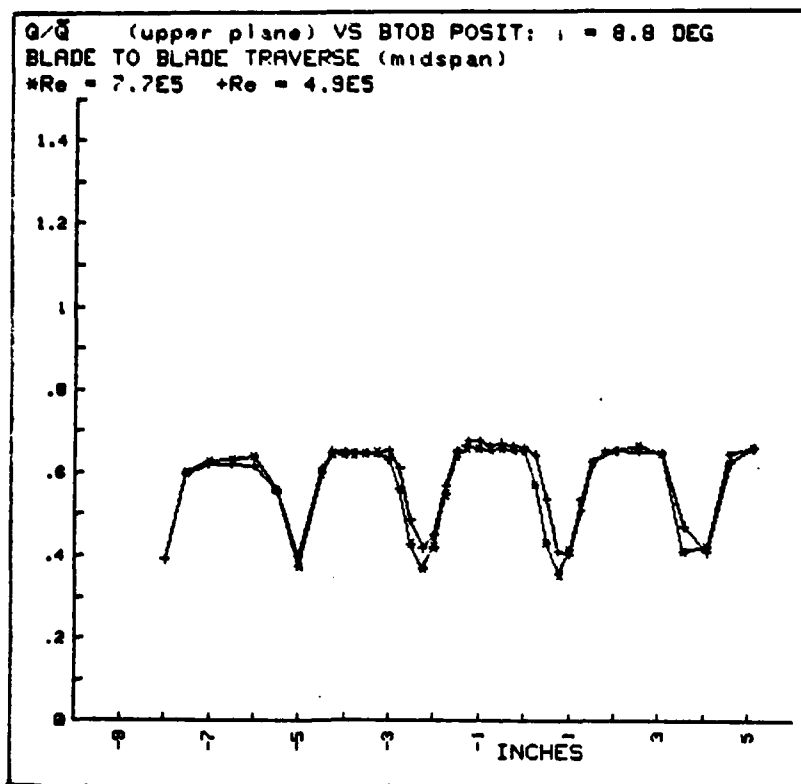


Fig. A.150

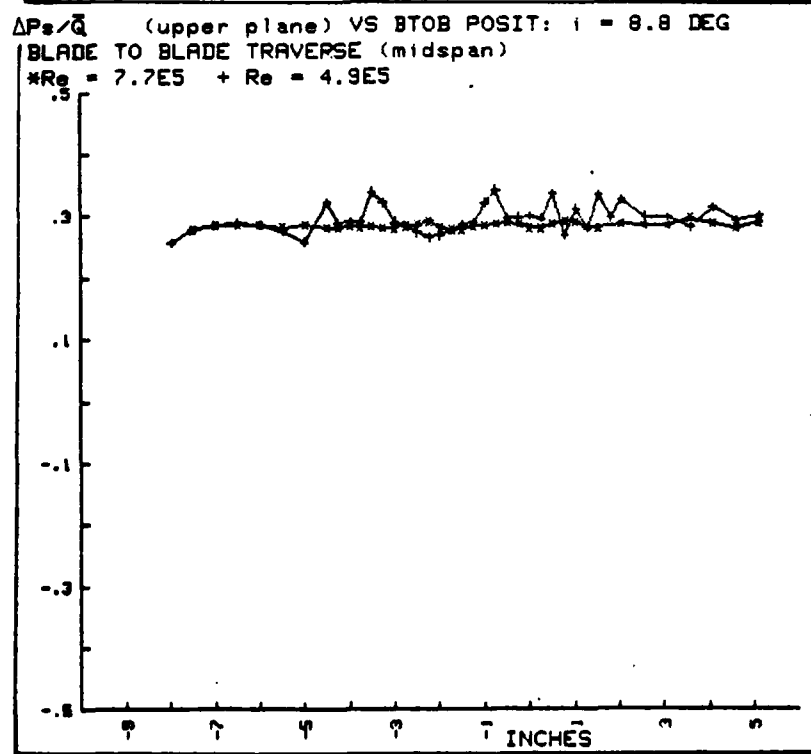


Fig. A.151

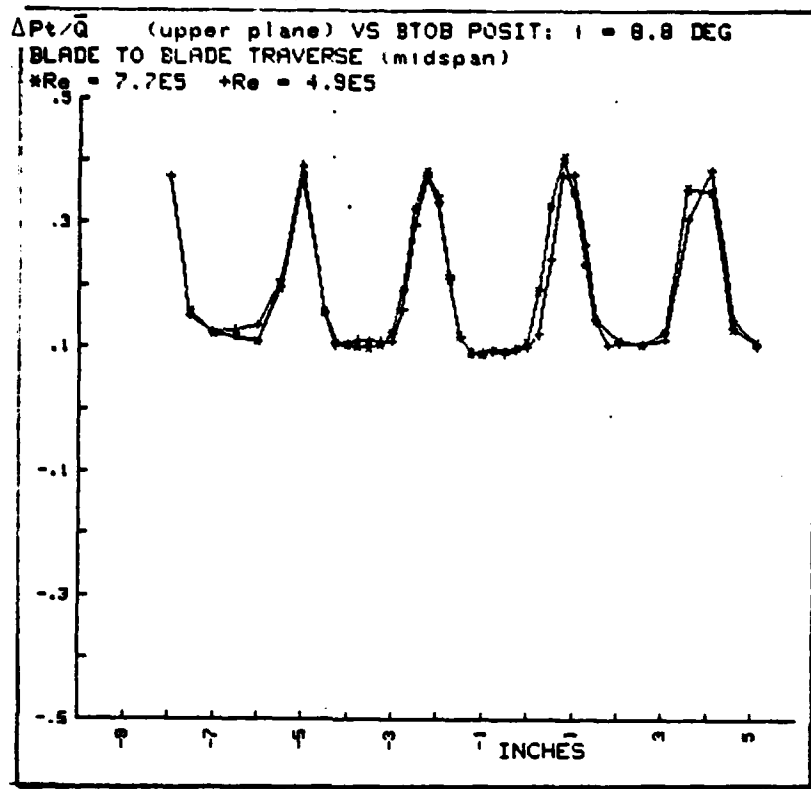


Fig. A.152

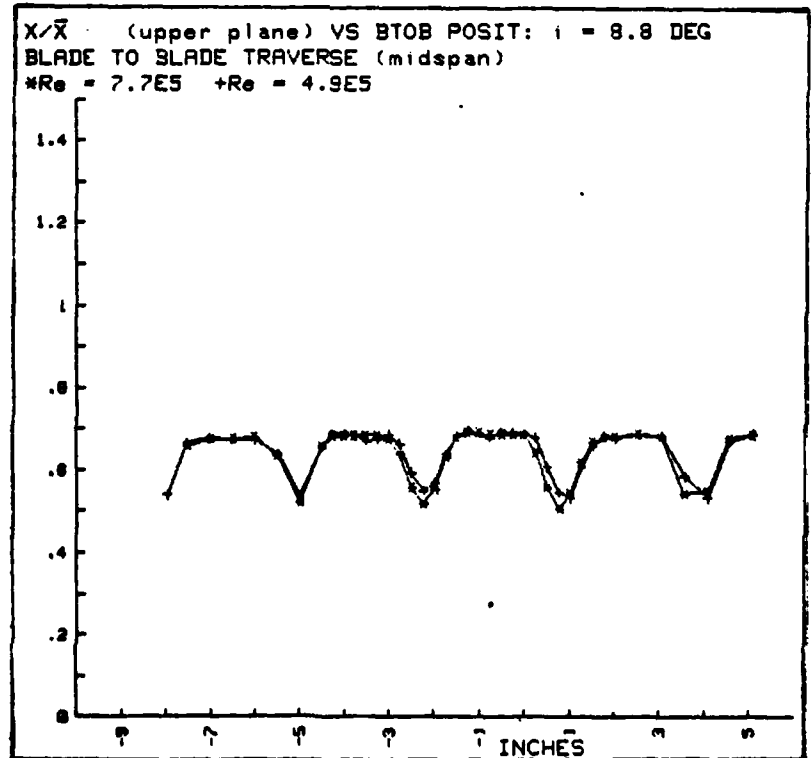


Fig. A.153

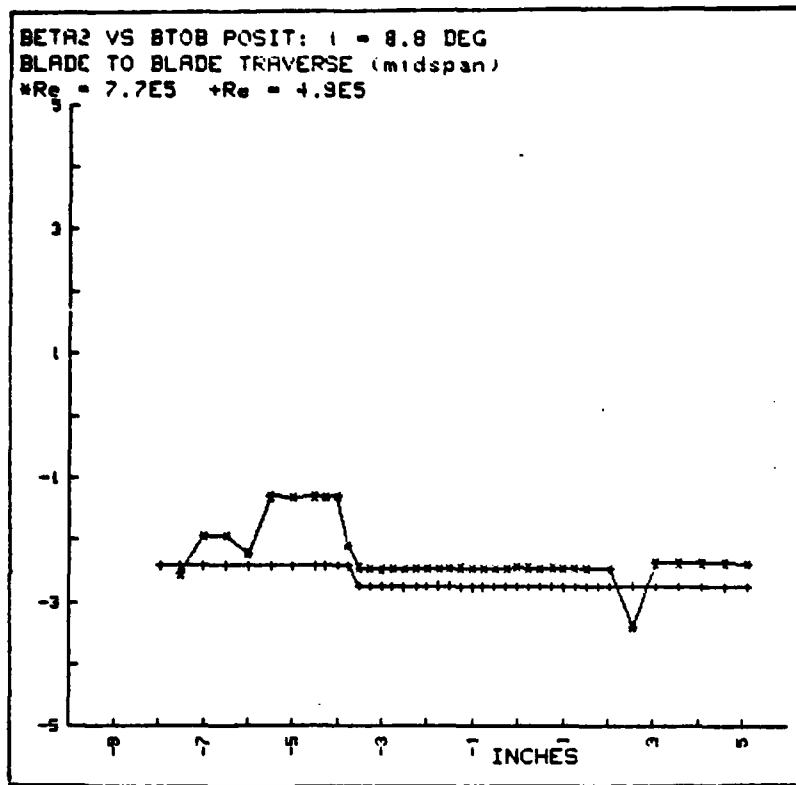


Fig. A.154

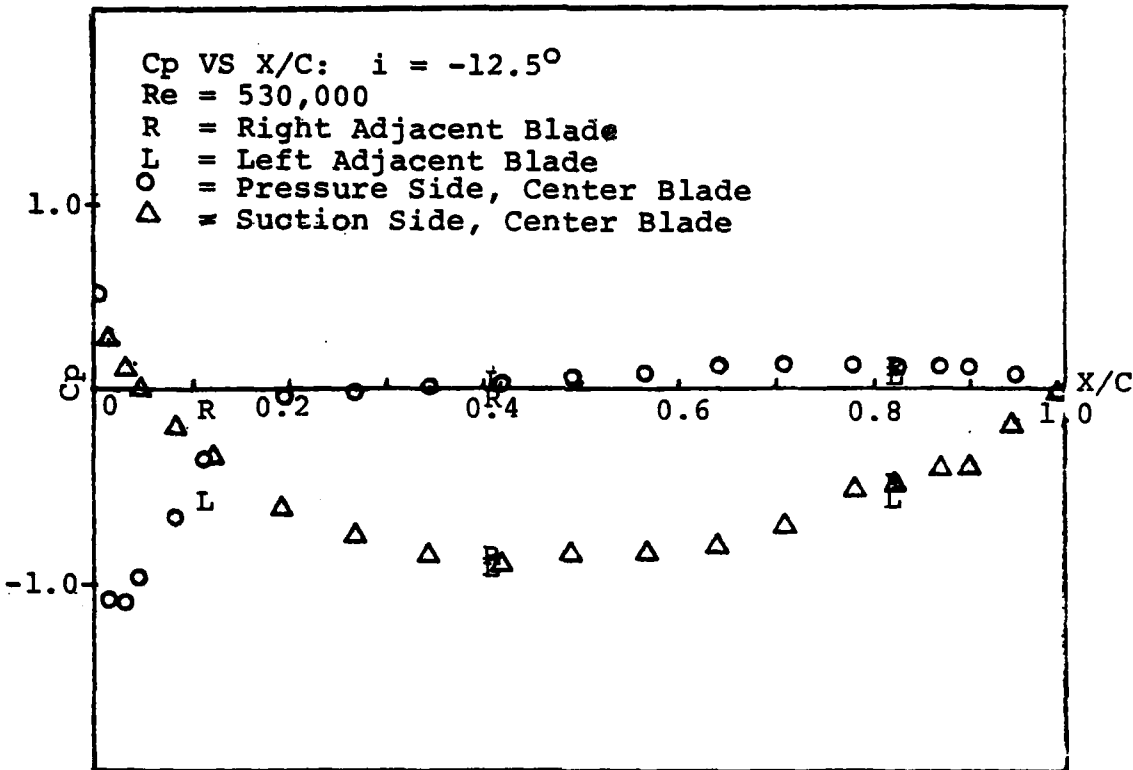


Fig. A.155

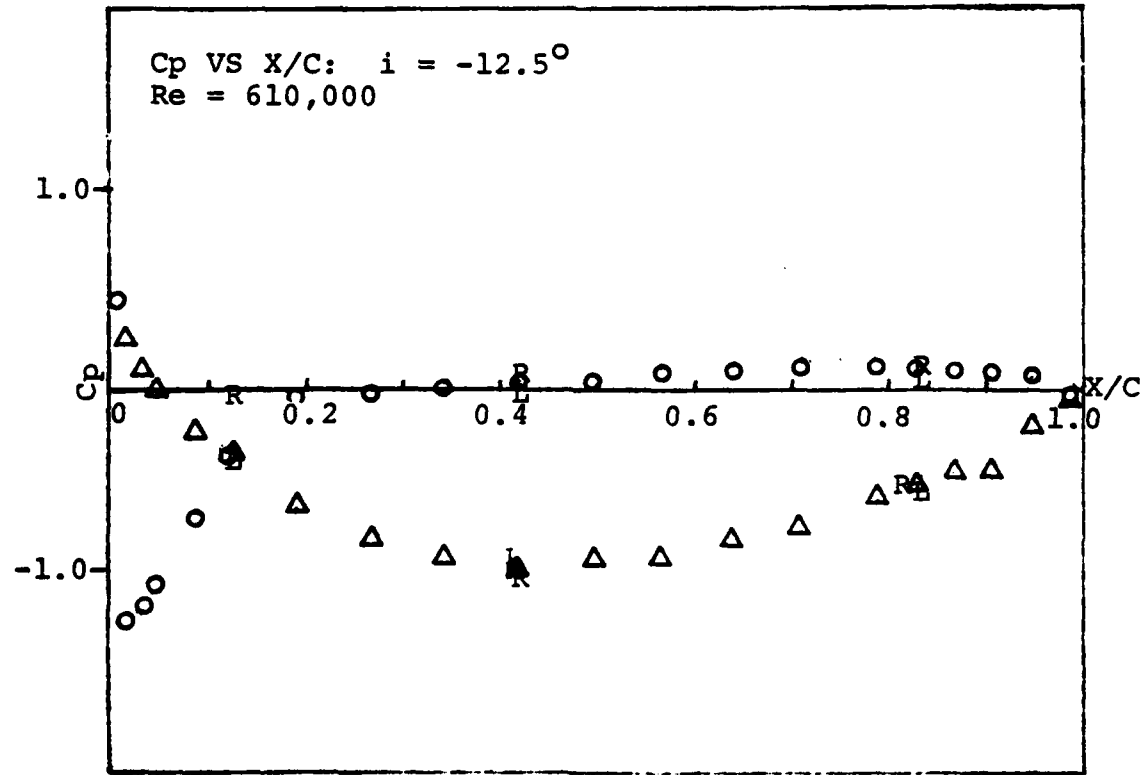


Fig. A.156

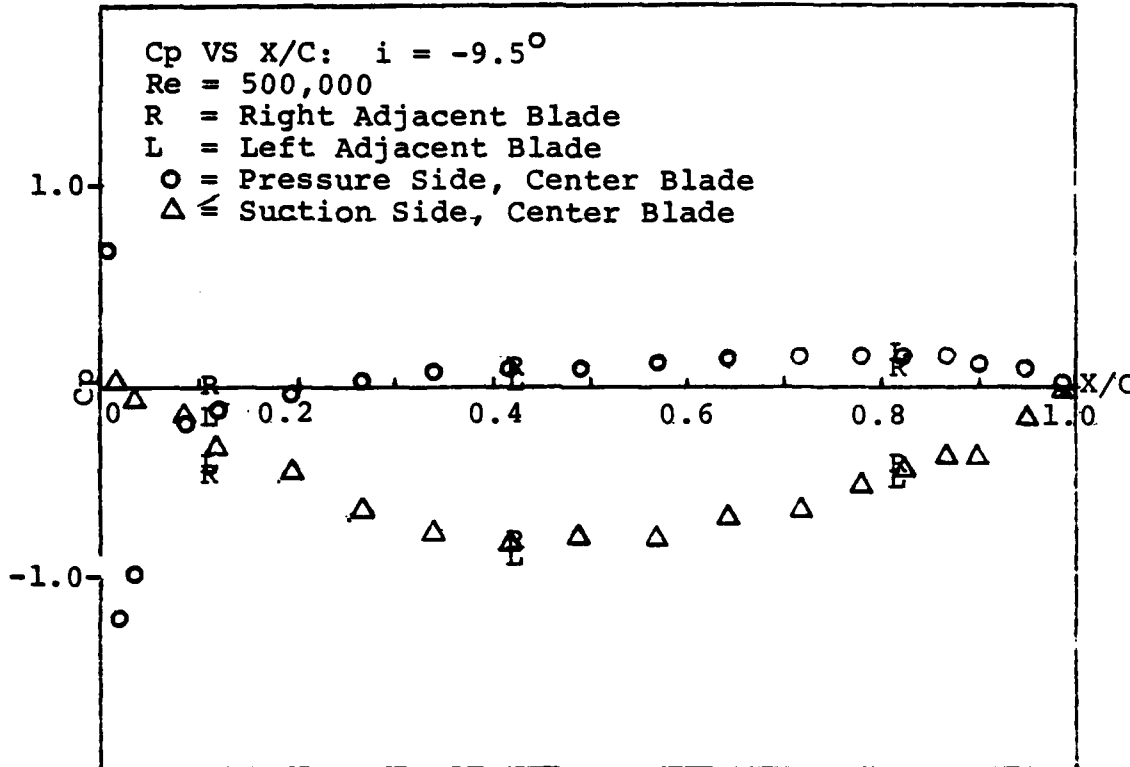


Fig. A.157

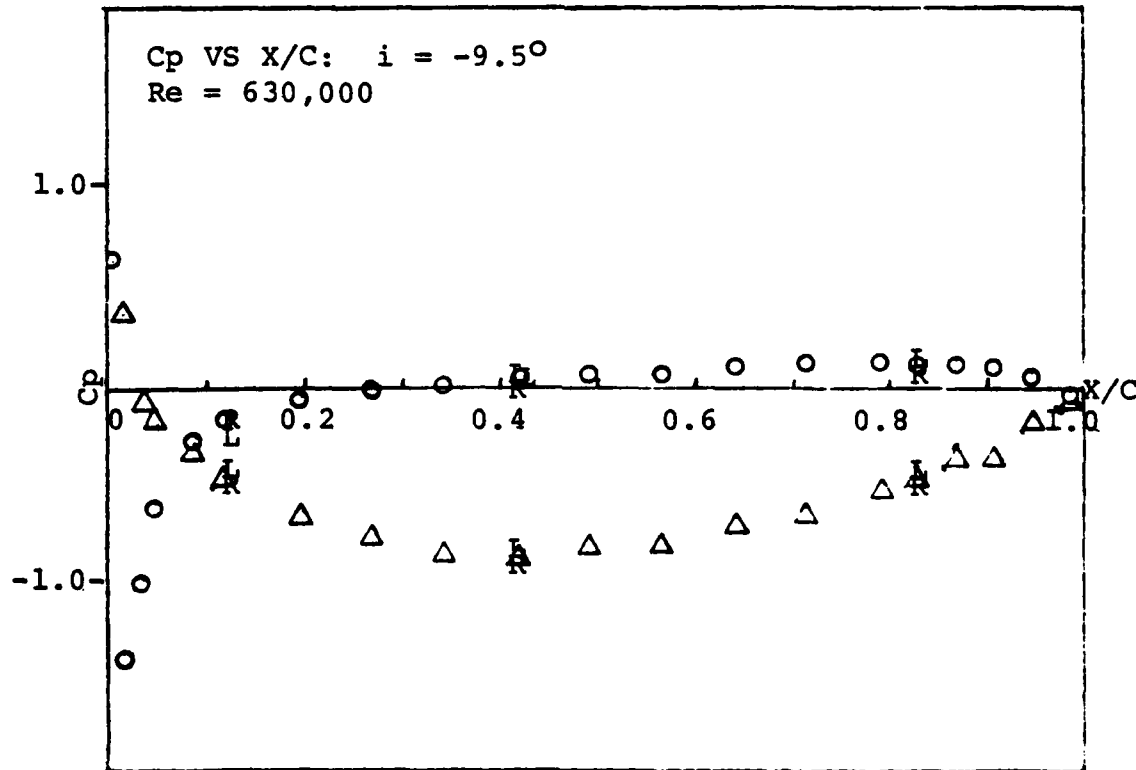


Fig. A.158  
150

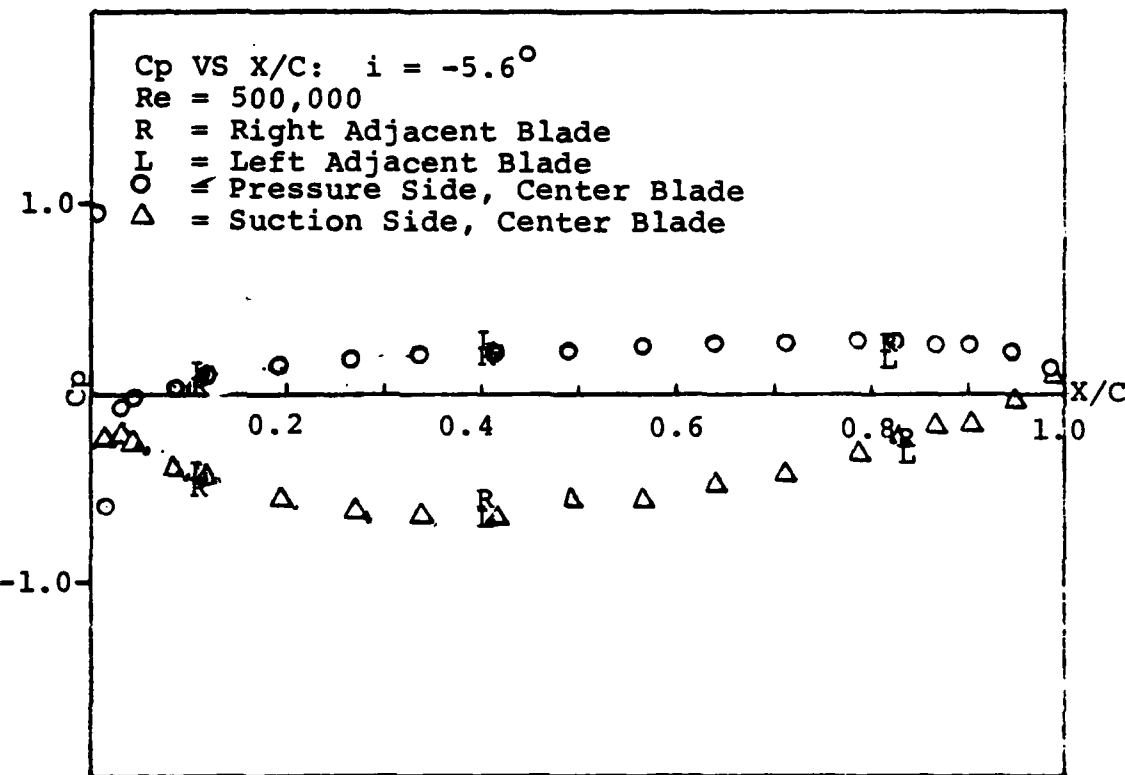


Fig. A.159

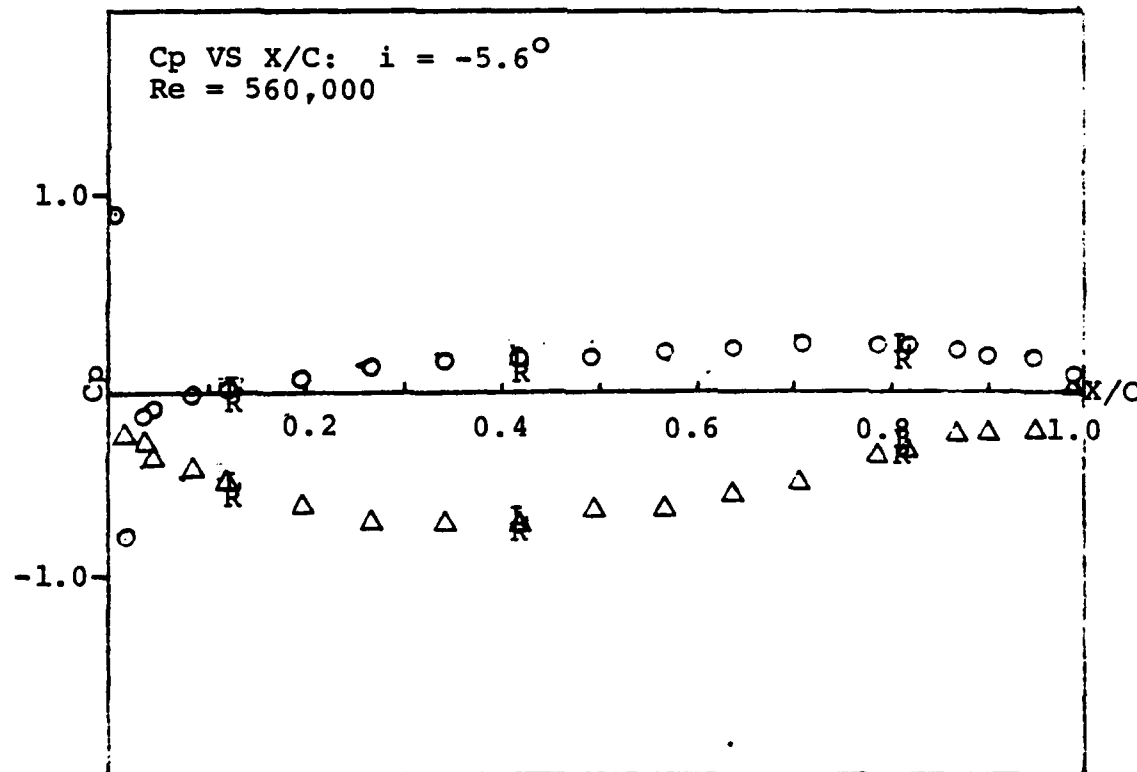


Fig. A.160  
151

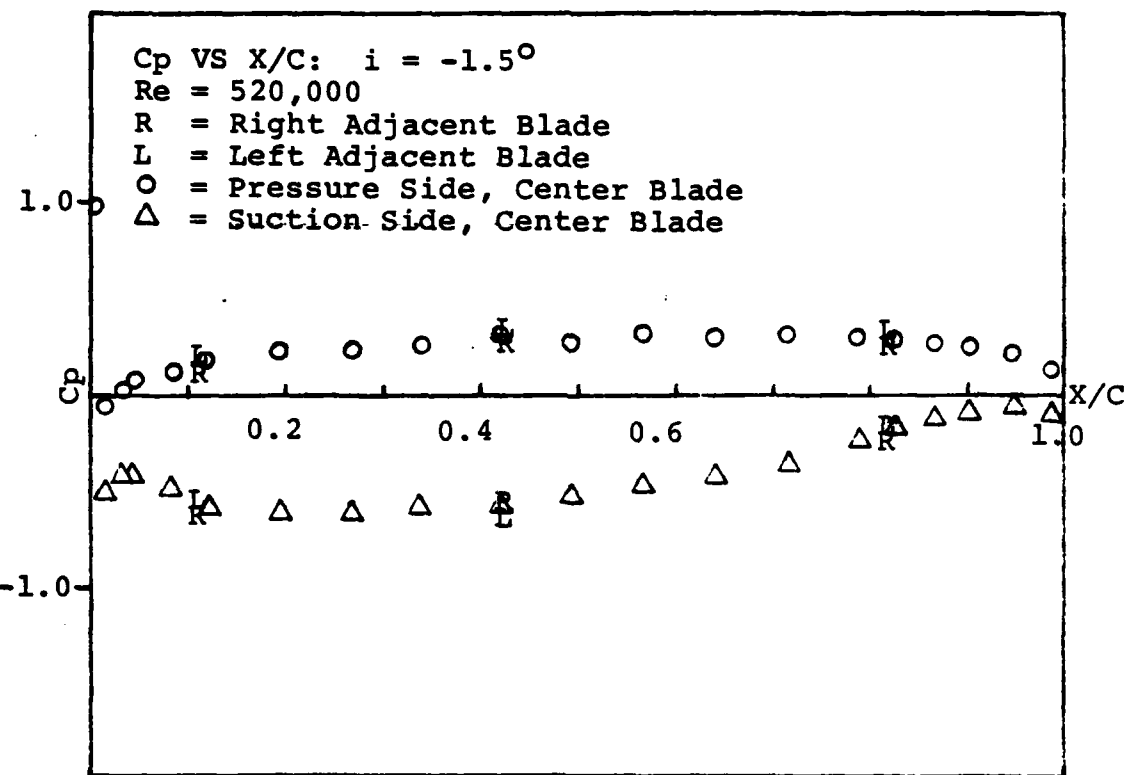


Fig. A.161

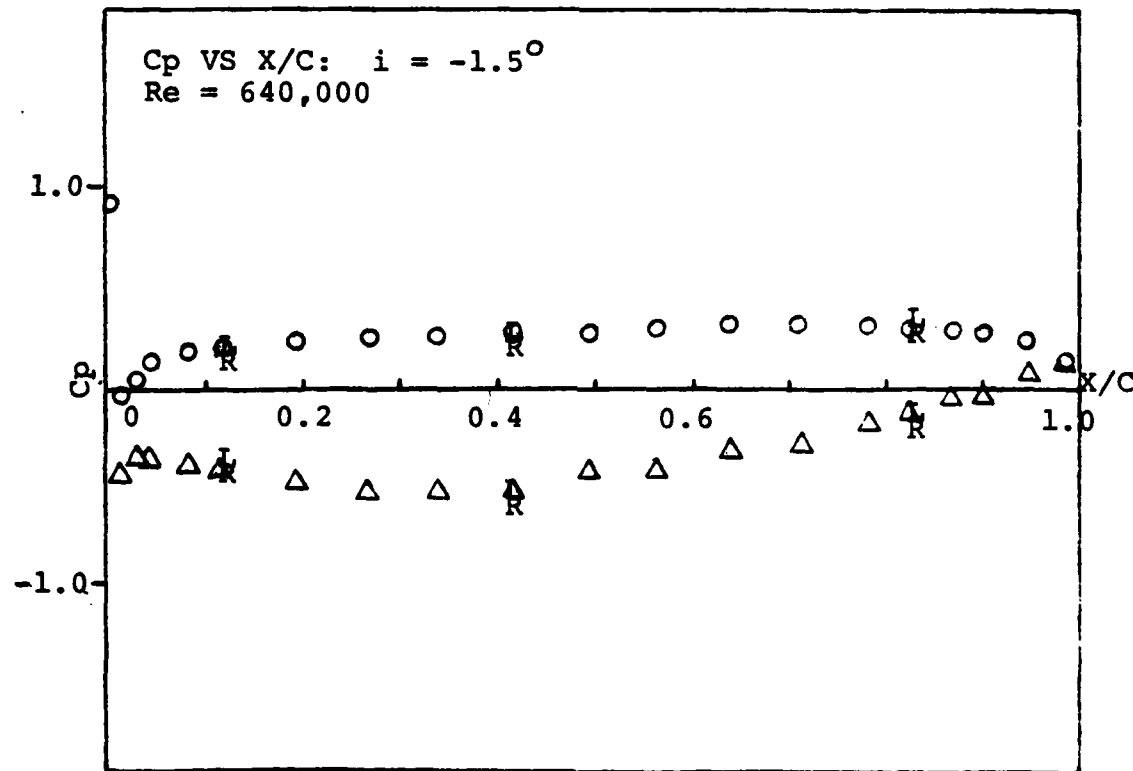


Fig. A.162

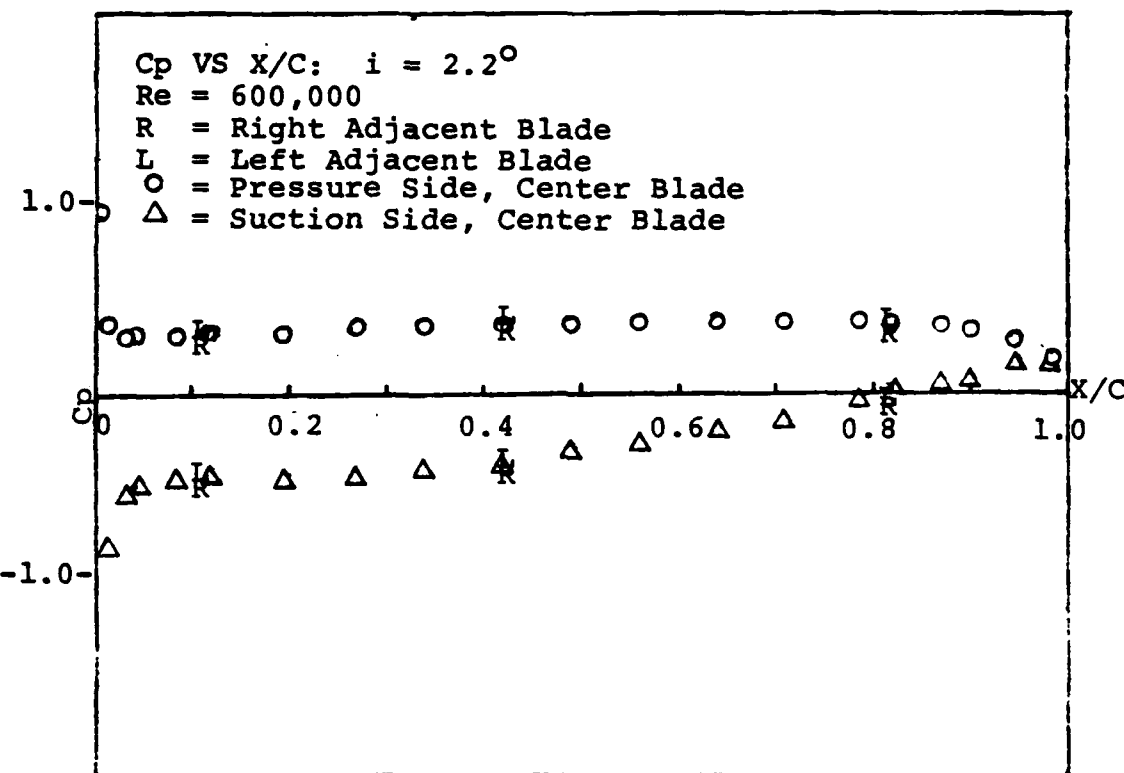


Fig. A.163

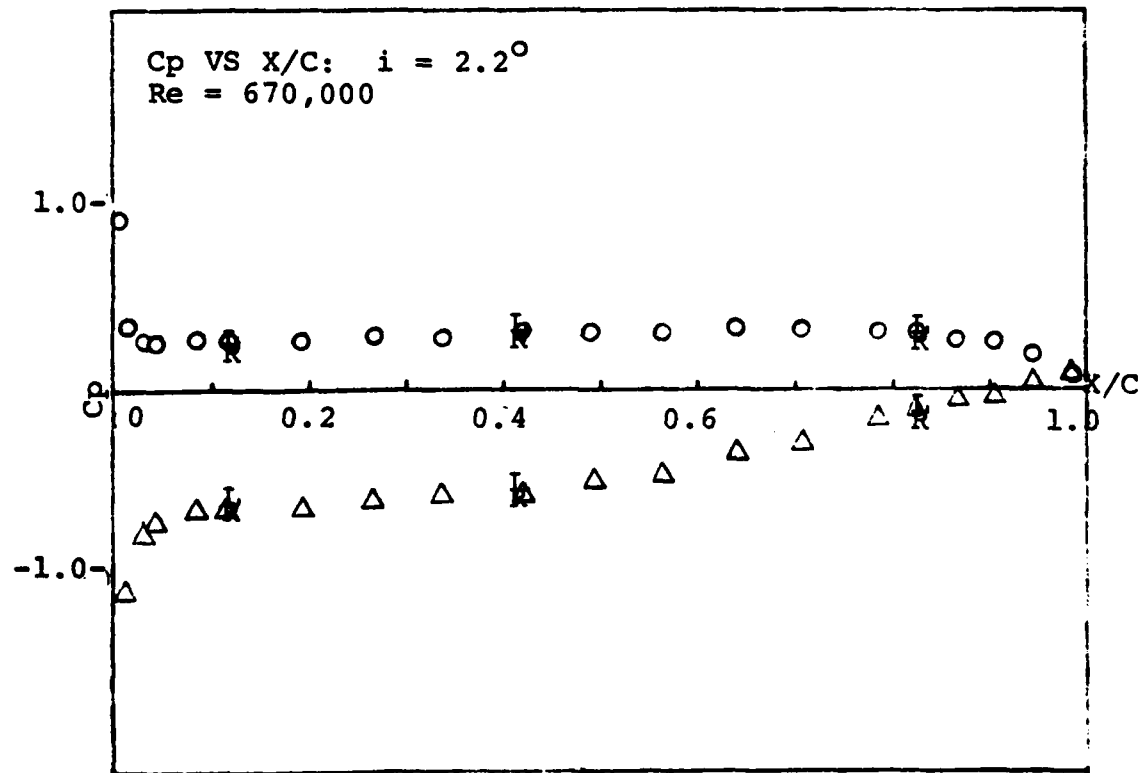


Fig. A.164

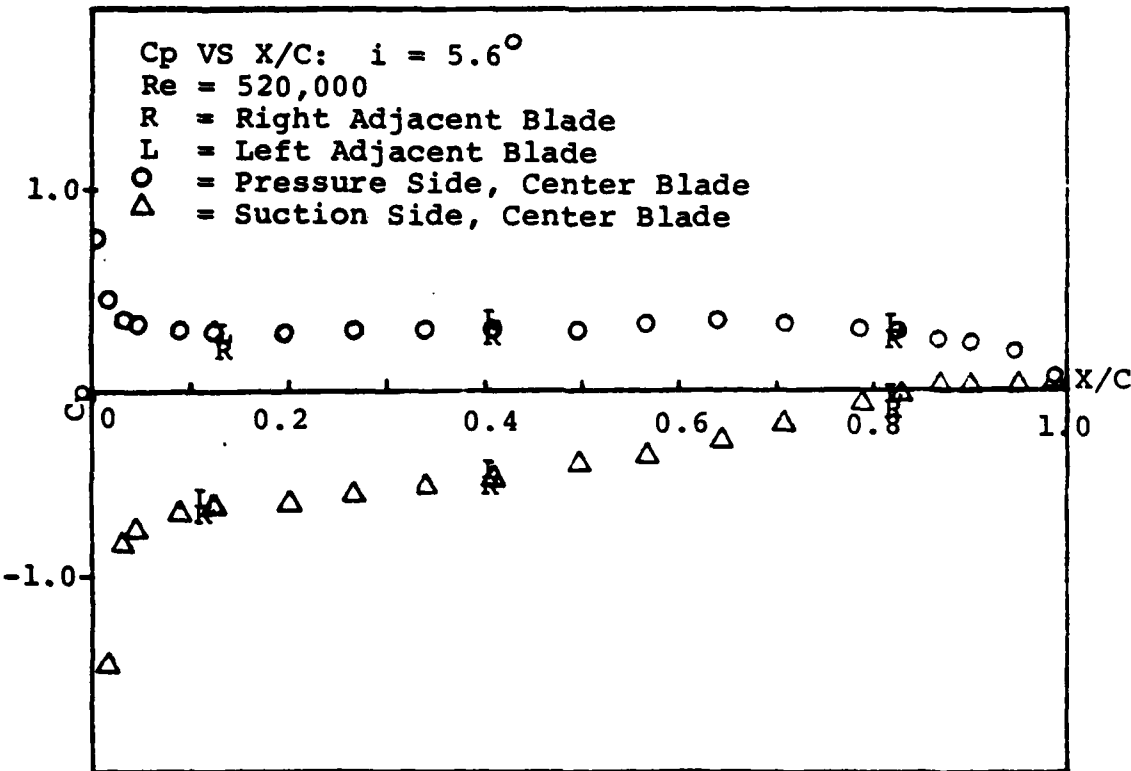


Fig. A.165

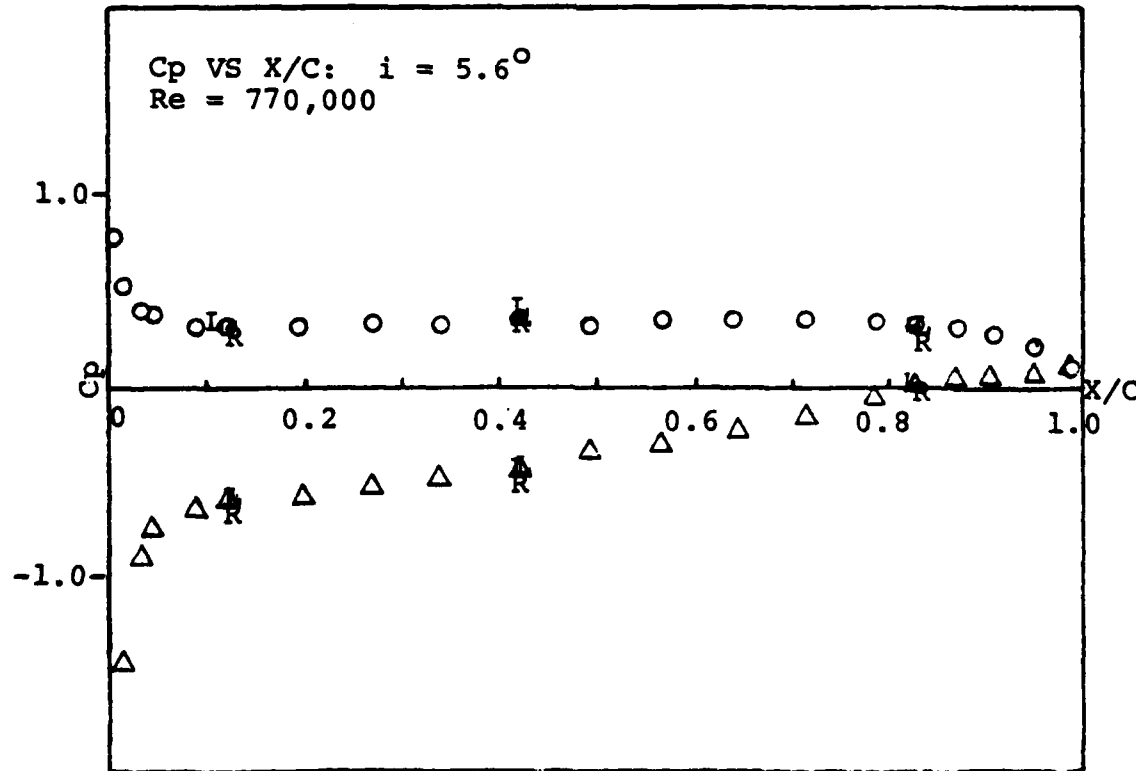


Fig. A.166

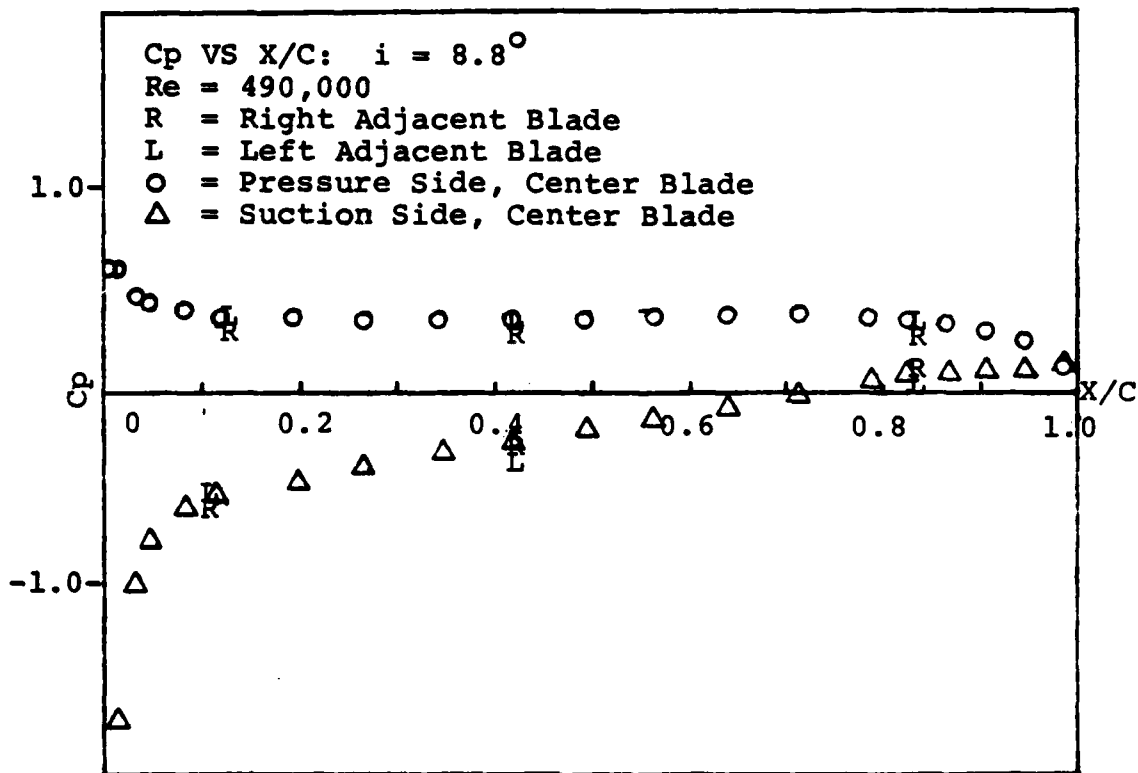


Fig. A.167

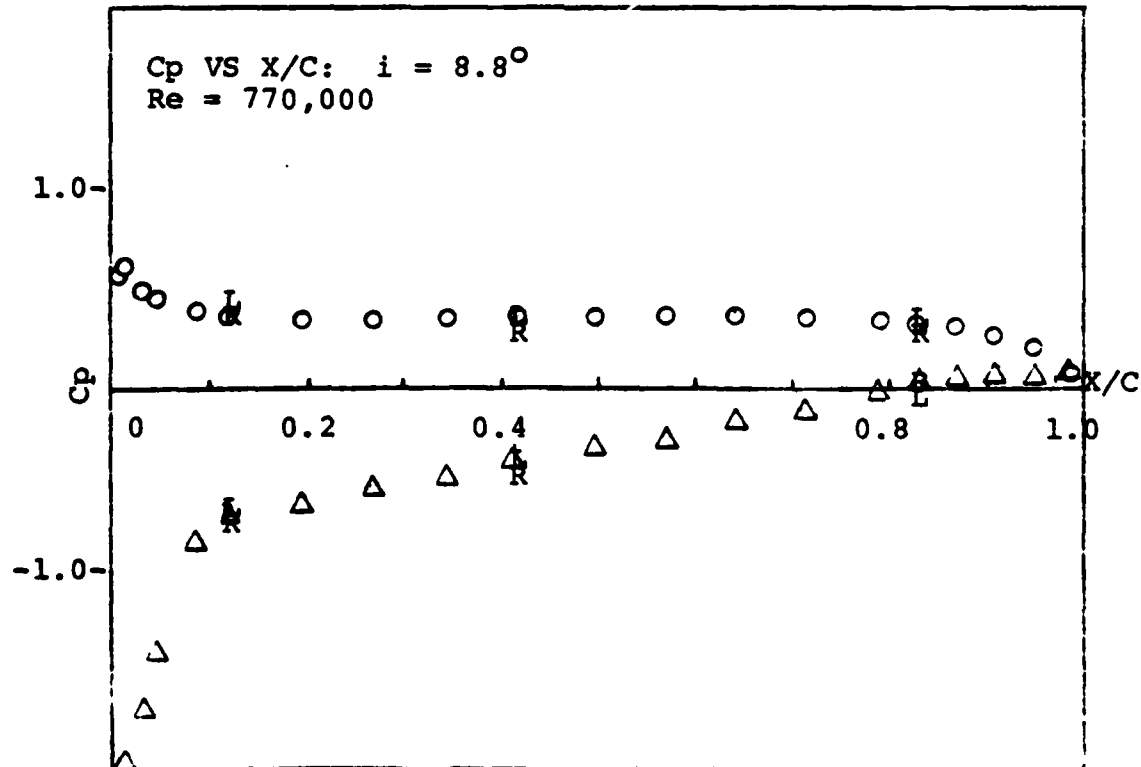


Fig. A.168

$$\beta_{\infty} = \tan^{-1} \left( \frac{\tan \beta_1 + \tan \beta_2}{2} \right)$$

$i = -12.5$  degrees  
 $Re = 611,000$

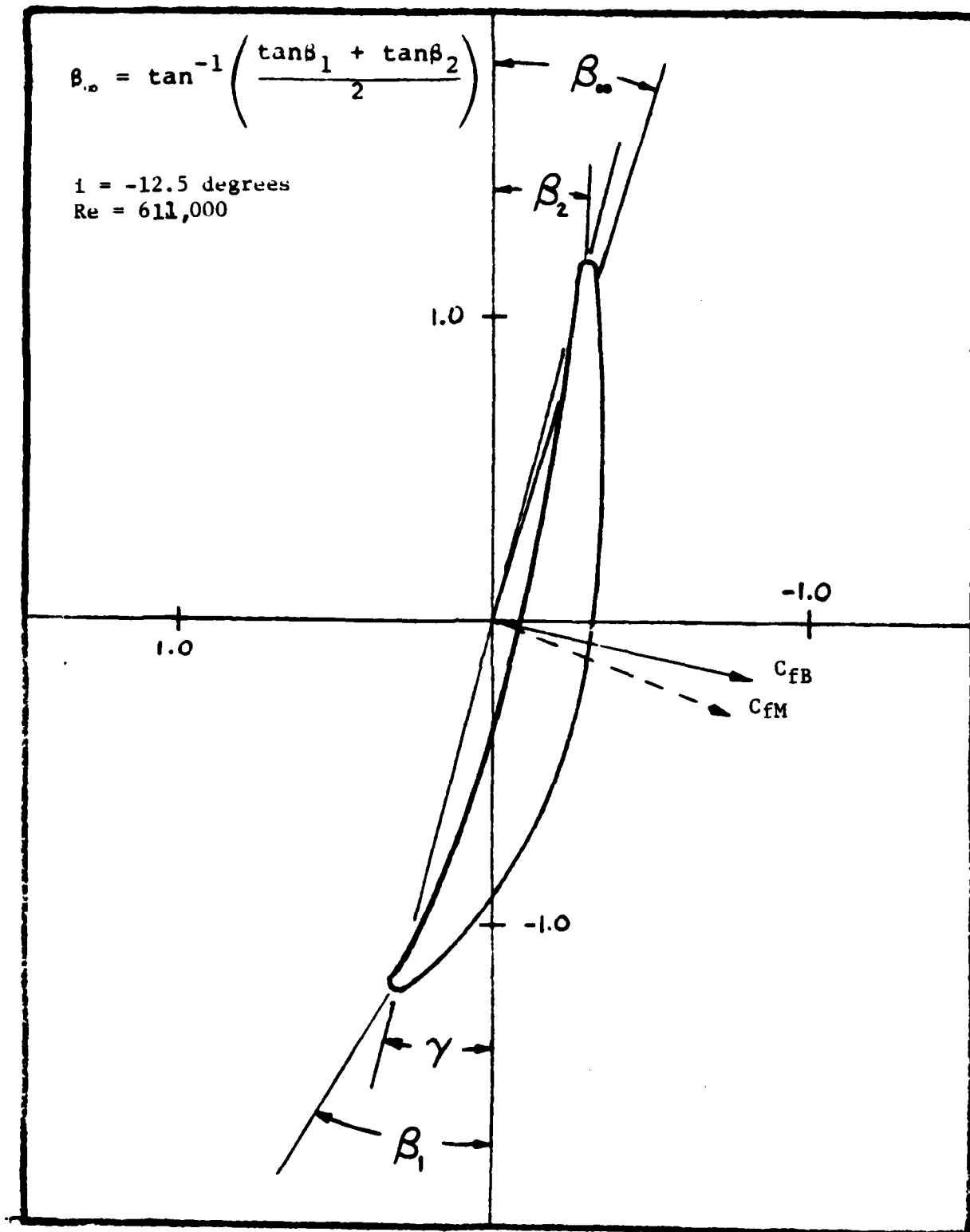


Fig. A.169

$$\beta_m = \tan^{-1} \left( \frac{\tan \beta_1 + \tan \beta_2}{2} \right)$$

$\delta = -12.39$  degrees  
 $Re = 53,500$

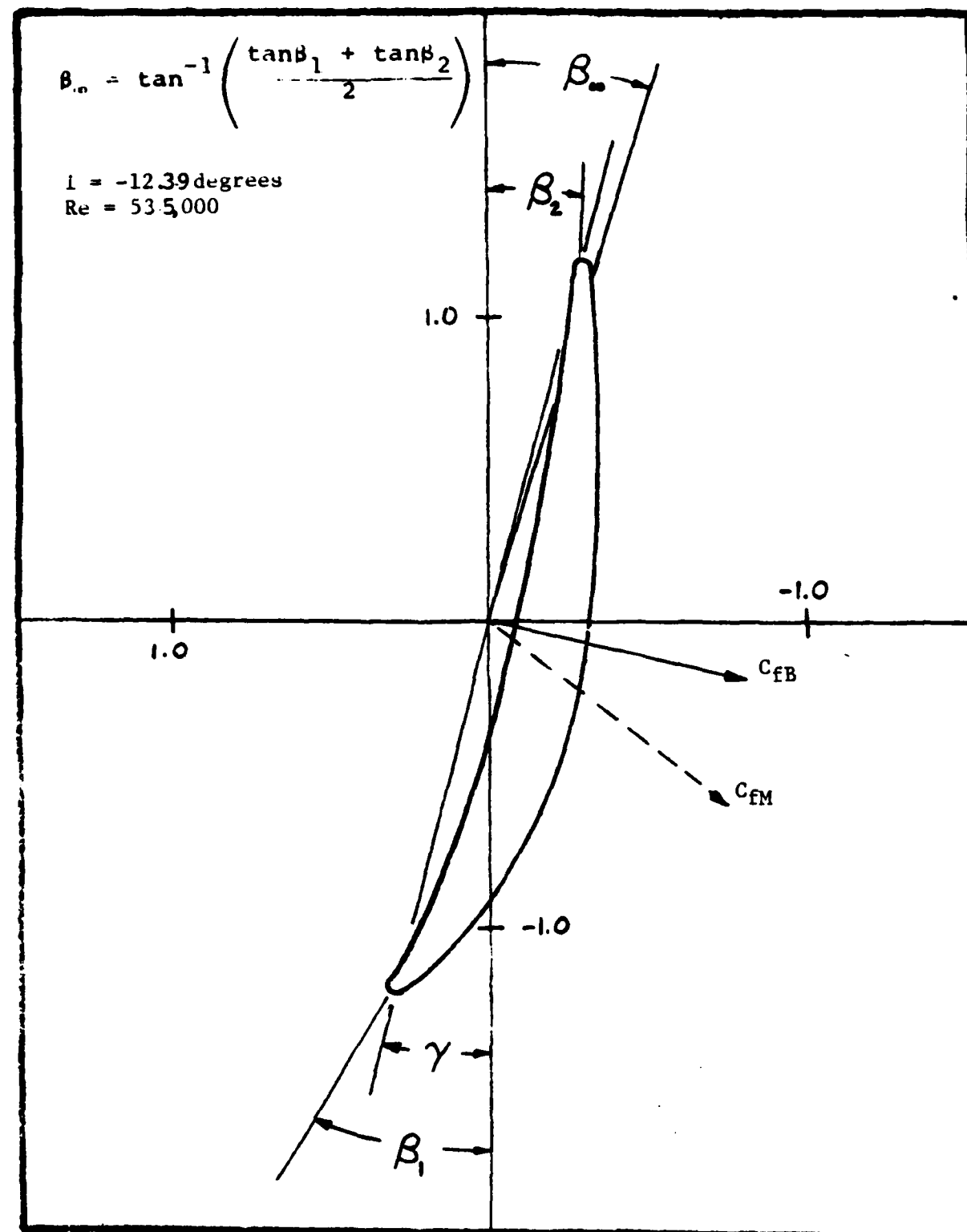


Fig. A.170

$$\beta_m = \tan^{-1} \left( \frac{\tan\beta_1 + \tan\beta_2}{2} \right)$$

$i = -9.58$  degrees  
 $Re = 626,000$

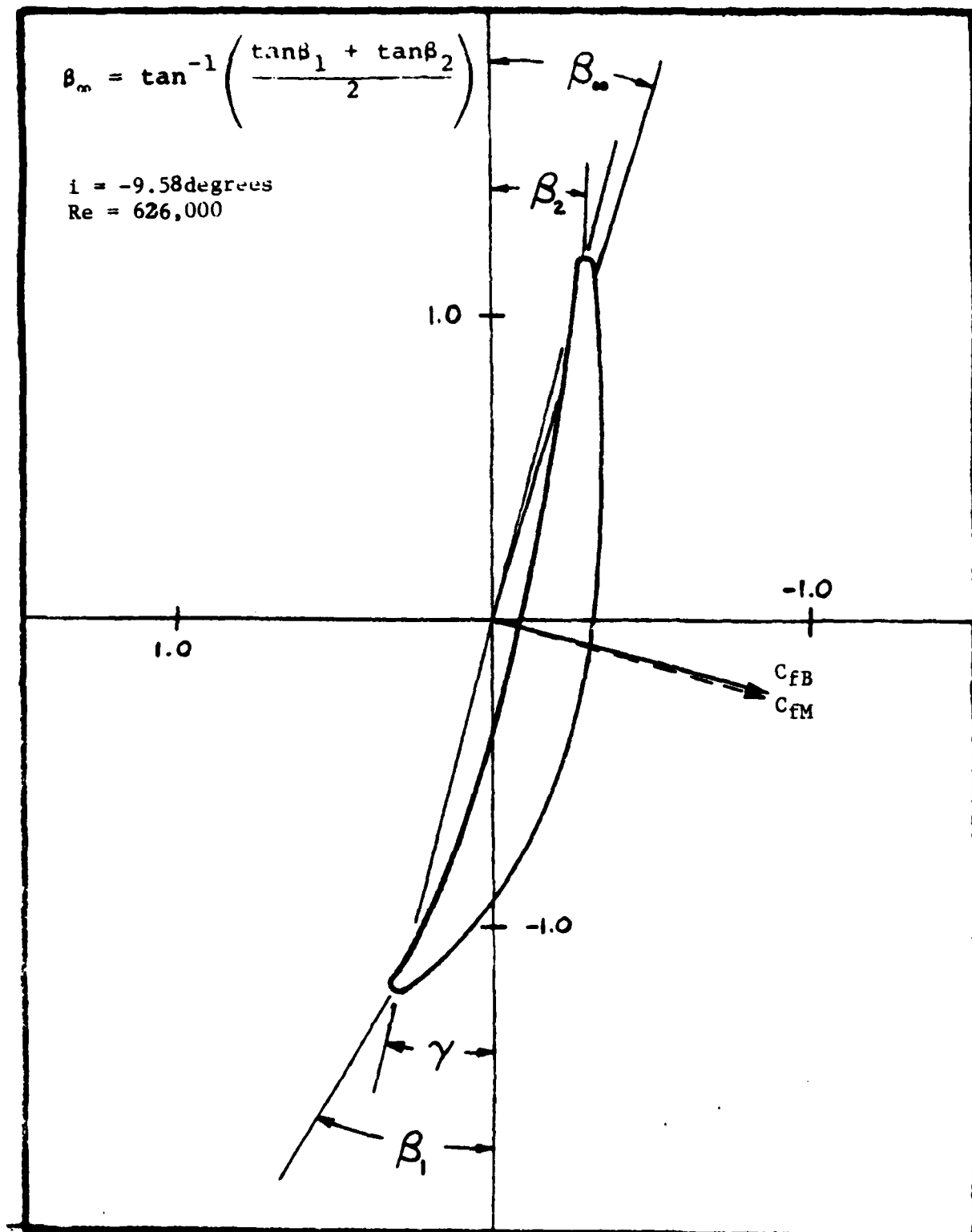


Fig. A.171

$$\beta_\infty = \tan^{-1} \left( \frac{\tan\beta_1 + \tan\beta_2}{2} \right)$$

$i = -9.23$  degrees  
 $Re = 503,000$

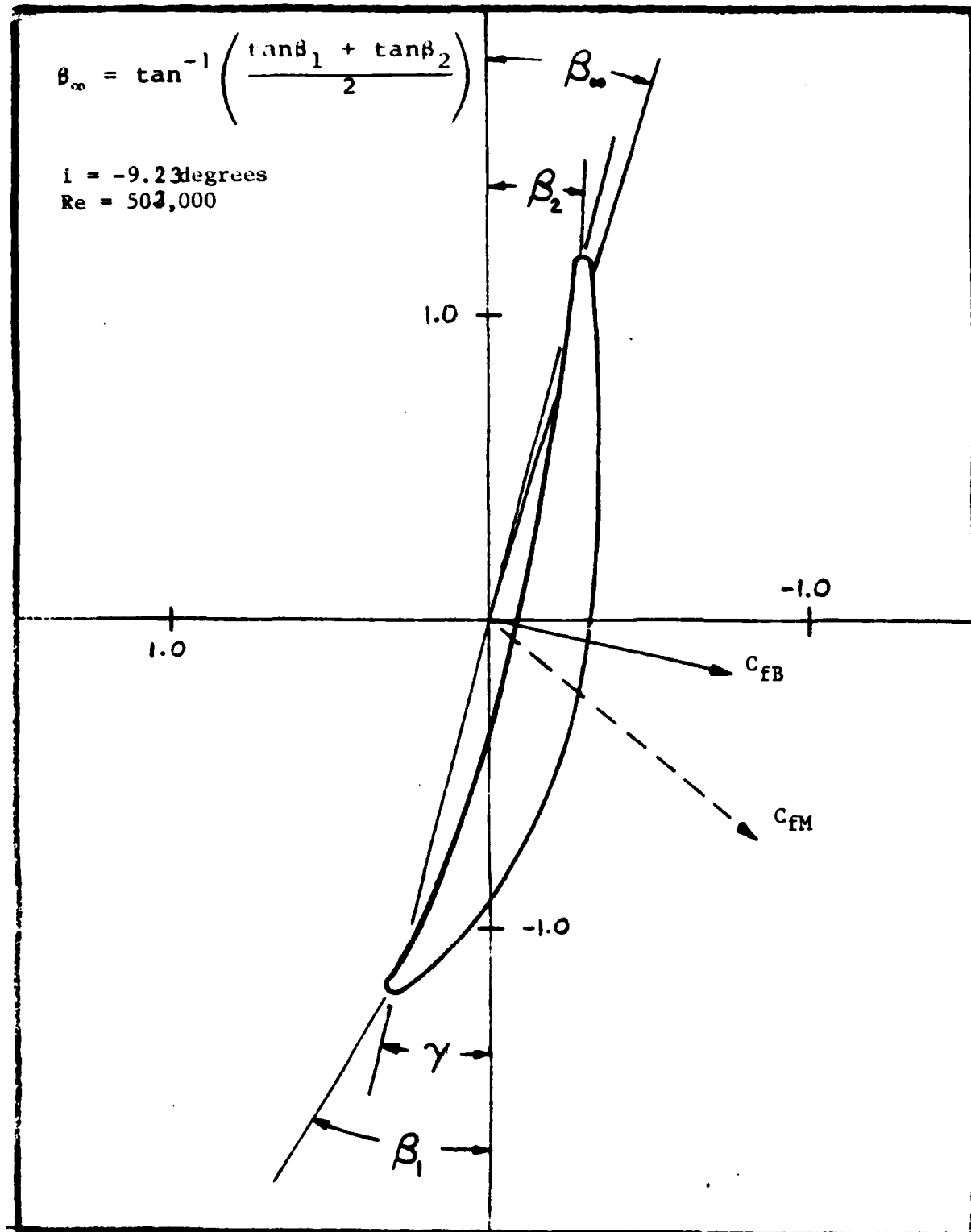


Fig. A.172

$$\beta_\infty = \tan^{-1} \left( \frac{\tan \beta_1 + \tan \beta_2}{2} \right)$$

$i = -5.8^\circ$  degrees  
 $Re = 560,000$

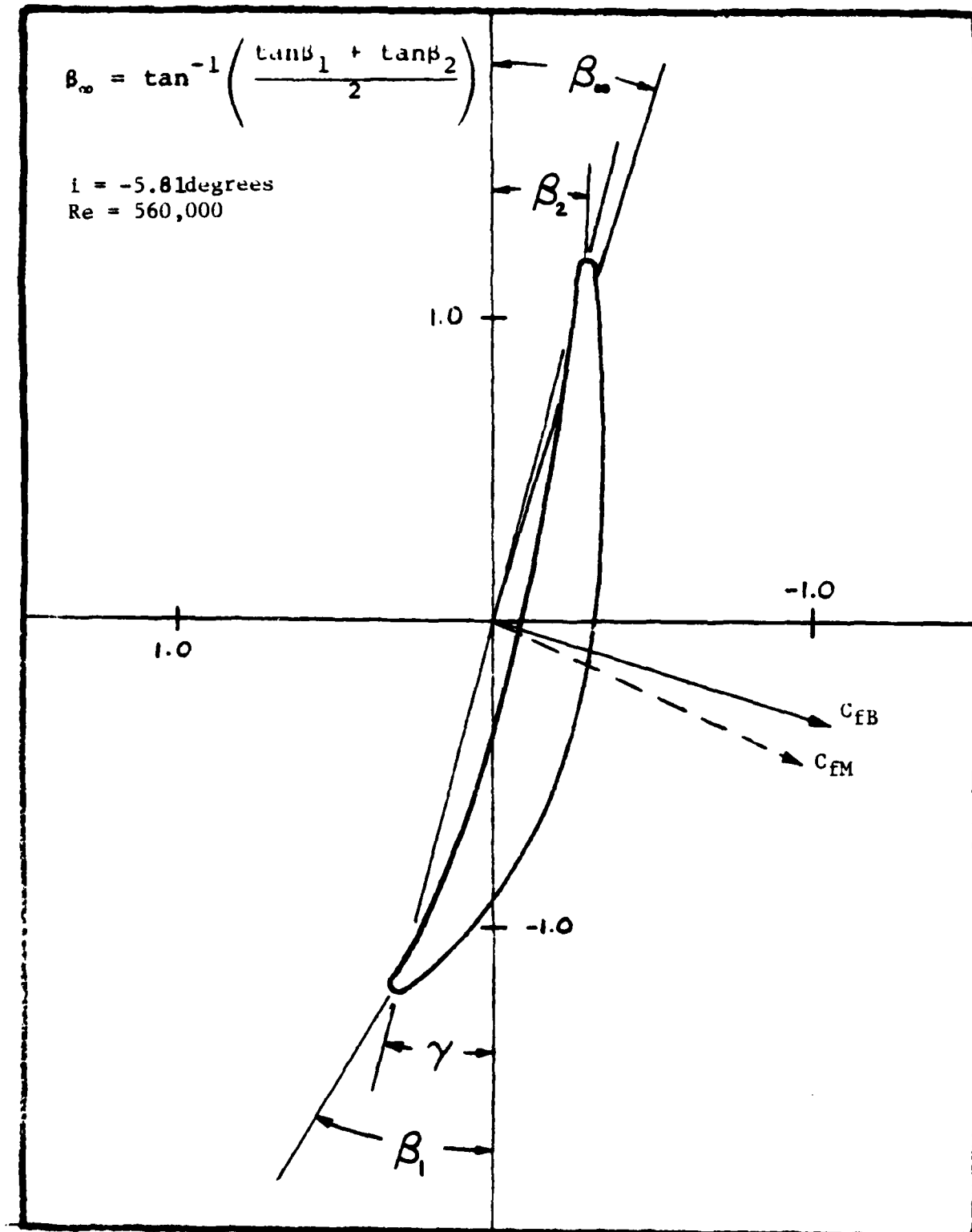


Fig. A.173

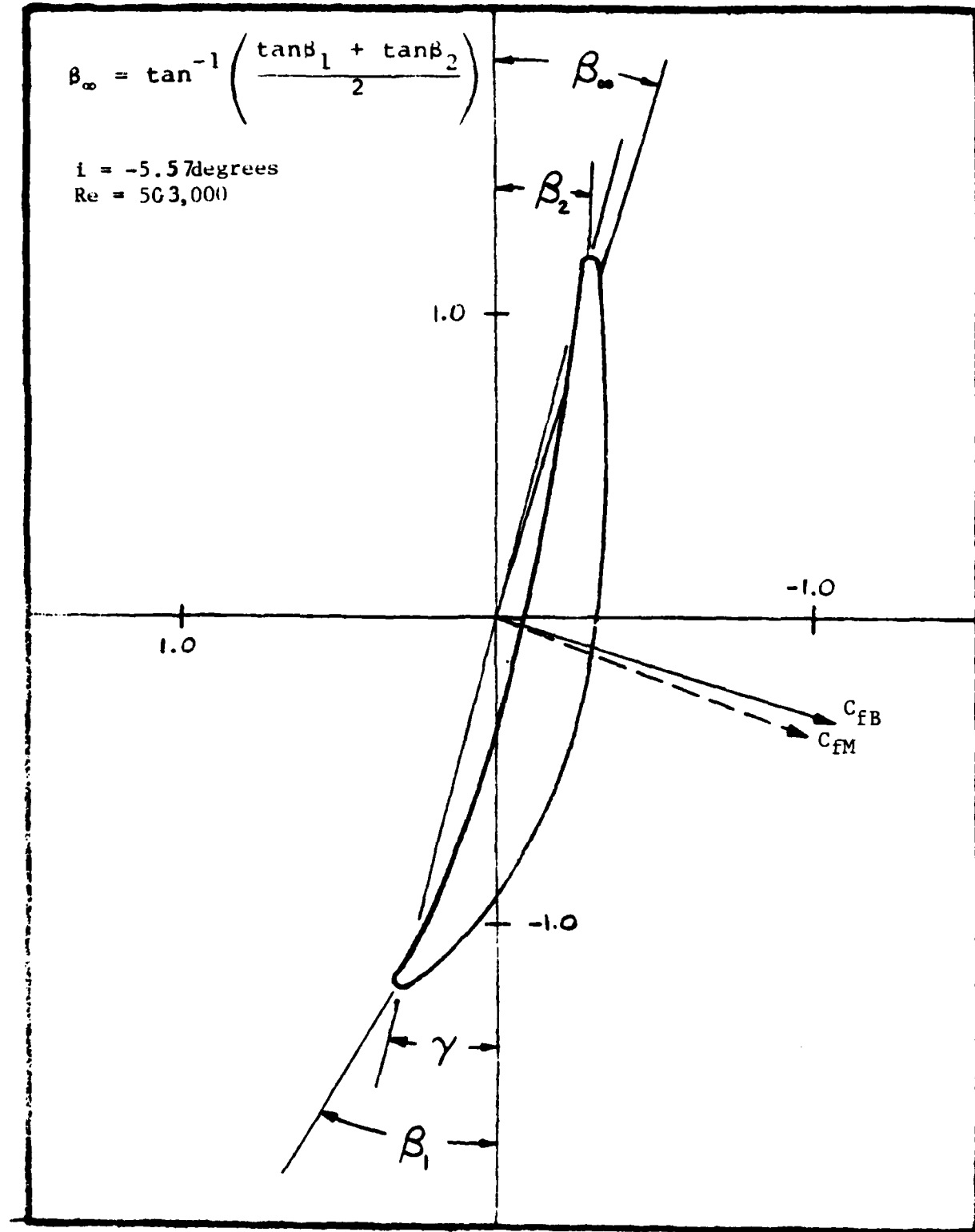


Fig. A.174

$$\beta_{\infty} = \tan^{-1} \left( \frac{\tan \beta_1 + \tan \beta_2}{2} \right)$$

$i = -1.59$  degrees  
 $Re = 643,000$

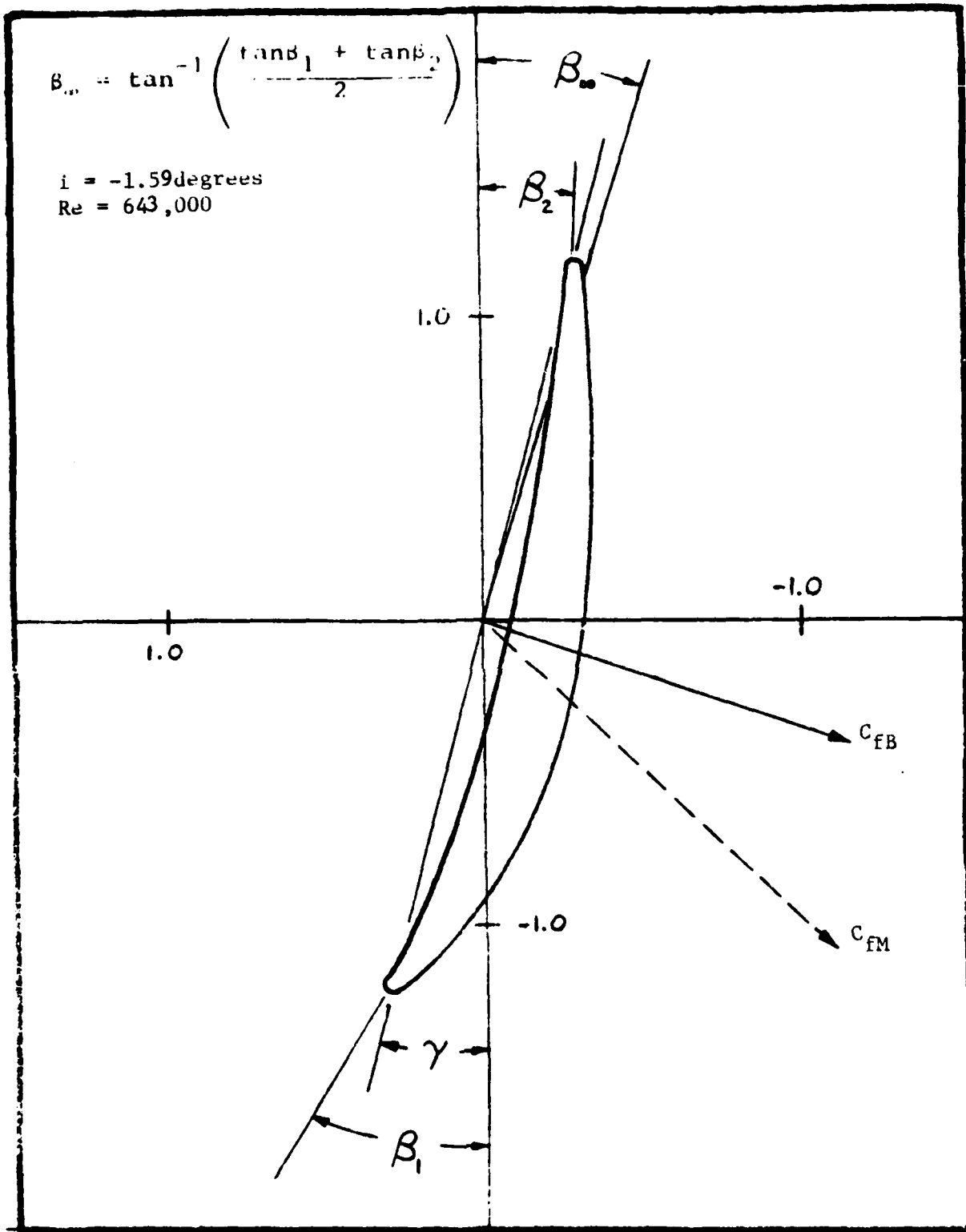


Fig. A.175

$$\beta_\infty = \tan^{-1} \left( \frac{\tan\beta_1 + \tan\beta_2}{2} \right)$$

$i = -1.5$  degrees  
 $Re = 525,000$

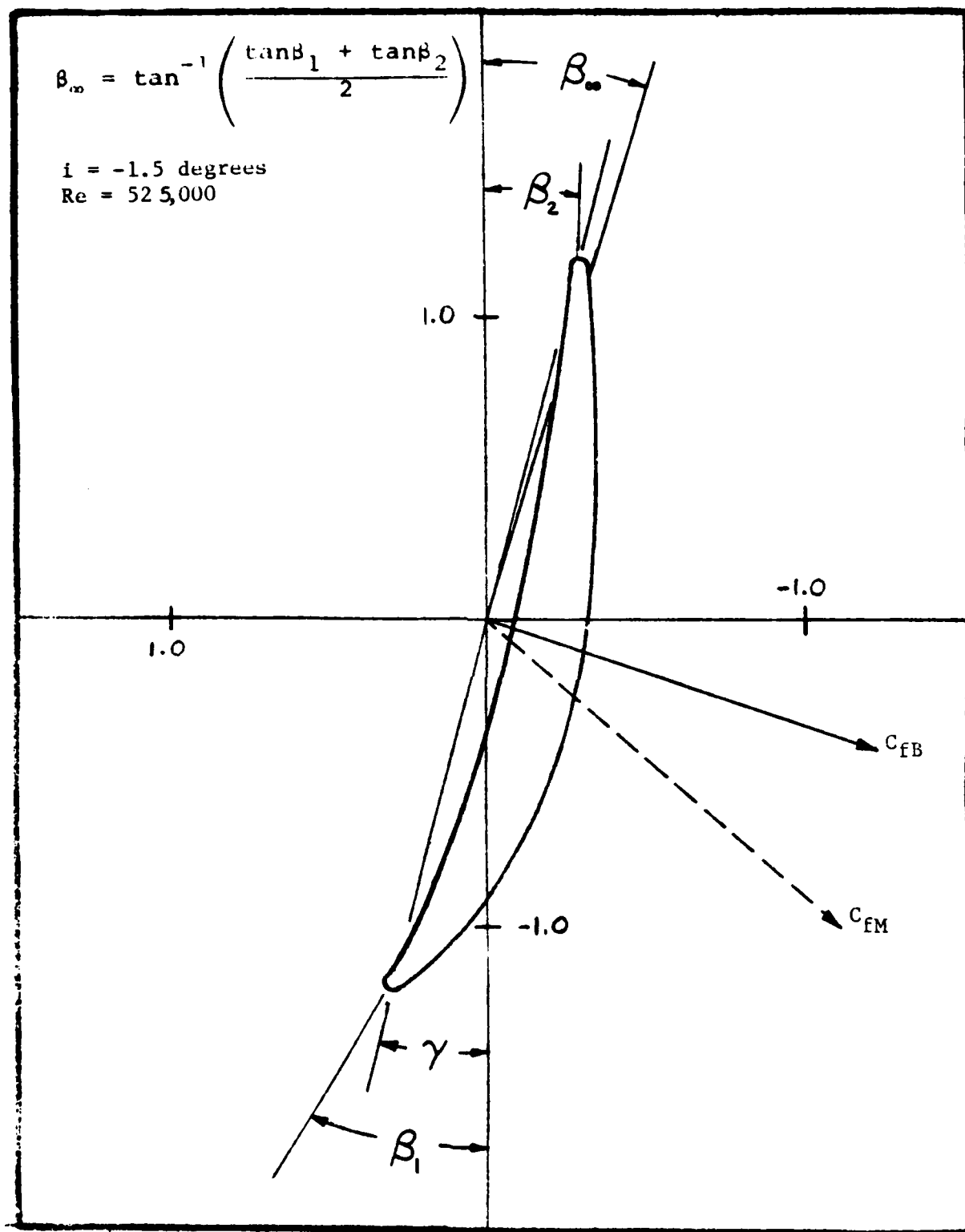


Fig. A.176

$$\beta_\infty = \tan^{-1} \left( \frac{\tan \beta_1 + \tan \beta_2}{2} \right)$$

$i = 2.27$  degrees  
 $Re = 676,000$

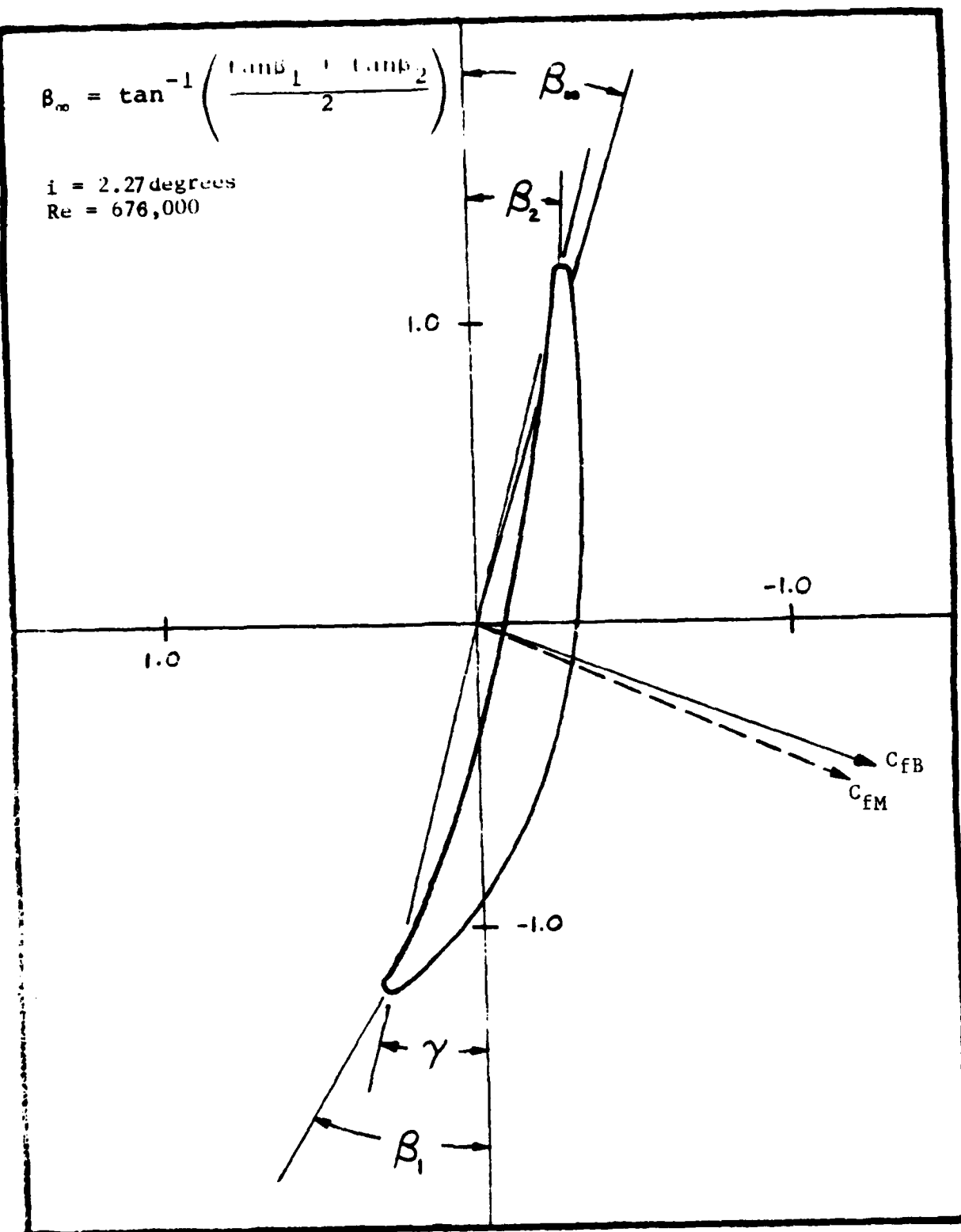


Fig. A.177

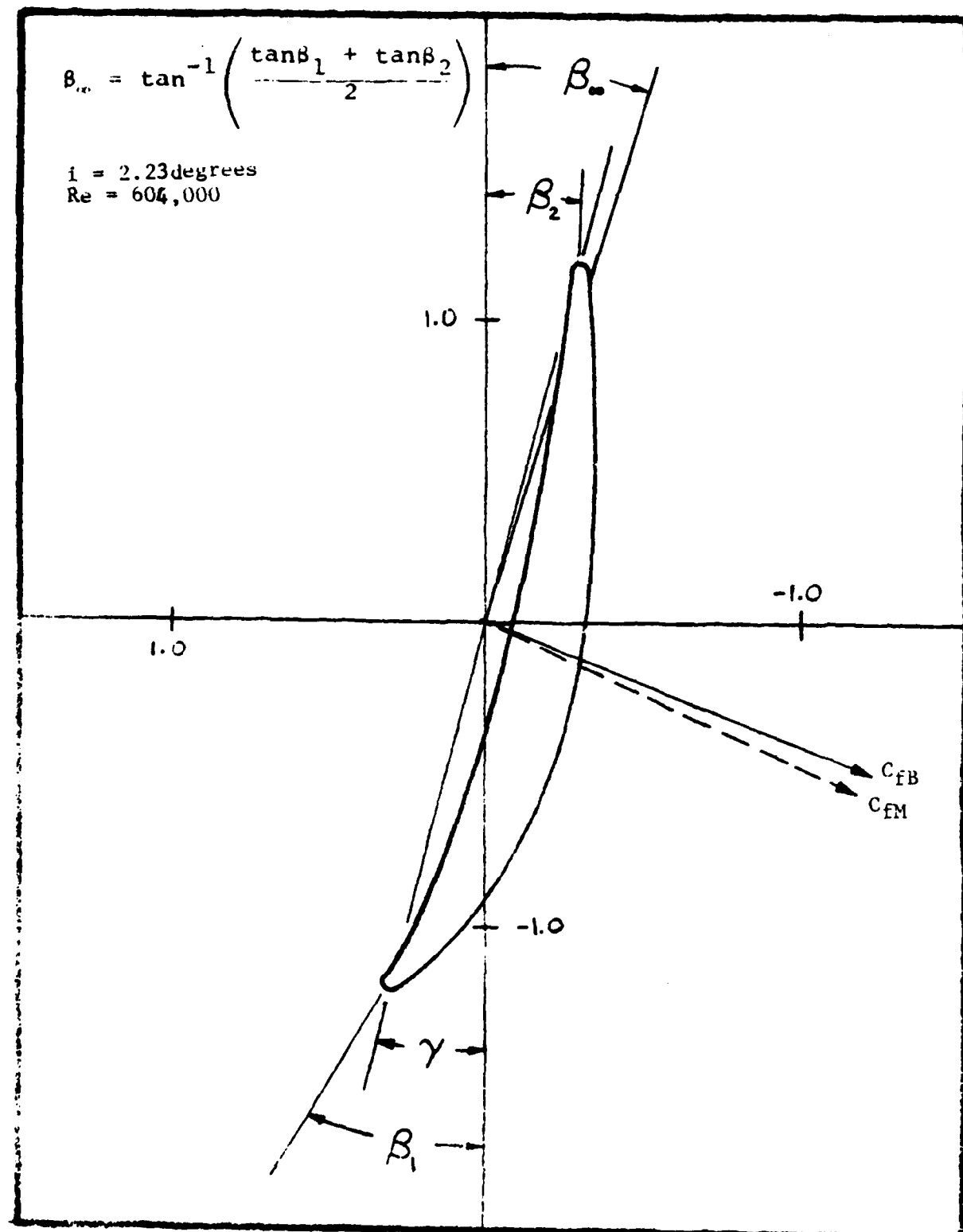


Fig. A.178

$$\beta_{\infty} = \tan^{-1} \left( \frac{\tan \beta_1 + \tan \beta_2}{2} \right)$$

$i = 5.99$  degrees  
 $Re = 771,000$

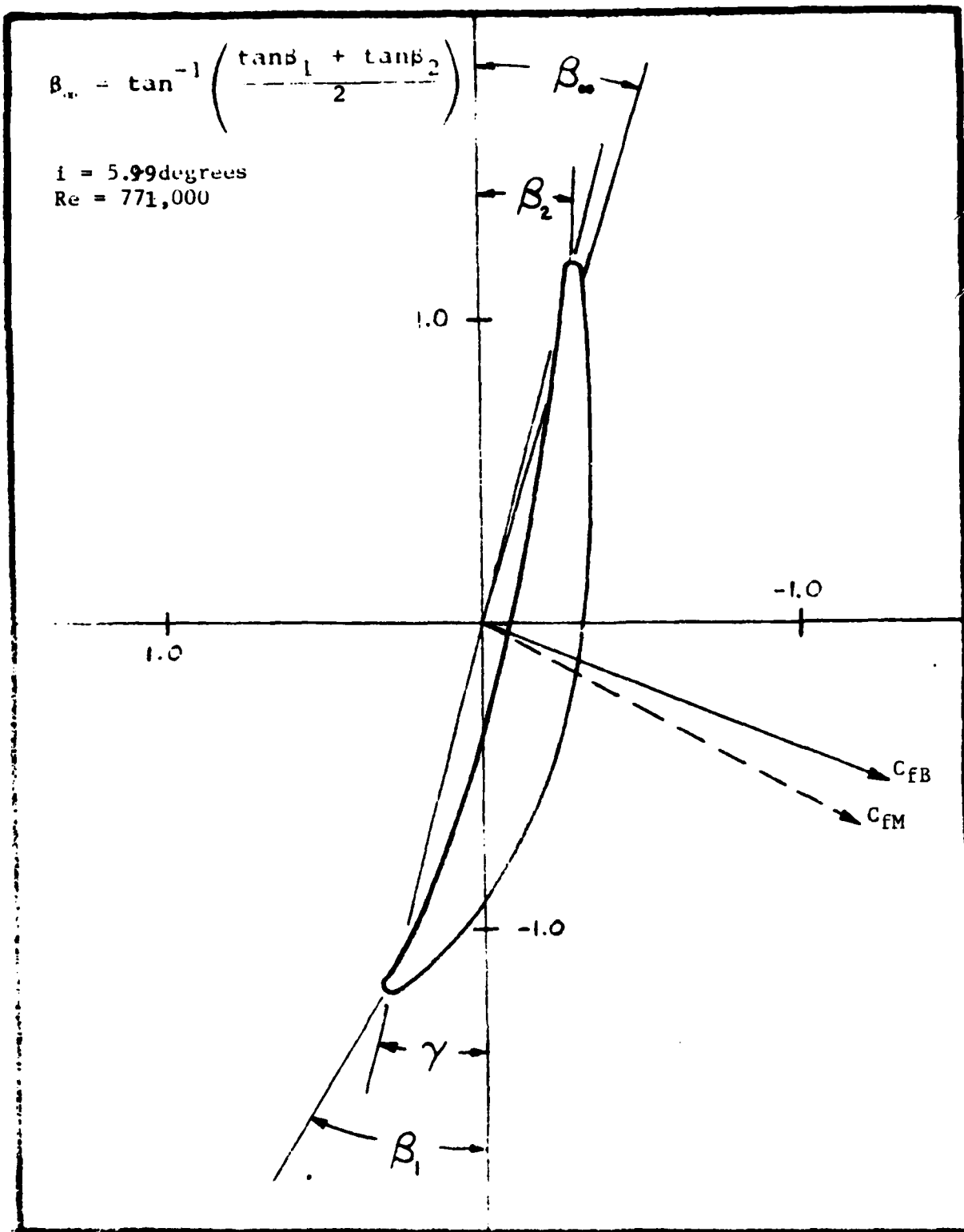


Fig. A.179

$$\beta_\infty = \tan^{-1} \left( \frac{\tan\beta_1 + \tan\beta_2}{2} \right)$$

$i = 5.54$  degrees  
 $Re = 518,000$

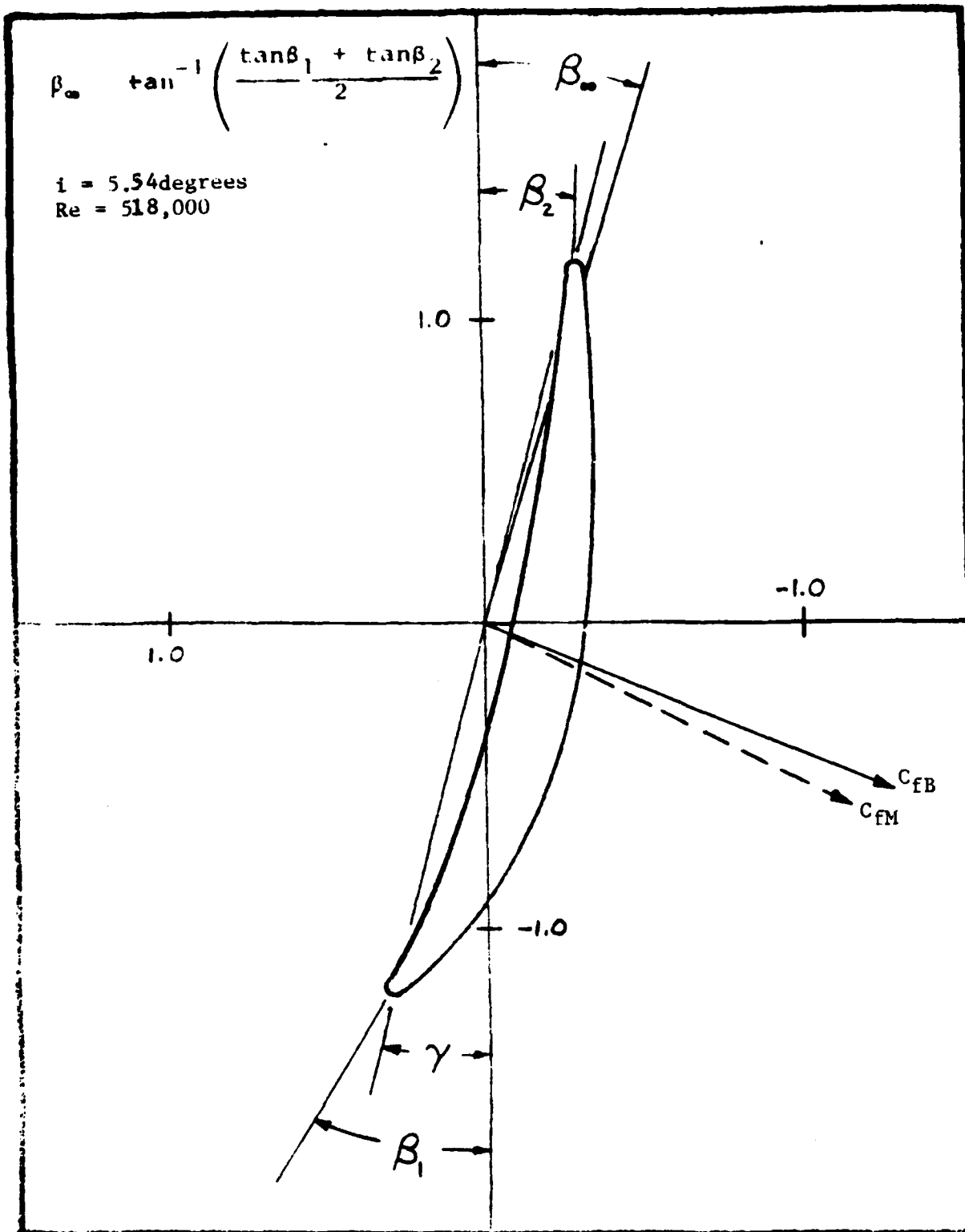


Fig. A.180

$$\beta_m = \tan^{-1} \left( \frac{\tan \beta_1 + \tan \beta_2}{2} \right)$$

$i = 8.79$  degrees  
 $Re = 768,000$

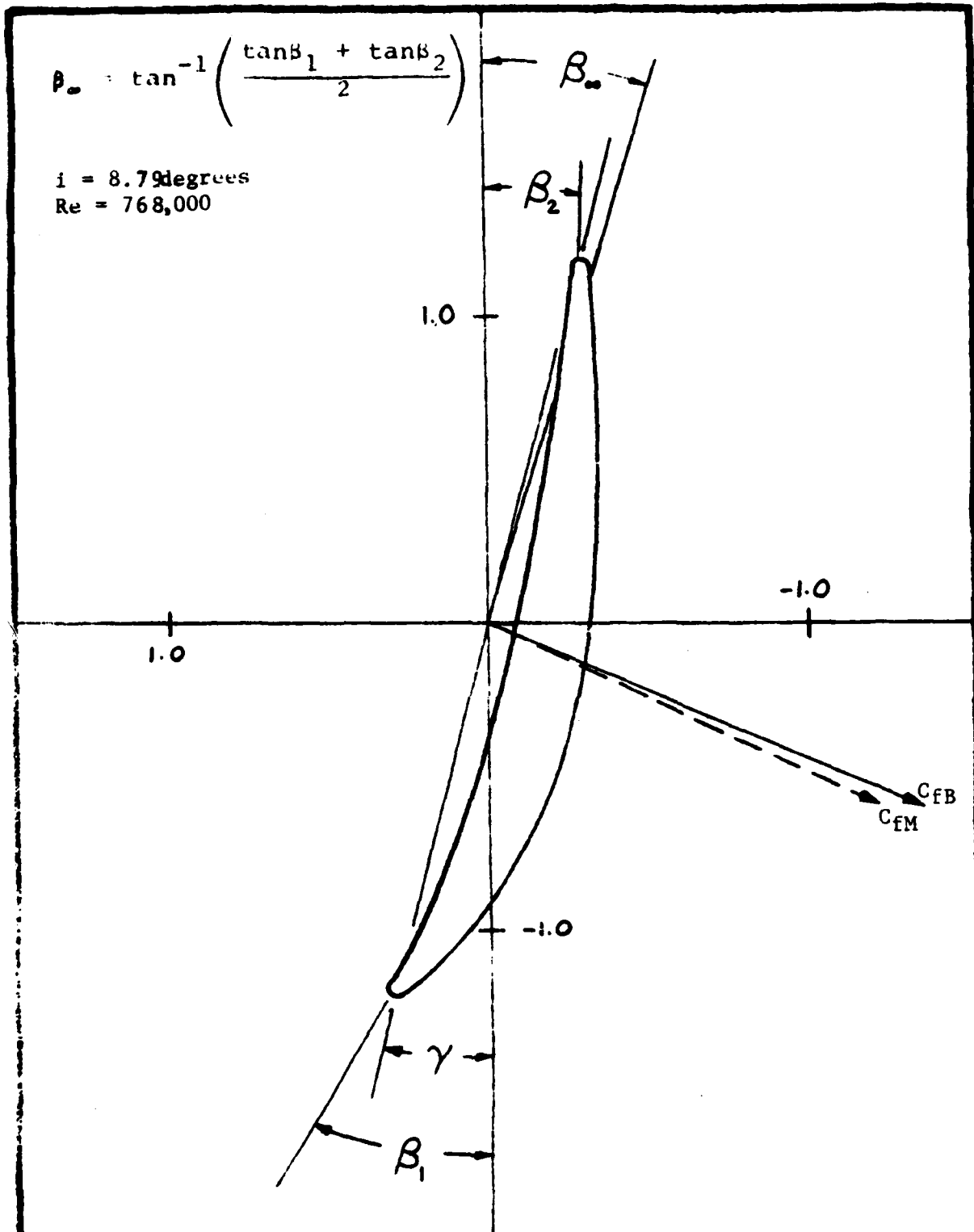


Fig. A.181

$$\beta_\infty = \tan^{-1} \left( \frac{\tan \beta_1 + \tan \beta_2}{2} \right)$$

$i = 8.76\text{ degrees}$   
 $\text{Re} = 493,000$

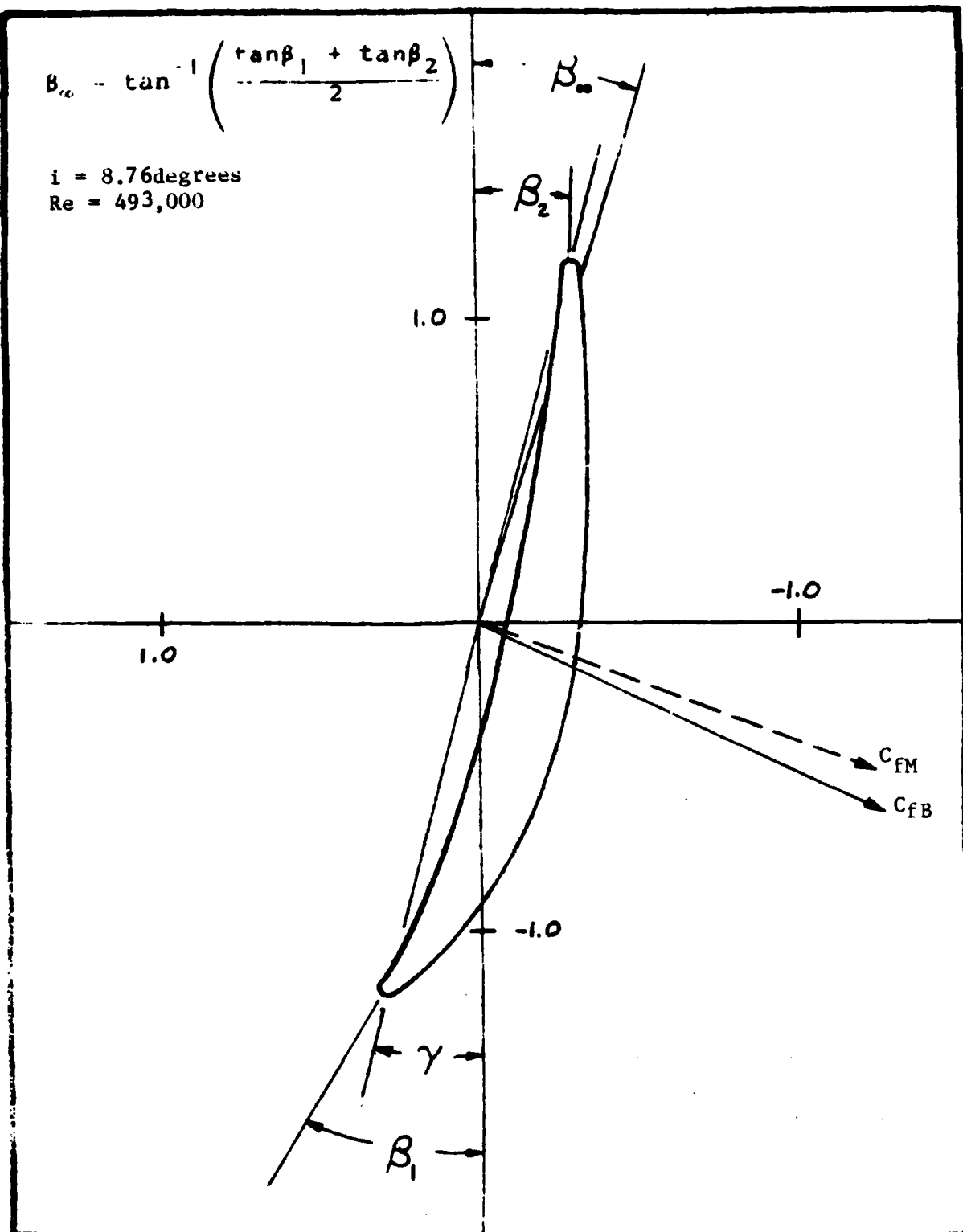


Fig. A.182

## APPENDIX B

### A. STORAGE OF EXPERIMENTAL DATA

#### 1. Storage Devices

##### a. Cassette Tape

All raw and reduced data acquired during the current study via the HP-3052A acquisition system were stored on cassette tape. Table B.1 summarizes the raw data file-names according to inlet air angle and cassette tape number. Tapes were filed with the Director, Turbopropulsion Laboratory, Naval Postgraduate School, Monterey, Ca.

##### b. File Naming Scheme

All files were named using a six character alphanumeric code that allowed the investigator to immediately identify stored data in any file and on what date it was recorded. Here is how the code works.

1st character: Indicates the type of traverse conducted ("B"lade-to blade, "S"panwise or "I"nstrumented blade data).

2nd character: Indicates the "state" of the data set (ra"W", re"D"uced or "F"inal).

3rd character: Indicates which probe was involved in taking the data set, either "U"pper or "L"ower. No letter here means that the probes acquired data simultaneously.

4th, 5th and 6th characters: These numbers indicate the julian date in 1983 that the test run was conducted.

For example, a file containing data from a raw blade-to-blade survey using the upper probe conducted on January 15, 1983 would be named BWU015. When upper and lower probes were traversed together the "U"pper or "L"ower character was dropped and the entire julian date filled the remaining four spaces. For example, if the upper and lower probes were both traversed in the blade-to-blade direction on January 15, 1983, the resultant raw data filename would be named BW3015.

Sometimes, in order to completely describe a reduced data file, parts of the julian date had to be sacrificed. Raw data from a spanwise survey of the upper probe one inch from the suction side of the centermost instrumented blade conducted on February 1, 1983 would be named SWSU32 ("S"panwise, ra"W", 1 inch from "S"uction side, "U"pper probe, julian date 30"32"). It should be noted that when spanwise surveys were conducted, both probes moved together. To preclude interference of the lower probe wake with the upper probe measurements, the upper probe was placed 1 inch from the suction side, and the lower probe was placed 1 inch from the pressure side of the center blade. The composite data file was named with the upper probe in mind, however, even though the lower probe was stationed at a different blade-to-blade position. For example, a raw spanwise survey named SWS077 would show that the upper probe was 1 inch from the

suction side of the center blade, while the lower probe was 1 inch from the pressure side.

Some specialized filenames reflect the type of data stored. Referencing constants calculated for a test conducted on February 15, 1983 would be named RC046A or RC046B where the "A" would mean that the referencing constants were calculated using the plenum total pressure and the lower wall static pressure as reference total and static pressures. "B" would indicate that the reference total and static pressures were supplied by the pitot-static probe.

## 2. Thesis Logbook

A chronological log of the present study with notes and printouts of all data files was deposited with the Director, Turbopropulsion Laboratory.

## B. PROBE CALIBRATION DATA

A folder documenting the calibration of United Sensor probes serial number 847-1 and 981-2 was filed with the Laboratory Manager, Turbopropulsion Laboratory. Non-dimensional velocity (X) and pitch angle (PHI) calibration files for both probes appear on each data storage cassette tape. Their names reflect the file type and the applicable probe. For example, the pitch angle calibration file for the 981 probe is named "PHI981", the X velocity calibration file for the 847 probe is named "X847", and so on.

TABLE B.I. RAW DATA STORAGE

$\beta_1$	Raw BTOB Data	Raw Spanwise Data	Raw Instrumented Blade Data	Tape Number
24.63	BW3144	SWS144	IW3144	11
24.74	BW3143	SWS143	IW3143	11
27.55	BW3123	SWS123 SWP123	IW3123	7
27.90	BW3125	SWS125 SWP125	IW3125	7
31.32	BW3119	SWS119 SWP119	IW3119	6
31.56	BW3121	SWS121 SWP123	IW3121	6
35.50	BW3138	SWS138	IW3138	10
35.60	BW3139	SWS139	IWL39B	10
39.02	BWU077 BWL077	SWU077 SWL077	IW077	2
38.68	BW3082	SW3082	IW082B	2
38.34	BW3097	SW3097	IW3097	3
38.89	BW3103	SW3103	IW3103	3
39.28	BW3127	SWS127 SWP127	IWL27B	8
39.40	BW3128	SWS128 SWP128	IW3128	8
39.16	BW3129	SWS129 SWP129	IW3129	9
39.36	BW3133	SWS133	IW3133	9
42.66	bw3109	sws109 swp109	iw3109	4
43.13	BW3110	SWS110 SWP110	IWL10B	4
45.92	BW3114	SWS114 SWP114	IW3114	5
45.89	bw3114	sws114 swp114	iw3114	5

## APPENDIX C

### EFFECT OF AVDR ON THE AXIAL FORCE COEFFICIENT DERIVED FROM PROBE SURVEY DATA.

The notation used in this section follows [Ref. 14] and [Ref. 15]. The application of the principle of momentum conservation to the control volume shown in Fig. C.1 results in the following expression for the resultant force on the control volume;

$$\bar{R}_w = \int_{S_1} \vec{V}_1 dm_1 - \int_{S_2} \vec{V}_2 dm_2 + \int_{S_1} d\vec{F}_1 + \int_{S_2} d\vec{F}_2 \\ + \int_{\textcircled{a}} d\vec{F}_a + \int_{\textcircled{b}} d\vec{F}_b$$

$$\Rightarrow R_{w_x} \hat{i}_x + R_{w_y} \hat{i}_y \quad (\text{C-1})$$

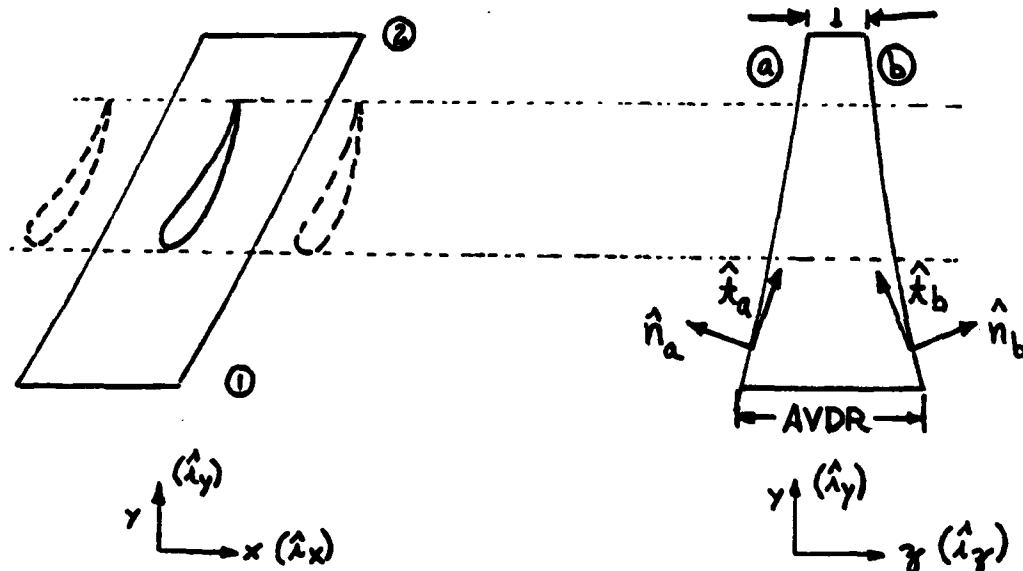


Figure C.1. Blade Space Control Volume

In the enlarged view of the edge of curved surface a, the unit outward normal vector,  $\hat{n}_a$ , is given by the relation

$$\hat{n}_a = \cos\alpha \hat{i}_y - \sin\alpha \hat{i}_z \quad (C-2)$$

and similarly, on surface b,  $\hat{n}_b$  is given by

$$\hat{n}_b = \cos\alpha \hat{i}_y + \sin\alpha \hat{i}_z \quad (C-3)$$

The elemental area "s" on the curved sidewall of the control volume can be expressed as the projection of an element of the base area  $ds$ , where

$$ds = dx dy \quad (C-4)$$

so that,

$$ds = \frac{dx dy}{\cos\alpha} \quad (C-5)$$

Resolving the elemental force,  $d\bar{F}$ , acting on the curved sidewalls of the control volume into normal and sheer components gives

$$d\bar{F} = -p \hat{n} ds - \tau \hat{t} ds \quad (C-6)$$

Neglecting wall friction,  $\tau$ , the tangential force becomes:

$$R_{w_t} = \int_{S_1} \rho_1 V_a V_{u_1} dA_1 - \int_{S_2} \rho_2 V_{a_2} V_{u_2} dA_2 \quad (C-7)$$

and the axial force becomes:

$$R_{w_a} = \int_{S_1} \rho_1 V_{a_1}^2 dA_1 - \int_{S_2} \rho_2 V_{a_2}^2 dA_2 + \int_{S_1} p_1 dA_1 - \int_{S_2} p_2 dA_2 + \int_a \hat{i}_y \cdot d\bar{F}_a + \int_b \hat{i}_y \cdot d\bar{F}_b \quad (C-8)$$

Using Eq. (C-2), Eq. (C-3), Eq. (C-5) and Eq. (C-6),

$$\begin{aligned}\int_a \hat{i}_y \cdot d\vec{F}_a &= \int_a \hat{i}_y [-p(\cos\alpha \cdot \hat{i}_y - \sin\alpha \cdot \hat{i}_x)] \frac{dx dy}{\cos\alpha} \\ &= \int_a -p dx dz\end{aligned}\quad (C-9)$$

and similarly,

$$\int_b \hat{i}_y \cdot d\vec{F}_b = \int_b -p dx dz \quad (C-10)$$

which represent additional axial force components due to pressure forces on the control volume side walls.

Equation (C-7) is identical to Eq. (B-3) of [Ref. 1] which was derived for a strictly two-dimensional flow. Substitution of Eq. (C-9) and Eq. (C-10) into Eq. (C-8) yields,

$$R_w = \int_0^S p_1 V_{a1}^2 (AVDR) dx - \int_0^S p_2 V_{a2}^2 dx + \int_0^S p_1 (AVDR) dx - \int_0^S p_2 dx - 2 \int_a^S p(y) dz dx \quad (C-11)$$

which contains a fifth axial force term not included by Cina, and a modification of the first and third terms resulting from the effects of AVDR.

Since the precise function  $p(y)$  is not known from station 1 to station 2, a linear change of pressure with  $y$  was assumed as depicted in Fig. C.2.

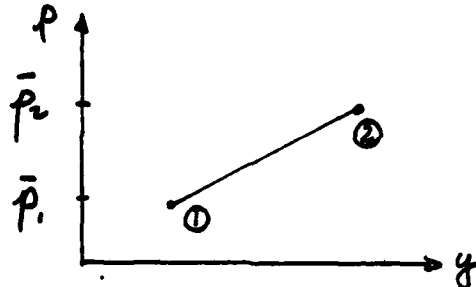


Figure C.2. Assumed Pressure Function

The fifth term of Eq. (C-11) can then be approximated as:

$$-2 \int_a^S p(y) dz dx = -S \left\{ \bar{p}_1 (AVDR-1) + \left[ \frac{\bar{p}_2 - \bar{p}_1}{2} \right] [AVDR-1] \right\} \quad (C-12)$$

Assuming that

$$\bar{p}_1 \cdot S \cdot AVDR = \int_0^S p_1 \cdot AVDR \cdot dx \quad (C-13)$$

substitution of Eq. (C-13) and Eq. (C-12) into Eq. (C-11)

yields,

$$R_{wa} = \int_0^S p_1 V_a^2 (AVDR) dx - \int_0^S p_2 V_{a_2}^2 dx + \int_0^S p_1 dx \\ - \int_0^S p_2 dx - \left\{ \left[ \frac{(\bar{p}_2 - \bar{p}_1)}{2} \right] [AVDR - 1] S \right\} \quad (C-14)$$

Equation (C-14) was reduced to force coefficient form using procedures explained in [Ref. 1] and then incorporated into existing software documented in [Ref. 8].

### LIST OF REFERENCES

1. Cina, Frank S., Subsonic Cascade Wind Tunnel Tests Using a Compressor Configuration of DCA Blades, M. S. Thesis: Naval Postgraduate School, Monterey, Ca., 1981.
2. Molloy, William D., Preliminary Measurements and Code Calculations of Flow Through a Cascade of DCA Blading at a Solidity of 1.67, M. S. Thesis, Naval Postgraduate School, Monterey, Ca., 1982.
3. Rose, Charles C., and Guttormson, Darold L., Installation and Test of a Rectilinear Cascade, M. S. Thesis, Naval Postgraduate School, Monterey, Ca., 1964.
4. Bartocci, J. E., An investigation of the Flow Conditions at the Lower Measurement Plane, and in the Plenum Chamber of the Rectilinear Cascade Test Facility, M. S. Thesis, Naval Postgraduate School, Monterey, Ca., 1966.
5. Moebius, Richard C., Analysis and Testing to Improve the Flow from the Plenum of a Subsonic Cascade Wind Tunnel, M. S. Thesis, Naval Postgraduate School, Monterey, Ca., 1980.
6. McGuire, Alan G., Determination of Boundary Layer Transition and Separation on Compressor Blades in a Large Subsonic Cascade, M. S. Thesis, Naval Postgraduate School, Monterey, Ca., 1983.
7. 3052A System Library (9845A), Hewlett Packard Company, 1978.
8. Turbopropulsion Laboratory, Naval Postgraduate School, Technical Note 80-03 (revised), Data Aquisition Programs for the Subsonic Cascade Wind Tunnel, by D. A. Duval, 1980 (revised by S. J. Himes, 1983).
9. NASA Report SP-36, Aerodynamic Design of Axial Flow Compressors, edited by Irving A. Johnson and Robert A. Bullock, 1965.
10. NASA Report 1016, Effect of Tunnel Configuration and Testing Technique on Cascade Performance, by John R. Erwin and James C. Emery, 1951.

11. Duval, David A., Evaluation of a Subsonic Cascade Wind Tunnel for Compressor Blade Testing, M. S. Thesis, Naval Postgraduate School, Monterey, Ca., 1980.
12. Contractor Report, Procedure and Computer Program for Approximation of Data (with Application to Multiple Sensor Probes), by H. Zebner, August 1980.
13. Turbopropulsion Laboratory, Naval Postgraduate School, Technical Note 82-03, Computer Software for the Calibration of Pneumatic and Temperature Probes, by F. Neuhoff, September 1982.
14. Vavra, Michael H., Aero-Thermodynamics and Flow in Turbomachines, Krieger, 1974.
15. Class Notes, Aerothermodynamics and Design of Turbomachines, R. P. Shreeve, Professor, October 1982.

INITIAL DISTRIBUTION LIST

	No. Copies
1. Defense Technical Information Center Cameron Station Alexandria, VA 22314	2
2. Library, Code 0142 Naval Postgraduate School Monterey, CA 93940	2
3. Department Chairman, Code 67 Department of Aeronautics Naval Postgraduate School Monterey, CA 93940	1
4. Director, Turbopropulsion Laboratory, Code 67Sf 1 Department of Aeronautics Naval Postgraduate School Monterey, CA 93940	
5. Mr. George Derderian Naval Air Systems Command Code AIR-310E Department of the Navy Washington, D. C. 20360	1
6. Dr. A. D. Wood Office of Naval Research Eastern/Central Regional Office 666 Summer Street Boston, MA 02210	1
7. Chief, Fan and Compressor Branch (Attn: Nelson Sanger) NASA Lewis Research Center Mail Stop 5-9 21000 Brookpark Road Cleveland, OH 44135	1
8. LCDR S. J. Himes, USN 4681 Revere Road Virginia Beach, VA 23456	1
9. Turbopropulsion Laboratory Code 67 Naval Postgraduate School Monterey, CA 93940	10

